Cellular functions and enzymatic activity of the poly(ADP-ribose) polymerase protein family

By

Sejal Vyas
B.S., Biochemistry and Molecular Biology
Pennsylvania State University, 2007

Submitted to the Department of Biology in Partial Fulfillment of the Requirements for the Degree of

Doctor of Philosophy

At the

Massachusetts Institute of Technology

February 2014

Signature of Author:.....

Sejal Vyas
Department of Biology
January 5th, 2014

Certified By:.....

Paul Chang
Assistant Professor of Biology
Thesis Supervisor

Accepted By:.....

Stephen P. Bell
Professor of Biology
Chair, Committee for Graduate Studies

Cellular functions and enzymatic activity of the poly(ADP-ribose) polymerase protein family

By

Sejal Vyas

Submitted to the Department of Biology in partial fulfillment of the requirements for the degree of Doctor of Philosophy

Abstract

The poly(ADP-ribose) polymerase (PARP) protein family consists of seventeen enzymes and generates ADP-ribose (ADPr) posttranslational modifications onto target proteins using NAD^+ as a substrate. While functions for PARPs in the nucleus, such as in DNA damage repair and transcriptional regulation, had been well studied, functions for PARPs outside the nucleus were largely unknown. The well known product of PARP activity is poly(ADP-ribose) (PAR), which is a structurally complex polymer that can be up to 200 units in length. Because the PARP family was identified based on sequence homology to the catalytic domain of PARP1, the founding PARP member and main generator of nuclear PAR modifications, it was thought that the remaining family members also synthesize PAR. However, bioinformatics analysis has predicted that many PARPs in fact generate only mono(ADP-ribose) (MAR) modifications. As yet, the catalytic activity of for the entire PARP family has not been experimentally verified.

We performed a systematic analysis of the PARP family to identify novel functions and determine the enzymatic activity for each PARP. First a family-wide localization and RNAi screen was performed to identify novel functions for PARP family members. From this work, we determined that the majority of PARPs are cytoplasmic and discovered new cytoplasmic functions for PARPs including actin cytoskeleton regulation and in regulation of membrane bound organelle structures. The enzymatic activity of each PARP was then analyzed to determine which types of ADPr modifications may be required for the PARP functions identified. We found that the majority of the PARP family proteins generate MAR modifications. Together, this work advances the understanding of PARP biology and identified novel PARP functions.

Thesis Supervisor: Paul Chang
Title: Assistant Professor of Biology

Table of Contents

Chapter 1. Introduction

Poly(ADP-ribose) polymerases (PARPs) post-translationally modify target proteins with ADP-ribose (ADPr) using NAD^+ as a substrate (Bürkle, 2005). Two forms of ADP-ribose are generated, monomers called mono(ADP-ribose) (MAR) or polymers called poly(ADP-ribose) (PAR). PAR was initially identified as polyadenylic nucleic acid and the enzymatic activity responsible for its synthesis was first reported in hen liver nuclear extracts in the 1960's (Chambon et al., 1963; Chambon et al., 1966). Purification of the first poly(ADP-ribose) polymerase activity from rat liver nuclei was reported shortly after and was shown to incorporate ADPr from substrate NAD^+ in a DNA dependent manner (Yamada et al., 1971; Okayama et al., 1977). The first PARP, nuclear PARP1, was cloned in 1987 followed by PARP2, another nuclear protein (Alkhatib et al., 1987; Cherney et al., 1987; Suzuki et al., 1987; Amé et al., 1999). It was not until much later that cytoplasmic PARPs were identified, with the discovery of PARP4 and PARP5a in 1999 (Kickhoefer et al., 1999; Smith and de Lange, 1999). The complete PARP family consisting of 17 PARPs was subsequently identified within the last decade based on sequence similarity with the catalytic domain of PARP1 (Amé et al., 2004).

PARP functions can be grouped into two general areas, regulation of cell physiology and of cell stress responses. Physiological functions include transcriptional regulation (Kraus and Lis, 2003), chromatin structure regulation (Dantzer and Santoro, 2013), cell migration (Aguiar et al., 2000; Vyas et al., 2013) and cell division (Dynek and Smith, 2004; Chang et al., 2005). Cell stress functions include regulation of the DNA damage response (Malanga and Althaus, 2005), heat shock response (Petesch and Lis,

2012; Di Giammartino et al., 2013), the cytoplasmic stress response (Leung et al., 2011), the unfolded protein response (Jwa and Chang, 2012) and the antiviral response (Gao et al., 2002).

Based on experimental data and computational analysis, each PARP is hypothesized to generate either PAR or MAR, but not both (Kleine et al., 2008). When generated *in vitro* PAR can contain up to 200 ADPr units in both linear and branched structures, while MAR is a single ADPr unit attached to a target protein (Alvarez-Gonzalez and Jacobson, 1987). The type of ADPr structure generated by each PARP is thought to depend on two factors. One is the primary amino acid sequence of the catalytic domain, specifically, the identity of amino acids that bind NAD^+ and catalyze the transfer of ADPr to target protein (Kleine et al., 2008). Additionally structural characteristics of the substrate and acceptor binding pockets within the catalytic domain are predicted to impact the type of ADPr modification generated (Kleine et al., 2008; Wahlberg et al., 2012).

In vivo, poly(ADP-ribosyl)ating PARPs are known to be primary acceptors of their own activity, with automodification often serving to nucleate protein complexes. While mono(ADP-ribosyl)ating PARPs have been demonstrated to automodify *in vitro*, less is known about their endogenous targets and whether they similarly serve as the main acceptors of their own activity *in vivo*. Additionally, automodification with PAR has been shown to downregulate the activity of poly(ADP-ribosyl)ating PARPs (Desmarais et al., 1991). If automodification is a significant *in vivo* activity of mono(ADP-ribosyl)ating PARPs, it remains to be seen what effect it has on enzymatic activity.

Cellular ADPr concentrations are regulated by a balance of PARP activity and hydrolysis by ADPr hydrolytic enzymes: poly(ADP-ribose) glycohydrolase (PARG), which hydrolyzes PAR chains, and the mono(ADP-ribose) hydrolases MacroD1, MacroD2 and terminal(ADP-ribose) glycohydrolase (TARG) which release ADPr at the site of protein attachment (Slade et al., 2011; Jankevicius et al., 2013; Rosenthal et al., 2013; Sharifi et al., 2013).

The primary focus of this review is to discuss new data regarding the function of the PARP family of proteins and to contextualize what is known about their structure and enzymatic activity into their newly identified cellular functions. Finally, we discuss exciting future directions for the PARP family.

Part 1. ADP-ribose modifications

Due to the major differences in size and structure, PAR and MAR exhibit distinct yet possibly overlapping mechanisms of function. Both PAR and MAR can modulate target protein function via covalent modification similar to traditional post-translation modifications such as phosphorylation (Johnson and Barford, 1993). However, given its large size and charge distribution, PAR can also bind specific proteins through non-covalent interactions to function as a protein-binding scaffold. In fact, 4 protein domains that bind with high affinity to PAR have been identified – WWE (tryptophan-tryptophan-glutamate), PBZ (poly(ADP-ribose) binding zinc finger), macro and a loosely defined PAR binding motif (Pleschke et al., 2000; Karras et al., 2005; Ahel et al., 2008; Wang et al., 2012). In contrast, only the macro domain can bind to MAR and therefore MAR appears to lack the ability to nucleate multiprotein complexes. Interestingly, there are differences in the type of ADPr recognized among distinct macro domains, first

identified in the histone variant macroH2A (Pehrson and Fried, 1992; Karras et al., 2005; Forst et al., 2013). For example, the macro domain of the mH2A and PARP9 can bind to PAR whereas the macro domains of PARP14 specifically bind to MARylated proteins (Karras et al., 2005; Forst et al., 2013).

Most of the experimental focus has been on PAR due to both historic and biological reasons. PAR was the first form of ADP-ribose identified, is more easily purified and studied due to stoichiometry and is less sensitive to degradation. However there are compelling reasons to study MAR - phylogenetic analysis of the PARP family across 77 species has shown that both PAR and MAR synthesis are evolutionarily conserved, indicating the importance of both types of ADPr modifications (Citarelli et al., 2010). Furthermore, bioinformatic analysis suggests that MAR is the most common product of PARP activity (Kleine et al., 2008).

Mono(ADP-ribose)

Although PARP-mediated MAR modifications are recently identified, mono(ADP-ribosyl)ating PARPs have many functions which include transcriptional regulation, actin cytoskeleton regulation and regulation of the unfolded protein response (Jwa and Chang, 2012; Feijs et al., 2013; Vyas et al., 2013). While the mechanism of function of MAR modifications is unclear for many of these cases, modification of the stress responsive kinase PERK (protein kinase RNA-like endoplasmic reticulum kinase) and IRE1α (inositol-requiring enzyme 1 α) by PARP16 upregulates their kinase activity, indicating that MAR is acting as a traditional posttranslational modification to modulate target protein activity (Jwa and Chang, 2012). Further insight can be taken from bacterial mono-ADP-ribosyltransferases (mARTs) that generate a biochemically

identical modifications albeit on distinct amino acids. mARTs mono(ADP-ribosyl)ate diverse host proteins to mediate pathogenicity including the translation factor EF-2 to inhibit protein translation, small GTPases to affect signal transduction pathways and the Rho-GTPase to alter actin cytoskeleton dynamics (Deng and Barbieri, 2008). In these cases, mono(ADP-ribosyl)ation of host proteins functions to disrupt interactions with binding partners, indicating that one mechanism of function for MAR is to alter target protein interactions. Finally, the binding of macro domain containing proteins to mono(ADP-ribosyl)ated proteins suggest that MAR modifications could also function as recruitment signals to sites of mono(ADP-ribosyl)ation (Karras et al., 2005; Forst et al., 2013)

Within the field of PARP biology, the existence of MAR modifications by PARPs is actually somewhat controversial, with some scientists interpreting the published data as evidence of single ADPr units, and others interpreting it as evidence of short ADPr modifications. While clearly distinct from the large polymers synthesized by PARPs 1, 2, 5a and 5b, it has not been explicitly shown for many of the proposed mono(ADP-ribosyl)ases whether the modification is truly a single ADPr unit or instead a short oligomer of a few ADPr units. For example, while PARP10 was initially published to possess polymerase activity, later work demonstrated only mono(ADP-ribosyl)ase activity for PARP10 (Yu et al., 2005; Kleine et al., 2008). Most work uses the resolution of PARPs as a discreet band at the expected molecular weight as opposed to smears on SDS-PAGE gels as evidence for mono(ADP-ribosyl)ation. However, as the molecular weight of a single ADPr unit is approximately 0.6 kDa, SDS-PAGE gels are insufficient to resolve the addition of a single unit versus an oligomer of a few units

versus modification by a single unit at multiple sites. Methods such as polyacrylamide sequencing gel, thin layer chromatography, HPLC or mass spectrometry analysis of ADPr modifications should instead be used to identify MAR modifications, as has been shown for PARP10 (Kleine et al., 2008; Sharifi et al., 2013).

The distinction between mono or oligo(ADP-ribose) synthesis activity is a subtle but important point as these two modifications would be substrates for different ADPr hydrolytic enzymes and therefore their turnover could be regulated by different mechanisms (Barkauskaite et al., 2013b). Additionally, as evidenced by the specificity of PARP14 binding to mono(ADP-ribosyl)ated protein whereas mH2A is able to bind poly(ADP-ribosyl)ated protein, there could be differences in binding of macro domain containing proteins to mono versus oligo(ADP-ribose) (Forst et al., 2013).

While PARPs are the only enzymes capable of PAR synthesis, other enzyme families also generate MAR modifications. These include the bacterial mARTs, and eukaryotic mono-ADP-ribosyltransferases such as ADP-ribosyltransferases (ARTs) and specific members of the sirtuin family (Tanny et al., 1999; Glowacki et al., 2002; Zhao et al., 2004; Haigis et al., 2006; Hawse and Wolberger, 2009). There are 7 vertebrate ARTs, 4 of which are expressed in humans as glycosylphosphatidylinositol-anchored membrane proteins (Glowacki et al., 2002; Di Girolamo et al., 2005; Masaharu et al., 2008). Eukaryotic ARTs are ecto-enzymes with arginine ADP-ribosyltransferases activity and have a R-S-EXE catalytic motif distinct from mono(ADP-ribosyl)ating PARPs (Glowacki et al., 2002). Eukaryotic mART activity was first reported in 1984 and found to modify some of the same targets as bacterial mART toxins, indicating the importance of MAR modifications in regulation of cell physiology (Moss and Vaughan,

1978; Lee and Iglewski, 1984). Finally, certain sirtuins, homologs of the yeast silencer information regulator proteins, possess mono-ADP-ribosyltransferase activity and are therefore another source of intracellular, physiological ADPr modifications. Humans express 7 sirtuin proteins whose primary activity is the mediation of NAD^+ dependent deacetylation of target proteins, resulting the production *O*-acetyl-ADP-ribose (Feldman et al., 2012). Specific sirtuins have also been shown to catalyze the transfer of ADP-ribose from NAD^+ onto arginine residues of target proteins, acting as ADP-ribosyltransferases (Haigis et al., 2006; Fahie et al., 2009). Whether PARPs with polymerase activity are able to use sirtuin-generated MAR modifications as a substrate for further elongation remains unknown.

Poly(ADP-ribose)

The size and charge distribution of PAR and the potentially complex structure that can result from the 1"-2' and branched 1"'-2" glycosidic linkages result in extensive protein binding, particularly to proteins that contain PAR-binding domains described above (Figure 1) (Alvarez-Gonzalez and Jacobson, 1987). Collectively, these domains are found in more than 400 cellular proteins, suggesting that protein binding to PAR is an important mechanism of PAR function. Therefore, in addition to altering target protein function by covalent modification, PAR can function as a reversible scaffold for non-covalent protein binding (Figure 2). Three examples of the scaffold function for PAR are in DNA damage repair, mitotic spindle assembly and in cytoplasmic stress granules (Ahel et al., 2008; Chang et al., 2009; Leung et al., 2011). In each example, the regulation of both PAR synthesis and hydrolysis are critical for the reversible assembly of protein complexes that respond to environmental and physiological signals.

The first well-studied function for PAR was during the DNA damage response due to the finding that PAR synthesis is stimulated upon DNA damage caused both by DNA strand breaks or chemical mutagenesis (Berger et al., 1979; Benjamin and Gill, 1980a; Benjamin and Gill, 1980b; Sugiyama et al., 1988). Upon DNA damage, PARPs 1 and 2 rapidly bind to DNA lesions, which upregulates their enzymatic activity and results in their automodification (Ikejima et al., 1990; Simonin et al., 1993; Amé et al., 1999; Malanga and Althaus, 2005; Mortusewicz et al., 2007; Langelier et al., 2012). Subsequently, DNA damage repair proteins such as XRCC1 (X-ray repair cross-complementing protein 1), APLF (Aprataxin and PNKP like factor) and DNA ligase III are recruited to sites of lesions through interaction with PARPs and PAR (Caldecott, 2003; El-Khamisy et al., 2003; Leppard et al., 2003; Ahel et al., 2008; Loeffler et al., 2011). Highlighting the importance of this protein recruitment, the base excision repair pathway is highly inefficient in PARP1 deficient cell extracts (Dantzer et al., 2000). In addition to the rapid PAR synthesis that occurs upon DNA damage, hydrolysis is also upregulated due to the recruitment of PARG to sites of DNA damage via an interaction with PAR, resulting in a PAR half life of ~40 sec in the absence of new polymerization (Alvarez-Gonzalez and Althaus, 1989; Mortusewicz et al., 2011). This reversibility is critical to allow for repair proteins to access damaged DNA and mediate the end to DNA damage signaling by PAR once the lesion is repaired.

Mitotic spindle assembly is a critical step of cell division and its misregulation can result in errors in chromosome segregation and cell death (Silkworth and Cimini, 2012). PAR was identified at the mitotic spindle and shown to be required for bipolar spindle organization (Chang et al., 2004). Mitotic spindle-associated PAR is generated by

spindle pole-localized PARP5a (Chang et al., 2005; Ha et al., 2012). PAR-modified PARP5a is sufficient to organize mitotic asters *in vitro* (Chang et al., 2009). Additionally, the spindle pole protein NuMA (nuclear mitotic apparatus protein) is both a PAR modification target for PARP5a and can bind to PAR (Chang et al., 2005; Chang et al., 2009). PARG is also enriched at centrosomes during mitosis, suggesting that regulation of PAR turnover is also important for the resolution of mitosis (Ohashi et al., 2003).

Finally, PAR appears to function as a scaffold in cytoplasmic stress granules, ribonucleoprotein particles enriched in translation initiation factors, poly-A mRNA and RNA binding proteins that form in response to multiple environmental stresses (Kedersha and Anderson, 2009). PAR, 5 PARPs and PARG are enriched in stress granules after stress induction, indicating that regulation of PAR metabolism at stress granules is critical (Leung et al., 2011). Interestingly, 4 of the 5 SG-PARPs also contain PAR binding domains and 2 of the 5 contain RNA binding domains, further supporting the role of PAR as a crosslinking scaffold for protein/PAR and protein/RNA interactions at these structures (Leung et al., 2011). Similar to DNA damage, the reversible nature of the PAR scaffold is critical for regulation of stress granule turnover dynamics. When PAR synthesis and degradation rates are altered by overexpression or knockdown of PARG, stress granule formation or disassembly kinetics are altered respectively (Leung et al., 2011).

Part 2. ADP-ribose synthesis

The mechanism of ADP-ribosylation by PARPs occurs via a transferase mechanism where PARPs mediate the cleavage of the glycosidic bond between the

nicotinamide and ribose moieties of NAD^+, transferring ADPr to the acceptor amino acid and releasing nicotinamide as a by-product (Bürkle, 2005) (Figure 3). Since nicotinamide is a precursor for NAD^+ biosynthesis it can be recycled in the NAD^+ salvage pathway (Revollo et al., 2004). Therefore, one consequence of PARP activity is the stimulation of NAD^+ biosynthesis (Houtkooper et al., 2010) (Figure 3). Additionally, nicotinamide and its analogs can inhibit PARP activity *in vitro* and *in vivo* and have been shown to delay DNA damage repair induced by ionizing radiation (Rankin et al., 1989; Zheng and Olive, 1996). Therefore, nicotinamide production upon stimulation of PARP activity has the potential to serve as both and positive and negative feedback mechanism.

Multiple features of the PARP catalytic domain are important for its enzymatic activity and are further predicted to impact its ability to generate MAR or PAR modifications. These include the primary sequence of the catalytic motif residues as well as structural elements that shape the substrate and acceptor binding pockets.

Specific amino acids requirements for ADP-ribosylation activity

The first PARP catalytic fragment to be crystallized was that of chicken PARP1 and the PARP fold was found to be structurally similar to catalytic domain of bacterial toxins such as diphtheria toxin (*Corynebacterium diphtheria*), exotoxin A (*Pseudomonas aeruginosa*), pertussis toxin (*Bordetella pertussis*) and cholera toxin (*Vibrio cholera*) (Ruf et al., 1996). Each of these toxins have mART activity, also using NAD^+ as a substrate to ADP-ribosylate host proteins (Deng and Barbieri, 2008). Aside from regions that form the NAD^+ binding pocket, there is little sequence similarity between PARP1 and these bacterial toxins (Domenighini et al., 1991). However, the core

catalytic triad motif of H-Y-E identified in *Pseudomonas* exotoxin A and diphtheria toxin is conserved in PARP1 (Domenighini and Rappuoli, 1996). Studies of these bacterial mARTs have demonstrated that the histidine is required for NAD^+ binding while the glutamate is required for catalytic activity (Carroll and Collier, 1984; Papini et al., 1989). Interestingly, while the catalytic glutamate residue is also required for the polymerase activity of PARP1, its mutation does not inhibit mono(ADP-ribosyl)ation activity, indicating a major distinction between PARPs and bacterial mARTs (Marsischky et al., 1995). The majority of the PARP family lacks the catalytic glutamate, instead containing amino acid substitutions of either isoleucine, leucine, valine or tyrosine at this position, and are therefore predicted to generate MAR (Otto et al., 2005; Kleine et al., 2008) (Table 1). Bacterial mARTs primarily target arginine side chains, although additional residues including diphthamide, cysteine and asparagine can also be modified by specific mART toxins (Van Ness et al., 1980; West et al., 1985; Sekine et al., 1989). In contrast, PARPs have been demonstrated to modify either acidic residues or lysines (Moss and Richardson, 1978; Vaughan and Moss, 1978; Kleine et al., 2008; Altmeyer et al., 2009; Messner et al., 2010; Castagnini et al., 2012).

Structural requirements for ADP-ribosylation activity

In addition to the primary sequence of the PARP catalytic triad, secondary structural features of the catalytic domain might also impact PARP activity. In particular, the Donor loop (D-loop) makes contacts with the substrate NAD^+ and is thought to act as a "lid" to help hold NAD^+ within the catalytic pocket. The D-loop has vastly different lengths and rigidities within the PARP family (Wahlberg et al., 2012) (Table 1). For example, PARP1 contains a long D-loop comprised of 12 residues, including 3 proline

residues contributing to the rigidity of the loop. Most of the remaining PARPs contain D-loops of 8 residues, resulting in a narrower pocket for NAD^+ binding. Differences in the D-loop length and structure could affect the dissociation constant of NAD^+ binding amongst the PARPs, contributing to differences in catalytic activity. For example, the difference in the amino acid composition of the PARP3 and PARP1 D-loop is thought to contribute to the inability of PARP3 to generate PAR despite containing a catalytic domain that is highly similar to that of PARP1.

Another structural element of the PARP catalytic domain is the acceptor pocket, which is partly lined by the loop between β sheets 4 and 5, referred to as the acceptor loop. This loop is implicated in the binding of either a protein substrate or an incoming ADP-ribose unit for bacterial mARTs or eukaryotic PARPs respectively (Ruf et al., 1998; Han and Tainer, 2002). The acceptor loop also varies greatly in length amongst the PARP family with DNA-dependent PARPs containing long acceptor loops ranging from 37-42 residues whereas the remaining PARP family members contain shorter acceptor loops of 2-14 residues (Otto et al., 2005) (Table 1). The longer acceptor loops found in the DNA-dependent PARPs are thought to help coordinate binding to an elongating PAR polymer. Therefore, the ability to bind to an incoming ADPr unit on a polymer chain could vary within the PARP family impacting the ability of specific family members to elongate a PAR chain.

Part 3. ADP-ribose hydrolysis

While the generation of ADPr modifications is critical for multiple stress responses and physiological, reversal of these modifications is equally important so that ADPr functions are temporally regulated. Prolonged activation of PARPs, for example

during irreparable DNA damage, has been proposed to result in cell death, highlighting the importance of balancing synthesis and turnover during normal cellular physiology (David et al., 2009). The regulation of ADPr synthesis and turnover ensures that a cell's response to physiological or environmental cues is precisely regulated, similar to the opposing actions of kinases and phosphatases in signal transduction cascades. In fact, the regulation of ADPr synthesis and turnover dynamics is critical as shown by growth inhibition upon heterologous expression of PARPs in yeast, which do not contain endogenous PARP or PARG enzymes, that can be relieved by coexpression of human PARG (Perkins et al., 2001). ADPr modifications can be degraded by the activity of various hydrolytic enzymes. PARG is responsible for hydrolyzing PAR, while 3 additional (ADP-ribosyl)hydrolases hydrolyze MAR (Figure 3). Each of these enzymes is defined by the presence of a structurally characterized ADPr binding macro domain.

PAR hydrolysis activity was first identified in 1971, although, due to difficulties in purification and sensitivity to proteolysis, it took many years to identify full length PARG and its relevant isoforms (Miwa and Sugimura, 1971; Lin et al., 1997; Meyer-Ficca et al., 2004; Bonicalzi et al., 2005). PARG is an essential protein in eukaryotes as PARG -/- mice are embryonic lethal (Koh et al., 2004). Three splice isoforms of PARG exist, of which two are cytoplasmic and one is nuclear (Meyer-Ficca et al., 2004). While two additional smaller isoforms have also been reported, one of which localizes to the mitochondrial matrix, they have been shown to be enzymatically inactive (Meyer et al., 2007; Niere et al., 2012). There are conflicting reports on the activity of PARG on the proximal protein-ADPr linkage. While the majority of reports demonstrate that PARG is inactive on the proximal ADPr unit, leaving a mono(ADP-ribosyl)ated protein, others

claim that PARG is able to remove the proximal residue from acidic linkages (Kleine et al., 2008; Slade et al., 2011; Barkauskaite et al., 2013a).

The catalytic signature sequence for PARG activity was identified in bovine PARG and used to identify isoforms over a range of eukaryotes (Patel et al., 2005). Additionally, divergent PARG homologs that contain the signature catalytic motif have been identified in many fungi and bacteria (Patel et al., 2005; Slade et al., 2011). Multiple PARG structures from protozoan, bacterial and mammalian sources have been solved confirming that PARG recognizes poly(ADP-ribosyl)ated substrates via its ADPr binding macro domain fold (Slade et al., 2011; Dunstan et al., 2012; Kim et al., 2012; Tucker et al., 2012). However, unlike other macro domain containing proteins, the PARG macro domain fold contains an additional loop that consists of the PARG catalytic motif, explaining the PAR hydrolysis activity for the PARG macro domain (Slade et al., 2011).

Interestingly, structural studies of a mammalian PARG have shown that while the canonical macro domain fold resembles that of a bacterial homolog, indicative of a conserved catalytic mechanism, there are additional unique structural elements in the substrate binding site of mammalian PARG (Kim et al., 2012). PARG purified from mammalian sources exhibits both exo- and endoglycosidic activity, although exoglycosidic hydrolysis resulting in ADPr release appears to be the dominant activity (Miwa et al., 1974; Hatakeyama et al., 1986; Braun and Panzeter..., 1994; Brochu et al., 1994; Barkauskaite et al., 2013a). In contrast, PARG from the bacteria *Thermospora curvata* is proposed to have only exoglycosidic activity (Slade et al., 2011). The structural differences of the substrate binding pocket have been postulated to account

for differences in endo versus exo-glycosidic activity of mammalian versus bacterial PARGs (Kim et al., 2012; Tucker et al., 2012).

Recently three enzymes were discovered that have mono(ADP-ribose) hydrolase activity. MacroD1, MacroD2 and TARG each remove the terminal ADPr attached to target proteins (Jankevicius et al., 2013; Rosenthal et al., 2013; Sharifi et al., 2013) (Figure 3). TARG deficiency is linked to a hereditary neurodegenerative disorder, further highlighting the physiological importance of ADPr turnover (Sharifi et al., 2013). MacroD1 and D2 where first identified as *O*-acetyl-ADP-ribose deacetylases, suggesting that these enzymes can hydrolyze modifications from both PARP and sirtuin activity (Chen et al., 2011). MacroD1 localizes to the mitochondria and MacroD2 localizes throughout the nucleus and cytoplasm, therefore, these enzymes are found in all cellular compartments where MAR and *O*-acetyl-ADP-ribose are generated (Neuvonen and Ahola, 2009). TARG is enriched in the nucleus and, similar to PARG, localizes to sites of microirradiation induced-DNA damage (Sharifi et al., 2013). Each of these enzymes is thought to remove MAR from acidic residues, although this has only been explicitly shown for MacroD2. In addition to hydrolyzing mono(ADP-ribosyl)ated substrate, TARG has also been shown to release PAR chains from protein, resulting in the generation of free polymer since TARG cannot hydrolyze the ribose-ribose glycosidic bonds (Sharifi et al., 2013) (Figure 3).

Finally, a distinct class of enzymes called ADP-ribosylhydrolases (ARHs) also has been demonstrated to hydrolyze ADPr modifications. The ARH family consists of 3 enzymes that are structurally unrelated to PARG and mono(ADP-ribosyl) hydrolases (Mueller-Dieckmann et al., 2006). ARH1 is demonstrated to specifically hydrolyze

arginine-ADPr linkages (Moss et al., 1992). In contrast, ARH3 is unable to cleave arginine-ADPr linkages but can hydrolyze *O*-acetyl-ADP-ribose, a product of sirtuin deacetylase activity (Ono et al., 2006). ARH3 has also been shown to be able to hydrolyze PAR *in vitro*, although with much lower activity compared to PARG (Oka et al., 2006). However, it is unclear if the PAR hydrolyzing activity by ARH3 occurs *in vivo*. Although ARH3 was shown to degrade mitochondrial matrix localized PAR, PAR accumulation was dependent on the targeting of the PARP1 catalytic domain to the mitochondria and therefore is not representative of physiological conditions (Niere et al., 2012).

The generation of free ADPr as a result of hydrolysis of PAR and MAR modifications has proposed functions as a signaling molecule through interactions with macro domain containing proteins, although this has not been mechanistically demonstrated (Karras et al., 2005). Importantly, free ADPr is a reducing sugar that can result in non-enzymatic protein glycation (Cervantes-Laurean et al., 1993). Non enzymatic glycation of histones by ADPr was demonstrated *in vitro* through formation of a ketoamine adduct onto amino groups (Cervantes-Laurean et al., 1996). Due to the inherent instability of the chemical linkage, the ketoamine adducts can be precursors to complex protein modifications and could possibly result in a functional decline of the protein (Verzijl et al., 2002). To protect cells from deleterious advanced glycation end products, free ADPr levels are controlled by ADPr pyrophosphatases, which hydrolyze ADPr to AMP and ribose 5-phosphate (Ribeiro et al., 1995; Fernández et al., 1996; Ribeiro et al., 2001) (Figure 3).

Part 4. The PARP Family

While the PARP family is defined by the presence of the PARP catalytic domain, individual PARPs contain many additional protein domains that can mediate interactions with nucleic acids, ADPr modifications and other proteins (Amé et al., 2004) (Figure 4, Table 2). These domains play important roles regulating PARP catalytic activity in response to physiological and environmental signals as well as mediating interactions with specific substrates and targeting PARPs to specific locations (Altmeyer et al., 2009; Loeffler et al., 2011; Jwa and Chang, 2012; Langelier et al., 2012). Based on their protein domain composition, PARPs are further grouped into 5 subfamilies: DNA Dependent, Tankyrase, CCCH-Zn Finger, Macro and Unclassified (Table 1).

The DNA dependent PARPs 1, 2 and 3 each contain distinct DNA-binding domains. PARP1 contains 3 Zinc finger motifs while the DNA-binding domains of PARPs 2 and 3 lack sequence homology to known DNA-binding motifs. The 54 amino acid N-terminal domain of PARP3 that is capable of binding DNA was also shown to be sufficient to target PARP3 to the centrosome (Augustin et al., 2003). In addition, PARP1 contains a BRCT (BRCA1 C terminus) domain that is critical for interactions with binding partners (Loeffler et al., 2011). The DNA dependent PARPs also contain a WGR (Tryptophan-Glycine-Arginine rich) domain of unknown function, although it has been shown to be required for enzymatic activity (Altmeyer et al., 2009).

Both tankyrases (PARPs 5a and 5b) contain a 24 ankyrin repeat domain that is required for binding to multiple target proteins as well as a SAM (sterile alpha motif) domain also predicted to be a protein-protein interaction module (Smith et al., 1998; Huang et al., 2009).

PARPs 7, 12 and 13 each contain at least one CCCH Zinc Finger motif, first identified to bind to AU-rich elements of mRNA in the RNA binding protein tristetraprolin and postulated to be RNA binding motifs (Lai et al., 1999). In addition, the CCCH Zinc finger PARPs each contain a PAR-binding WWE domain (Wang et al., 2012), giving them the potential to integrate PAR signaling in the regulation of RNA.

Macro PARPs 9, 14 and 15 each contain multiple ADPr binding macro domains (Karras et al., 2005). PARP14 additionally contains a PAR binding WWE domain.

Finally, within the unclassified PARPs, PARP4 contains a BRCT domain, VWFA (von Willebrand factor A) domain and a VIT (vault inter alpha trypsin) domain, PARP10 contains both RNA recognition and ubiquitin interaction motifs, PARP11 contains a WWE domain and PARP16 contains a transmembrane domain. PARPs 6 and 8 do not contain any defined protein domains, however the N terminal portions of PARPs 6 and 8 share 69% sequence identity.

PARP functions are largely defined by their subfamily categorization. While some PARPs within subfamilies have overlapping roles, it is becoming increasingly clear that there are critical functional differences between PARPs in the same subfamily with regards to localization patterns and enzymatic activity. This leads to a new functional categorization of the PARPs that takes into account subcellular localizations as well as activity (Figure 4).

Nuclear PAR-generating PARPs

Because PAR was originally identified in the nucleus, nuclear PAR and PARP functions are the most well studied. These functions include maintenance of genome integrity and transcriptional regulation and are carried out by PARPs 1 and 2. While

both generate branched PAR modifications, PARP1 is highly abundant (0.5-2X10^6 copies/cell) and generates the majority of nuclear PAR (Alvarez-Gonzalez and Jacobson, 1987; Yamanaka et al., 1988; Amé et al., 1999). Although PARP1 and 2 display some functional redundancy as evidenced by single knockout mice for each being fertile and viable in normal growth conditions, PARP1 knockout mice are more sensitive to exposure to specific types of genotoxic stress (Wang et al., 1995; de Murcia et al., 1997). PARP1 and PARP2 double knockout mice display embryonic lethality, indicating the requirement of nuclear poly(ADP-ribosylation) for development (Ménissier de Murcia et al., 2003) .

PARP1 and 2 are best studied in DNA damage repair (reviewed in Malanga and Althaus, 2005; De Vos et al., 2012). PARP1 binds to multiple DNA damage structures such as single strand breaks, double strand breaks and overhangs, as well as recombination intermediates (Lonskaya, 2005; Lilyestrom et al., 2010). In contrast, PARP2 was shown to bind to double strand breaks with low affinity although it bound to various other structures including overhangs and short gaps (Kutuzov et al., 2013). This difference in binding affinity is likely a result of distinct DNA binding domains: PARP1 contains 3 zinc fingers with zinc finger 2 having high affinity for double strand breaks whereas the DNA binding domain of PARP2 has an unknown structure and does not have sequence homology with known DNA binding motifs (Langelier et al., 2012; Kutuzov et al., 2013). This likely explains the sensitivity of PARP1 knockout mice to DNA damaging agents such as γ-irradiation and the differences in recruitment kinetics of PARP1 and PARP2 to DNA damage induced by microirradiation, both of which result in double strand breaks (de Murcia et al., 1997; Mortusewicz et al., 2007). Similar to

functions in recognizing damaged DNA structures, PARP1 and 2 are also required to resolve replication forks stalled by hydroxyurea treatment or topoisomerase I inhibition via binding to ssDNA structures or single strand breaks respectively (Bryant et al., 2009; Ray Chaudhuri et al., 2012).

In addition to their role in maintaining genome integrity, PARPs 1 and 2 have important functions in transcriptional regulation (reviewed in Kraus and Lis, 2003; Wacker et al., 2007; Kraus, 2008; Luo and Kraus, 2012; Szántó et al., 2012). PARP1 and 2 can regulate transcription both through direct interactions with transcription factors and through chromatin remodeling. PARP1 has been shown to interact with many transcription factors at gene promoters and its role as either a transcriptional enhancer or repressor as well as the requirement for enzymatic activity for function is context specific (Kraus and Lis, 2003). Knockdown of PARP1 results in the misregulation of approximately 1200 genes and PARP1 binds at promoters of positively and negatively regulated target genes, suggesting a direct function in transcriptional regulation (Frizzell et al., 2009). While specific mechanisms for transcriptional regulation by PARP2 are less well known, it has been shown to regulate multiple transcription factors (summarized in Szántó et al., 2012). For example, PARP2 -\- mice have decreased expression PPARγ/RXR targets and PARP2 was demonstrated to bind promoters of PPARγ/RXR target genes, suggesting a transcriptional co-activator function for PARP2 (Bai et al., 2007).

Transcriptional regulation via chromatin remodeling by PARP1 is exemplified in the heat shock response. The function of PARP1 during heat shock-specific transcription was first demonstrated in *Drosophila* salivary gland chromosomes where

PARP1 was required for the formation of PAR-enriched chromosomal puffs and induction of *Hsp70* transcription (Tulin and Spradling, 2003). This was further shown in mammalian cells where PARP1 and PAR were required for nucleosome loss at the *Hsp70* locus and full induction of *Hsp70* transcription with PARP1 activation dependent on the recruitment of a histone acetylase to the *Hsp70* locus (Petesch and Lis, 2008, 2012). PARP2 can also affect transcription through chromatin modification and in one example was shown to recruit histone deacetylases and a histone methyltransferase to the promoter of cell cycle-related genes in a non-enzymatic manner, resulting in transcriptional repression (Liang et al., 2013).

PARPs 1 and 2 have many additional nuclear functions including heterochromatin establishment (Dantzer and Santoro, 2013), maintenance of telomere integrity (Dantzer et al., 2004) and repression of polyadenylation during heat shock (Di Giammartino et al., 2013). During mitosis, PARP2 is enriched at centromeres and has been shown to be required for faithful meiosis I during spermatogenesis (Dantzer et al., 2006). In addition, while PARP1 and 2 are primarily enriched in the nucleus, they have also been detected in centrosomes and PARP1 depletion was shown to result in centrosome hyperamplification, suggesting a role in centrosome regulation (Kanai et al., 2003; Vyas et al., 2013)

Cytoplasmic PAR-generating PARPs

PARPs 5a and 5b are the only cytoplasmic PARPs that generate PAR. They have highly conserved domain architecture and are termed tankyrases (TNKS1 and TNKS2 respectively) due to the presence of multiple copies of the ankyrin domain and because PARP5a was initially shown to interact with TRF1 (telomeric repeat binding

factor 1) (Smith et al., 1998). Both tankyrases generate linear PAR modifications (Cook et al., 2002; Rippmann et al., 2002). Similar to PARPs 1 and 2, PARP5a and 5b single knockout mice are viable whereas double knockout mice are embryonic lethal, indicating functional redundancy and requirement of cytoplasmic PAR modifications in development (Hsiao et al., 2006; Chiang et al., 2008).

Although both PARP5a and 5b were shown to exhibit primarily cytoplasmic, perinuclear localization patterns, they were first identified through interactions with TRF1 (Smith et al., 1998; Smith and de Lange, 1999; Kaminker et al., 2001; Cook et al., 2002; Vyas et al., 2013). Importantly, while PARP5a was shown to localize to telomeres, this localization was dependent on an interaction with TRF1, as PARP5a does not contain a nuclear localization sequence and exogenous PARP5a does not exhibit a telomeric localization pattern unless it is coexpressed with TRF1 (Smith and de Lange, 1999). It is possible that a small percent of PARP5a and 5b interact with telomeres during cell division when the cytoplasm and nucleoplasm intermix, explaining telomere localization during interphase (Smith et al., 1998; Smith and de Lange, 1999). Although both have been implicated in regulation of telomere length via modification and inhibition of the DNA binding ability of TRF1, these conclusions were drawn from experiments in which PARP5a and 5b containing exogenous nuclear localization sequences were overexpressed and therefore are not representative physiological conditions (Smith et al., 1998; Smith and de Lange, 2000; Cook et al., 2002; Hsiao et al., 2006). Indeed, PARP5a and 5b single knockout mice do not display any defects in telomere length, maintenance or capping (Hsiao et al., 2006; Chiang et al., 2008).

PARP5a was also shown to localize to the nuclear envelope, centrosome and mitotic spindle pole (Smith and de Lange, 1999; Chang et al., 2005). Consistent with its localization to the mitotic spindle, PARP5a is required for proper cell division as its knockdown causes misaligned chromosomes, disordered spindles and supernumerary spindle poles, ultimately resulting in a decrease in cell viability (Chang et al., 2005; Vyas et al., 2013). While PARP5b also localizes to the mitotic spindle, knockdown does not result in similar defects in spindle structure (Vyas et al., 2013). However, since PARP5a -/- mice are viable, PARP5b may be able to compensate for the critical function of PARP5a in cell division in animals (Chiang et al., 2008).

One functional outcome of PARP5a and PARP5b modification of acceptor proteins is their subsequent targeting for ubiquitin-proteasome mediated degradation. For example, both PARP5a and 5b were found to interact and poly(ADP-ribosyl)ate Axin, a member of a multiprotein complex that causes degradation of the Wnt-regulated transcription factor β-catenin, targeting it for ubiquitin-proteasome mediated degradation (Huang et al., 2009). Degradation of PARylated Axin is mediated by a WWE-domain containing E3 ubiquitin ligase, indicating that recognition of PAR is important for this function (Zhang et al., 2011). PARylation of TRF1 by PARP5a as well as PAR-automodification of PARP5a also results in subsequent ubiquitin-proteasome mediated degradation (Chang et al., 2003; Yeh et al., 2006).

While the structures of PARP5a and 5b are highly conserved, only PARP5a has been implicated in additional cytoplasmic functions. PARP5a is enriched in stress granules upon exposure to multiple environmental stresses (Leung et al., 2011). Additionally, PARP5a localizes to GLUT4 positive storage vesicles where it is in

implicated in insulin stimulated exocytosis of GLUT4 vesicles via an interaction with IRAP (insulin-responsive peptidase) (Chi and Lodish, 2000; Yeh et al., 2007). These cellular functions unique to PARP5a could potentially be due to an additional N-terminal HPS (histidine-proline-serine) domain not found in PARP5b.

Cytoplasmic and Nuclear MAR-generating PARPs

PARPs 3, 7, 10 and 14 are found in both the cytoplasm and nucleus and have unique functions in each compartment. The factors regulating the subcellular localization of these proteins are unknown. While PARP10 actively shuttles between the two compartments, it is unclear whether the nuclear and cytoplasmic fractions of PARPs 3, 7 and 14 represent two distinct, separately regulated pools or if there is crosstalk between the compartments.

PARP3 differs from its subfamily members in that it does not have polymerase activity (Loseva et al., 2010). Similar to PARPs1 and 2, PARP3 is also implicated in DNA damage repair and transcriptional regulation within the nucleus (Rouleau et al., 2011; Rulten et al., 2011). There are mixed reports on the DNA dependence of PARP3 activity, with one claiming that PARP3 is not activated by DNA whereas another identified an increase in activity upon addition of DNA with double strand breaks (Loseva et al., 2010; Rulten et al., 2011). Consistent with double strand break mediated activation, knockdown of PARP3 delays DNA damage repair following γ-irradiation (Rulten et al., 2011).

PARP3 also functions in transcriptional regulation, binding downstream of the transcription start sites of various developmental genes (Rouleau et al., 2011). PARP3 deficiency impaired expression of cell fate specifiers *sox9a* and *dlx3b/dlx4b*, resulting in

defects in early zebrafish development, although the mechanism of transcriptional regulation by PARP3 is unknown (Rouleau et al., 2011). PARP3 is enriched at polycomb group (PcG) bodies, protein complexes that mediate epigenetic transcriptional repression via histone modifications and are critical regulators of embryogenesis and development and PcG components co-immunoprecipitate with PARP3 (Rouleau et al., 2007). Therefore, PARP3 may effect transcription through its interactions with PcGs as opposed to acting a transcriptional co-factor similar to PARPs 1 and 2.

PARP3 also localizes to the cytoplasm as evidenced by immunostaining and cell fractionation (Rouleau et al., 2011; Vyas et al., 2013). Although cytoplasmic functions are largely unknown, PARP3 has been identified at centrosomes and was implicated in cell cycle progression (Augustin et al., 2003; Vyas et al., 2013).

PARP7 was first identified as tiPARP since it is upregulated by the environmental toxin 2,3,7,8-tetracholordibenzo-p-dioxin (TCDD) in hepatocyte cell lines in a manner dependent on aryl hydrocarbon receptor (AHR), a ligand-activated transcription factor (Ma et al., 2001; Ma, 2002). PARP7 overexpression mimics the cytotoxic effects of TCDD, including suppression of gluconeogenesis, suggesting that it is a key mediator of TCDD toxicity (Diani-Moore et al., 2010). Further work demonstrated the PARP7 dependent ADP-ribosylation of PEPCK (phosphoenolpyruvate carboxykinase), a key regulator of gluconeogenesis (Diani-Moore et al., 2013). PARP7 is also enriched at nuclear foci, colocalizing with AHR in the nucleus and inhibiting the expression of AHR target genes in a negative feedback loop (MacPherson et al., 2013). During mitosis,

PARP7 knockdown results in a significant enrichment of cells in pre-metaphase, suggesting that it is involved in the regulation of mitotic progression (Vyas et al., 2013).

While PARP10 is primarily cytoplasmic, it was initially identified as a c-myc interacting protein that was able to inhibit transformation of rat embryo fibroblasts when coexpressed with c-Myc/Ha-Ras independent of catalytic activity, suggesting that a nuclear PARP10 pool also exists (Yu et al., 2005; Vyas et al., 2013). PARP10 accumulation in the nucleus has been observed upon inhibition of export and mutation of its nuclear export signal, suggesting that while PARP10 is normally efficiently exported resulting in its predominant cytoplasmic localization, it actively shuttles between the two compartments (Yu et al., 2005; Kleine et al., 2012). PARP10 overexpression interferes with cell viability and induce apoptosis, with the pro-apoptotic effect being dependent both the RRM and PARP10 catalytic activity (Chou et al., 2006; Herzog et al., 2013). Recently, PARP10 was also shown to regulate NF-κB signaling in a manner dependent on both poly-ubiquitin binding and catalytic activity, with exogenous PARP10 expression resulting in the inhibition of downstream target expression in response to interleukin-1β (IL-1β) and tumour necrosis factor-α (TNFα) (Verheugd et al., 2013). Exogenous PARP10 expression altered the poly-ubiquitination state of several signaling intermediates, a modification required to transduce IL-1β and TNFα signals to the nucleus (Verheugd et al., 2013). In the cytoplasm, PARP10 is enriched in poly-ubiquitin containing foci that can interact with p62-positive autophagosomes (Kleine et al., 2012). Since induction of NF-κB signaling can regulate autophagy, PARP10 may represent a critical link between these two pathways (Trocoli and Djavaheri-Mergny, 2011).

PARP14 has been implicated in both nuclear and cytoplasmic processes. In the nucleus, PARP14 regulates interleukin-4 signaling by acting as a transcriptional co-activator of the transcription factor Stat6 in a mechanism that is dependent on catalytic activity (Goenka and Boothby, 2006; Goenka et al., 2007). PARP14 -/- mice are deficient in IL-4 mediated proliferation and survival of B cells and have delayed Myc-induced B cell lymphomagenesis, highlighting the role of PARP14 in B cell lineages (Cho et al., 2009; Cho et al., 2011). Recently, PARP14 has also been implicated in mediating JNK (Jun N-terminal kinase) pro-survival signaling in multiple myeloma cells and was found to be highly expressed in neoplastic myeloma plasma cells compared to normal plasma cells (Barbarulo et al., 2013). PARP14 is also enriched at the plasma membrane in focal adhesion structures, with PARP14 knockdown resulting in defects in cell migration suggestive of a misregulation of focal adhesion dynamics (Vyas et al., 2013). While the mechanism of PARP14 subcellular localization regulation is unknown, recent work demonstrating that PARP14 can bind to mono(ADP-ribosyl)ated protein substrates via its macro domains raises the possibility that its localization can be regulated through binding interactions (Forst et al., 2013).

Cytoplasmic MAR-generating PARPs

PARPs 4, 6, 8, 11, 12, 15 and 16 are primarily cytoplasmic generators of MAR. Interestingly, most of these PARPs do not belong to a specific subfamily and instead contain domains not found in other PARPs or lack identifiable protein domains. Additionally, many have distinct sub-cytoplasmic localizations, suggesting that they are regulated by independent mechanisms.

PARP4 was originally identified as vPARP due to its presence in vault particles,

cytoplasmic ribonucleoprotein complexes comprised mainly of major vault protein (MVP) (Kickhoefer et al., 1999). Vault particles are highly conserved structures that have been postulated to mediate multidrug resistance and to regulate intracellular signal transduction and immune responses (Berger et al., 2009). However, it is unclear mechanistically how vault particles mediate these potential functions and what role PARP4 plays in the structure or function of vault particles (Berger et al., 2009). PARP4 likely does not contribute to vault particle structure as PARP4 -/- mice contain structurally intact vault particles (Liu et al., 2004). Because vault particles also contain telomerase associated protein (TEP1) and PARP4 was found to associate with TEP1 in a yeast two hybrid, the effect on telomere length was also analyzed in PARP4 -/- mice. However, PARP4 was dispensable for the maintenance of telomere length in vivo (Liu et al., 2004). Therefore, cellular functions for PARP4 are still largely unknown.

PARP16 was recently demonstrated to be an endoplasmic reticulum (ER) C-tail anchored transmembrane protein, with its PARP catalytic domain facing the cytoplasm (Di Paola et al., 2012; Jwa and Chang, 2012). Modification targets for PARP16 include karyopherin-β1, PERK and IRE1α (Di Paola et al., 2012; Jwa and Chang, 2012). PARP16 mediated ADP-ribosylation of PERK and IRE1α was shown to be required for their activation and induction of the unfolded protein response (Jwa and Chang, 2012).

The remaining cytoplasmic, MAR generating PARPs have either unknown or poorly understood cellular functions. PARPs 6 and 8 have no identifiable protein domains outside of the PARP catalytic domain, although they share portions of high sequence homology. While knockdown of PARP8 results in nuclear morphology defects, similar defects were not found in PARP6 knockdown cells (Vyas et al., 2013).

Interestingly, PARP8 contains a N-terminal region and insertion within the regions of homology not found in PARP6, potentially contributing to its unique function in nuclear envelope integrity (Vyas et al., 2013). PARP12 is enriched in the Golgi, although its function at this location is unclear (Vyas et al., 2013). Overexpression of PARP12 disrupts Golgi structure, causing a dispersal of the Golgi and increase in Golgi area, suggesting that PARP12 misregulation can result in structural defects in the Golgi (Vyas et al., 2013). In addition, PARP12 and PARP15 are enriched in stress granules upon cytoplasmic stress, potentially mediated by the RNA binding CCCH-Zn Finger domain and PAR binding WWE domain of PARP12 and the ADPr binding macro domain of PARP15 (Leung et al., 2011). The protein domain structure of PARP11 resembles that of the CCCH-Zn Finger PARPs with regards to the presence of a WWE domain immediately preceding the catalytic domain. However, PARP11 does not have any known cellular functions.

Inactive PARPs

Interestingly, 2 PARPs that lack catalytic activity have critical cellular functions. PARP9 was originally identified as BAL1 (B-aggressive lymphoma 1) because it is expressed at higher levels in fatal high-risk diffuse large B-cell lymphomas when compared to cured, low risk tumors (Aguiar et al., 2000). Additionally, PARP9 overexpression promotes migration of B-cell lymphomas, suggesting a function in regulation of cell motility (Aguiar et al., 2000). Our findings that PARP9 knockdown results in defects in actin cytoskeleton regulation further support functions for PARP9 in the cell migration (Vyas et al., 2013). Previous work has demonstrated a nucleocytoplasmic shuttling for PARP9 mediated by a PARP9 binding partner BBAP (B

cell aggressive and BAL1 binding partner) and interferon-γ dependent induction of PARP9 expression (Juszczynski et al., 2006).

PARP13 was first identified as the antiviral factor ZAP (zinc finger antiviral protein) due to its ability to bind and cause the degradation of the moloney murine leukemia retroviral RNA via recruitment of the exosome, an RNA degrading multiprotein complex (Gao et al., 2002; Guo et al., 2004; Guo et al., 2007). Subsequently, PARP13 expression was also shown to inhibit the replication of the multiple Alphaviruses, which are also RNA viruses, but does not produce a general antiviral state as other RNA and DNA viruses retain the ability to replicate in PARP13 expressing cells, suggesting specificity in the recognition of viral RNA by PARP13 (Bick et al., 2003). Additionally, PARP13 is enriched in cytoplasmic stress granules in response to various environmental stress signals and interacts with the Ago2, a critical component of the RNAi pathway, resulting in the downregulation of Ago2-mediated microRNA silencing activity (Leung et al., 2011; Seo et al., 2013).

Conclusion

Recent discoveries in the PARP field have expanded the cellular functions for PARPs and ADPr modifications and shattered previous perceptions of PARPs and PAR being an exclusively nuclear phenomenon. The prevalence of PARPs with mono(ADP-ribosyl)ase activity also demonstrates the importance of these once unrealized PARP modifications. Further understanding of mechanisms of regulation of PARP activity as well as identification of PARP specific protein targets will be critical for furthering our

understanding of how this protein family carries out its numerous, diverse cellular functions.

Mono(ADP-ribosyl)ation is particularly interesting because in addition to causing an alteration in target protein function as a singular modification, MAR could be an intermediate for PAR synthesis onto a target protein, with PARPs cooperatively functioning to generate polymer. In this hypothesis, certain PARPs may function to prime targets for modification, which are then elongated by PARPs with polymerase activity (Figure 3). While recombinant PARP1 purifications that lack any other PARP enzymes are capable of producing polymer *in vitro,* priming may represent a mechanism of regulation of polymer synthesis, potentially effecting the kinetics of polymer synthesis *in vivo* (Langelier et al., 2011).

The presence of PARPs with each of the predicted activities in both the cytoplasm and nucleus and the identification of cellular complexes containing PARPs with both MAR and PAR synthesis activities suggests that this type of cooperative PARP function could occur (Kleine et al., 2008; Vyas et al., 2013). For example, PARP3, which exhibits MAR activity, has been shown to heterodimerize with PARP1, stimulating PARP1 activity in the absence of DNA damage (Loseva et al., 2010). While the mechanism of PARP1 activation by PARP3 is unclear, one possibility is that PARP3 could modify PARP1 in trans, providing a platform for polymer elongation by PARP1. Another example is found in cytoplasmic stress granules, which contain a single PARP capable of PAR synthesis, PARP5a, and 3 additional MAR generating PARPs which may provide initiating modifications that are subsequently converted to PAR by PARP5a activity (Leung et al., 2011). It will be critical to further investigate the ability of

poly(ADP-ribosyl)ating PARPs to elongate MAR modifications in order to determine if this type of cooperative function can occur.

Conversely, mono(ADP-ribosyl)ated proteins may be protected from further elongation by binding of macro domain containing proteins, resulting in the capping of the ADPr modification. For example, PARP14 was shown to bind specifically to mono(ADP-ribosyl)ated PARP10 but not poly(ADP-ribosyl)ated PARP1 via its macro domain (Forst et al., 2013). Capped MAR modifications could be poised for elongation to polymer upon physiological or environmental signals, allowing a cell to rapidly respond to various stimuli. In this case, MAR modifications could function similarly to paused RNA polymerase II at the 5' ends of genes and Ago2-miRNA silenced mRNA transcripts, which are poised for transcription and translation respectively. Since the elongation versus capping of a MAR modification would lead to distinct functional outcomes, MAR modifications are particularly interesting as they offer the cell a versatile platform for intricate regulation of protein-protein interactions.

Figures and Tables

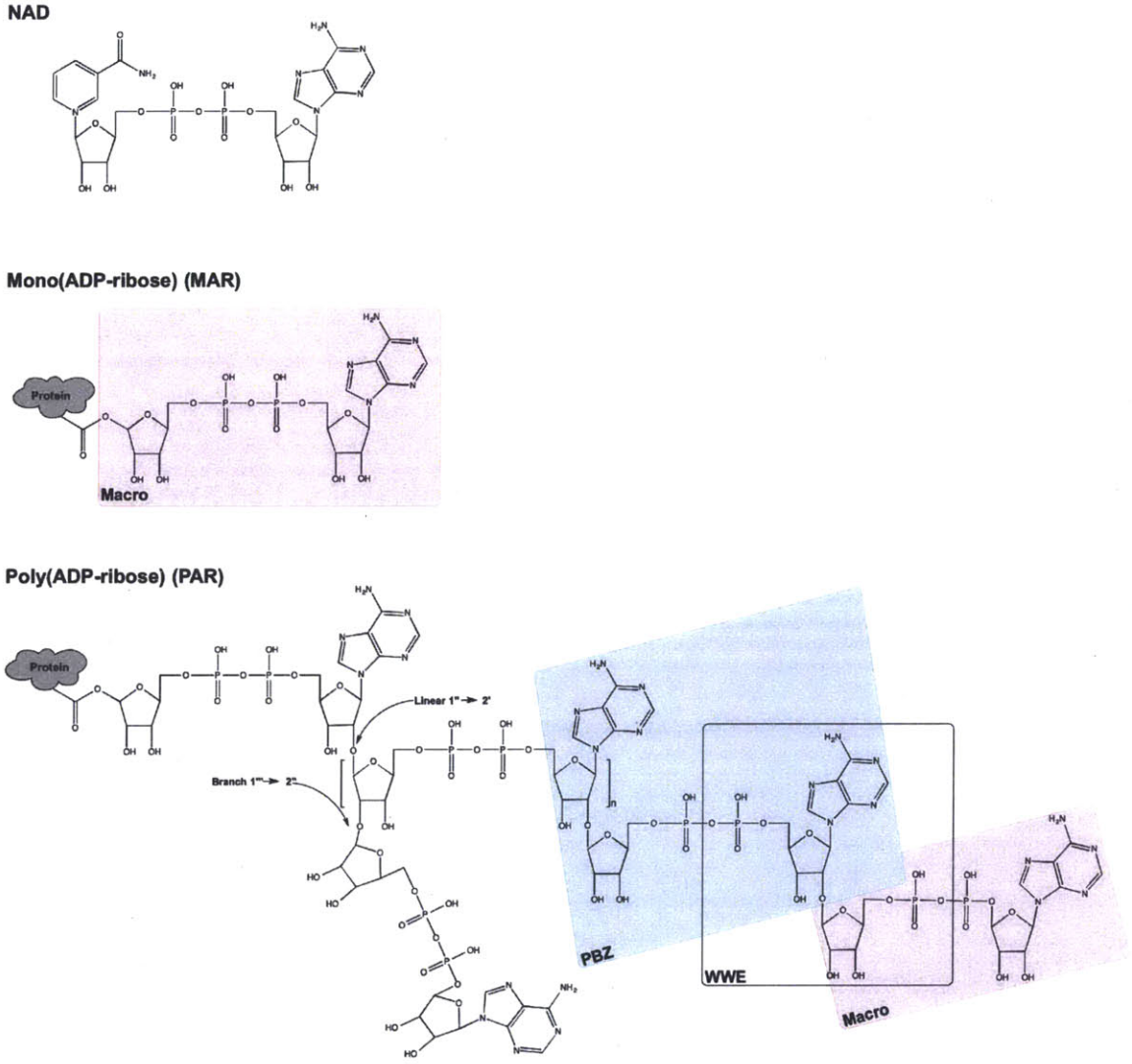

Figure 1. Structure of ADP-ribose modifications
The structures of NAD^+, the substrate for ADPr modifications, and two types of ADPr modifications, mono(ADP-ribose) (MAR) and poly(ADP-ribose) (PAR) are depicted with ester linkages to the acceptor protein. ADPr units in PAR chains linked by glycosidic bonds between and can either be linear (1"-2' linkage) or branched (1"'-2" linkage). Additionally, regions of MAR and PAR detected by different ADPr binding protein domains are outlined.

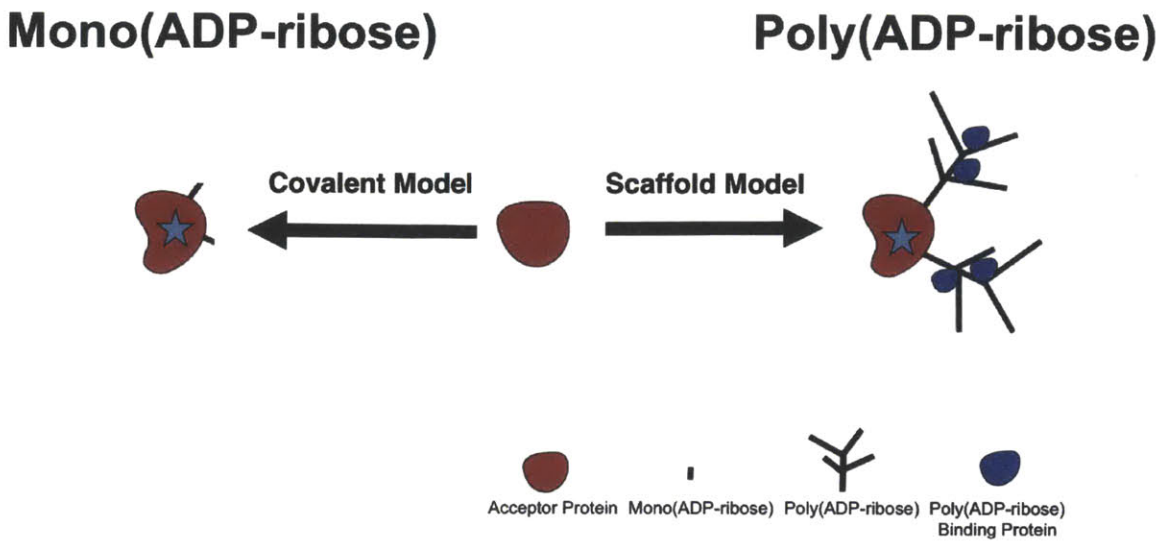

Figure 2. Mechanisms of function of ADP-ribose posttranslational modifications Mono(ADP-ribose) can alter target protein activity through covalent modification, similar to traditional posttranslational modifications such as phosphorylation. Poly(ADP-ribose), in addition to alter target protein activity via covalent modification, can bind to proteins non-covalently and function as a scaffold for the assembly of multiprotein complexes.

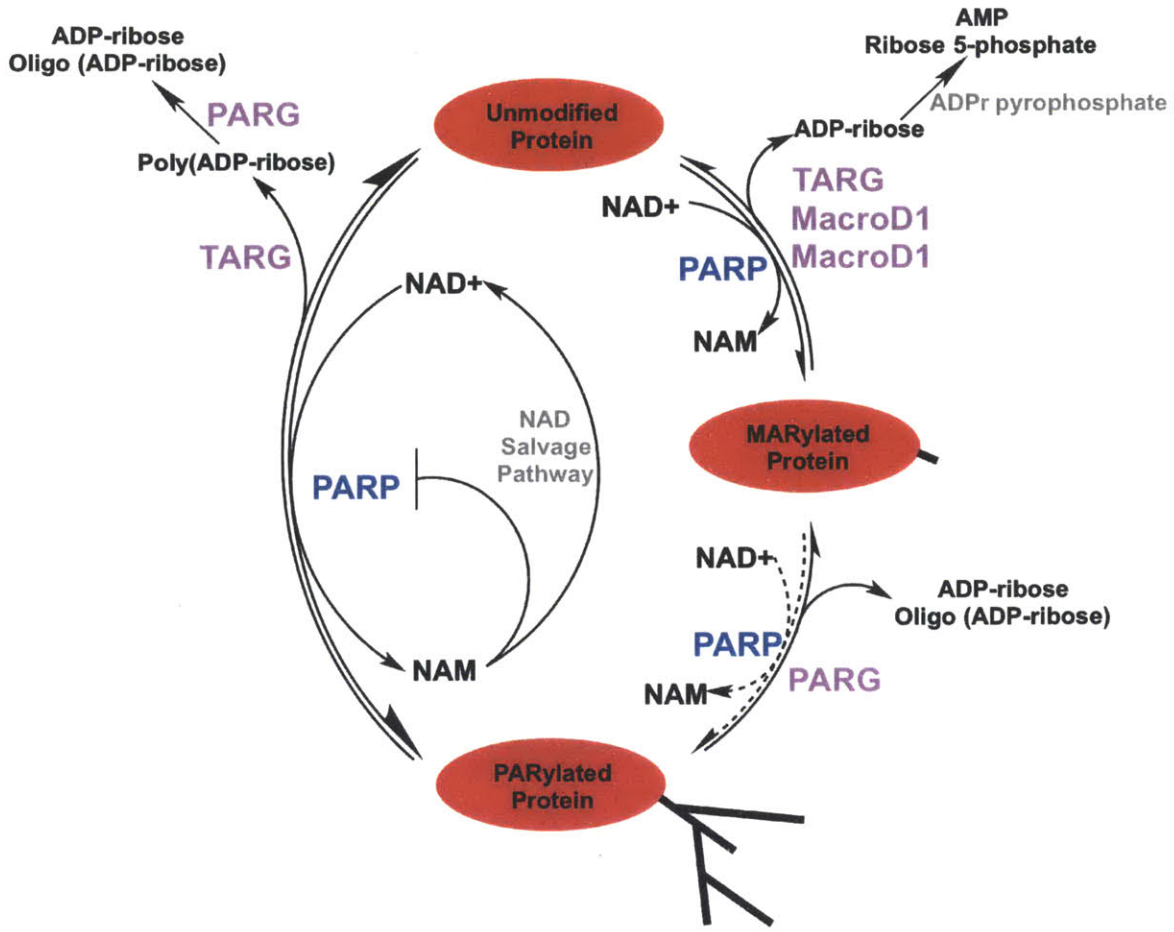

Figure 3. Metabolism of ADP-ribose modifications
Poly(ADP-ribose) polymerases (PARPs) use NAD^+ as a substrate to modify target proteins with mono or poly(ADP-ribose), releasing nicotinamide (NAM) as a by-product. NAM can inhibit PARP activity and is recycled through the NAD^+ salvage pathway. Whether mono(ADP-ribosyl)ation of a protein serves as a primer for further elongation is unclear (dashed line). Exo or endoglycosidic poly(ADP-ribose) glycohydrolase (PARG) activity results in the hydrolysis of poly(ADP-ribose), releasing ADPr or oligo(ADP-ribose) respectively. Mono(ADP-ribose) hydrolases MacroD1, MacroD2 and terminal (ADP-ribose) glycohydrolase (TARG) hydrolyze proximal protein-ADPr linkages. TARG is also able to hydrolyze the proximal ADPr-protein linkage of polymer chains, releasing free poly(ADP-ribose) that can be further hydrolyzed to oligo or mono(ADP-ribose) by PARG activity. Free ADPr released by PARG and mono(ADP-ribose) hydrolase activity can be hydrolyzed to AMP and ribose 5-phosphate by ADPr pyrophosphatases.

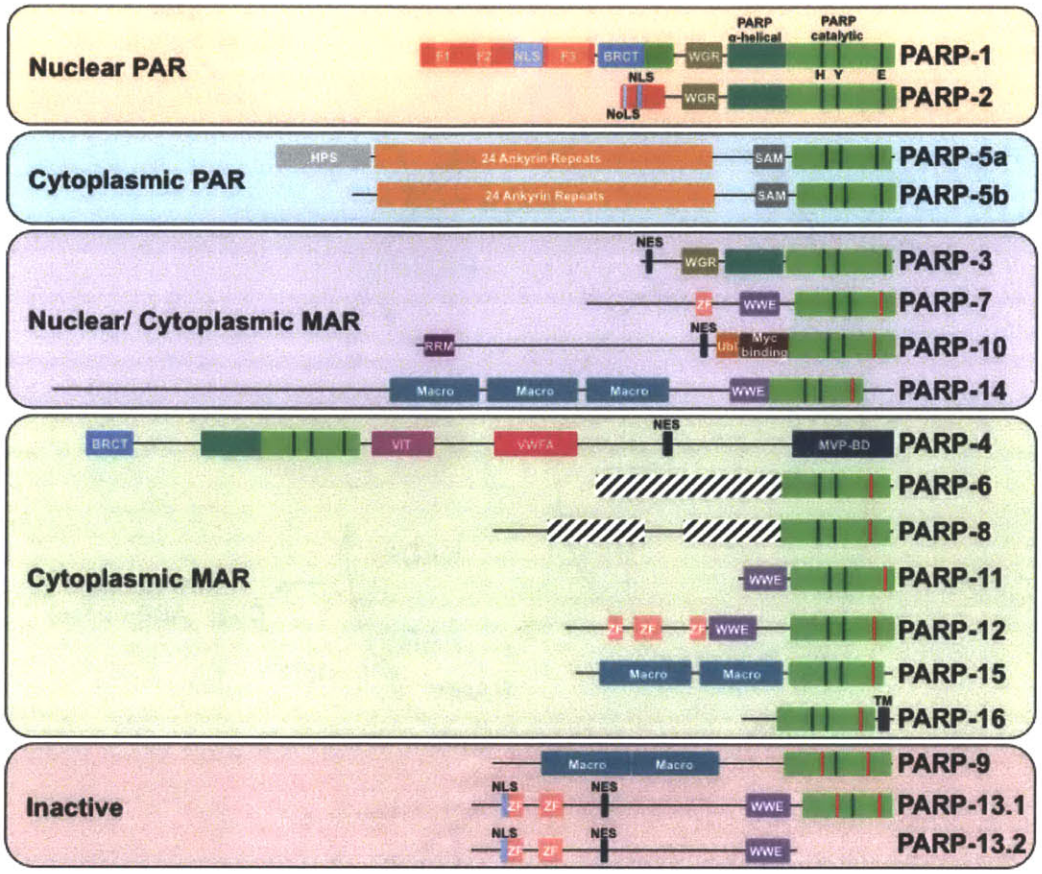

Figure 4. Domain architecture of PARP family members
PARPs are grouped according functional classifications of localization patterns and enzymatic activity. See Table 2 for summary of known functions for domains. Within the PARP catalytic domain, the catalytic triad residues are indicated by dashes – green dashes indicate presence of canonical catalytic triad amino acid while red dashes indicate substitution for a different amino acid. NLS: Nuclear Localization Sequence, NES: Nuclear Export Sequence, NoLS: Nucleolar Localization Sequence, TM: Transmembrane Domain

Subfamily	PARP	Other Names	Catalytic Motif	D loop Length	Acceptor Loop Length	Major Functions
DNA Dependent	1	PARP ARTD1	H-Y-E	12	37	DNA Damage Transcription Regulation Chromatin Structure
	2	ARTD2	H-Y-E	12	40	DNA Damage Transcription Regulation Chromatin Structure
	3	ARTD3	H-Y-E	8	42	Transcription Regulation
Tankyrase	5a	TNKS1 ARTD5	H-Y-E	7	10	Cell Division Protein Degradation Cytoplasmic Stress Response
	5b	TNKS2 ARTD6	H-Y-E	7	10	Protein Degradation
CCCH Zn Finger	7	tiPARP ARTD14	H-Y-I	?	6	Mediation of TCDD toxicity Cell Division
	12	ARTD12	H-Y-I	8	6	Cytoplasmic Stress Response
	13	ZAP ZC3HAV1 ARTD13	Y-Y-V	8	6	Antiviral Response Cytoplasmic Stress Response
Macro	9	BAL1 ARTD9	Q-Y-T	?	6	Cell Migration
	14	BAL2 ARTD8	H-Y-L	8	6	Cell Migration Signal Transduction
	15	BAL3 ARTD7	H-Y-L	8	6	Cytoplasmic Stress Response
Unclassified	4	vPARP ARTD4	H-Y-E	?	14	?
	6	ARTD17	H-Y-I	?	2	?
	8	ARTD16	H-Y-I	?	2	Nuclear Envelope Integrity
	10	ARTD10	H-Y-I	8	6	NF-κB Signaling Apoptosis
	11	ARTD11	H-Y-I	?	6	?
	16	ARTD15	H-Y-Y	9	13	Unfolded Protein Response

Table 1. Catalytic elements and major functions of PARP family members.

Interaction	Domain	Found In
Nucleic Acid	Zinc Finger	1
	DNA Binding Domain (Unknown structure)	2, 3
	CCCH Zinc Finger	7, 12, 13
	RRM (RNA Recognition Motif)	10
ADPr Modification	WWE (Trp-Trp-Glu)	7, 11, 12, 13, 14
	Macro	9, 14, 15
Protein	BRCT (BRCA1 C terminus)	1, 4
	Ankyrin	5a, 5b
	SAM (Sterile Alpha Motif)	5a, 5b
Unknown	WGR (Trp-Gly-Arg)	1, 2, 3
	VWFA (von Willebrand Factor A)	4
	VIT (Vault inter alpha trypsin)	4
	HPS (His-Pro-Ser)	5a

Table 2. Summary of known protein domains found in PARP family.

References

Aguiar, R., Yakushijin, Y., Kharbanda, S., Salgia, R., Fletcher, J., and Shipp, M. (2000). BAL is a novel risk-related gene in diffuse large B-cell lymphomas that enhances cellular migration. Blood 96, 4328-4334.

Ahel, I., Ahel, D., Matsusaka, T., Clark, A., Pines, J., Boulton, S., and West, S. (2008). Poly(ADP-ribose)-binding zinc finger motifs in DNA repair/checkpoint proteins. Nature 451, 81-85.

Alkhatib, H., Chen, D., Cherney, B., Bhatia, K., Notario, V., Giri, C., Stein, G., Slattery, E., Roeder, R., and Smulson, M. (1987). Cloning and expression of cDNA for human poly(ADP-ribose) polymerase. Proceedings of the National Academy of Sciences of the United States of America 84, 1224-1228.

Altmeyer, M., Messner, S., Hassa, P., Fey, M., and Hottiger, M. (2009). Molecular mechanism of poly(ADP-ribosyl)ation by PARP1 and identification of lysine residues as ADP-ribose acceptor sites. Nucleic acids research 37, 3723-3738.

Alvarez-Gonzalez, R., and Althaus, F. (1989). Poly(ADP-ribose) catabolism in mammalian cells exposed to DNA-damaging agents. Mutation research 218, 67-74.

Alvarez-Gonzalez, R., and Jacobson, M. (1987). Characterization of polymers of adenosine diphosphate ribose generated in vitro and in vivo. Biochemistry 26, 3218-3224.

Amé, J., Rolli, V., Schreiber, V., Niedergang, C., Apiou, F., Decker, P., Muller, S., Höger, T., Ménissier-de Murcia, J., and de Murcia, G. (1999). PARP-2, A novel mammalian DNA damage-dependent poly(ADP-ribose) polymerase. The Journal of biological chemistry 274, 17860-17868.

Amé, J.-C., Spenlehauer, C., and de Murcia, G. (2004). The PARP superfamily. BioEssays : news and reviews in molecular, cellular and developmental biology 26, 882-893.

Augustin, A., Spenlehauer, C., Dumond, H., Ménissier-De Murcia, J., Piel, M., Schmit, A.-C., Apiou, F., Vonesch, J.-L., Kock, M., Bornens, M., and De Murcia, G. (2003). PARP-3 localizes preferentially to the daughter centriole and interferes with the G1/S cell cycle progression. Journal of cell science 116, 1551-1562.

Bai, P., Houten, S., Huber, A., Schreiber, V., Watanabe, M., Kiss, B., de Murcia, G., Auwerx, J., and Ménissier-de Murcia, J. (2007). Poly(ADP-ribose) polymerase-2 [corrected] controls adipocyte differentiation and adipose tissue function through the regulation of the activity of the retinoid X receptor/peroxisome proliferator-activated receptor-gamma [corrected] heterodimer. The Journal of biological chemistry 282, 37738-37746.

Barbarulo, A., Iansante, V., Chaidos, A., Naresh, K., Rahemtulla, A., Franzoso, G., Karadimitris, A., Haskard, D., Papa, S., and Bubici, C. (2013). Poly(ADP-ribose) polymerase family member 14 (PARP14) is a novel effector of the JNK2-dependent pro-survival signal in multiple myeloma. Oncogene 32, 4231-4242.

Barkauskaite, E., Brassington, A., Tan, E., Warwicker, J., Dunstan, M., Banos, B., Lafite, P., Ahel, M., Mitchison, T., Ahel, I., and Leys, D. (2013a). Visualization of poly(ADP-ribose) bound to PARG reveals inherent balance between exo- and endo-glycohydrolase activities. Nature communications 4, 2164.

Barkauskaite, E., Jankevicius, G., Ladurner, A., Ahel, I., and Timinszky, G. (2013b). The recognition and removal of cellular poly(ADP-ribose) signals. The FEBS journal 280, 3491-3507.

Benjamin, R., and Gill, D. (1980a). Poly(ADP-ribose) synthesis in vitro programmed by damaged DNA. A comparison of DNA molecules containing different types of strand breaks. The Journal of biological chemistry 255, 10502-10508.

Benjamin, R.C., and Gill, D.M. (1980b). ADP-ribosylation in mammalian cell ghosts. Dependence of poly (ADP-ribose) synthesis on strand breakage in DNA. Journal of Biological Chemistry 255, 10493-10501.

Berger, N., Sikorski, G., Petzold, S., and Kurohara, K. (1979). Association of poly(adenosine diphosphoribose) synthesis with DNA damage and repair in normal human lymphocytes. The Journal of clinical investigation 63, 1164-1171.

Berger, W., Steiner, E., Grusch, M., Elbling, L., and Micksche, M. (2009). Vaults and the major vault protein: novel roles in signal pathway regulation and immunity. Cellular and molecular life sciences : CMLS 66, 43-61.

Bick, M., Carroll, J.-W.N., Gao, G., Goff, S., Rice, C., and MacDonald, M. (2003). Expression of the zinc-finger antiviral protein inhibits alphavirus replication. Journal of virology 77, 11555-11562.

Bonicalzi, M.E., Haince, J.F., Droit, A., and Poirier, G. (2005). Regulation of poly(ADP-ribose) metabolism by poly(ADP-ribose) glycohydrolase: where and when? Cellular and molecular life sciences : CMLS 62, 739-750.

Braun, S., and Panzeter..., P. (1994). Endoglycosidic cleavage of branched polymers by poly (ADP - ribose) glycohydrolase. European Journal of ···.

Brochu, G., Duchaine, C., Thibeault, L., Lagueux, J., Shah, G., and Poirier, G. (1994). Mode of action of poly(ADP-ribose) glycohydrolase. Biochimica et biophysica acta 1219, 342-350.

Bryant, H., Petermann, E., Schultz, N., Jemth, A.-S., Loseva, O., Issaeva, N., Johansson, F., Fernandez, S., McGlynn, P., and Helleday, T. (2009). PARP is activated at stalled forks to mediate Mre11-dependent replication restart and recombination. The EMBO journal 28, 2601-2615.

Bürkle, A. (2005). Poly(ADP-ribose). The most elaborate metabolite of NAD+. The FEBS journal 272, 4576-4589.

Caldecott, K. (2003). XRCC1 and DNA strand break repair. DNA repair 2, 955-969.

Carroll, S.F., and Collier, R.J. (1984). NAD binding site of diphtheria toxin: identification of a residue within the nicotinamide subsite by photochemical modification with NAD. Proceedings of the National Academy of Sciences of the United States of America 81, 3307-3311.

Castagnini, M., Picchianti, M., Talluri, E., Biagini, M., Del Vecchio, M., Di Procolo, P., Norais, N., Nardi-Dei, V., and Balducci, E. (2012). Arginine-specific mono ADP-ribosylation in vitro of antimicrobial peptides by ADP-ribosylating toxins. PloS one 7.

Cervantes-Laurean, D., Jacobson, E., and Jacobson, M. (1996). Glycation and glycoxidation of histones by ADP-ribose. The Journal of biological chemistry 271, 10461-10469.

Cervantes-Laurean, D., Minter, D., Jacobson, E., and Jacobson, M. (1993). Protein glycation by ADP-ribose: studies of model conjugates. Biochemistry 32, 1528-1534.

Chambon, P., Weill, J.D., Doly, J., Strosser, M.T., and Mandel, P. (1966). On the formation of a novel adenylic compound by enzymatic extracts of liver nuclei. Biochemical and Biophysical Research Communications 25.

Chambon, P., Weill, J.D., and Mandel, P. (1963). Nicotinamide mononucleotide activation of new DNA-dependent polyadenylic acid synthesizing nuclear enzyme. Biochemical and biophysical research communications 11, 39-43.

Chang, P., Coughlin, M., and Mitchison, T. (2005). Tankyrase-1 polymerization of poly(ADP-ribose) is required for spindle structure and function. Nature cell biology 7, 1133-1139.

Chang, P., Coughlin, M., and Mitchison, T.J. (2009). Interaction between Poly(ADP-ribose) and NuMA contributes to mitotic spindle pole assembly. Molecular biology of the cell 20, 4575-4585.

Chang, P., Jacobson, M.K., and Mitchison, T.J. (2004). Poly(ADP-ribose) is required for spindle assembly and structure. Nature 432, 645-649.

Chang, W., Dynek, J., and Smith, S. (2003). TRF1 is degraded by ubiquitin-mediated proteolysis after release from telomeres. Genes & development 17, 1328-1333.

Chen, D., Vollmar, M., Rossi, M., Phillips, C., Kraehenbuehl, R., Slade, D., Mehrotra, P., von Delft, F., Crosthwaite, S., Gileadi, O., Denu, J., and Ahel, I. (2011). Identification of macrodomain proteins as novel O-acetyl-ADP-ribose deacetylases. The Journal of biological chemistry 286, 13261-13271.

Cherney, B., McBride, O., Chen, D., Alkhatib, H., Bhatia, K., Hensley, P., and Smulson, M. (1987). cDNA sequence, protein structure, and chromosomal location of the human gene for poly(ADP-ribose) polymerase. Proceedings of the National Academy of Sciences of the United States of America 84, 8370-8374.

Chi, N., and Lodish, H. (2000). Tankyrase is a golgi-associated mitogen-activated protein kinase substrate that interacts with IRAP in GLUT4 vesicles. The Journal of biological chemistry 275, 38437-38444.

Chiang, Y., Hsiao, S., Yver, D., Cushman, S., Tessarollo, L., Smith, S., and Hodes, R. (2008). Tankyrase 1 and tankyrase 2 are essential but redundant for mouse embryonic development. PloS one 3.

Cho, S., Ahn, A., Bhargava, P., Lee, C.-H., Eischen, C., McGuinness, O., and Boothby, M. (2011). Glycolytic rate and lymphomagenesis depend on PARP14, an ADP ribosyltransferase of the B aggressive lymphoma (BAL) family. Proceedings of the National Academy of Sciences of the United States of America 108, 15972-15977.

Cho, S., Goenka, S., Henttinen, T., Gudapati, P., Reinikainen, A., Eischen, C., Lahesmaa, R., and Boothby, M. (2009). PARP-14, a member of the B aggressive lymphoma family, transduces survival signals in primary B cells. Blood 113, 2416-2425.

Chou, H.-Y.E., Chou, H., and Lee, S.-C. (2006). CDK-dependent activation of poly(ADP-ribose) polymerase member 10 (PARP10). The Journal of biological chemistry 281, 15201-15207.

Citarelli, M., Teotia, S., and Lamb, R. (2010). Evolutionary history of the poly(ADP-ribose) polymerase gene family in eukaryotes. BMC evolutionary biology 10, 308.
Cook, B., Dynek, J., Chang, W., Shostak, G., and Smith, S. (2002). Role for the related poly(ADP-Ribose) polymerases tankyrase 1 and 2 at human telomeres. Molecular and cellular biology 22, 332-342.
Dantzer, F., de La Rubia, G., Ménissier-De Murcia, J., Hostomsky, Z., de Murcia, G., and Schreiber, V. (2000). Base excision repair is impaired in mammalian cells lacking Poly(ADP-ribose) polymerase-1. Biochemistry 39, 7559-7569.
Dantzer, F., Giraud-Panis, M.-J., Jaco, I., Amé, J.-C., Schultz, I., Blasco, M., Koering, C.-E., Gilson, E., Ménissier-de Murcia, J., de Murcia, G., and Schreiber, V. (2004). Functional interaction between poly(ADP-Ribose) polymerase 2 (PARP-2) and TRF2: PARP activity negatively regulates TRF2. Molecular and cellular biology 24, 1595-1607.
Dantzer, F., Mark, M., Quenet, D., Scherthan, H., Huber, A., Liebe, B., Monaco, L., Chicheportiche, A., Sassone-Corsi, P., de Murcia, G., and Ménissier-de Murcia, J. (2006). Poly(ADP-ribose) polymerase-2 contributes to the fidelity of male meiosis I and spermiogenesis. Proceedings of the National Academy of Sciences of the United States of America 103, 14854-14859.
Dantzer, F., and Santoro, R. (2013). The expanding role of PARPs in the establishment and maintenance of heterochromatin. The FEBS journal 280, 3508-3518.
David, K.K., Andrabi, S.A., Dawson, T.M., and Dawson, V.L. (2009). Parthanatos, a messenger of death. Frontiers in bioscience 14, 1116-1128.
de Murcia, J., Niedergang, C., Trucco, C., Ricoul, M., Dutrillaux, B., Mark, M., Oliver, F., Masson, M., Dierich, A., LeMeur, M., Walztinger, C., Chambon, P., and de Murcia, G. (1997). Requirement of poly(ADP-ribose) polymerase in recovery from DNA damage in mice and in cells. Proceedings of the National Academy of Sciences of the United States of America 94, 7303-7307.
De Vos, M., Schreiber, V., and Dantzer, F. (2012). The diverse roles and clinical relevance of PARPs in DNA damage repair: current state of the art. Biochemical pharmacology 84, 137-146.
Deng, Q., and Barbieri, J. (2008). Molecular mechanisms of the cytotoxicity of ADP-ribosylating toxins. Annual review of microbiology 62, 271-288.
Desmarais, Y., Menard, L., Lagueux, J., and Poirier, G.G. (1991). Enzymological properties of poly(ADP-ribose)polymerase: characterization of automodification sites and NADase activity. Biochim Biophys Acta 1078, 179-186.
Di Giammartino, D., Shi, Y., and Manley, J. (2013). PARP1 represses PAP and inhibits polyadenylation during heat shock. Molecular cell 49, 7-17.
Di Girolamo, M., Dani, N., Stilla, A., and Corda, D. (2005). Physiological relevance of the endogenous mono(ADP-ribosyl)ation of cellular proteins. The FEBS journal 272, 4565-4575.
Di Paola, S., Micaroni, M., Di Tullio, G., Buccione, R., and Di Girolamo, M. (2012). PARP16/ARTD15 is a novel endoplasmic-reticulum-associated mono-ADP-ribosyltransferase that interacts with, and modifies karyopherin-ß1. PloS one 7.
Diani-Moore, S., Ram, P., Li, X., Mondal, P., Youn, D., Sauve, A., and Rifkind, A. (2010). Identification of the aryl hydrocarbon receptor target gene TiPARP as a mediator of suppression of hepatic gluconeogenesis by 2,3,7,8-

tetrachlorodibenzo-p-dioxin and of nicotinamide as a corrective agent for this effect. The Journal of biological chemistry 285, 38801-38810.
Diani-Moore, S., Zhang, S., Ram, P., and Rifkind, A. (2013). Aryl hydrocarbon receptor activation by dioxin targets phosphoenolpyruvate carboxykinase (PEPCK) for ADP-ribosylation via 2,3,7,8-tetrachlorodibenzo-p-dioxin (TCDD)-inducible poly(ADP-ribose) polymerase (TiPARP). The Journal of biological chemistry 288, 21514-21525.
Domenighini, M., Montecucco, C., Ripka, W.C., and Rappuoli, R. (1991). Computer modelling of the NAD binding site of ADP-ribosylating toxins: active-site structure and mechanism of NAD binding. Molecular Microbiology 5.
Domenighini, M., and Rappuoli, R. (1996). Three conserved consensus sequences identify the NAD-binding site of ADP-ribosylating enzymes, expressed by eukaryotes, bacteria and T-even bacteriophages. Molecular microbiology 21, 667-674.
Dunstan, M., Barkauskaite, E., Lafite, P., Knezevic, C., Brassington, A., Ahel, M., Hergenrother, P., Leys, D., and Ahel, I. (2012). Structure and mechanism of a canonical poly(ADP-ribose) glycohydrolase. Nature communications 3, 878.
Dynek, J., and Smith, S. (2004). Resolution of sister telomere association is required for progression through mitosis. Science (New York, NY) 304, 97-100.
El-Khamisy, S., Masutani, M., Suzuki, H., and Caldecott, K. (2003). A requirement for PARP-1 for the assembly or stability of XRCC1 nuclear foci at sites of oxidative DNA damage. Nucleic acids research 31, 5526-5533.
Fahie, K., Hu, P., Swatkoski, S., Cotter, R., Zhang, Y., and Wolberger, C. (2009). Side chain specificity of ADP-ribosylation by a sirtuin. The FEBS journal 276, 7159-7176.
Feijs, K., Verheugd, P., and Lüscher, B. (2013). Expanding functions of intracellular resident mono-ADP-ribosylation in cell physiology. The FEBS journal 280, 3519-3529.
Feldman, J., Dittenhafer-Reed, K., and Denu, J. (2012). Sirtuin catalysis and regulation. The Journal of biological chemistry 287, 42419-42427.
Fernández, A., Ribeiro, J., Costas, M., Pinto, R., Canales, J., and Cameselle, J. (1996). Specific ADP-ribose pyrophosphatase from Artemia cysts and rat liver: effects of nitroprusside, fluoride and ionic strength. Biochimica et biophysica acta 1290, 121-127.
Forst, A., Karlberg, T., Herzog, N., Thorsell, A.-G., Gross, A., Feijs, K., Verheugd, P., Kursula, P., Nijmeijer, B., Kremmer, E., Kleine, H., Ladurner, A., Schüler, H., and Lüscher, B. (2013). Recognition of mono-ADP-ribosylated ARTD10 substrates by ARTD8 macrodomains. Structure (London, England : 1993) 21, 462-475.
Frizzell, K., Gamble, M., Berrocal, J., Zhang, T., Krishnakumar, R., Cen, Y., Sauve, A., and Kraus, W. (2009). Global analysis of transcriptional regulation by poly(ADP-ribose) polymerase-1 and poly(ADP-ribose) glycohydrolase in MCF-7 human breast cancer cells. The Journal of biological chemistry 284, 33926-33938.
Gao, G., Guo, X., and Goff, S. (2002). Inhibition of retroviral RNA production by ZAP, a CCCH-type zinc finger protein. Science (New York, NY) 297, 1703-1706.
Glowacki, G., Braren, R., Firner, K., Nissen, M., Kühl, M., Reche, P., Bazan, F., Cetkovic-Cvrlje, M., Leiter, E., Haag, F., and Koch-Nolte, F. (2002). The family of

toxin-related ecto-ADP-ribosyltransferases in humans and the mouse. Protein science : a publication of the Protein Society 11, 1657-1670.
Goenka, S., and Boothby, M. (2006). Selective potentiation of Stat-dependent gene expression by collaborator of Stat6 (CoaSt6), a transcriptional cofactor. Proceedings of the National Academy of Sciences of the United States of America 103, 4210-4215.
Goenka, S., Cho, S., and Boothby, M. (2007). Collaborator of Stat6 (CoaSt6)-associated poly(ADP-ribose) polymerase activity modulates Stat6-dependent gene transcription. The Journal of biological chemistry 282, 18732-18739.
Guo, X., Carroll, J.-W.N., Macdonald, M., Goff, S., and Gao, G. (2004). The zinc finger antiviral protein directly binds to specific viral mRNAs through the CCCH zinc finger motifs. Journal of virology 78, 12781-12787.
Guo, X., Ma, J., Sun, J., and Gao, G. (2007). The zinc-finger antiviral protein recruits the RNA processing exosome to degrade the target mRNA. Proceedings of the National Academy of Sciences of the United States of America 104, 151-156.
Ha, G.H., Kim, H.S., Go, H., Lee, H., Seimiya, H., Chung, D., and Lee, C.W. (2012). Tankyrase-1 function at telomeres and during mitosis is regulated by Polo-like kinase-1-mediated phosphorylation. Cell death and differentiation 19, 321-332.
Haigis, M., Mostoslavsky, R., Haigis, K., Fahie, K., Christodoulou, D., Murphy, A., Valenzuela, D., Yancopoulos, G., Karow, M., Blander, G., Wolberger, C., Prolla, T., Weindruch, R., Alt, F., and Guarente, L. (2006). SIRT4 inhibits glutamate dehydrogenase and opposes the effects of calorie restriction in pancreatic beta cells. Cell 126, 941-954.
Han, S., and Tainer, J.A. (2002). The ARTT motif and a unified structural understanding of substrate recognition in ADP-ribosylating bacterial toxins and eukaryotic ADP-ribosyltransferases. International journal of medical microbiology : IJMM 291, 523-529.
Hatakeyama, K., Nemoto, Y., Ueda, K., and Hayaishi, O. (1986). Purification and characterization of poly(ADP-ribose) glycohydrolase. Different modes of action on large and small poly(ADP-ribose). The Journal of biological chemistry 261, 14902-14911.
Hawse, W., and Wolberger, C. (2009). Structure-based mechanism of ADP-ribosylation by sirtuins. The Journal of biological chemistry 284, 33654-33661.
Herzog, N., Hartkamp, J., Verheugd, P., Treude, F., Forst, A., Feijs, K., Lippok, B., Kremmer, E., Kleine, H., and Lüscher, B. (2013). Caspase-dependent cleavage of the mono-ADP-ribosyltransferase ARTD10 interferes with its pro-apoptotic function. The FEBS journal 280, 1330-1343.
Houtkooper, R., Cantó, C., Wanders, R., and Auwerx, J. (2010). The secret life of NAD+: an old metabolite controlling new metabolic signaling pathways. Endocrine reviews 31, 194-223.
Hsiao, S., Poitras, M., Cook, B., Liu, Y., and Smith, S. (2006). Tankyrase 2 poly(ADP-ribose) polymerase domain-deleted mice exhibit growth defects but have normal telomere length and capping. Molecular and cellular biology 26, 2044-2054.
Huang, S.-M.A., Mishina, Y., Liu, S., Cheung, A., Stegmeier, F., Michaud, G., Charlat, O., Wiellette, E., Zhang, Y., Wiessner, S., Hild, M., Shi, X., Wilson, C., Mickanin, C., Myer, V., Fazal, A., Tomlinson, R., Serluca, F., Shao, W., Cheng, H., Shultz,

M., Rau, C., Schirle, M., Schlegl, J., Ghidelli, S., Fawell, S., Lu, C., Curtis, D., Kirschner, M., Lengauer, C., Finan, P., Tallarico, J., Bouwmeester, T., Porter, J., Bauer, A., and Cong, F. (2009). Tankyrase inhibition stabilizes axin and antagonizes Wnt signalling. Nature 461, 614-620.

Ikejima, M., Noguchi, S., Yamashita, R., Ogura, T., Sugimura, T., Gill, D., and Miwa, M. (1990). The zinc fingers of human poly(ADP-ribose) polymerase are differentially required for the recognition of DNA breaks and nicks and the consequent enzyme activation. Other structures recognize intact DNA. The Journal of biological chemistry 265, 21907-21913.

Jankevicius, G., Hassler, M., Golia, B., Rybin, V., Zacharias, M., Timinszky, G., and Ladurner, A. (2013). A family of macrodomain proteins reverses cellular mono-ADP-ribosylation. Nature structural & molecular biology 20, 508-514.

Johnson, L., and Barford, D. (1993). The effects of phosphorylation on the structure and function of proteins. Annual review of biophysics and biomolecular structure 22, 199-232.

Juszczynski, P., Kutok, J., Li, C., Mitra, J., Aguiar, R., and Shipp, M. (2006). BAL1 and BBAP are regulated by a gamma interferon-responsive bidirectional promoter and are overexpressed in diffuse large B-cell lymphomas with a prominent inflammatory infiltrate. Molecular and cellular biology 26, 5348-5359.

Jwa, M., and Chang, P. (2012). PARP16 is a tail-anchored endoplasmic reticulum protein required for the PERK- and IRE1alpha-mediated unfolded protein response. Nature cell biology 14, 1223-1230.

Kaminker, P., Kim, S., Taylor, R., Zebarjadian, Y., Funk, W., Morin, G., Yaswen, P., and Campisi, J. (2001). TANK2, a new TRF1-associated poly(ADP-ribose) polymerase, causes rapid induction of cell death upon overexpression. The Journal of biological chemistry 276, 35891-35899.

Kanai, M., Tong, W.-M., Sugihara, E., Wang, Z.-Q., Fukasawa, K., and Miwa, M. (2003). Involvement of poly(ADP-Ribose) polymerase 1 and poly(ADP-Ribosyl)ation in regulation of centrosome function. Molecular and cellular biology 23, 2451-2462.

Karras, G., Kustatscher, G., Buhecha, H., Allen, M., Pugieux, C.l., Sait, F., Bycroft, M., and Ladurner, A. (2005). The macro domain is an ADP-ribose binding module. The EMBO journal 24, 1911-1920.

Kedersha, N., and Anderson, P. (2009). Regulation of translation by stress granules and processing bodies. Progress in molecular biology and translational science 90, 155-185.

Kickhoefer, V.A., Siva, A.C., Kedersha, N.L., Inman, E.M., Ruland, C., Streuli, M., and Rome, L.H. (1999). The 193-kD vault protein, VPARP, is a novel poly(ADP-ribose) polymerase. The Journal of cell biology 146, 917-928.

Kim, I.-K., Kiefer, J., Ho, C., Stegeman, R., Classen, S., Tainer, J., and Ellenberger, T. (2012). Structure of mammalian poly(ADP-ribose) glycohydrolase reveals a flexible tyrosine clasp as a substrate-binding element. Nature structural & molecular biology 19, 653-656.

Kleine, H., Herrmann, A., Lamark, T., Forst, A., Verheugd, P., Lüscher-Firzlaff, J., Lippok, B., Feijs, K., Herzog, N., Kremmer, E., Johansen, T., Müller-Newen, G., and Lüscher, B. (2012). Dynamic subcellular localization of the mono-ADP-

ribosyltransferase ARTD10 and interaction with the ubiquitin receptor p62. Cell communication and signaling : CCS 10, 28.
Kleine, H., Poreba, E., Lesniewicz, K., Hassa, P.O., Hottiger, M.O., Litchfield, D.W., Shilton, B.H., and Luscher, B. (2008). Substrate-assisted catalysis by PARP10 limits its activity to mono-ADP-ribosylation. Molecular cell 32, 57-69.
Koh, D., Lawler, A., Poitras, M., Sasaki, M., Wattler, S., Nehls, M., St√ ∂ ger, T., Poirier, G., Dawson, V., and Dawson, T. (2004). Failure to degrade poly(ADP-ribose) causes increased sensitivity to cytotoxicity and early embryonic lethality. Proceedings of the National Academy of Sciences of the United States of America 101, 17699-17704.
Kraus, W. (2008). Transcriptional control by PARP-1: chromatin modulation, enhancer-binding, coregulation, and insulation. Current opinion in cell biology 20, 294-302.
Kraus, W., and Lis, J. (2003). PARP goes transcription. Cell 113, 677-683.
Kutuzov, M., Khodyreva, S., Amé, J.-C., Ilina, E., Sukhanova, M., Schreiber, V., and Lavrik, O. (2013). Interaction of PARP-2 with DNA structures mimicking DNA repair intermediates and consequences on activity of base excision repair proteins. Biochimie 95, 1208-1215.
Lai, W., Carballo, E., Strum, J., Kennington, E., Phillips, R., and Blackshear, P. (1999). Evidence that tristetraprolin binds to AU-rich elements and promotes the deadenylation and destabilization of tumor necrosis factor alpha mRNA. Molecular and cellular biology 19, 4311-4323.
Langelier, M.-F., Planck, J., Roy, S., and Pascal, J. (2012). Structural basis for DNA damage-dependent poly(ADP-ribosyl)ation by human PARP-1. Science (New York, NY) 336, 728-732.
Langelier, M.-F., Planck, J., Servent, K., and Pascal, J. (2011). Purification of human PARP-1 and PARP-1 domains from Escherichia coli for structural and biochemical analysis. Methods in molecular biology (Clifton, NJ) 780, 209-226.
Lee, H., and Iglewski, W. (1984). Cellular ADP-ribosyltransferase with the same mechanism of action as diphtheria toxin and Pseudomonas toxin A. Proceedings of the National Academy of Sciences of the United States of America 81, 2703-2707.
Leppard, J., Dong, Z., Mackey, Z., and Tomkinson, A. (2003). Physical and functional interaction between DNA ligase IIIalpha and poly(ADP-Ribose) polymerase 1 in DNA single-strand break repair. Molecular and cellular biology 23, 5919-5927.
Leung, A., Vyas, S., Rood, J., Bhutkar, A., Sharp, P., and Chang, P. (2011). Poly(ADP-ribose) regulates stress responses and microRNA activity in the cytoplasm. Molecular cell 42, 489-499.
Liang, Y.-C., Hsu, C.-Y., Yao, Y.-L., and Yang, W.-M. (2013). PARP-2 regulates cell cycle-related genes through histone deacetylation and methylation independently of poly(ADP-ribosyl)ation. Biochemical and biophysical research communications 431, 58-64.
Lilyestrom, W., van der Woerd, M., Clark, N., and Luger, K. (2010). Structural and biophysical studies of human PARP-1 in complex with damaged DNA. Journal of molecular biology 395, 983-994.

Lin, W., Ame, J.C., Aboul-Ela, N., Jacobson, E.L., and Jacobson, M.K. (1997). Isolation and characterization of the cDNA encoding bovine poly(ADP-ribose) glycohydrolase. The Journal of biological chemistry 272, 11895-11901.

Liu, Y., Snow, B., Kickhoefer, V., Erdmann, N., Zhou, W., Wakeham, A., Gomez, M., Rome, L., and Harrington, L. (2004). Vault poly(ADP-ribose) polymerase is associated with mammalian telomerase and is dispensable for telomerase function and vault structure in vivo. Molecular and cellular biology 24, 5314-5323.

Loeffler, P., Cuneo, M., Mueller, G., DeRose, E., Gabel, S., and London, R. (2011). Structural studies of the PARP-1 BRCT domain. BMC structural biology 11, 37.

Lonskaya, I. (2005). Regulation of Poly(ADP-ribose) Polymerase-1 by DNA Structure-specific Binding. Journal of Biological Chemistry 280.

Loseva, O., Jemth, A.-S., Bryant, H., Schüler, H., Lehtiö, L., Karlberg, T., and Helleday, T. (2010). PARP-3 is a mono-ADP-ribosylase that activates PARP-1 in the absence of DNA. The Journal of biological chemistry 285, 8054-8060.

Luo, X., and Kraus, W. (2012). On PAR with PARP: cellular stress signaling through poly(ADP-ribose) and PARP-1. Genes & development 26, 417-432.

Ma, Q. (2002). Induction and superinduction of 2,3,7,8-tetrachlorodibenzo-rho-dioxin-inducible poly(ADP-ribose) polymerase: role of the aryl hydrocarbon receptor/aryl hydrocarbon receptor nuclear translocator transcription activation domains and a labile transcription repressor. Arch Biochem Biophys 404, 309-316.

Ma, Q., Baldwin, K., Renzelli, A., McDaniel, A., and Dong, L. (2001). TCDD-inducible poly(ADP-ribose) polymerase: a novel response to 2,3,7,8-tetrachlorodibenzo-p-dioxin. Biochemical and biophysical research communications 289, 499-506.

MacPherson, L., Tamblyn, L., Rajendra, S., Bralha, F., McPherson, J., and Matthews, J. (2013). 2,3,7,8-Tetrachlorodibenzo-p-dioxin poly(ADP-ribose) polymerase (TiPARP, ARTD14) is a mono-ADP-ribosyltransferase and repressor of aryl hydrocarbon receptor transactivation. Nucleic acids research 41, 1604-1621.

Malanga, M., and Althaus, F. (2005). The role of poly(ADP-ribose) in the DNA damage signaling network. Biochemistry and cell biology = Biochimie et biologie cellulaire 83, 354-364.

Marsischky, G.T., Wilson, B.A., and Collier, R.J. (1995). Role of glutamic acid 988 of human poly-ADP-ribose polymerase in polymer formation. Evidence for active site similarities to the ADP-ribosylating toxins. The Journal of biological chemistry 270, 3247-3254.

Masaharu, T., Mai, T., Makoto, S., Yoshinori, T., Takeshi, U., and Mikako, T. (2008). Glycosylphosphatidylinositol-anchored arginine-specific ADP-ribosyltransferase7.1 (Art7.1) on chicken B cells: the possible role of Art7 in B cell receptor signalling and proliferation. Molecular and cellular biochemistry 320.

Ménissier de Murcia, J., Ricoul, M., Tartier, L., Niedergang, C., Huber, A., Dantzer, F., Schreiber, V., Amé, J.-C., Dierich, A., LeMeur, M., Sabatier, L., Chambon, P., and de Murcia, G. (2003). Functional interaction between PARP-1 and PARP-2 in chromosome stability and embryonic development in mouse. The EMBO journal 22, 2255-2263.

Messner, S., Altmeyer, M., Zhao, H., Pozivil, A., Roschitzki, B., Gehrig, P., Rutishauser, D., Huang, D., Caflisch, A., and Hottiger, M. (2010). PARP1 ADP-ribosylates lysine residues of the core histone tails. Nucleic acids research 38, 6350-6362.

Meyer, R., Meyer-Ficca, M., Whatcott, C., Jacobson, E., and Jacobson, M. (2007). Two small enzyme isoforms mediate mammalian mitochondrial poly(ADP-ribose) glycohydrolase (PARG) activity. Experimental cell research 313, 2920-2936.
Meyer-Ficca, M.L., Meyer, R.G., Coyle, D.L., Jacobson, E.L., and Jacobson, M.K. (2004). Human poly(ADP-ribose) glycohydrolase is expressed in alternative splice variants yielding isoforms that localize to different cell compartments. Experimental cell research 297, 521-532.
Miwa, M., and Sugimura, T. (1971). Splitting of the ribose-ribose linkage of poly(adenosine diphosphate-robose) by a calf thymus extract. The Journal of biological chemistry 246, 6362-6364.
Miwa, M., Tanaka, M., Matsushima, T., and Sugimura, T. (1974). Purification and properties of glycohydrolase from calf thymus splitting ribose-ribose linkages of poly(adenosine diphosphate ribose). The Journal of biological chemistry 249, 3475-3482.
Mortusewicz, O., Amé, J.-C., Schreiber, V., and Leonhardt, H. (2007). Feedback-regulated poly(ADP-ribosyl)ation by PARP-1 is required for rapid response to DNA damage in living cells. Nucleic acids research 35, 7665-7675.
Mortusewicz, O., Fouquerel, E., Amé, J.-C., Leonhardt, H., and Schreiber, V. (2011). PARG is recruited to DNA damage sites through poly(ADP-ribose)- and PCNA-dependent mechanisms. Nucleic acids research 39, 5045-5056.
Moss, J., and Richardson, S. (1978). Activation of adenylate cyclase by heat-labile Escherichia coli enterotoxin. Evidence for ADP-ribosyltransferase activity similar to that of choleragen. The Journal of clinical investigation 62, 281-285.
Moss, J., Stanley, S.J., Nightingale, M.S., Murtagh, J.J., Jr., Monaco, L., Mishima, K., Chen, H.C., Williamson, K.C., and Tsai, S.C. (1992). Molecular and immunological characterization of ADP-ribosylarginine hydrolases. The Journal of biological chemistry 267, 10481-10488.
Moss, J., and Vaughan, M. (1978). Isolation of an avian erythrocyte protein possessing ADP-ribosyltransferase activity and capable of activating adenylate cyclase. Proceedings of the National Academy of Sciences of the United States of America 75, 3621-3624.
Mueller-Dieckmann, C., Kernstock, S., Lisurek, M., von Kries, J., Haag, F., Weiss, M., and Koch-Nolte, F. (2006). The structure of human ADP-ribosylhydrolase 3 (ARH3) provides insights into the reversibility of protein ADP-ribosylation. Proceedings of the National Academy of Sciences of the United States of America 103, 15026-15031.
Neuvonen, M., and Ahola, T. (2009). Differential activities of cellular and viral macro domain proteins in binding of ADP-ribose metabolites. Journal of molecular biology 385, 212-225.
Niere, M., Mashimo, M., Agledal, L., Dölle, C., Kasamatsu, A., Kato, J., Moss, J., and Ziegler, M. (2012). ADP-ribosylhydrolase 3 (ARH3), not poly(ADP-ribose) glycohydrolase (PARG) isoforms, is responsible for degradation of mitochondrial matrix-associated poly(ADP-ribose). The Journal of biological chemistry 287, 16088-16102.
Ohashi, S., Kanai, M., Hanai, S., Uchiumi, F., Maruta, H., Tanuma, S.-i., and Miwa, M. (2003). Subcellular localization of poly(ADP-ribose) glycohydrolase in

mammalian cells. Biochemical and biophysical research communications 307, 915-921.
Oka, S., Kato, J., and Moss, J. (2006). Identification and characterization of a mammalian 39-kDa poly(ADP-ribose) glycohydrolase. The Journal of biological chemistry 281, 705-713.
Okayama, H., Edson, C., Fukushima, M., Ueda, K., and Hayaishi, O. (1977). Purification and properties of poly(adenosine diphosphate ribose) synthetase. The Journal of biological chemistry 252, 7000-7005.
Ono, T., Kasamatsu, A., Oka, S., and Moss, J. (2006). The 39-kDa poly(ADP-ribose) glycohydrolase ARH3 hydrolyzes O-acetyl-ADP-ribose, a product of the Sir2 family of acetyl-histone deacetylases. Proceedings of the National Academy of Sciences of the United States of America 103, 16687-16691.
Otto, H., Reche, P., Bazan, F., Dittmar, K., Haag, F., and Koch-Nolte, F. (2005). In silico characterization of the family of PARP-like poly(ADP-ribosyl)transferases (pARTs). BMC genomics 6, 139.
Papini, E., Schiavo, G., Sandona, D., Rappuoli, R., and Montecucco, C. (1989). Histidine 21 is at the NAD+ binding site of diphtheria toxin. The Journal of biological chemistry 264, 12385-12388.
Patel, C., Koh, D., Jacobson, M., and Oliveira, M. (2005). Identification of three critical acidic residues of poly(ADP-ribose) glycohydrolase involved in catalysis: determining the PARG catalytic domain. The Biochemical journal 388, 493-500.
Pehrson, J., and Fried, V. (1992). MacroH2A, a core histone containing a large nonhistone region. Science (New York, NY) 257, 1398-1400.
Perkins, E., Sun, D., Nguyen, A., Tulac, S., Francesco, M., Tavana, H., Nguyen, H., Tugendreich, S., Barthmaier, P., Couto, J., Yeh, E., Thode, S., Jarnagin, K., Jain, A., Morgans, D., and Melese, T. (2001). Novel inhibitors of poly(ADP-ribose) polymerase/PARP1 and PARP2 identified using a cell-based screen in yeast. Cancer research 61, 4175-4183.
Petesch, S., and Lis, J. (2008). Rapid, transcription-independent loss of nucleosomes over a large chromatin domain at Hsp70 loci. Cell 134, 74-84.
Petesch, S., and Lis, J. (2012). Activator-induced spread of poly(ADP-ribose) polymerase promotes nucleosome loss at Hsp70. Molecular cell 45, 64-74.
Pleschke, J., Kleczkowska, H., Strohm, M., and Althaus, F. (2000). Poly(ADP-ribose) binds to specific domains in DNA damage checkpoint proteins. The Journal of biological chemistry 275, 40974-40980.
Rankin, P., Jacobson, E., Benjamin, R., Moss, J., and Jacobson, M. (1989). Quantitative studies of inhibitors of ADP-ribosylation in vitro and in vivo. The Journal of biological chemistry 264, 4312-4317.
Ray Chaudhuri, A., Hashimoto, Y., Herrador, R., Neelsen, K., Fachinetti, D., Bermejo, R., Cocito, A., Costanzo, V., and Lopes, M. (2012). Topoisomerase I poisoning results in PARP-mediated replication fork reversal. Nature structural & molecular biology 19, 417-423.
Revollo, J., Grimm, A., and Imai, S.-i. (2004). The NAD biosynthesis pathway mediated by nicotinamide phosphoribosyltransferase regulates Sir2 activity in mammalian cells. The Journal of biological chemistry 279, 50754-50763.

Ribeiro, J., Cameselle, J., Fernández, A., Canales, J., Pinto, R., and Costas, M. (1995). Inhibition and ADP-ribose pyrophosphatase-I by nitric-oxide-generating systems: a mechanism linking nitric oxide to processes dependent on free ADP-ribose. Biochemical and biophysical research communications 213, 1075-1081.

Ribeiro, J., Carloto, A., Costas, M., and Cameselle, J. (2001). Human placenta hydrolases active on free ADP-ribose: an ADP-sugar pyrophosphatase and a specific ADP-ribose pyrophosphatase. Biochimica et biophysica acta 1526, 86-94.

Rippmann, J., Damm, K., and Schnapp, A. (2002). Functional characterization of the poly(ADP-ribose) polymerase activity of tankyrase 1, a potential regulator of telomere length. Journal of molecular biology 323, 217-224.

Rosenthal, F., Feijs, K., Frugier, E., Bonalli, M., Forst, A., Imhof, R., Winkler, H., Fischer, D., Caflisch, A., Hassa, P., Lüscher, B., and Hottiger, M. (2013). Macrodomain-containing proteins are new mono-ADP-ribosylhydrolases. Nature structural & molecular biology 20, 502-507.

Rouleau, M., McDonald, D., Gagné, P., Ouellet, M.E., Droit, A., Hunter, J., Dutertre, S., Prigent, C., Hendzel, M., and Poirier, G. (2007). PARP-3 associates with polycomb group bodies and with components of the DNA damage repair machinery. Journal of cellular biochemistry 100, 385-401.

Rouleau, M., Saxena, V., Rodrigue, A., Paquet, E., Gagnon, A., Hendzel, M., Masson, J.-Y., Ekker, M., and Poirier, G. (2011). A key role for poly(ADP-ribose) polymerase 3 in ectodermal specification and neural crest development. PloS one 6.

Ruf, A., Mennissier de Murcia, J., de Murcia, G., and Schulz, G.E. (1996). Structure of the catalytic fragment of poly(AD-ribose) polymerase from chicken. Proceedings of the National Academy of Sciences of the United States of America 93, 7481-7485.

Ruf, A., Rolli, V., de Murcia, G., and Schulz, G. (1998). The mechanism of the elongation and branching reaction of poly(ADP-ribose) polymerase as derived from crystal structures and mutagenesis. Journal of molecular biology 278, 57-65.

Rulten, S., Fisher, A., Robert, I., Zuma, M., Rouleau, M., Ju, L., Poirier, G., Reina-San-Martin, B., and Caldecott, K. (2011). PARP-3 and APLF function together to accelerate nonhomologous end-joining. Molecular cell 41, 33-45.

Sekine, A., Fujiwara, M., and Narumiya, S. (1989). Asparagine residue in the rho gene product is the modification site for botulinum ADP-ribosyltransferase. The Journal of biological chemistry 264, 8602-8605.

Seo, G., Kincaid, R., Phanaksri, T., Burke, J., Pare, J., Cox, J., Hsiang, T.-Y., Krug, R., and Sullivan, C. (2013). Reciprocal Inhibition between Intracellular Antiviral Signaling and the RNAi Machinery in Mammalian Cells. Cell host & microbe.

Sharifi, R., Morra, R., Appel, C., Tallis, M., Chioza, B., Jankevicius, G., Simpson, M., Matic, I., Ozkan, E., Golia, B., Schellenberg, M., Weston, R., Williams, J., Rossi, M., Galehdari, H., Krahn, J., Wan, A., Trembath, R., Crosby, A., Ahel, D., Hay, R., Ladurner, A., Timinszky, G., Williams, R., and Ahel, I. (2013). Deficiency of terminal ADP-ribose protein glycohydrolase TARG1/C6orf130 in neurodegenerative disease. The EMBO journal 32, 1225-1237.

Silkworth, W.T., and Cimini, D. (2012). Transient defects of mitotic spindle geometry and chromosome segregation errors. Cell Div 7, 19.
Simonin, F., Höfferer, L., Panzeter, P., Muller, S., de Murcia, G., and Althaus, F. (1993). The carboxyl-terminal domain of human poly(ADP-ribose) polymerase. Overproduction in Escherichia coli, large scale purification, and characterization. The Journal of biological chemistry 268, 13454-13461.
Slade, D., Dunstan, M., Barkauskaite, E., Weston, R., Lafite, P., Dixon, N., Ahel, M., Leys, D., and Ahel, I. (2011). The structure and catalytic mechanism of a poly(ADP-ribose) glycohydrolase. Nature 477, 616-620.
Smith, S., and de Lange, T. (1999). Cell cycle dependent localization of the telomeric PARP, tankyrase, to nuclear pore complexes and centrosomes. Journal of cell science 112 (Pt 21), 3649-3656.
Smith, S., and de Lange, T. (2000). Tankyrase promotes telomere elongation in human cells. Current biology : CB 10, 1299-1302.
Smith, S., Giriat, I., Schmitt, A., and de Lange, T. (1998). Tankyrase, a poly(ADP-ribose) polymerase at human telomeres. Science (New York, NY) 282, 1484-1487.
Sugiyama, M., Costa, M., Nakagawa, T., Hidaka, T., and Ogura, R. (1988). Stimulation of polyadenosine diphosphoribose synthesis by DNA lesions induced by sodium chromate in Chinese hamster V-79 cells. Cancer research 48, 1100-1104.
Suzuki, H., Uchida, K., Shima, H., Sato, T., Okamoto, T., Kimura, T., and Miwa, M. (1987). Molecular cloning of cDNA for human poly(ADP-ribose) polymerase and expression of its gene during HL-60 cell differentiation. Biochemical and biophysical research communications 146, 403-409.
Szántó, M., Brunyánszki, A., Kiss, B., Nagy, L., Gergely, P., Virág, L., and Bai, P. (2012). Poly(ADP-ribose) polymerase-2: emerging transcriptional roles of a DNA-repair protein. Cellular and molecular life sciences : CMLS 69, 4079-4092.
Tanny, J., Dowd, G., Huang, J., Hilz, H., and Moazed, D. (1999). An enzymatic activity in the yeast Sir2 protein that is essential for gene silencing. Cell 99, 735-745.
Trocoli, A., and Djavaheri-Mergny, M. (2011). The complex interplay between autophagy and NF-κB signaling pathways in cancer cells. American journal of cancer ….
Tucker, J., Bennett, N., Brassington, C., Durant, S., Hassall, G., Holdgate, G., McAlister, M., Nissink, J., Truman, C., and Watson, M. (2012). Structures of the human poly (ADP-ribose) glycohydrolase catalytic domain confirm catalytic mechanism and explain inhibition by ADP-HPD derivatives. PloS one 7.
Tulin, A., and Spradling, A. (2003). Chromatin loosening by poly(ADP)-ribose polymerase (PARP) at Drosophila puff loci. Science (New York, NY) 299, 560-562.
Van Ness, B., Howard, J., and Bodley, J. (1980). ADP-ribosylation of elongation factor 2 by diphtheria toxin. NMR spectra and proposed structures of ribosyl-diphthamide and its hydrolysis products. The Journal of biological chemistry 255, 10710-10716.
Vaughan, M., and Moss, J. (1978). Mechanism of action of choleragen. Journal of supramolecular structure 8, 473-488.

Verheugd, P., Forst, A., Milke, L., Herzog, N., Feijs, K., Kremmer, E., Kleine, H., and Lüscher, B. (2013). Regulation of NF-κB signalling by the mono-ADP-ribosyltransferase ARTD10. Nature communications 4, 1683.

Verzijl, N., DeGroot, J., Ben, Z., Brau-Benjamin, O., Maroudas, A., Bank, R., Mizrahi, J., Schalkwijk, C., Thorpe, S., Baynes, J., Bijlsma, J., Lafeber, F., and TeKoppele, J. (2002). Crosslinking by advanced glycation end products increases the stiffness of the collagen network in human articular cartilage: a possible mechanism through which age is a risk factor for osteoarthritis. Arthritis and rheumatism 46, 114-123.

Vyas, S., Chesarone-Cataldo, M., Todorova, T., Huang, Y.H., and Chang, P. (2013). A systematic analysis of the PARP protein family identifies new functions critical for cell physiology. Nature communications 4, 2240.

Wacker, D.A., Frizzell, K.M., Zhang, T., and Kraus, W.L. (2007). Regulation of chromatin structure and chromatin-dependent transcription by poly(ADP-ribose) polymerase-1: possible targets for drug-based therapies. Sub-cellular biochemistry 41, 45-69.

Wahlberg, E., Karlberg, T., Kouznetsova, E., Markova, N., Macchiarulo, A., Thorsell, A.-G., Pol, E., Frostell, Å., Ekblad, T., Öncü, D., Kull, B., Robertson, G., Pellicciari, R., Schüler, H., and Weigelt, J. (2012). Family-wide chemical profiling and structural analysis of PARP and tankyrase inhibitors. Nature biotechnology 30, 283-288.

Wang, Z., Auer, B., Stingl, L., Berghammer, H., Haidacher, D., Schweiger, M., and Wagner, E. (1995). Mice lacking ADPRT and poly(ADP-ribosyl)ation develop normally but are susceptible to skin disease. Genes & development 9, 509-520.

Wang, Z., Michaud, G., Cheng, Z., Zhang, Y., Hinds, T., Fan, E., Cong, F., and Xu, W. (2012). Recognition of the iso-ADP-ribose moiety in poly(ADP-ribose) by WWE domains suggests a general mechanism for poly(ADP-ribosyl)ation-dependent ubiquitination. Genes & development 26, 235-240.

West, R., Moss, J., Vaughan, M., and Liu, T. (1985). Pertussis toxin-catalyzed ADP-ribosylation of transducin. Cysteine 347 is the ADP-ribose acceptor site. The Journal of biological chemistry 260, 14428-14430.

Yamada, M., Miwa, M., and Sugimura, T. (1971). Studies on poly (adenosine diphosphate-ribose). X. Properties of a partially purified poly (adenosine diphosphate-ribose) polymerase. Arch Biochem Biophys 146, 579-586.

Yamanaka, H., Penning, C., Willis, E., Wasson, D., and Carson, D. (1988). Characterization of human poly(ADP-ribose) polymerase with autoantibodies. The Journal of biological chemistry 263, 3879-3883.

Yeh, T.-Y.J., Meyer, T., Schwesinger, C., Tsun, Z.-Y., Lee, R., and Chi, N.-W. (2006). Tankyrase recruitment to the lateral membrane in polarized epithelial cells: regulation by cell-cell contact and protein poly(ADP-ribosyl)ation. The Biochemical journal 399, 415-425.

Yeh, T.-Y.J., Sbodio, J., Tsun, Z.-Y., Luo, B., and Chi, N.-W. (2007). Insulin-stimulated exocytosis of GLUT4 is enhanced by IRAP and its partner tankyrase. The Biochemical journal 402, 279-290.

Yu, M., Schreek, S., Cerni, C., Schamberger, C., Lesniewicz, K., Poreba, E., Vervoorts, J., Walsemann, G., Grötzinger, J., Kremmer, E., Mehraein, Y., Mertsching, J.,

Kraft, R., Austen, M., Lüscher-Firzlaff, J., and Lüscher, B. (2005). PARP-10, a novel Myc-interacting protein with poly(ADP-ribose) polymerase activity, inhibits transformation. Oncogene 24, 1982-1993.

Zhang, Y., Liu, S., Mickanin, C., Feng, Y., Charlat, O., Michaud, G., Schirle, M., Shi, X., Hild, M., Bauer, A., Myer, V., Finan, P., Porter, J., Huang, S.-M.A., and Cong, F. (2011). RNF146 is a poly(ADP-ribose)-directed E3 ligase that regulates axin degradation and Wnt signalling. Nature cell biology 13, 623-629.

Zhao, K., Harshaw, R., Chai, X., and Marmorstein, R. (2004). Structural basis for nicotinamide cleavage and ADP-ribose transfer by NAD(+)-dependent Sir2 histone/protein deacetylases. Proceedings of the National Academy of Sciences of the United States of America 101, 8563-8568.

Zheng, H., and Olive, P. (1996). Reduction of tumor hypoxia and inhibition of DNA repair by nicotinamide after irradiation of SCCVII murine tumors and normal tissues. Cancer research 56, 2801-2808.

Chapter 2. A systematic analysis of the PARP protein family identifies new functions critical for cell physiology

Sejal Vyas[1,2], Melissa Chesarone-Cataldo[1,2], Tanya Todorova[1,2], Yun-Han Huang[2], and Paul Chang[1,2]

[1]Koch Institute for Integrative Cancer Research, [2]Department of Biology, Massachusetts Institute of Technology, Cambridge, MA 02139, USA

S.V. designed and performed PARP localization and knock-down experiments and PAR cell cycle analysis. S.V. and M.C-C designed and performed experiments for PARP14 specific experiments. T.T. determined the effects of PARP12 overexpression on Golgi structure. Y-H.H. generated the full length GFP-PARP14 construct. P.C., S.V. and M.C-C conceived and designed experiments. S.V., M.C-C. and P.C. wrote the manuscript.

Published as
Vyas, S., Chesarone-Cataldo, M., Todorova, T., Huang, Y-H. and Chang, P. (2013). A systematic analysis of the PARP protein family identified new functions critical for cell physiology. *Nat. Commun.* 4, doi 10.1038/ncomms3240.

The poly(ADP-ribose) polymerase (PARP) family of proteins use NAD^+ as their substrate to modify acceptor proteins with adenosine diphosphate-ribose (ADPr) modifications. The function of most PARPs under physiological conditions is unknown. Here, to better understand this protein family, we systematically analyze the cell cycle localization of each PARP and of poly(ADP-ribose), a product of PARP activity, then identify the knockdown phenotype of each protein and perform secondary assays to elucidate function. We show that most PARPs are cytoplasmic, identify cell cycle differences in the ratio of nuclear to cytoplasmic poly(ADP-ribose), and identify four phenotypic classes of PARP function. These include the regulation of membrane structures, cell viability, cell division, and the actin cytoskeleton. Further analysis of PARP14 shows that it is a component of focal adhesion complexes required for proper cell motility and focal adhesion function. In total, we show that PARP proteins are critical regulators of eukaryotic physiology.

Introduction

Post-translational protein modifications such as phosphorylation, ubiquitination, and acetylation are critical for regulating acceptor protein function (Mann and Jensen, 2003). A less well-understood modification is ADP-ribosylation, in which units of ADP-ribose (ADPr) are added onto acceptor proteins using NAD^+ as substrate (Bürkle, 2005). Proteins can be modified by polymers of ADPr (poly(ADP-ribose) or PAR), that vary in length and extent of branching, or by shorter modifications such as mono(ADP-ribose) (MAR). The best known functions of ADP-ribosylation occur during regulation of

cell stress responses such as DNA damage (Malanga and Althaus, 2005), apoptosis (Koh et al., 2005), heat shock (Petesch and Lis, 2008), cytoplasmic stress (Leung et al., 2011) and the unfolded protein response (Jwa and Chang, 2012). However it has become increasingly clear that ADP-ribose modifications are critical for cell physiology under non-stress conditions, since cell division, transcription and chromatin structure regulation all require ADP-ribosylation (Chang et al., 2004; Chang et al., 2005; Schreiber et al., 2006; Hassa and Hottiger, 2008; Chang et al., 2009; Ha et al., 2012).

Poly(ADP-ribose) polymerases (PARPs; also known as ADP-ribosyl transferases (ARTDs)) are a family of enzymes found in eukaryotes and prokaryotes that generate ADP-ribose modifications onto acceptor proteins (Bürkle, 2005; Hassa and Hottiger, 2008; Slade et al., 2011). Humans are thought to express 17 PARPs identified on the basis of sequence homology to the catalytic domain of PARP1 (Amé et al., 2004; Hottiger et al., 2010) (for a summary of PARP/ARTD nomenclature see Table 1). The PARP family is further grouped into four subfamilies based on the presence of functionally characterized domains in regions outside the PARP domain: *DNA-dependent PARPs*, initially thought to require DNA binding for enzymatic activity; *tankyrases*, with protein-binding ankyrin repeats; *CCCH zinc finger PARPs* that contain CCCH zinc finger domains shown to bind viral RNA; and *macro PARPs*, with ADPr-binding macro domains (Karras et al., 2005). The remaining PARPs are referred to as *unclassified PARPs*. A diagram of the PARPs, including motifs and domains, is provided in Figure 1A (a more thorough description of the PARP family is reviewed in Meyer-Ficca et al., 2005; Schreiber et al., 2006; Hassa and Hottiger, 2008; Rouleau et

al., 2010). Both the expression pattern of the various PARPs in human somatic cells and the physiological function of the majority of PARPs have not been established.

Based on the experimental study of a subset of PARPs combined with bioinformatic analysis, each PARP is predicted to exhibit either MAR or PAR synthesis activity, or catalytic inactivity (Kleine et al., 2008). Sequence analysis predicts that DNA-dependent PARPs, tankyrases, and PARP4 generate PAR; PARP9 and 13 are catalytically inactive; and all other PARPs generate MAR (Kleine et al., 2008). Specific amino acid residues that have been identified as targets of PARP modification include glutamic acid, aspartic acid and lysine residues (Barkauskaite et al., 2013).

To better understand the PARPs and PAR, we performed a systems-level analysis of each PARP protein and the PAR polymer, examining localization and expression throughout the cell cycle. We then examined the knock-down phenotype of each PARP and performed follow up analyses to help elucidate function. This work identifies new physiological functions for the PARP family, including the regulation of cell viability, cellular membrane structures, and the actin cytoskeleton. Finally, we closely examined the function of PARP14, a member of the actin cytoskeleton-regulating MacroPARPs. We report that PARP14 is a component of focal adhesion complexes that regulates the strength and stability of cellular attachment to substrate.

Results

Most human PARPs are expressed and most are cytoplasmic

To examine PARP expression levels in human somatic cells, we analyzed transcript abundance using Illumina RNA-sequencing of HeLa cells originally derived from transformed cervical cancer cells, and retinal primary epithelial (RPE1) cells

immortalized via hTERT expression. Fragments Per Kilobase of transcript per Million fragments mapped (FPKM) values for each PARP, poly(ADP-ribose) glycohydrolase (PARG), a PAR hydrolyzing enzyme, and standard normalizing controls (actin and GAPDH), are shown in Table 2. With the exception of PARP15 (omitted from subsequent analyses), all PARPs were expressed in both epithelial cell lines, with relative expression levels varying by several orders of magnitude.

Localization was then analyzed using a library of N-terminal GFP fusions and affinity-purified peptide antibodies generated for each PARP. Specificity of each reagent was cross-verified by staining and blotting GFP-PARP expressing HeLa cells with corresponding anti-PARP antibodies (Supplementary Figure S1). GFP-PARP expressing cells exhibited overlapping GFP and antibody staining patterns when fixed and stained with anti-PARP antibody (Supplementary Figure S1A, S1B). To further confirm that the N-terminal GFP fusions did not disrupt PARP localization, we analyzed the localization of N-terminal fusions of the much smaller streptavidin binding peptide (38 amino acid) to select PARPs. SBP-PARP and GFP-PARP localization patterns were identical (Supplementary Figure S1C). In general, expression of GFP-PARP fusions did not result in cellular phenotypes, however instances where phenotypes were detected are noted below. PARP antibodies verified in this manner were then used to stain interphase (Figure 1B) and mitotic (Figure 1C) cells. Localization was highly similar in HeLa and hTERT-RPE1 cells (Figure 1, Supplementary Figure S2).

Cell cycle localization was then analyzed in RPE1 cells arrested in G_o/G_1, S-phase and mitosis (Supplementary Figure S2B-D). Cell cycle state was confirmed via centrin staining, to identify single centriole pairs present in G_o/G_1 (Vorobjev and

Chentsov Yu, 1982), EdU labeling for S-phase, and tubulin staining to identify mitotic spindles present during mitosis. Most PARPs were cytoplasmic throughout the cell cycle, exhibiting additional enrichment at specific organelles. Six PARPs from three subfamilies localized to the centrosome: PARP2 and 3 in G_o/G_1 (Supplementary Figure S2B; centrosomal localization for PARP3 and 5a were previously identified (Smith and de Lange, 1999; Augustin et al., 2003), PARP11 and PARP5b during mitosis (Supplementary Figure S3A), and PARP5a and 8 throughout the cell cycle (Supplementary Figure S3A). Multiple PARPs and the previous identification of PARG at this site suggest that ADPr is actively regulated there (Ohashi et al., 2003). Five PARPs from three subfamilies localized to membranous organelles: PARP8 to nuclear envelope, PARP12 to Golgi (Supplementary Figure S3B), PARP9 and 14 to plasma membrane (Supplementary Figure S3C) and PARP16 to endoplasmic reticulum (Supplementary Figure S3D). Finally, 4 PARPs from two subfamilies localized to the mitotic spindle: PARP5a and 5b and unclassified PARP8 and 11 localized to spindle poles (Smith and de Lange, 1999; Chang et al., 2005, 2009) (Supplementary Figure S3A). PARP localization, largely consistent with knock-down phenotypes, is summarized below and in Table 1.

All DNA-dependent PARPs were nuclear during interphase, with PARP2 and 3 exhibiting additional cytoplasmic localization (Figure 1B). Consistent with previous studies (Augustin et al., 2003; Rouleau et al., 2007), PARP3 localization varied with the cell cycle, with centrosomal and nuclear enrichment in G_o/G_1 and cytoplasmic enrichment in S-phase (Supplementary Figure S2B, S2C). During mitosis, PARP1 was

enriched at chromatin, and PARP2 and 3 were cytoplasmic (Figure 1C, Supplementary Figure S2D).

Both tankyrases localized to cytoplasmic puncta during interphase (Figure 1B). During mitosis, PARP5a and 5b localized to the mitotic spindle pole (Kaminker et al., 2001; Chang et al., 2005). We identified additional localization for PARP5b throughout the spindle (Figure 1C, Supplementary Figure S2D).

The CCCH Zn finger PARPs were primarily cytoplasmic during interphase, exhibiting punctate localizations (Figure 1B). In addition, PARP7 localized to nuclear foci, PARP12 exhibited juxtanuclear localization resembling Golgi staining, and PARP13 exhibited a ~4-5 fold variability in expression between clusters of cells, suggesting clonal variability (Figure 1B). Cells expressing high concentrations of GFP-PARP12 and 13 assembled stress granules in the cytoplasm as previously described (Leung et al., 2011). PARP12 localization to the Golgi was confirmed by co-localization with trans Golgi protein p230 (Supplementary Figure S3B). Overexpression of GFP-PARP12 blocked PARP12 localization to the Golgi and disrupted Golgi structure, analyzed via staining of p230, a trans Golgi marker (Supplementary Figure S4A, S4B). While p230 staining intensity was unaltered in cells overexpressing GFP-PARP12, Golgi area increased ~1.58 fold relative to control cells. No such defects were found in untransfected, GFP-overexpressing and GFP-PARP13.2 overexpressing cells suggesting that the Golgi defects were specific to PARP12 overexpression (Supplementary Figure S4B). During mitosis, all CCCH Zn finger PARPs localized to the cytoplasm (Figure 1C, Supplementary Figure S2D).

Macro PARPs 9 and 14 were primarily cytoplasmic with additional nuclear localization consistent with previous studies (Figure 1B) (Goenka and Boothby, 2006; Juszczynski et al., 2006; Yanagawa et al., 2007). Nuclear PARP9 staining was highly enriched in S-phase arrested cells (Supplementary Figure S1A, S2C) suggesting that the previously described nucleo-cytoplasmic shuttling of PARP9 might be cell cycle-regulated (Juszczynski et al., 2006). In addition, PARP9 and 14 exhibited enriched localization at the cell periphery (Figure 1B). Both proteins were later confirmed to co-localize with actin filaments, motile elements of the actin cytoskeleton that are enriched at the cell periphery (Supplementary Figure S3C). Such enrichment was particularly prominent in cells fixed with 10% Trichloroacetic acid (TCA), conditions ideal for staining cortical proteins (Yonemura et al., 2004) (Supplementary Figure S3C). During mitosis, all macro PARPs were cytoplasmic; PARP9 staining was diffuse while PARP14 staining was punctate (Figure 1C, Supplementary Figure S2D).

Previous reports identified cytoplasmic localization for PARP4 (Kickhoefer et al., 1999), and cytoplasmic and nuclear localizations for PARP10, with a nuclear enrichment upon inhibition of nuclear export (Yu et al., 2005). Each unclassified PARP localized to cytoplasm during interphase, with PARP4 and 11 exhibiting additional nuclear localization (Figure 1B). PARP4 staining at the nucleus is likely non-specific as knock-down of PARP4 (see below) resulted in reduction of cytoplasmic, but not nuclear signal (Figure 3). PARP8 was enriched at the nuclear envelope in fixed cells (Figure 1B) and cells expressing high concentrations of GFP-PARP8 exhibited nuclear accumulation of the protein (Supplementary Figure S1A, B). PARP10 was punctate in the cytoplasm and largely absent from the nucleus. Similar to PARP13, PARP10

expression varied ~6-7 fold among small clusters of cells (Figure 1B). Cells with increased expression of PARP10 exhibited strong cytoplasmic juxtanuclear staining. Finally, PARP16 exhibited reticular membrane localization that co-localized with DiI, consistent with our previous results identifying it as an endoplasmic reticulum protein (Jwa and Chang, 2012) (Supplementary Figure S3D). Cells expressing high concentrations of GFP-PARP16 contained DiI positive membrane structures as previously shown (Jwa and Chang, 2012) (Supplementary Figure S4C).

During mitosis, all unclassified PARPs localized throughout the cytoplasm. With the exception of PARP4, cytoplasmic staining was punctate (Figure 1C, Supplementary Figure S2D). PARP8 and 11 exhibited strong staining at the spindle poles as shown by co-staining with centrin (Figure 1C, Supplementary Figure S3A). No centriolar staining was identified for PARP11 during interphase, suggesting the localization is specific to mitosis (Figure 1C, Supplementary Figure S3A).

Poly(ADP-ribose) is found throughout the cell

The predominant cytoplasmic localization of the PARPs and their cell cycle dependent localization patterns suggested that previously undetected cytoplasmic ADPr, generated in a cell cycle dependent manner, could exist. Since reagents to label MAR are not well characterized (Meyer and Hilz, 1986; Karras et al., 2005), we focused on PAR, for which several well-characterized antibodies are available.

We examined PAR localization in asynchronous, G_0/G_1, S-phase, and mitosis arrested HeLa cells, and HeLa cells treated with H_2O_2 to induce DNA damage, resulting in upregulated PAR synthesis in the nucleus (Junod et al., 1989) (Figure 2A,

Supplementary Figures S5A & S5C). Cells were fixed with methanol (MeOH) or 20% TCA to minimize post-fixation PAR synthesis then stained with two antibodies generated against distinct PAR antigens: Tulip chicken anti-PAR IgY (Figure 2A) and BD rabbit anti-PAR (Kirsten et al., 2004) (Supplementary Figure S5C). Cell cycle arrest was verified as above. Each fixation condition and antibody yielded similar results.

Significant amounts of PAR were detected in both cytoplasm and nucleus of asynchronous cells, H_2O_2 treated cells, and during all cell cycle stages (Figure 2A, Supplementary Figure S5A & S5C). Staining in the interphase cytoplasm and nucleus appeared both diffuse and punctate, with increased nuclear PAR staining during S-phase. Such staining was punctate and distinct from nuclear staining during other cell cycle stages suggesting S-phase specific functions for these puncta. In addition, PAR was also significantly enriched at the interphase centrosome and mitotic spindle poles, consistent with PARP localization described above, and previous results (Kanai et al., 2003; Chang et al., 2004; Chang et al., 2005, 2009) (Figure 2A, Supplementary Figure S5C).

To biochemically validate cell cycle dependent differences in PAR concentrations between the cellular compartments, the nuclear to cytoplasmic ratio of PAR was determined by generating nuclear and cytoplasmic extracts from H_2O_2 treated, asynchronous, and G_o/G_1 and S phase-arrested cells. Extracts were immunoblotted with chIgY and BD anti-PAR (Figure 2B, Supplementary Figure S5B & S5D), and the nuclear to cytoplasmic PAR ratios determined by integrating signal intensities of each lane of the blots (Figure 2C, n=3). During G_o/G1, the ratio was 0.57 +/- 0.11 and 0.51 +/- 0.15 for the chIgY and BD PAR antibodies respectively, and during S-phase this

ratio increases to 1.3 +/- 0.33 and 1.2 +/- 0.39 respectively for each antibody. During DNA damage the ratio of nuclear to cytoplasmic PAR is 2.03 +/-0.55 and 1.94+/-0.29 for chIgY and BD PAR antibodies respectively. Additionally, immunoblotting for PAR in asynchronous and mitotically arrested cells demonstrated increased PAR concentrations during mitosis, consistent with previous reports (Chang et al., 2009) (Figure 2B, Supplementary Figure S5D). Thus significant amounts of PAR exist in the cytoplasm, and the relative amounts of PAR in the cytoplasm and nucleus change with the cell cycle.

PARP knock-down phenotypes

We next examined the phenotypes of PARP knock-down via RNAi, focusing on changes in cell viability and morphology. For PARPs with unpublished phenotypes, at least eight siRNAs were generated. To verify phenotypes, at least two siRNAs demonstrating > 80% protein knock-down via immunoblot and cell staining were required to result in similar phenotypes (Figure 3A, 3B, Table S1). For PARPs 1, 2, 3, 4, 5a, 5b and 7, published siRNA sequences were utilized (Chang et al., 2005; Neumann et al., 2010). Published shRNA sequences for PARP10 knock-down were ineffective in our siRNA assays, therefore new siRNAs were screened (Chou et al., 2006). In all cases non-targeting siRNAs were used as control.

Cell viability was examined via seed assay in which PARPs were knocked-down, total cell number quantitated, and cells replated at the same density. Cell number was determined 24 or 72h post seeding and the ratio of cell number at each time point to initial seed number used to assess defects in cell viability. PARP knock-downs that

resulted in a fold change of at least two standard deviations were considered to cause viability defects (Figure 3C).

Cell morphology was assayed by comparing PARP and DNA staining in control and knock-down cells, then verified by follow-up assays. In total, both assays identify four phenotypes upon PARP knockdown: decreased cell viability, defects in the actin cytoskeleton, defects in internal membrane structure, and defects in mitosis.

Knock-down of individual DNA-dependent PARPs did not result in observable changes in cell viability or morphological defects suggesting that each is non-essential (Figure 3A, 3C).

PARP5a knock-down resulted in mitotic arrest, increased mitotic index confirmed by phosphoH3 staining (~13% mitotic index in knock-down cells vs. ~3% in control) and decreased cell viability (Figure 3A & 3C), consistent with our previous results and work by others (Dynek and Smith, 2004; Chang et al., 2005, 2009; Ha et al., 2012). PARP5b knock-down did not result in observable phenotypes or decreased viability (Figure 3A, 3C).

Consistent with previous reports, PARP7 knock-down resulted in increased mitotic index confirmed by phosphoH3 staining (~6% in knock-down cells vs. ~3% in control) (Neumann et al., 2010) (Figure 3A, Supplementary Figure S6). A significant decrease in cell viability was not observed in PARP7 knock-downs, suggesting that knock-down cells are able to undergo mitosis (Figure 3C). Neither PARP12 nor 13 knock-down resulted in morphological phenotypes, however PARP13 knock-down resulted in significantly decreased cell viability (Figure 3A,C).

Knock-down of each macro PARP resulted in cell morphology defects (Figure 3A). Roughly 25% of PARP9 knock-down cells exhibited pronounced membrane blebbing phenotypes. This phenotype was not likely due to apoptosis, as a substantial increase in apoptotic nuclei, identified by the presence of highly condensed DNA via Hoescht staining, was not observed (~3.5% in PARP9 knock-downs vs. 1% in control) (Figure 3A). PARP14 knock-down resulted in decreased cell viability (Figure 3C) and dramatic alterations in cell morphology, as ~60% of cells had elongated processes extending far from the cell body (Figure 3A, see below).

Knock-down of PARP4, 6 and 10 did not result in obvious morphological defects or decreased cell viability (Figure 3A, 3C). In contrast, PARP8 and 16 knock-down resulted in cell morphology defects, with ~50% of PARP8 knock-downs and ~30% of PARP16 knock-down cells appearing completely round (Figure 3A). PARP16 knock-down cells exhibiting the round cell phenotype were always found in pairs while round PARP8 knock-downs were individual cells. PARP8 knock-down resulted in the most pronounced decrease in cell viability of all PARPs (Figure 3C). PARP11 siRNAs were ineffective for knock-down and therefore we cannot report on phenotype.

PARP knock-down phenotypes identify new cellular functions

Cell morphology phenotypes identified in initial RNAi screens led us to design secondary assays to better understand function. Macro PARP knock-down phenotypes were reminiscent of actin cytoskeletal misregulation (Fackler and Grosse, 2008; Pollard and Cooper, 2009). We therefore stained control, PARP9 and 14 knock-down cells with phalloidin, a filamentous actin (F-actin) label (PARP9 knockdowns), or an actin

antibody (PARP14 knock-downs) (Figure 4). In control cells, PARP9 strongly co-localized with F-actin at the cell cortex, while PARP14 localized to the ends of actin fibers specifically at cell protrusions in a staining pattern consistent with focal adhesion structures (Figure 4, arrowheads). Both PARP9 and 14 knock-downs exhibited highly abnormal F-actin staining suggesting functions in actin cytoskeletal regulation; PARP9 knockdowns contained multiple actin-rich membrane blebs and PARP14 knock-down cells exhibited highly elongated actin-rich processes (Figure 4, arrows; Supplementary Figure S3C). These results are consistent with previous reports implicating this subfamily in the regulation of cell migration in B-cell lymphomas (Aguiar et al., 2000).

The round cell phenotypes suggested that PARP8 and 16 knockdowns exhibited defects in membrane structure. Due to its nuclear envelope localization, we stained control and PARP8 knock-down cells with an antibody against the nuclear envelope protein Lamin A/C. PARP8 staining co-localized with Lamin A/C in control cells, and was largely undetectable at the nuclear envelope after PARP8 knockdown. The average size of nuclei in PARP8 knock-down cells was slightly smaller than control cells (~180 +/- 50 μm^2 in knock-downs, n=360 cells vs. 205 +/- 54 μm^2 in controls, n=282 cells). Lamin A/C staining identified multilobed nuclei in the knockdowns (~14% in knock-downs vs. 0.7% in controls, n>400 cells) suggesting structural defects in the nuclear envelope, or a misregulation of nuclear envelope biogenesis (Figure 4). Together PARP8 localization to the nuclear envelope and the defects in nuclear envelope structure upon knockdown suggest that it is a critical nuclear envelope protein. PARP16 knockdown resulted in the accumulation of pairs of round cells, reminiscent of defective cytokinesis. PARP16 localization to membrane prompted us to examine

membrane structure in the PARP16 knock-downs by staining with DiI (Figure 4). Total intensity of DiI staining was unchanged, however PARP16 knock-downs exhibited a disruption of organized reticular membrane staining (Figure 4), perhaps a result of the dramatic change in cell morphology. It is unclear if this phenotype relates to PARP16 function in the unfolded protein response (Jwa and Chang, 2012), however activation of the unfolded protein response is known to result in cytokinesis defects in *S. cervisiae* (Bicknell et al., 2007).

PARP5a and 7 knock-downs were stained for tubulin to examine spindle structure. Consistent with previous results, control cells exhibited PARP5a staining at spindle poles, and knock-down cells lacking PARP5a staining at spindle poles contained multiple microtubule foci and improperly aligned chromosomes (~58% of mitotic cells with improperly aligned chromosomes for knock-downs vs. 3% in controls, n>30 mitotic cells) (Dynek and Smith, 2004; Chang et al., 2005, 2009) (Figure 4, Supplementary Figure S6). In contrast, PARP7 did not localize to the mitotic spindle in control cells. Tubulin staining of PARP7 knock-downs revealed a disproportionate increase in pre-metaphase cells among mitotic cells (~57% in PARP7 knock-down vs. ~19% in controls, n>50 mitotic cells), a mitotic defect distinct from that of PARP5a knock-down (Figure 4, Supplementary Figure S6). Since the increase in mitotic index was mild (~6% vs. ~3% for control cells) and PARP7 knock-down did not significantly decrease cell viability, our results suggest that PARP7 is not required for spindle function, but that its knock-down increases the length of pre-metaphase mitosis.

PARP14 is a focal adhesion protein

The PARP14 knock-down phenotype was particularly striking prompting us to closely examine its function in actin cytoskeletal regulation. Both PARP14 siRNAs resulted in cells that were elongated and contained dendritic-like membrane protrusions emanating from the cell body (Figure 5A, B). These extended cellular protrusions were substantial- PARP14 knock-downs measured ~3 times longer than control cells (n=20 cells) (Figure 5B). Greater than 60% of PARP14 knock-down cells exhibited these extended protrusions in contrast to control knock-down cells that contained similar protrusions in ~5% of the population (n=3, 200 cells counted for each condition) (Figure 5B).

To better understand how these extended protrusions were generated, we analyzed control and PARP14 knock-downs using real-time imaging. In control cells, small membrane protrusions were generated and quickly retracted as cells moved in different directions (Figure 5C, Supplementary **Movie 1)**. In PARP14 knock-downs, cells appeared unable to retract protrusions efficiently, resulting in highly elongated extensions (Figure 5C, Supplementary **Movie 2)**. Thus, abnormal membrane protrusions appeared to result from defective retraction of protrusions normally generated in migrating cells. Retraction of protrusions was so defective in PARP14 knock-downs that cells stretched into severely elongated shapes as they explored the substrate (Figure 5C, Supplementary **Movie 2)**.

A major control point in cell migration is the assembly, maturation and disassembly of focal adhesions (FA)s, multi-protein complexes that serve as connections between the substrate and the actin cytoskeleton (Burridge et al., 1988). FA regulation requires the ordered recruitment of FA proteins and the strength and

stability of FAs depends on the protein composition of the FA (Kuo et al., 2011). Cells must balance FA strength so that adhesions are strong enough to pull the cell forward, but sufficiently labile so that they can be rapidly disassembled as the cell moves. The PARP14 knock-down phenotype suggested defects in FA function.

A previous proteomic study identified PARP14 protein in purified FAs isolated from HFF-1 cells, consistent with the PARP14 staining at cell protrusions we observed (Kuo et al., 2011) (Figure 4, Supplementary Figure S3C). We therefore examined PARP14 localization at FAs in HeLa cells grown on fibronectin coated coverslips (to mimic extra-cellular substrate). Cells were fixed and stained with antibodies against PARP14 and known FA components. PARP14 localized to the ends of actin stress fibers, similar to other FA proteins, and co-localized with Vinculin, VASP and Paxillin (Figure 5D). The specificity of PARP14 localization at FAs was confirmed by examining PARP14 antibody staining at FAs after targeted knock-down (Figure 5E). PARP14 knock-down resulted in near complete depletion of PARP14 staining at FAs, while VASP staining was maintained. In addition to validating the specificity of PARP14 localization to the FA, this result also indicates that PARP14 is not required for general FA assembly (Figure 5E). Importantly, such siRNA treatments did not deplete cytoplasmic or nuclear PARP14 staining, suggesting that staining at these locations is either non-specific or represents siRNA-resistant populations of PARP14.

PARP14 regulates focal adhesion function

For cells to properly retract membrane protrusions, they must be able to efficiently breakdown FAs in a process called FA turnover (Webb et al., 2004). The

inability of PARP14 knock-down cells to properly retract membrane protrusions, combined with its localization to FAs, suggested that PARP14 functions in FA turnover. Therefore we examined FA adhesive force in control and PARP14 knock-downs using three independent assays. First we utilized a trypsin-based detachment assay measuring time required to detach cells from substrate (Bhattacharya et al., 2009). PARP14 knock-down cells were more resistant to trypsinization than controls, with ~ 2 times more cells remaining adhered after similar periods of trypsinization (Figure 6A). Second we employed a centrifugation assay comparing the number of cells remaining adhered to substrate after constant application of centrifugal force. Approximately 5 times more PARP14 knock-down cells remained adhered to substrate after centrifugation compared to controls (Figure 6B). Third, we used a cell-spreading assay measuring the area of cell spreading per unit time (Figure 6C). At early time points when cells adhered to substrate but had not yet formed defined FAs, control and PARP14 knock-downs were of similar size suggesting that the morphological defects observed in PARP14 knock-downs were dependent on FA formation and not simply a property of the cells themselves. As cells assembled FAs and spread onto substrate, PARP14 knock-down cells covered ~twice the surface area of control cells at each time point (Figure 6C). These three independent assays suggest that the adhesive strength between FAs and substrate is stronger in PARP14 knock-downs relative to control. It is likely that this increased adhesive strength leads to slowed FA disassembly and prevents cellular protrusions from properly retracting.

Discussion

The initial bioinformatic identification of 17 human PARP genes suggested that PARPs function in more biological pathways than previously imagined (Amé et al., 2004; Otto et al., 2005). Our analysis confirms the diversity of PARP function and leads to several important conclusions regarding the protein family. First, nearly all (16 of 17) of the PARPs predicted to exist in humans are expressed in epithelial cells collected from the retina and cervical tumors- tissues of diverse origin. This suggests ubiquitous expression of most PARPs among human tissues. Second, PARPs are predominantly cytoplasmic proteins, and a significant amount of one product of PARP activity, PAR, is present in the cytoplasm. Third, PAR synthesis/hydrolysis appears to be cell cycle regulated as the ratio of PAR synthesis/hydrolysis in the nucleus and cytoplasm changes during specific cell cycle stages. This suggests cell cycle specific functions for PAR. Finally, PARP proteins are important regulators of somatic cell physiology and function in multiple diverse pathways.

The importance of nuclear PARP function in the physiology of the cell is well established. PARP1/PARP2 regulate critical physiological functions in the nucleus, and while neither PARP1 nor PARP2 are essential for life, PARP1/2 double knockout mice are non-viable suggesting that the activity of a least one of these PARPs is essential (de Murcia et al., 1997; Ménissier de Murcia et al., 2003). Our data suggests that PARP function in the cytoplasm is equally important. All multicellular eukaryotes encode both nuclear and cytoplasmic PARPs with vertebrates containing the most PARPs (Citarelli et al., 2010). The additional PARPs found in vertebrates are cytoplasmic, and each PARP identified as essential for cell viability is found in the cytoplasm of all vertebrates

suggesting that vertebrate evolution led to an increased requirement for cytoplasmic PARP function (Citarelli et al., 2010).

Each of the PARP knock-down phenotypes points to a remarkable diversity of function among this family of proteins. Such diversity is likely conferred by the diverse functional domains present outside of the conserved PARP domain, such as the DNA binding domains of DNA dependent PARPs, and the ADP-ribose binding Macro domains of the Macro PARPs (Karras et al., 2005). The similarity of localization and function of subfamily members demonstrates the importance of these functional domains and suggest that in addition to previously described roles in regulation of PARP enzymatic activity they can target PARPs to specific cellular locations (Loseva et al., 2010; Gibson and Kraus, 2012) (Figure 1A and Table 1).

The defects in cell viability in PARP5a, 8, and 14 knockdowns are not surprising given their phenotypes. In contrast, PARP13 knock-downs did not result in obvious morphological defects, thus its requirement for cell viability is unclear. PARP13 has been shown to be an important regulator of mRNA, targeting viral RNA for degradation, and regulating cellular mRNA post-transcriptionally by regulating miRNA activity (Guo et al., 2007; Leung et al., 2011). Since cell cycle progression is regulated by miRNA activity it is possible that the decreased cell viability resulting from PARP13 knock-down results from misregulation of miRNA function or that the cell viability defect is due to general misregulation of mRNA metabolism (Cirera-Salinas et al., 2012).

Our PARP8, 12 and 16 data suggest potential functions for PARPs in the assembly or maintenance of membranous organelles. Each of the structures to which PARP8, 12 and 16 localize are derived from endoplasmic reticulum, and require

trafficking from the endoplasmic reticulum for function, processes regulated by glycosylation (Sciaky et al., 1997). Perhaps ADP-ribose could serve a similar function as glycosylation in vesicle trafficking either by functioning as a trafficking signal, or by regulating glycosylation of target proteins.

Finally, Macro PARPs had been postulated to regulate B cell motility via unknown mechanisms, with overexpression of PARP9 resulting in increased migration of B-cell lymphomas (Aguiar et al., 2000). Our results provide a potential explanation for these observations by demonstrating that macro PARPs localize to the motile elements of the actin cytoskeleton and exhibit cytoskeletal defects upon knock-down. Interestingly, PARP14 expression is upregulated in multiple myelomas and has been shown to regulate IL-4 mediated B-cell survival (Cho et al., 2011; Barbarulo et al., 2013). As such, PARP14 has been mentioned as a possible target for therapeutic inhibition of multiple myelomas. It is unclear if there is a connection between this specific PARP14 function in these specialized cell types and PARP14 function at FAs. However, it is possible that inhibiting the enzymatic activity of PARP14 could also affect cellular adhesiveness, making PARP14 an attractive target for the therapeutic inhibition of metastatic cancers in addition to multiple myelomas.

Materials and Methods

Cell Culture and Reagents

Cells were grown at 37°C and 5% CO_2. HeLa cells (ATCC) were passaged in DMEM + 10% fetal bovine serum (FBS) (Tissue Culture Biologicals) + penicillin/streptomycin (Invitrogen); hTERT-RPE1 cells (ATCC) in Ham's F12/DMEM (1:1) (Mediatech) + 10% FBS, penicillin/streptomycin, and 0.01mg/mL hygromycin B (Invitrogen). Anti-PARP

peptide antibodies were generated and affinity purified using a standard protocol (Harlow and Lane, 1999). Antibodies (stored at 1mg/ml) were used at 1:100 for IF and 1:1000 for IB. Additional antibodies used were anti-pADPr (chIgY, Tulip Biolabs, 1:100 IF, 1:500 IB; 51-811KD, BD Pharmingen, 1:100 IF, 1:500 IB), anti-PARP1 (PA3-951, Affinity Bioreagents, 1:1000 IB), anti-PARP5a (H350, Santa Cruz, 1:100 IF, 1:1000 IB), anti-PARP14 (HPA012063, 1:100 IB; HPA008846, 1:100 IF, Sigma Aldrich), anti-GFP (ab1218, Abcam 1:100 IF; JL8, Clontech 1:2500 IB), anti-Tubulin (YL1/2, Abcam, 1:1000 IF, 1:5000 IB), anti-lamin A/C (ab8984, Abcam, 1:100 IF), anti-actin (A3853, Sigma Aldrich, 1:100 IF), anti-vasp (a kind gift from F. Gertler, 1:500 IF), anti-zyxin (ab71842, Abcam, 1:200 IF), anti-paxillin (610051, BD Biosciences, 1:1000 IF), anti-vinculin (Sigma Aldrich, 1:200 IF), anti-p230 (611280, BD Transduction Laboratories, 1:200), anti-gamma tubulin (GTU88, Sigma-Aldrich, 1:10000 IF), anti pH2AX (05-636, Millipore, 1:100 IF), anti-centrin (a kind gift from J. Salisbury, 1:1000 IF), anti-SBP (ab119491, Abcam, 1:500 IF). Secondary antibodies, phalloidin, DiI, EdU labeling kit and Hoechst 33342 were from Invitrogen. siRNA oligonucleotides were purchased from Invitrogen (Stealth or Silencer Select) or Dharmacon (siGenome) (Table S1).

Transfections

HeLa cells were transfected using Lipofectamine 2000 (Invitrogen) according to manufacturer protocols. For RNAi of PARPs-1-4, HeLa cells were transfected with 20 nM siRNA for at least 24 h prior to splitting onto coverslips. Knock-down analysis was performed 48 h post transfection. For PARPs 5a-16, HeLa cells were transfected with 20 nM siRNA for at least 24 h. Cells were split and re-transfected the following day with identical concentrations of siRNA for 24 h prior to splitting. Knock-down analysis was

performed 96 h after initial transfection. AllStars negative control siRNA (Qiagen) was used as control. For further validation of PARP14 knock-down phenotype, HeLa cells were transfected with 25nM siRNA and allowed to incubate in transfection mixture for at least 48 hr prior to splitting.

Immunofluorescence

For all transfections, cells were plated on coverslips 6 h post transfections. For G_0/G_1 arrests, cells were plated at 50% confluence and serum starved for 72 h. For S phase arrest, cells were treated with 5 µg/mL aphidicolin for 16 h. For mitotic arrest, cells were treated with either 200 or 400 nM nocodazole for 16 h. Coverslips were fixed in either -20° MeOH for 5 min, 10 or 20% TCA (Fluka) for 15 min at 4°, or 4% formaldehyde (Polysciences) in PBS (Invitrogen) for 15 min followed by extraction with 0.5% Triton-X100 (Sigma) in PBS for 10 min. For validation of PARP14 localization, cells were grown on fibronectin coated coverslips and fixed in 10% TCA. Coverslips were blocked in abdil (PBS containing 4% BSA, 0.1% Triton X-100, and 0.02% sodium azide) then incubated with primary and secondary antibodies for 45 min. All antibody dilutions were generated in abdil. For quantitation of golgi area in PARP12 overexpression and nuclear area in PARP8 knock-downs, NIS-Elements software was used to generate a region of interest around the golgi/nucleus and the area of the ROI was determined.

Viability Assay

Following RNAi knock-down, cells were counted using a Cellometer automated cell counter then normalized and split in duplicate. Living cells were then counted after 24 and 72 h using trypan blue exclusion and a Cellometer automated cell counter. Viability was assessed by calculating the fold change in cell number relative to cell number

initially seeded. PARPs whose knock-down resulted in a decrease in fold change compared to control knock-down of at least two standard deviations were considered to have an effect on viability. Three independent experiments were performed for viability analysis.

Real Time Imaging

Control and PARP14 knock-down HeLa cells were split into 6 well glass bottom plates (Greiner Bio-One) coated with fibronectin and grown overnight. Cells were rinsed with PBS and changed into CO_2-independent medium containing 10% FBS (Invitrogen) for imaging. Brightfield images were collected every 5 min for 16 hrs. All live imaging was preformed using a Nikon TiEclipse microscope equipped with an environmental chamber with CO_2 and temperature control and Hamamatsu ORCA R^2 digital camera.

Cell adhesion assays

For trypsin-based assays, cells were sparsely seeded onto fibronectin coated plates and then incubated overnight. The next morning, the number of cells in each well was calculated. Cells were washed 2x with PBS and then treated with 0.025% trypsin in DMEM. At the indicated time points, the number of cells released into the media and the number of cells remaining on the plate was counted.

For centrifugal-based assays, cells were cells were sparsely seeded onto fibronectin coated plates and then incubated overnight. The next morning, the number of cells in each well was calculated. Cells were washed 3x with PBS and then centrifuged inverted for 30 min at 2,000 g. The number of cells remaining in each well after centrifugation was then counted.

For cell spreading assays, plated cells were gently trypsinized, resuspended in DMEM,

and then allowed to recover for 10 min at 37^0C. Cells were then very sparsely seeded onto fibronectin coated-coverslips. At the indicated time points after plating, coverslips were gently washed with PBS, then fixed and stained.

RNA sequencing

Total RNA was purified from HeLa and hTERT-RPE1 cells using a Qiagen RNeasy kit. The samples were poly-A purified and cDNA libraries were synthesized using the Illumina Tru-Seq protocol. The libraries were sequenced on Illumina HiSeq2000 obtaining 40nt single end reads. The reads were mapped to the Human genome (hg19) using bowtie2 version 2.0.0-beta6, samtools version 0.1.18 and tophat version 2.0.4.

Acknowledgments

The authors wish to dedicate this paper to the memory of Officer Sean Collier, for his caring service to the MIT community and for his sacrifice. We apologize to those that we were unable to cite due to space limitations. We thank A. West, and T. Sangpo for technical support; C. Whittaker of the Bioinformatics and Computing Facility at the Swanson Biotechnology Center, David H. Koch Institute for Integrative Cancer Research at MIT, for computational analysis; J. Rood, P. Ohi, J. Saeij, M. Vander Heiden and F. Solomon for comments. Funding for this project was provided while P.C. was a Rita Allen Foundation Scholar, a Kimmel Foundation for Cancer Research Scholar, and a Howard S. and Linda B. Stern Career Development Assistant Professor. This work was partially supported by Cancer Center Support (core; grant P30-CA14051), RO1GM087465 from the National Institutes of Health to PC, and funds from the Jeptha H and Emily V. Wade Fund, and Curt and Kathy Marble to P.C. M.C-C. was partially supported by NIH Grant 1F32GM103089-01.

Figures and Tables

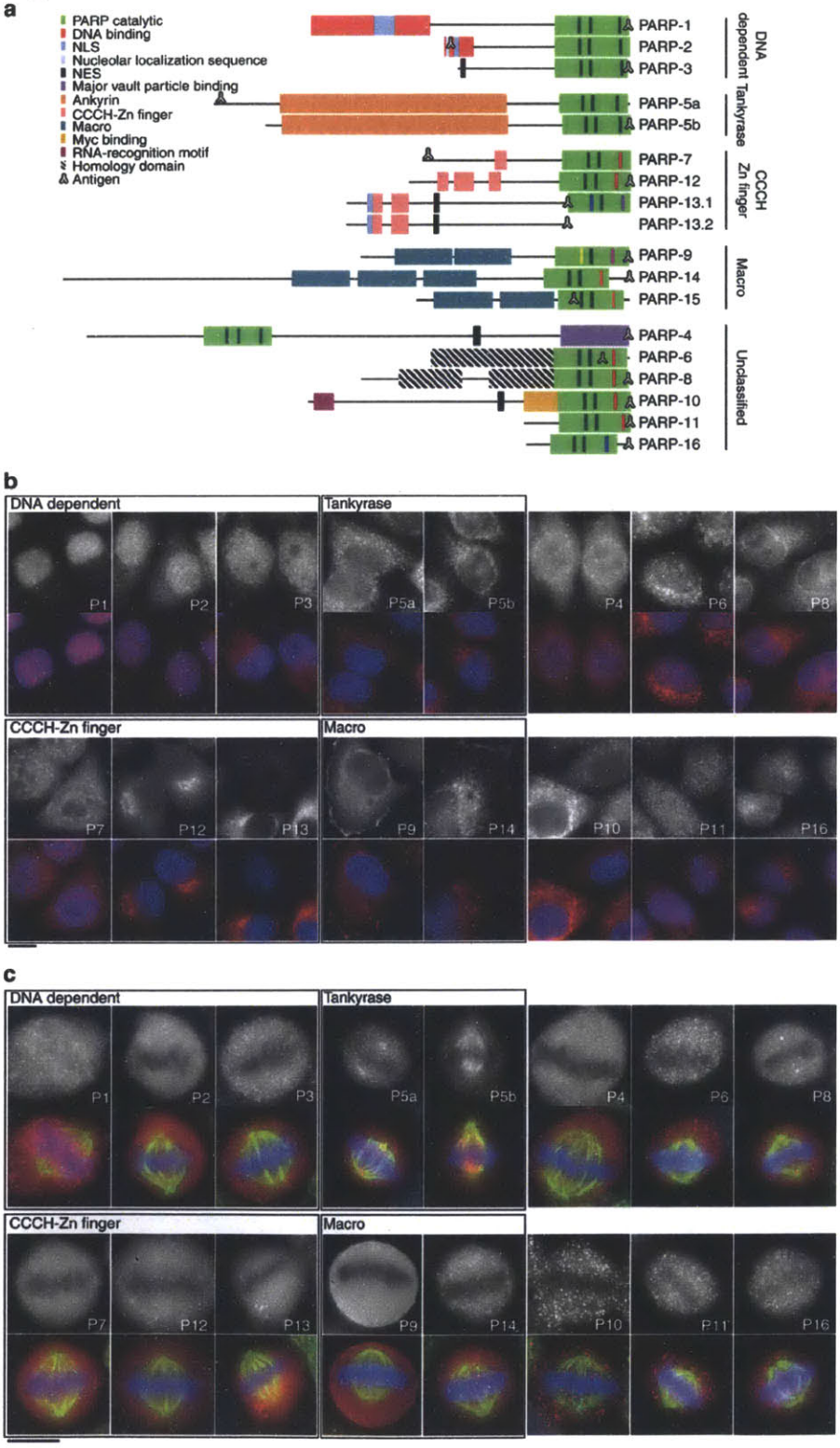

Figure 1. PARPs localize throughout the cell

A) Domain structure of PARP proteins. Functional domains are indicated and green dashes within the catalytic domain indicate H-Y-E amino acids thought to be required for PAR synthesis activity. Dashes with different colors indicate the replacement of these amino acids with the following residues: I (red), Y (blue), V (purple), Q (yellow), T (pink), L (orange). B-C) HeLa cells were fixed then stained with affinity-purified antibodies generated against each PARP. Data is presented in PARP subfamily groupings, labeled in boxes, with each PARP labeled as P(x). A summary of localization patterns is provided in Table 1. B) Interphase localization of PARP proteins. Most PARPs are cytoplasmic (top). Merge (below) shows PARP (red) and Hoechst 33342 staining (blue). C) PARP localization in mitotic cells (top). A subset of PARPs localize to the mitotic spindle (P5a, 5b, 8,11). Merge (below) shows PARP (red), tubulin (green) and Hoechst 33342 (blue) staining. Scale bars, 10 μm. See also Supplementary Figures S1-S3 and Tables 1-2.

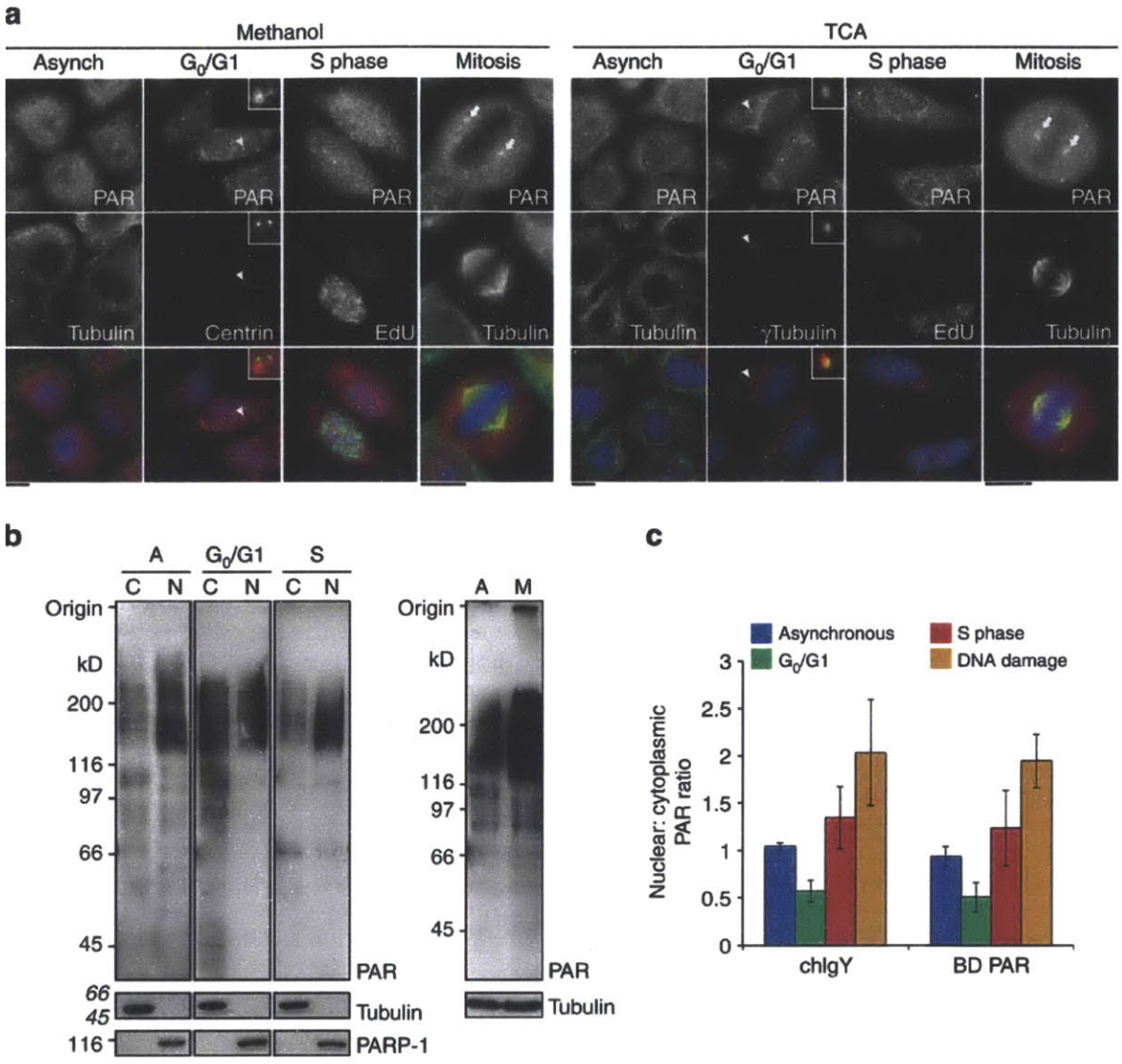
a
Methanol
TCA
Asynch
G0/G1
S phase
Mitosis
PAR
Tubulin
Centrin
EdU
γTubulin
b
A
G0/G1
S
C N C N C N
Origin
kD
200
116
97
66
45
PAR
Tubulin
PARP-1
A M
c
Asynchronous
S phase
G0/G1
DNA damage
Nuclear: cytoplasmic PAR ratio
3
2.5
2
1.5
1
0.5
0
chIgY
BD PAR

Figure 2. Poly(ADP-ribose) is localized to the cytoplasm and nucleus throughout the cell cycle.

A) Asynchronous populations of HeLa cells (Asynch) or cells arrested in G0/G1, S phase or mitosis were fixed with MeOH or TCA and then stained for PAR (Tulip chIgY), and Centrin or γ-Tubulin, to identify single centriole pairs found during Go/G1, EdU, incorporated during S phase, and Tubulin, to stain mitotic spindles. In asynchronous cells and during Go/G1, S phase and mitosis, PAR staining was punctate with strong staining at the centrosome (arrowhead) and poles of the mitotic spindle (arrows). S-phase cells exhibited increased punctate staining in the nucleus relative to Go/G1 cells. Merge shows PAR (red), cell cycle markers (green) and Hoechst 33342 (blue). Scale bars, 10 mm. B) Cytoplasmic (C) and nuclear (N) extracts prepared from identical cell pellets, then normalized to cell volume, were generated from asynchronous, Go/G1 and S-phase-arrested cells. Extracts were immunoblotted with Tulip chIgY anti-PAR antibody. Cytoplasmic and nuclear extracts were further examined for the presence of tubulin, a cytoplasmic protein, or PARP1, a nuclear protein, to assay for contamination between the fractions. Total cell extracts were also prepared from asynchronous (A) and mitotic (M) cells and immunoblotted with Tulip chIgY anti-PAR antibody. Positions of molecular-weight markers are indicated on the right in black, and molecular weights shown in italics identify the closest markers above and below the cropped region. C) Quantitation of signal intensity of PAR immunoblots using chIgY and BD PAR antibodies. The ratio of nuclear to cytoplasmic PAR increases during S phase and DNA damage. The integrated intensity over the entire lane was determined, and the ratio of nuclear:cytoplasmic signal was calculated. Error bars represent s.d., n=3. See also Supplementary Fig. S5.

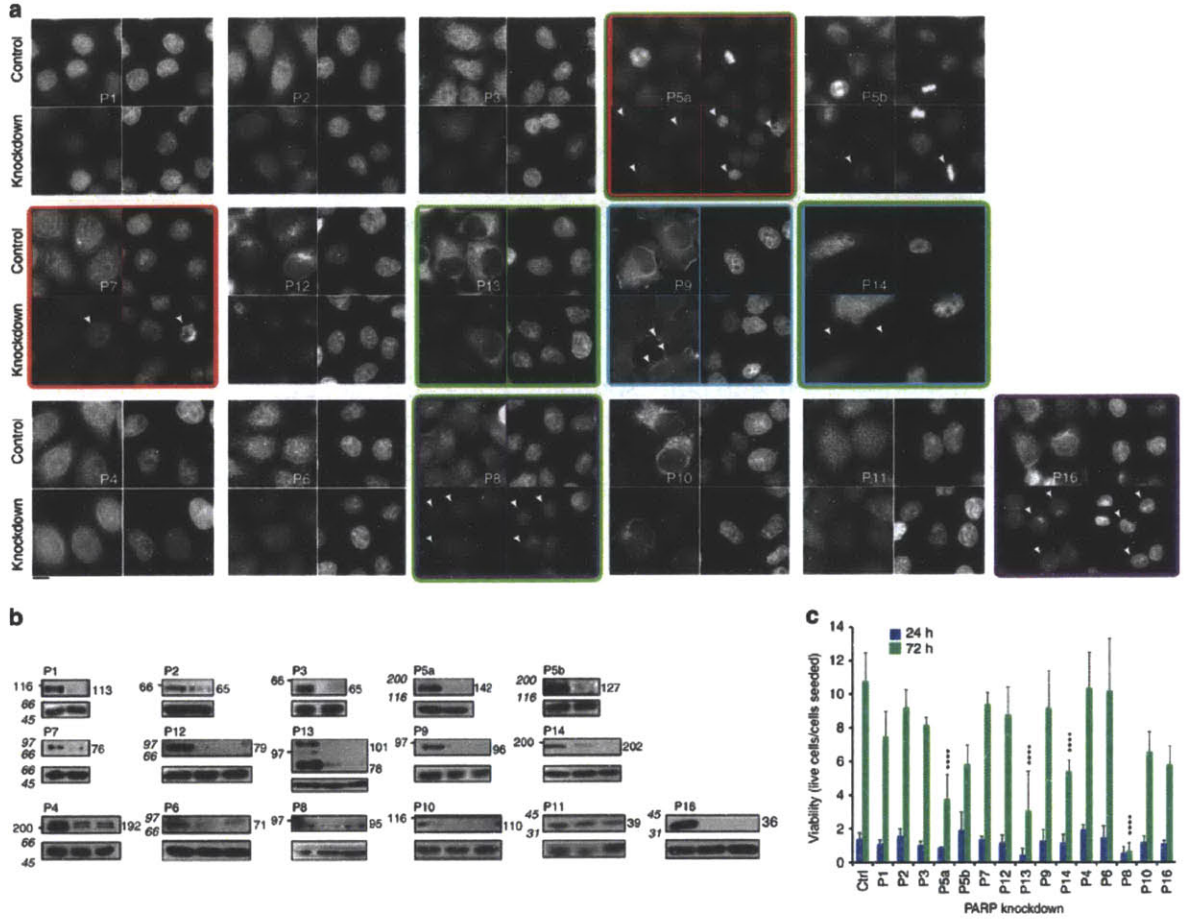
a
Control
Knockdown
P1
P2
P3
P5a
P5b
P7
P12
P13
P9
P14
P4
P6
P8
P10
P11
P16
b
c
24 h
72 h
Viability (live cells/cells seeded)
Ctrl
PARP knockdown

Figure 3. Knock-down phenotypes of the PARP family

PARP knock-down results in cell viability, membrane, actin cytoskeleton, and mitosis phenotypes. PARP expression was knocked-down via siRNA transfection in HeLa cells. Cells were then stained for each PARP (A) and immunoblot analysis performed to confirm knock-down (B). A) Cells were transfected with control siRNAs (Control) or siRNAs specific for each PARP (Knock-down) then stained for PARP (left) and Hoechst 33342 (right). Knock-down identified 4 phenotypes: defects in membranes (purple boxes), actin cytoskeleton (cyan boxes), mitosis (red boxes), and cell viability (green boxes). Arrowheads indicate cells exhibiting knock-down. Scale bar, 10 μm. B) Lysates from HeLa cells transfected with control (left lane) or PARP-specific siRNA (right lane(s)) were immunoblotted with corresponding anti-PARP antibody. Positions of molecular weight markers are indicated on the right in black, molecular weights shown in red identify the closest markers above and below the cropped region and the approximate molecular weight (kDa) of the relevant PARP in each knock-down is indicated to the left of each PARP blot. The corresponding tubulin blot is included as a loading control (lower panels). C) Cell number was analyzed 24h and 72h after knock-down of each PARP and presented as fold change relative to the initial number of cells seeded. PARP knock-downs that resulted in a decrease in viability of > 2 standard deviations relative to control knock-downs where identified as defective in cell viability. Error bars represent standard deviation, n=3, ****$p<0.00001$, Student's T test. See also Supplementary Figure S6 and Table 1.

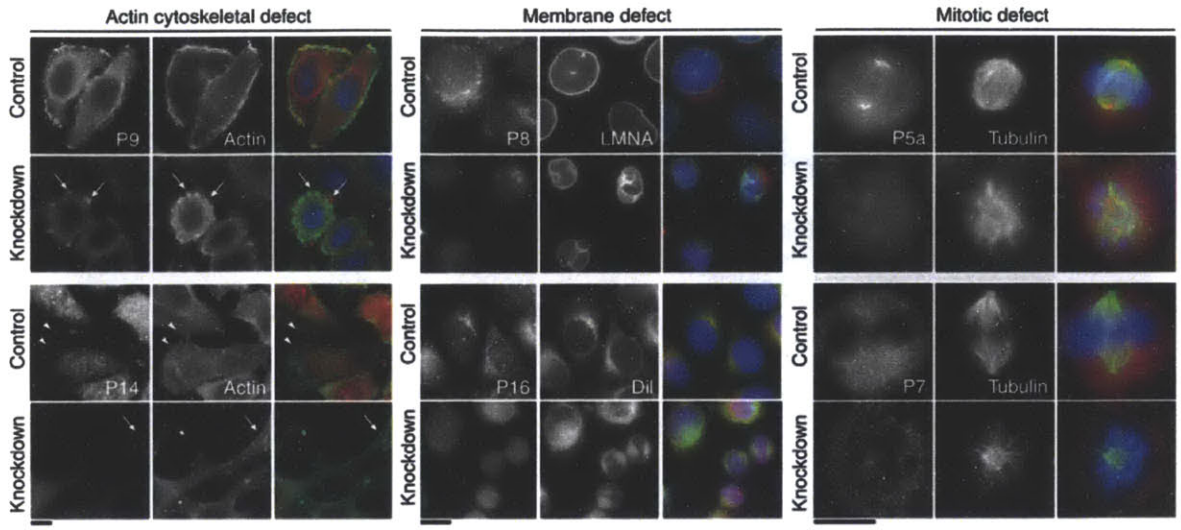

Figure 4. Analysis of knock-down phenotypes identifies new PARP functions
Morphological phenotypes identified upon PARP knock-down were grouped into actin cytoskeletal, membrane or mitotic defects then analyzed to determine biological function. Control and Knock-down cells stained with Hoechst 33342 (blue) and antibodies against the knocked-down PARP (red). Cells exhibiting Actin Cytoskeletal Defects were co-stained with phalloidin (P9) or an actin antibody (P14) to stain filamentous Actin (green), Membrane Defects for Lamin A/C (LMNA) or DiI (green) and mitotic defects for Tubulin (green). PARP9 (P9) co-localized with actin in control cells. Knock-down resulted in actin rich blebs shown by Arrows. PARP14 (P14) localized to cell protrusions in control cells (Arrowheads), identified in Figure 5 as focal adhesions. P14 knockdowns exhibited severe morphological defects with assembly of extended cellular protrusions (Arrowheads). PARP8 (P8) co-localized with LMNA in control cells, but not knockdown cells. PARP8 knockdown resulted in abnormal, bilobed nuclei. PARP16 (P16) co-localized with the membrane dye DiI in control cells. Knock-down resulted in pairs of round cells. PARP5a (P5a), but not PARP7 (P7) localized to the mitotic spindle. Knockdown of P5a resulted in multipolar spindles, while P7 knockdown resulted in an increase in pre-metaphase spindles. Actin cytoskeletal defects are further examined in Figure 5-6, and mitotic defects in Supplementary Figure S6. Scale bars, 10 μm.

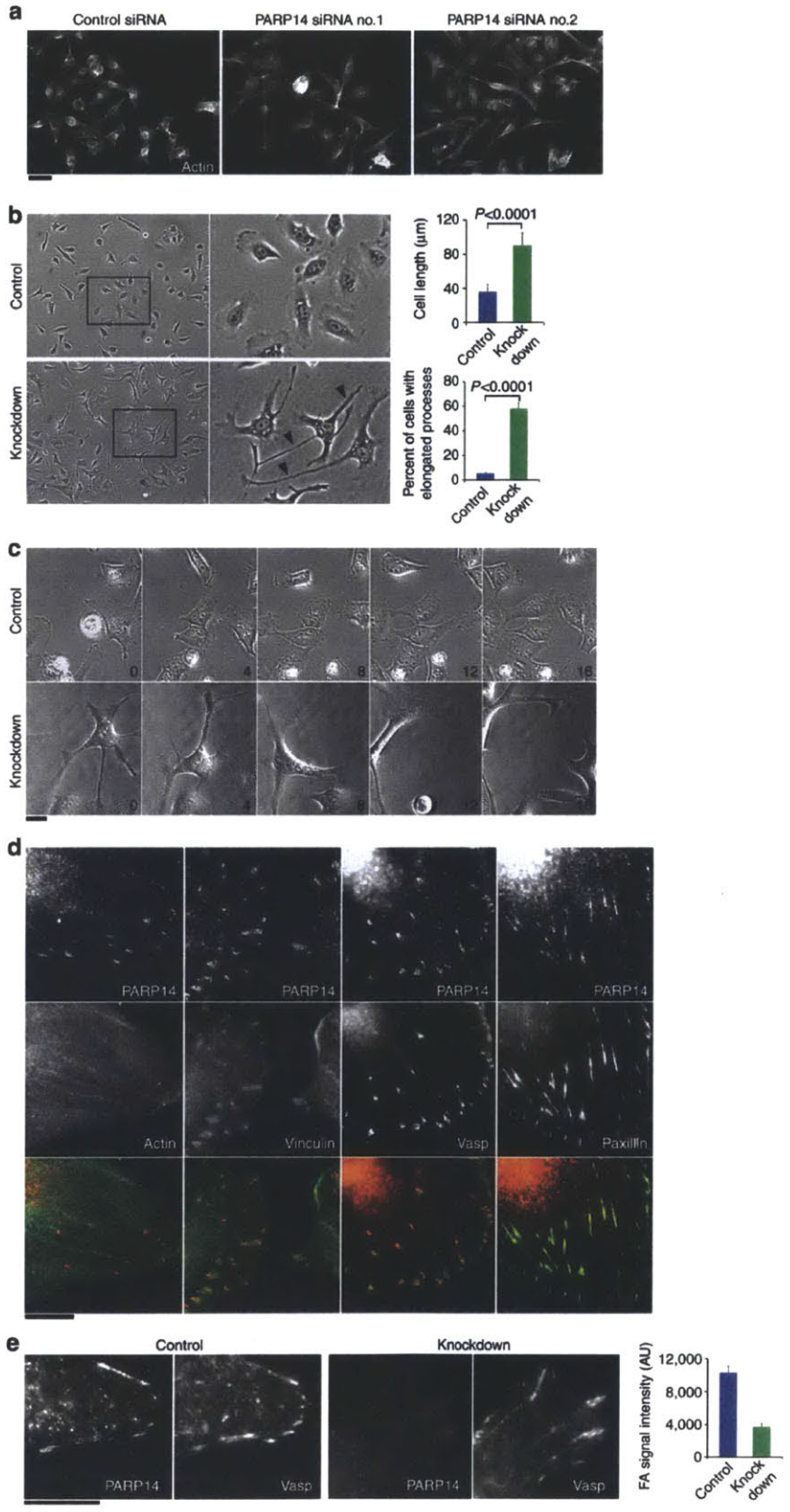
a
Control siRNA
PARP14 siRNA no.1
PARP14 siRNA no.2
Actin
b
Control
Knockdown
Cell length (μm)
P<0.0001
Control
Knock down
Percent of cells with elongated processes
P<0.0001
Control
Knock down
c
Control
Knockdown
0
4
8
12
16
d
PARP14
Actin
Vinculin
Vasp
Paxillin
e
Control
Knockdown
PARP14
Vasp
PARP14
Vasp
FA signal intensity (AU)
12,000
8,000
4,000
0
Control
Knock down

Figure 5. PARP14 is a focal adhesion protein whose knock-down results in abnormal cell morphology and cell migration defects

A) HeLa cells were transfected with control siRNA or siRNA 1 or 2 directed against distinct PARP14 sequences, then stained with Phalloidin. Both PARP14 siRNAs result in similar cell phenotypes containing extended cellular protrusions. Scale Bar, 50 μm. B) Bright field images of representative fields of control and PARP14 siRNA treated cells. Extended cellular protrusions in PARP14 siRNA treated cells are marked with Arrowheads. Quantitation of maximum cell length (n=20 cells) and percent cells displaying extended cellular protrusions (n=3, 200 cells counted per condition) shown at left. Error bars represent standard deviation. Significance determined by student's t-test. C) Still images of the indicated time points of movies taken of control and PARP14 siRNA treated cells undergoing random migration on the substrate fibronectin. See also **Supplementary Movie 1** (Control cells) and **Supplementary Movie 2** (PARP14 depleted cells). Scale bar, 25 μm. D) HeLa cells plated on fibronectin fixed with TCA and stained for PARP14 (red), and the indicated focal adhesion proteins (green). Scale bar, 10 μm. E) Control and PARP14 knock-down cells fixed with TCA and co-stained for PARP14 and Vasp. PARP14 knock-down results in loss of signal at focal adhesions demonstrating the specificity of focal adhesion staining (arrows). The intensity of PARP14 signal at focal adhesions was quantified in both control and PARP14 knock-down cells. Scale bar, 10 μm.

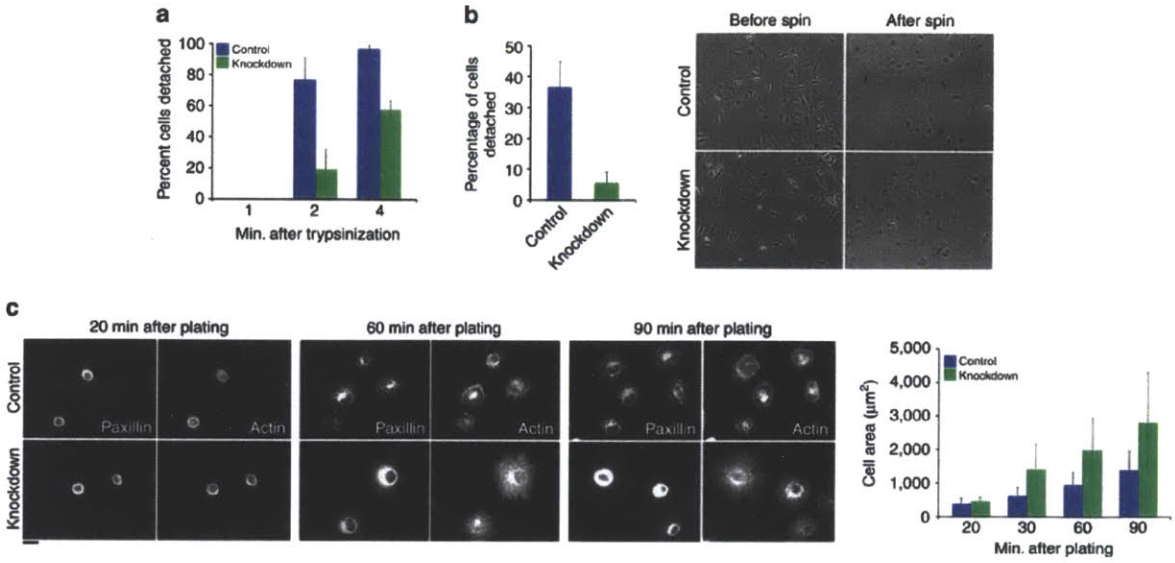

Figure 6. PARP14 depletion from focal adhesions results in increased adhesive strength.

A) Control or PARP14 siRNA treated cells plated on fibronectin were treated with trypsin for the indicated times and percent cells detached quantified at each time point. Error bars represent standard deviation. B) Control or PARP14 siRNA treated cells plated on fibronectin were subjected to a constant centrifugal force (2,000 g) for 30 min and the number of cells detached during centrifugation quantified. Representative images of control and PARP14 knock-down cells before and after centrifugation shown at right. Error bars represent standard deviation. C) Control or PARP14 siRNA treated cells were allowed to adhere to a fibronectin coated plate for the indicated times, fixed and stained with anti-paxillin and phalloidin, and the area of individual cells quantified at each timepoint. Error bars represent standard deviation. Representative images of control or PARP14 knock-down cells at each time point are shown. Scale bar, 25 μm.

Subfamily	PARP	Other Names	Localization			Knock-down
			Interphase		Mitosis	
			Cytoplasmic	Nuclear		
DNA Dependent	PARP-1	PARP, ARTD1		Diffuse	Chromatin	
	PARP-2	ARTD2	Punctate	Punctate	Diffuse, Cytoplasmic	
	PARP-3	ARTD3	Punctate	Punctate	Punctate, Cytoplasmic	
Tankyrase	PARP-5a	TNKS1, ARTD5	Punctate, Centrosome		Spindle Pole	Mitotic Defect, Viability Defect
	PARP-5b	TNKS2, ARTD6	Punctate		Spindle	
CCCH Zn Finger	PARP-7	tiPARP, ARTD14	Punctate	Punctate	Diffuse, Cytoplasmic	Mitotic Defect
	PARP-12	ARTD12	Punctate, Golgi		Punctate, Cytoplasmic	
	PARP-13	ZAP, ARTD13	Punctate		Punctate, Cytoplasmic	Viability Defect
Macro	PARP-9	BAL1, ARTD9	Diffuse, Plasma Membrane	Diffuse	Diffuse, Cytoplasmic	Actin Cytoskeletal Defect
	PARP-14	BAL2, ARTD8	Punctate, Focal Adhesions	Punctate	Punctate, Cytoplasmic	Actin Cytoskeletal Defect, Viability Defect
	PARP-15	BAL3, ARTD7	Not Assayed	Not Assayed	Not Assayed	Not Assayed
Unclassified	PARP-4	vPARP, ARTD4	Punctate	Diffuse	Diffuse, Cytoplasmic	
	PARP-6	ARTD17	Punctate		Punctate, Cytoplasmic	
	PARP-8	ARTD16	Punctate, Centrosome, Nuclear Envelope		Spindle Pole	Membrane Defect, Viability Defect
	PARP-10	ARTD10	Punctate		Punctate, Cytoplasmic	
	PARP-11	ARTD11	Punctate	Punctate	Centriole	Not Assayed
	PARP-16	ARTD15	Punctate, Reticular		Punctate, Cytoplasmic	Membrane Defect

Table 1. Summary of PARP localization and knock-down phenotypes.

Subfamily	Gene/ PARP	FPKM	
		HeLa	hTERT-RPE1
	Actin	11.61	12.503
	GAPDH	11.966	13.776
	PARG	4.298	4.043
DNA Dependent	1	6.871	5.399
	2	4.338	4.639
	3	2.848	3.418
Tankyrase	5a	2.528	3.553
	5b	4.271	4.547
CCCH-Zn Finger	7	3.422	4.705
	12	3.377	2.253
	13	4.983	3.666
Macro	9	3.038	2.584
	14	0.044	2.114
	15	0	0
Unclassified	4	4.537	4.87
	6	5.153	6.073
	8	0.012	1.914
	10	2.4	0.352
	11	0.055	0.037
	16	2.849	1.963

Table 2. FPKM values for PARP transcripts in HeLa and hTERT-RPE1 cells.

References

Aguiar, R., Yakushijin, Y., Kharbanda, S., Salgia, R., Fletcher, J., and Shipp, M. (2000). BAL is a novel risk-related gene in diffuse large B-cell lymphomas that enhances cellular migration. Blood 96, 4328-4334.

Amé, J.-C., Spenlehauer, C., and de Murcia, G. (2004). The PARP superfamily. BioEssays : news and reviews in molecular, cellular and developmental biology 26, 882-893.

Augustin, A., Spenlehauer, C., Dumond, H., Ménissier-De Murcia, J., Piel, M., Schmit, A.-C., Apiou, F., Vonesch, J.-L., Kock, M., Bornens, M., and De Murcia, G. (2003). PARP-3 localizes preferentially to the daughter centriole and interferes with the G1/S cell cycle progression. Journal of cell science 116, 1551-1562.

Barbarulo, A., Iansante, V., Chaidos, A., Naresh, K., Rahemtulla, A., Franzoso, G., Karadimitris, A., Haskard, D., Papa, S., and Bubici, C. (2013). Poly(ADP-ribose) polymerase family member 14 (PARP14) is a novel effector of the JNK2-dependent pro-survival signal in multiple myeloma. Oncogene 32, 4231-4242.

Barkauskaite, E., Jankevicius, G., Ladurner, A., Ahel, I., and Timinszky, G. (2013). The recognition and removal of cellular poly(ADP-ribose) signals. The FEBS journal 280, 3491-3507.

Bhattacharya, R., Gonzalez, A., Debiase, P., Trejo, H., Goldman, R., Flitney, F., and Jones, J. (2009). Recruitment of vimentin to the cell surface by beta3 integrin and plectin mediates adhesion strength. Journal of cell science 122, 1390-1400.

Bicknell, A., Babour, A., Federovitch, C., and Niwa, M. (2007). A novel role in cytokinesis reveals a housekeeping function for the unfolded protein response. The Journal of cell biology 177, 1017-1027.

Bürkle, A. (2005). Poly(ADP-ribose). The most elaborate metabolite of NAD+. The FEBS journal 272, 4576-4589.

Burridge, K., Fath, K., Kelly, T., Nuckolls, G., and Turner, C. (1988). Focal adhesions: transmembrane junctions between the extracellular matrix and the cytoskeleton. Annual review of cell biology 4, 487-525.

Chang, P., Coughlin, M., and Mitchison, T.J. (2005). Tankyrase-1 polymerization of poly(ADP-ribose) is required for spindle structure and function. Nature cell biology 7, 1133-1139.

Chang, P., Coughlin, M., and Mitchison, T.J. (2009). Interaction between Poly(ADP-ribose) and NuMA contributes to mitotic spindle pole assembly. Molecular biology of the cell 20, 4575-4585.

Chang, P., Jacobson, M.K., and Mitchison, T.J. (2004). Poly(ADP-ribose) is required for spindle assembly and structure. Nature 432, 645-649.

Cho, S., Ahn, A., Bhargava, P., Lee, C.-H., Eischen, C., McGuinness, O., and Boothby, M. (2011). Glycolytic rate and lymphomagenesis depend on PARP14, an ADP ribosyltransferase of the B aggressive lymphoma (BAL) family. Proceedings of the National Academy of Sciences of the United States of America 108, 15972-15977.

Chou, H.-Y.E., Chou, H., and Lee, S.-C. (2006). CDK-dependent activation of poly(ADP-ribose) polymerase member 10 (PARP10). The Journal of biological chemistry 281, 15201-15207.

Cirera-Salinas, D., Pauta, M., Allen, R., Salerno, A., Ramírez, C., Chamorro-Jorganes, A., Wanschel, A., Lasuncion, M., Morales-Ruiz, M., Suarez, Y., Baldan, Á., Esplugues, E., and Fernández-Hernando, C. (2012). Mir-33 regulates cell proliferation and cell cycle progression. Cell cycle (Georgetown, Tex) 11, 922-933.

Citarelli, M., Teotia, S., and Lamb, R. (2010). Evolutionary history of the poly(ADP-ribose) polymerase gene family in eukaryotes. BMC evolutionary biology 10, 308.

de Murcia, J., Niedergang, C., Trucco, C., Ricoul, M., Dutrillaux, B., Mark, M., Oliver, F., Masson, M., Dierich, A., LeMeur, M., Walztinger, C., Chambon, P., and de Murcia, G. (1997). Requirement of poly(ADP-ribose) polymerase in recovery from DNA damage in mice and in cells. Proceedings of the National Academy of Sciences of the United States of America 94, 7303-7307.

Dynek, J., and Smith, S. (2004). Resolution of sister telomere association is required for progression through mitosis. Science (New York, NY) 304, 97-100.

Fackler, O., and Grosse, R. (2008). Cell motility through plasma membrane blebbing. The Journal of cell biology 181, 879-884.

Gibson, B., and Kraus, W. (2012). New insights into the molecular and cellular functions of poly(ADP-ribose) and PARPs. Nature reviews Molecular cell biology 13, 411-424.

Goenka, S., and Boothby, M. (2006). Selective potentiation of Stat-dependent gene expression by collaborator of Stat6 (CoaSt6), a transcriptional cofactor. Proceedings of the National Academy of Sciences of the United States of America 103, 4210-4215.

Guo, X., Ma, J., Sun, J., and Gao, G. (2007). The zinc-finger antiviral protein recruits the RNA processing exosome to degrade the target mRNA. Proceedings of the National Academy of Sciences of the United States of America 104, 151-156.

Ha, G.H., Kim, H.S., Go, H., Lee, H., Seimiya, H., Chung, D., and Lee, C.W. (2012). Tankyrase-1 function at telomeres and during mitosis is regulated by Polo-like kinase-1-mediated phosphorylation. Cell death and differentiation 19, 321-332.

Hassa, P.O., and Hottiger, M.O. (2008). The diverse biological roles of mammalian PARPS, a small but powerful family of poly-ADP-ribose polymerases. Front Biosci 13, 3046-3082.

Hottiger, M., Hassa, P., Lüscher, B., Schüler, H., and Koch-Nolte, F. (2010). Toward a unified nomenclature for mammalian ADP-ribosyltransferases. Trends in biochemical sciences 35, 208-219.

Junod, A., Jornot, L., and Petersen, H. (1989). Differential effects of hyperoxia and hydrogen peroxide on DNA damage, polyadenosine diphosphate-ribose polymerase activity, and nicotinamide adenine dinucleotide and adenosine triphosphate contents in cultured endothelial cells and fibroblasts. Journal of cellular physiology 140, 177-185.

Juszczynski, P., Kutok, J., Li, C., Mitra, J., Aguiar, R., and Shipp, M. (2006). BAL1 and BBAP are regulated by a gamma interferon-responsive bidirectional promoter and are overexpressed in diffuse large B-cell lymphomas with a prominent inflammatory infiltrate. Molecular and cellular biology 26, 5348-5359.

Jwa, M., and Chang, P. (2012). PARP16 is a tail-anchored endoplasmic reticulum protein required for the PERK- and IRE1alpha-mediated unfolded protein response. Nature cell biology 14, 1223-1230.

Kaminker, P., Kim, S., Taylor, R., Zebarjadian, Y., Funk, W., Morin, G., Yaswen, P., and Campisi, J. (2001). TANK2, a new TRF1-associated poly(ADP-ribose) polymerase, causes rapid induction of cell death upon overexpression. The Journal of biological chemistry 276, 35891-35899.

Kanai, M., Tong, W.-M., Sugihara, E., Wang, Z.-Q., Fukasawa, K., and Miwa, M. (2003). Involvement of poly(ADP-Ribose) polymerase 1 and poly(ADP-Ribosyl)ation in regulation of centrosome function. Molecular and cellular biology 23, 2451-2462.

Karras, G., Kustatscher, G., Buhecha, H., Allen, M., Pugieux, C.I., Sait, F., Bycroft, M., and Ladurner, A. (2005). The macro domain is an ADP-ribose binding module. The EMBO journal 24, 1911-1920.

Kickhoefer, V.A., Siva, A.C., Kedersha, N.L., Inman, E.M., Ruland, C., Streuli, M., and Rome, L.H. (1999). The 193-kD vault protein, VPARP, is a novel poly(ADP-ribose) polymerase. The Journal of cell biology 146, 917-928.

Kirsten, E., Kun, E., Mendeleyev, J., and Ordahl, C.P. (2004). Activity assays for poly-ADP ribose polymerase. Methods Mol Biol 287, 137-149.

Kleine, H., Poreba, E., Lesniewicz, K., Hassa, P.O., Hottiger, M.O., Litchfield, D.W., Shilton, B.H., and Luscher, B. (2008). Substrate-assisted catalysis by PARP10 limits its activity to mono-ADP-ribosylation. Molecular cell 32, 57-69.

Koh, D.W., Dawson, T.M., and Dawson, V.L. (2005). Mediation of cell death by poly(ADP-ribose) polymerase-1. Pharmacol Res 52, 5-14.

Kuo, J.-C., Han, X., Hsiao, C.-T., Yates, J., and Waterman, C. (2011). Analysis of the myosin-II-responsive focal adhesion proteome reveals a role for β-Pix in negative regulation of focal adhesion maturation. Nature cell biology 13, 383-393.

Leung, A., Vyas, S., Rood, J., Bhutkar, A., Sharp, P., and Chang, P. (2011). Poly(ADP-ribose) regulates stress responses and microRNA activity in the cytoplasm. Molecular cell 42, 489-499.

Loseva, O., Jemth, A.-S., Bryant, H., Schüler, H., Lehtiö, L., Karlberg, T., and Helleday, T. (2010). PARP-3 is a mono-ADP-ribosylase that activates PARP-1 in the absence of DNA. The Journal of biological chemistry 285, 8054-8060.

Malanga, M., and Althaus, F. (2005). The role of poly(ADP-ribose) in the DNA damage signaling network. Biochemistry and cell biology = Biochimie et biologie cellulaire 83, 354-364.

Mann, M., and Jensen, O. (2003). Proteomic analysis of post-translational modifications. Nature biotechnology 21, 255-261.

Ménissier de Murcia, J., Ricoul, M., Tartier, L., Niedergang, C., Huber, A., Dantzer, F., Schreiber, V., Amé, J.-C., Dierich, A., LeMeur, M., Sabatier, L., Chambon, P., and de Murcia, G. (2003). Functional interaction between PARP-1 and PARP-2 in chromosome stability and embryonic development in mouse. The EMBO journal 22, 2255-2263.

Meyer, T., and Hilz, H. (1986). Production of anti-(ADP-ribose) antibodies with the aid of a dinucleotide-pyrophosphatase-resistant hapten and their application for the detection of mono(ADP-ribosyl)ated polypeptides. Eur J Biochem 155, 157-165.

Meyer-Ficca, M., Meyer, R., Jacobson, E., and Jacobson, M. (2005). Poly(ADP-ribose) polymerases: managing genome stability. The international journal of biochemistry & cell biology 37, 920-926.

Neumann, B., Walter, T., Hériché, J.-K., Bulkescher, J., Erfle, H., Conrad, C., Rogers, P., Poser, I., Held, M., Liebel, U., Cetin, C., Sieckmann, F., Pau, G., Kabbe, R., Wünsche, A., Satagopam, V., Schmitz, M., Chapuis, C., Gerlich, D., Schneider, R., Eils, R., Huber, W., Peters, J.-M., Hyman, A., Durbin, R., Pepperkok, R., and Ellenberg, J. (2010). Phenotypic profiling of the human genome by time-lapse microscopy reveals cell division genes. Nature 464, 721-727.

Ohashi, S., Kanai, M., Hanai, S., Uchiumi, F., Maruta, H., Tanuma, S.-i., and Miwa, M. (2003). Subcellular localization of poly(ADP-ribose) glycohydrolase in mammalian cells. Biochemical and biophysical research communications 307, 915-921.

Otto, H., Reche, P., Bazan, F., Dittmar, K., Haag, F., and Koch-Nolte, F. (2005). In silico characterization of the family of PARP-like poly(ADP-ribosyl)transferases (pARTs). BMC genomics 6, 139.

Petesch, S., and Lis, J. (2008). Rapid, transcription-independent loss of nucleosomes over a large chromatin domain at Hsp70 loci. Cell 134, 74-84.

Pollard, T., and Cooper, J. (2009). Actin, a central player in cell shape and movement. Science (New York, NY) 326, 1208-1212.

Rouleau, M., McDonald, D., Gagné, P., Ouellet, M.E., Droit, A., Hunter, J., Dutertre, S., Prigent, C., Hendzel, M., and Poirier, G. (2007). PARP-3 associates with polycomb group bodies and with components of the DNA damage repair machinery. Journal of cellular biochemistry 100, 385-401.

Rouleau, M.I., Patel, A., Hendzel, M., Kaufmann, S., and Poirier, G. (2010). PARP inhibition: PARP1 and beyond. Nature reviews Cancer 10, 293-301.

Schreiber, V.r., Dantzer, F.ß., Ame, J.-C., and de Murcia, G. (2006). Poly(ADP-ribose): novel functions for an old molecule. Nature reviews Molecular cell biology 7, 517-528.

Sciaky, N., Presley, J., Smith, C., Zaal, K., Cole, N., Moreira, J., Terasaki, M., Siggia, E., and Lippincott-Schwartz, J. (1997). Golgi tubule traffic and the effects of brefeldin A visualized in living cells. The Journal of cell biology 139, 1137-1155.

Slade, D., Dunstan, M., Barkauskaite, E., Weston, R., Lafite, P., Dixon, N., Ahel, M., Leys, D., and Ahel, I. (2011). The structure and catalytic mechanism of a poly(ADP-ribose) glycohydrolase. Nature 477, 616-620.

Smith, S., and de Lange, T. (1999). Cell cycle dependent localization of the telomeric PARP, tankyrase, to nuclear pore complexes and centrosomes. Journal of cell science 112 (Pt 21), 3649-3656.

Vorobjev, I., and Chentsov Yu, S. (1982). Centrioles in the cell cycle. I. Epithelial cells. The Journal of cell biology 93, 938-949.

Webb, D., Donais, K., Whitmore, L., Thomas, S., Turner, C., Parsons, J., and Horwitz, A. (2004). FAK-Src signalling through paxillin, ERK and MLCK regulates adhesion disassembly. Nature cell biology 6, 154-161.

Yanagawa, T., Funasaka, T., Tsutsumi, S., Hu, H., Watanabe, H., and Raz, A. (2007). Regulation of Phosphoglucose Isomerase/Autocrine Motility Factor Activities by the Poly(ADP-Ribose) Polymerase Family-14. Cancer Research 67.

Yonemura, S., Hirao-Minakuchi, K., and Nishimura, Y. (2004). Rho localization in cells and tissues. Experimental cell research 295, 300-314.

Yu, M., Schreek, S., Cerni, C., Schamberger, C., Lesniewicz, K., Poreba, E., Vervoorts, J., Walsemann, G., Grötzinger, J., Kremmer, E., Mehraein, Y., Mertsching, J., Kraft, R., Austen, M., Lüscher-Firzlaff, J., and Lüscher, B. (2005). PARP-10, a novel Myc-interacting protein with poly(ADP-ribose) polymerase activity, inhibits transformation. Oncogene 24, 1982-1993.

Vyas et al., *Nature Communications* 2013
Supplementary Material

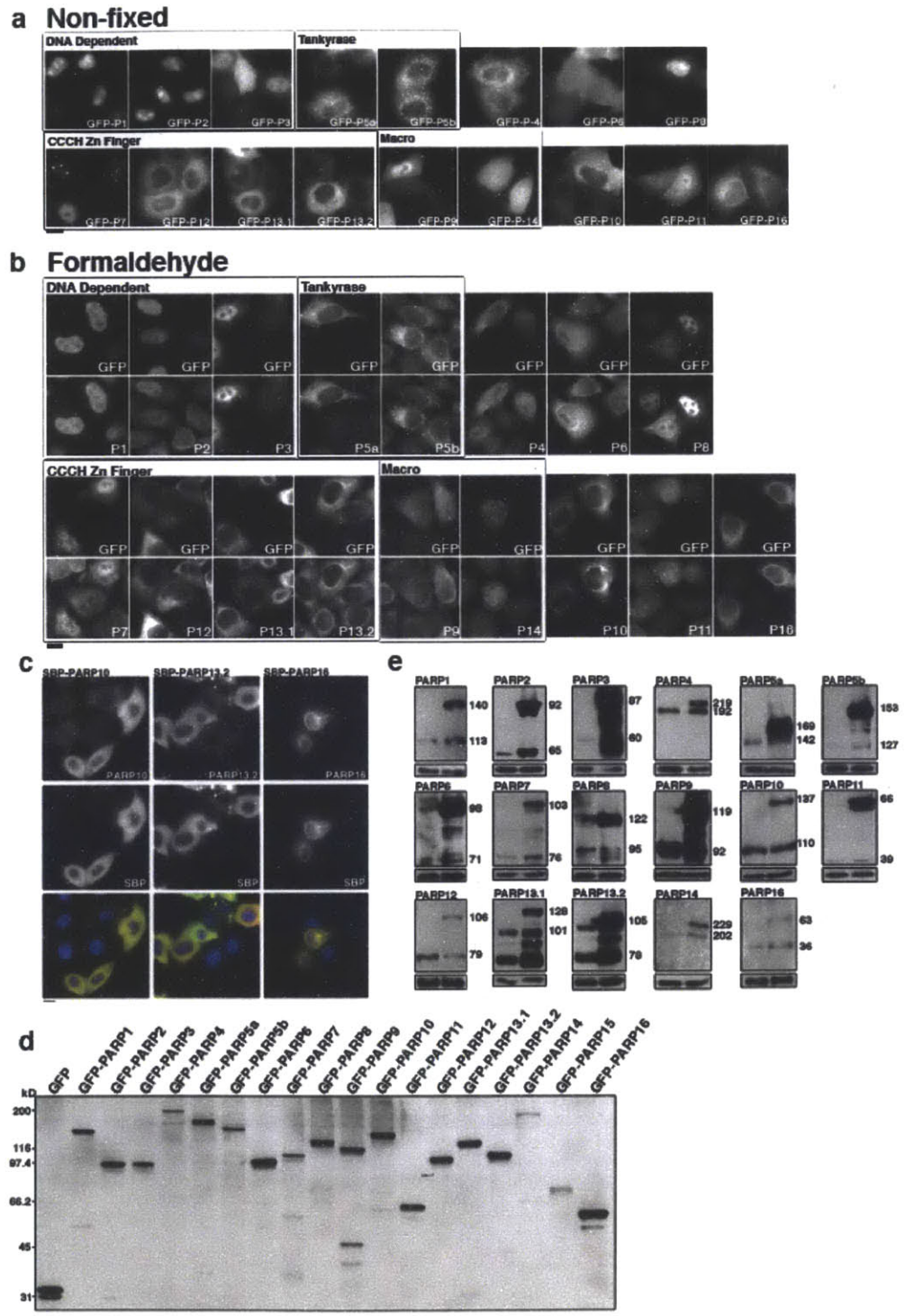

Supplementary Figure S1. PARP localization patterns using GFP-PARP and PARP-specific antibody libraries

GFP-PARP localization in non-fixed (A) and formaldehyde fixed (B) GFP-PARPx transfected HeLa cells. Fixed cells were costained with GFP (top) and PARP-specific (bottom) antibodies to verify reactivity and localization of PARP antibodies. Scale bars, 10 μm. C) Streptavidin binding peptide tagged PARPs 10, 13.2 and 16 were expressed in HeLa cells and stained with antibodies against SBP (green) and each PARP (red) Localization of SBP tagged PARPs is identical to GFP tag, suggesting that the tag is not effecting PARP localization patterns. Scale bar, 10 μm. D) GFP-PARPx transfected HeLa lysates were immunoblotted using an antibody against GFP to verify correct molecular weight of each GFP-PARP fusion construct. E) Untransfected (left lane) and GFP-PARPx transfected (right lane) HeLa cells were immunoblotted with corresponding PARP antibody to determine specificity of each antibody. The corresponding tubulin blot is included as a loading control (lower panels). Approximate molecular weights of endogenous PARPs and overexpressed GFP-PARP fusions are indicated.

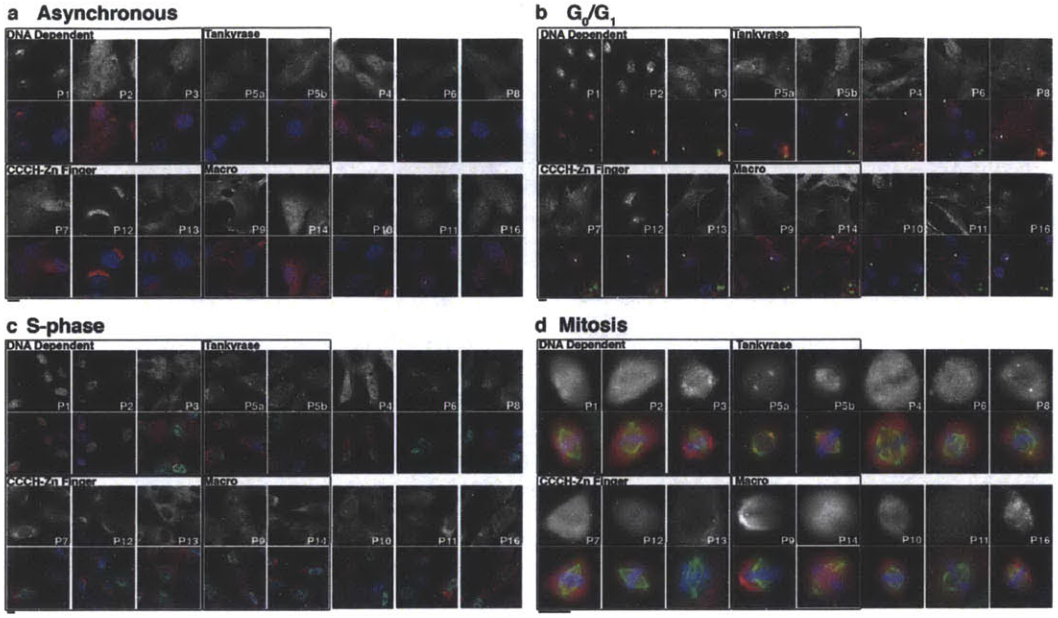

Supplementary Figure S2. Cell cycle specific PARP localization patterns
A) Asynchronous hTERT-RPE1 cells were fixed with formaldehyde and stained with PARP specific antibodies. B) hTERT-RPE1 were arrested in G0/G1 via serum starvation and costained with PARP antibodies (red) and centrin (green) to identify G_0/G_1 cells. Arrowheads indicate area of inset. C) hTERT-RPE1 were arrested in S-phase via aphidicolin treatment and stained with PARP antibodies (red). The detection of EdU (green), a nucleotide analog, incorporated during a 20 min aphidicolin washout, was used to identify S phase cells. D) Mitotic hTERT-RPE1 cells were costained with PARP antibodies (red) and tubulin (green). DNA was stained with Hoechst 33342, shown in blue. Scale bars, 10 µm.

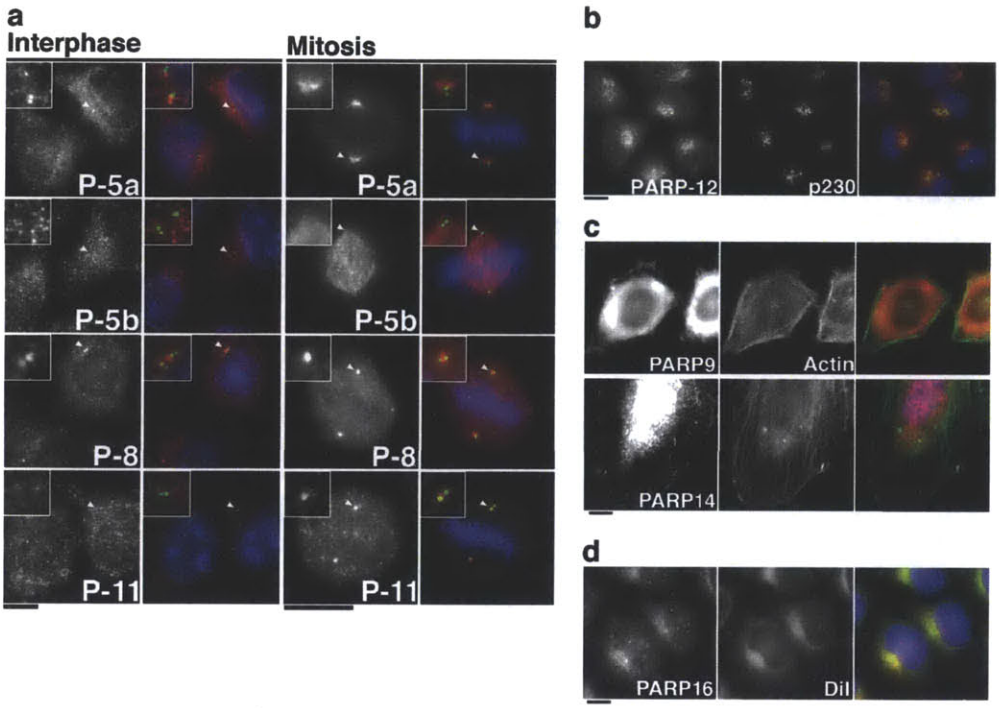

Supplementary Figure S3. Subcellular localization validation of centrosomal, Golgi, cytoskeletal, and membrane localized PARPs

A) Interphase and mitotic HeLa cells were stained with antibodies against the indicated PARP and centrin to demonstrate centrosomal localization patterns. Color merge shows PARP (red), centrin (green), and Hoechst 33342 (blue) costaining. Arrowheads indicate area of inset. B) Interphase HeLa cells were stained with antibodies against PARP12 and the trans Golgi marker p230, confirming a Golgi localization pattern for PARP12. C) Interphase HeLa cells were stained with antibodies against the indicated macro PARP and actin to demonstrate localization patterns consistent with functions in cell motility. Cells were fixed with 10% TCA to preserve membrane signal. D) Interphase HeLa cells were stained with antibodies against PARP16 and the lipophilic membrane dye DiI, demonstrating colocalization with DiI positive membrane structures. Scale bars, 10 μm.

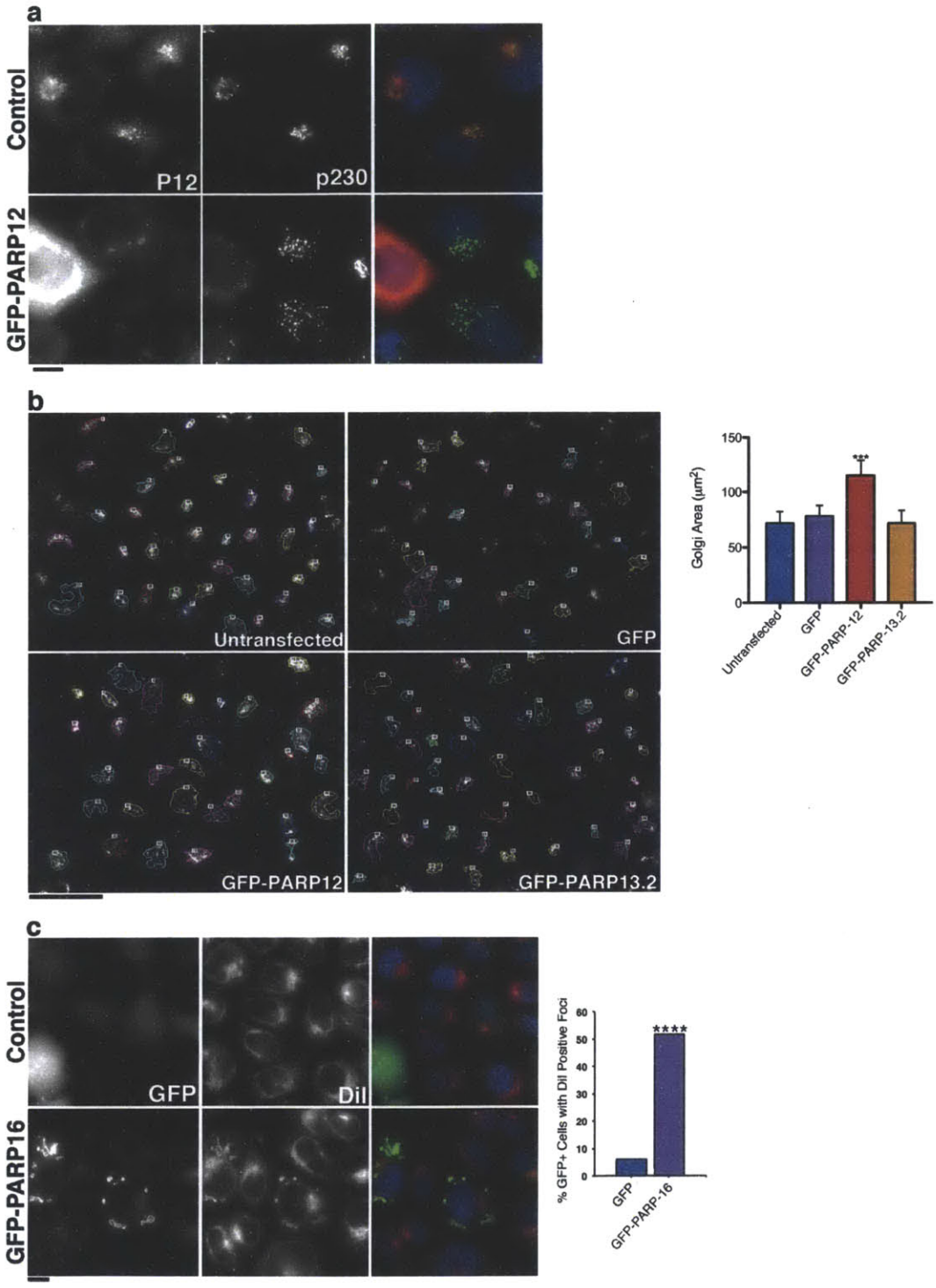
a
Control
GFP-PARP12
P12
p230
b
Untransfected
GFP
GFP-PARP12
GFP-PARP13.2
Golgi Area (μm²)
150
100
50
0
***
Untransfected
GFP
GFP-PARP-12
GFP-PARP-13.2
c
Control
GFP-PARP16
GFP
DiI
% GFP+ Cells with DiI Positive Foci
60
50
40
30
20
10
0
****
GFP
GFP-PARP-16

Supplementary Figure S4. PARP Overexpression phenotypes

A) Control and GFP-PARP12 overexpressing cells were costained antibodies against PARP12 (red) and p230 (green). DNA was stained with Hoechst 33342 (blue). Scale bar, 10 μm. B) GFP-PARP12 overexpression resulted in increased Golgi area relative to control overexpression as determined by p230 staining while GFP alone or GFP-PARP13.2 overexpression did not result in changes in Golgi size (***$p<0.0001$, $n \geq 46$, one way ANOVA, error bars indicate 95% CI of the mean). Golgi size in untransfected (n=77), GFP transfected (n=97), GFP-PARP12 transfected (n=107) and GFP-PARP13.2 (n=46) transfected cells was determined by staining with the trans-Golgi marker p230, tracing the area enclosed within the p230 signal, then calculating the area of the tracings. Data were analyzed via one-way ANOVA, comparing each data set to the untransfected data set. GFP-PARP12 overexpressing cells contained Golgi ~1.58 fold larger than Golgi found in nontransfected control cells while GFP and GFP-PARP13.2 overexpression did not result in a change in Golgi size relative to controls. Images show representative data. Scale bar, 50 μm. C) Overexpression of GFP-PARP16 resulted in the assembly of abnormal structures identified as membranous by DiI staining. Such structures were not seen in control cells overexpressing GFP. Graph shows percent of GFP transfected cells with DiI positive foci (****$p<.0001$, $n \geq 34$, Fisher's exact test). Scale bar, 10 μm.

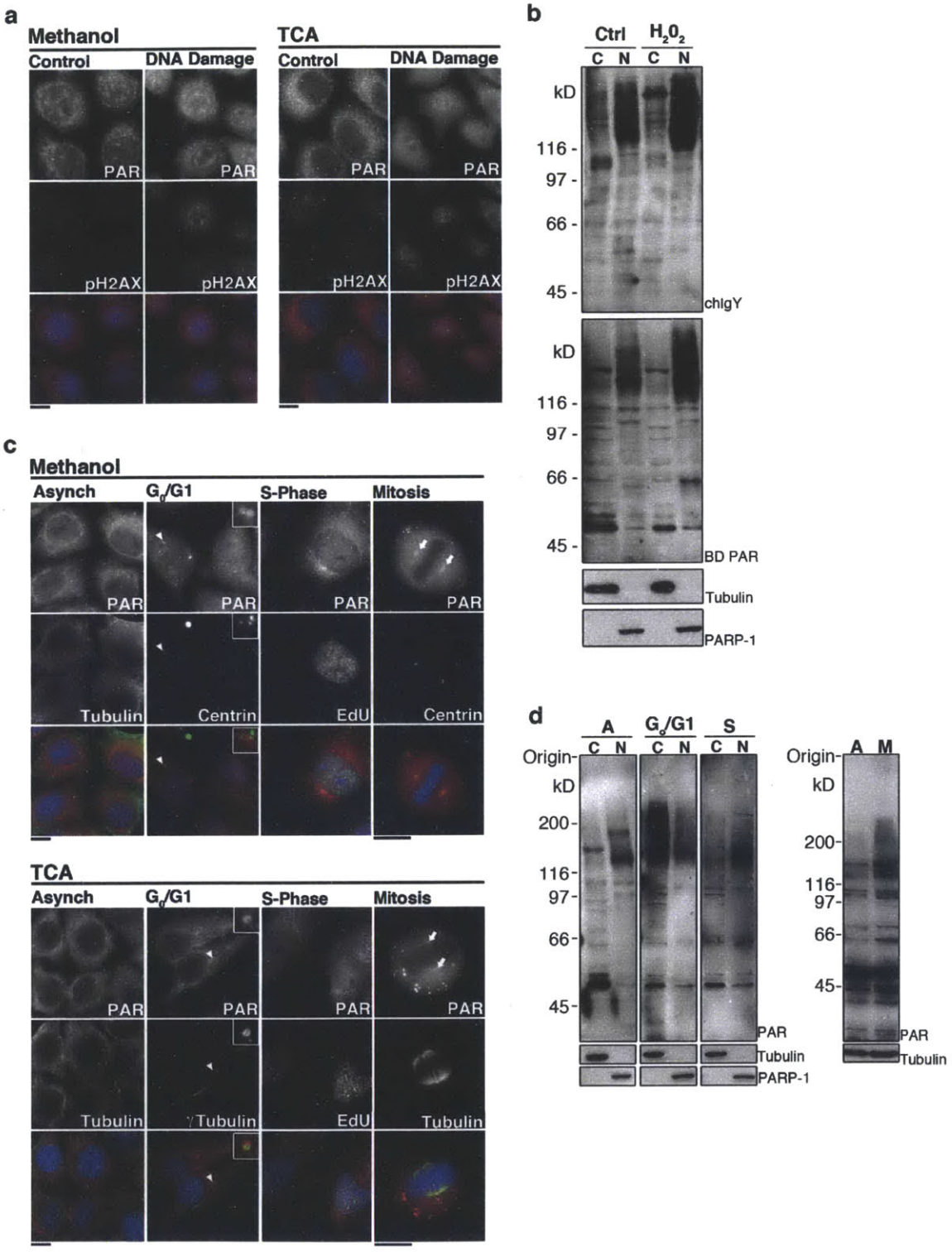
a
Methanol
Control
DNA Damage
TCA
Control
DNA Damage
PAR
pH2AX
b
Ctrl
H_2O_2
C N C N
kD
116 -
97 -
66 -
45 -
chIgY
BD PAR
Tubulin
PARP-1
c
Methanol
Asynch
G_0/G1
S-Phase
Mitosis
PAR
Tubulin
Centrin
EdU
TCA
γTubulin
d
A
G_0/G1
S
M
Origin-
200-
PAR
Tubulin
PARP-1

Supplementary Figure S5. Poly (ADP-ribose) localization throughout the cell cycle

A) HeLa cells were either untreated (Control) or treated with H_2O_2 (DNA Damage) to verify accurate PAR staining. Cells were fixed with either Methanol or TCA and stained for PAR (chIgY). Both fixation conditions demonstrate an increase in nuclear PAR upon induction of DNA damage, indicated by pH2AX staining. Scale bar, 10 μm. B) Cytoplasmic (C) and nuclear (N) extracts were prepared from untreated and H_2O_2 treated cells and immunoblotted using chIgY and BD PAR pADPr antibodies, confirming an increase in nuclear PAR levels during DNA damage conditions. C) Asynchronous HeLa cells or cells arrested in G_0/G_1, S-phase and mitosis were fixed in either Methanol or TCA then stained for PAR (BD PAR) and the cell cycle markers Centrin or g-Tubulin, to identify single centriole pairs found only during G_0/G_1, EdU, incorporated during S-phase, and Tubulin, to stain mitotic spindles. In Asynchronous cells and during G_0/G_1, S-phase, and Mitosis, pADPr staining appears diffuse and punctate with strong staining at the centrosome (arrowhead), and poles of the mitotic spindle (arrows). Merge shows PAR in red, cell cycle markers in green and Hoechst 33342 in blue. Scale bars, 10 μm. D) Cytoplasmic (C) and nuclear (N) extracts were prepared from asynchronous, G_0/G_1 and S-phase arrested cells and immunoblotted with BD PAR anti-PAR antibody. G_o/G_1 cells have higher levels of cytoplasmic PAR while S-phase cells have increased nuclear pADPr. Total cell extracts were prepared for asynchronous (A) and mitotic (M) cells and immunoblotted with BD PAR anti-PAR antibody, displaying increased levels of PAR during mitosis.

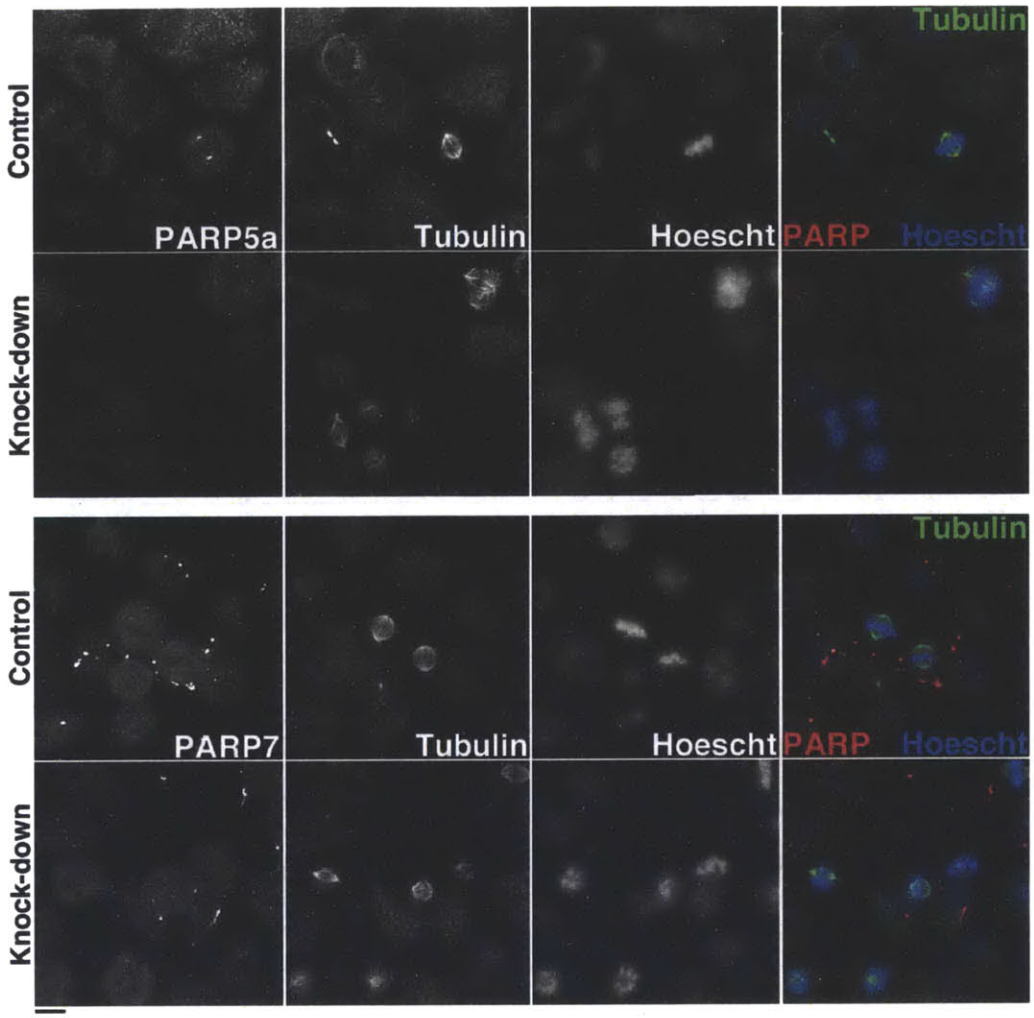

Supplementary Figure S6. PARP knock-down phenotypes

Control HeLa cells or cells in which either PARP-5a or -7 were knocked-down were stained with the corresponding PARP antibody and tubulin to examine spindle structure. PARP-5a knock-down resulted in an increased mitotic index (~13% vs. ~3% for controls), disorganized spindles, and supernumerary spindle poles. PARP-7 knock-down cells exhibited an increase in pre-metaphase mitotic spindles

	siRNA-1		siRNA-2		
PARP	Sequence	Company	Sequence	Company	Published
1	GCCUCCGCUCCUGAACAAU	Dharmacon	N/A		Chang et al. Nat Cell Bio.7, 1133 (2005)
2	AAUCAGUGUAAUGAACUACUA	Dharmacon	N/A		Chang et al. Nat Cell Bio.7, 1133 (2005)
3	GGACCCAGGUGUAUGAGGACUACAA	Invitrogen Stealth	N/A		Chang et al. Nat Cell Bio.7, 1133 (2005)
4	AAACAAGGAUUUCUACUAAGA	Dharmacon	AAAGAUCGUGGUGUGCAAAGA	Dharmacon	Chang et al. Nat Cell Bio.7, 1133 (2005)
5a	CAGUAACAAUUCACCGUCGUCCUCU	Invitrogen Stealth	N/A		Chang et al. Nat Cell Bio.7, 1133 (2005)
5b	GCUUCAGAAUGGUGCAAAU	Dharmacon	N/A		Chang et al. Nat Cell Bio.7, 1133 (2005)
6	s32505	Invitrogen Silencer Select	s32504	Invitrogen Silencer Select	N/A
7	s24857 GUGAUAAGCUGAGUACUGATT	Invitrogen Silencer Select	s24858 GCUCCUGUUUUAUACUGCUTT	Invitrogen Silencer Select	Neumann et al. Nature 464, 721 (2010)
8	GGAAGAUUCUGAAGGUGACAAUGAU	Invitrogen Stealth	GCCUUAUGUGAAGUGAUCACCUCAU	Invitrogen Stealth	N/A
9	D-014734-03	Dharmacon	D-014734-01	Dharmacon	N/A
10	GCCUGGUGGAGAUGGUGCUAUUGAU	Invitrogen Stealth	AGACGUCGCUCUCUUGCCACUUGAA	Invitrogen Stealth	N/A
12	s34882	Invitrogen Silencer Select	s34883	Invitrogen Silencer Select	N/A
13	GCUCACGGAACUAUGAGCUGAGUUU	Invitrogen Stealth	GCUGACCCAAGAGUAGCACUUGUUA	Invitrogen Stealth	N/A
14	D-023583-02	Dharmacon	s29270	Invitrogen Silencer Select	N/A
16	CCCAAGUACUUCGUGGUCACCAAUA	Invitrogen Stealth	GAGACCAAAGGAGAACGAGACCUAA	Invitrogen Stealth	N/A

Supplementary Table 1. PARP siRNA sequences

Chapter 3. Analysis of poly(ADP-ribose) polymerase (PARP) enzymatic activity identifies mono(ADP-ribosyl)ation as the primary PARP catalytic activity

Sejal Vyas[1,2] and Paul Chang[1,2]

[1]*Koch Institute for Integrative Cancer Research,* [2]*Department of Biology, Massachusetts Institute of Technology, Cambridge, MA 02139, USA*

Correspondence: P.C. (pchang2@mit.edu)

Abstract

The poly(ADP-ribose) polymerase protein family generates ADPr modifications onto target proteins using NAD^+ as substrate. While PARPs have been historically thought to generate poly(ADP-ribose) (PAR), recent work has predicted that many PARPs instead catalyze mono(ADP-ribose) modifications based the amino acid composition of the catalytic triad motif. To experimentally test these predictions, we performed *in vitro* NAD^+ incorporation reactions for the entire PARP family and confirmed the identity of the ADPr modifications generated via enzymatic hydrolysis and chemical release. Reaction products were then analyzed for size via thin layer chromatography and high resolution sequencing gel analysis. Our results demonstrate that the majority of PARPs generate MAR modifications rather than PAR and that the amino acid composition of the catalytic triad is not the sole indicator of PAR synthesis. While the primary sequence of PARP3 and 4predicts poly(ADP-ribose) synthesis, both only generate MAR suggesting that structural features of the PARP catalytic domain also impact enzymatic activity. This work establishes the catalytic activity of an entire enzyme family.

Introduction

The seventeen-member poly(ADP-ribose) polymerase (PARP) protein family generates ADP-ribose (ADPr) modifications onto target proteins using NAD^+ as a substrate (Ame et al., 2004). The most well understood PARP functions involve poly(ADP-ribose) (PAR) synthesis and include physiological functions in cell division (Chang et al., 2004; Chang et al., 2005, 2009) transcriptional regulation (reviewed in Ji and Tulin, 2010) and regulation of protein degradation (Huang et al., 2009; Zhang et al., 2011). PAR also functions during cell stress responses such as DNA damage (Malanga and Althaus, 2005), heat shock (Petesch and Lis, 2012; Di Giammartino et al., 2013), and the cytoplasmic stress response (Leung et al., 2011). Recently, it was shown that certain PARPs, such as PARP10 can only generate mono(ADP-ribose) (MAR) (Kleine et al., 2008). Based on amino acid sequence analysis other PARP family members are also thought to be limited to MAR synthesis (Kleine et al., 2008). Many functions have been identified for PARPs predicted to generate MAR, including actin cytoskeletal regulation (PARP14) (Vyas et al., 2013), regulation of the unfolded protein response (PARP16) (Jwa and Chang, 2012), transcriptional regulation (PARP3, 7 and 14) (Goenka and Boothby, 2006; Goenka et al., 2007; Rouleau et al., 2011; MacPherson et al., 2013) and in the regulation of multiple signal transduction pathways (PARP10 and 14) (Cho et al., 2009; Barbarulo et al., 2013; Verheugd et al., 2013)

The type of ADPr modification generated by PARPs has critical impacts on potential mechanisms of function. While MAR modifications add single ADPr units on to proteins, PAR is a structurally complex polymer that can be up to 200 units in length when generated *in vitro*, and can contain both linear and branched glycosidic linkages

(Alvarez-Gonzalez and Jacobson, 1987). Although both can regulate target protein function via direct covalent modification, PAR can also recruit binding proteins that contain characterized PAR binding motifs including PBZ, WWE, Macro and PBM motifs (Pleschke et al., 2000; Karras et al., 2005; Ahel et al., 2008; Wang et al., 2012). As such PAR can act as a reversible protein binding scaffold for the nucleation of multiprotein complexes. Therefore, identifying the type of ADPr modifications generated by each PARP is critical to understanding specific mechanisms of PARP function.

The primary predictors of PARP enzymatic activity are thought to be the primary sequence of the amino acids that catalyze the ADP-ribose transfer reaction, as well as structural elements of the PARP catalytic domain that either mediate binding of the catalytic domain to substrate, or incoming ADPr residues of the growing polymer. The PARP catalytic domain contains a signature H-Y-E motif originally identified in various bacterial mono-ADP-ribosyltransferase (mART) toxins that also mediate ADP-ribose transfer. Histidine and tyrosine residues were shown to be required for binding of the substrate NAD^+ and the glutamate for catalysis (Carroll and Collier, 1984; Papini et al., 1989; Brenda et al., 1990). Comparative analysis of catalytic domains of bacterial mARTs and eukaryotic PARPs identified common structural features in the substrate binding pockets and superimposablity of the catalytic residues (Domenighini and Rappuoli, 1996). Mutation of the corresponding catalytic glutamate in PARP1 to glutamine resulted in over 2000 fold reduction in elongation activity, although mono(ADP-ribosyl)ase activity was retained (Marsischky et al., 1995). Interestingly, most PARPs have an isoleucine, leucine or tyrosine in place of the catalytic glutamate and are therefore predicted to generate MAR (Kleine et al., 2008) (Table 1).

Additionally, two PARPs also contain amino acid substitutions for the NAD^+ binding histidine and are predicted to be inactive (Kleine et al., 2008).

Secondary structural features of the PARP catalytic domain are also predicted to influence catalytic activity. In addition to the NAD^+ binding residues of the catalytic triad, the Donor loop (D-loop) shapes the substrate binding pocket and interacts with NAD^+ (Wahlberg et al., 2012). This loop varies greatly in size and rigidity within the PARP family and analysis of the binding of small molecule PARP inhibitors to PARP catalytic domains identified the D-loop as a structural element that contributed to differential inhibitor binding (Wahlberg et al., 2012). Therefore, the shape of the substrate binding pocket, partly lined by the D-loop, could contribute to differences in the strength of NAD^+ binding among the PARPs and impact catalytic activity or enzyme kinetics. Another structural component of the PARP catalytic domain is the acceptor pocket, which is partly lined by the loop between β sheets 4 and 5 and referred to as the acceptor loop. This loop is implicated in the binding of either a protein substrate or ADP-ribose acceptor for bacterial mARTs or eukaryotic PARPs respectively and varies greatly in length among the PARP family (Ruf et al., 1998; Han and Tainer, 2002; Otto et al., 2005). Therefore, the ability to bind to an incoming ADPr unit on a polymer chain could vary within the PARP family and impact the ability to elongate a PAR chain or create a branched modification.

While recent work has provided experimental evidence in support of many of the predicted PARP activities, most use the resolution of automodified PARPs as a discreet band rather than a smear indicative of PARylation to show MARylation (summarized in Table1). However, since a single ADPr unit would add 0.6 kDa to a protein, the

resolution in an SDS-PAGE gel is not sufficient to distinguish addition of a single ADPr unit versus a short oligomer (Aguiar et al., 2005; Kleine et al., 2008; Loseva et al., 2010; MacPherson et al., 2013).

Recently, we identified 4 classes of PARP function: regulation of the actin cytoskeleton, membranous organelles and cell division and cell viability (Vyas et al., 2013). To further determine which types of ADPr modifications are functioning in these distinct cellular pathways, we performed automodification assays for the entire PARP family. In order to further confirm that the modifications observed were truly MAR and not short oligomers of ADPr, we utilized ADPr hydrolyzing enzymes that act on distinct ADPr modifications and chemical treatments to release the ADPr modification at the site of protein linkage, allowing length determination. These assays suggest that the primary activity for the majority of PARPs is MAR synthesis.

Results

The majority of PARPs do not exhibit poly(ADP-ribosyl)ation activity

To assess enzymatic activity of the PARPs, we purified each protein and performed standard automodification assays (Figure 1A) (Slade et al., 2011). As the majority of PARP activity is primarily directed towards the PARP itself, automodification is an effective measure of enzymatic activity (Lindahl et al., 1995; Rippmann et al., 2002). N-terminal GFP fusions to each full-length PARP were expressed and purified from human 293F cells. Bead-bound GFP-PARPs were incubated with 5 or 10μM NAD^+ supplemented with a constant ratio of ^{32}P-NAD^+ (Figure 1A). We chose to use lower concentrations of cold NAD^+ than standard PARP automodification reactions in order to increase the ratio of hot:cold NAD^+ due to the weak signal incorporated by

many PARPs during initial analysis This is potentially critical for detection of short ADPr oligomers where the ^{32}P-NAD$^+$ could be outcompeted by unlabeled NAD$^+$. Importantly, PARP1 was able to generate polymers at these low NAD$^+$ concentrations, indicating that NAD$^+$ is not a limiting reagent in our reactions (Figure 1).

We confirmed that the N-terminal GFP tag does not interfere with PARP enzymatic activity under these conditions. A similar analysis was used to show that the TAP tag (similar in size to GFP) on either end of a PARP does not affect enzymatic activity (Kleine et al., 2008). Both N- and C-terminal GFP fusions to PARP-1 incorporated similar amounts of ^{32}P-ADPr, suggesting that the GFP tag does not affect enzymatic activity of the PARPs (Figure S1A). Additionally, to ensure that the on bead incorporation reaction does not interfere with enzymatic activity, we compared the NAD$^+$ incorporation activity of bead bound GFP-PARP10 and SBP-PARP10 to soluble PARP10 in which the purification tag was proteolytically cleaved (Figure S1B). These results indicated that the bead-bound protein did not interfere with NAD$^+$ incorporation activity.

Previous work by Kleine et al. defined three categories of PARP enzymatic activity based on the presence of the H-Y-E catalytic triad: 1) MAR synthesis, identified by ADPr incorporation at the PARP's molecular weight with no shift in electrophoretic mobility; 2) PAR synthesis, identified by incorporation at and above the PARP's molecular weight resulting in dramatic mobility shifts and smearing of signal; or 3) catalytic inactivity, identified by no incorporated ^{32}P-ADPr (Kleine et al., 2008). In addition to the primary sequence of the catalytic motif, we have further grouped the PARPs based on structural components from available crystal structures of catalytic

domain (Figure 1B, Table 1). Based on the patterns of incorporation detected, both features of the catalytic domain appear to impact enzymatic activity.

H-Y-E with long donor and acceptor loop

PARP1 and 2 incorporated NAD^+ in a manner consistent with PAR synthesis activity, consistent with previously published reports (Alvarez-Gonzalez and Jacobson, 1987; Amé et al., 1999) (Figure 1A). Additionally, both PARP1 and 2 automodification reactions had signal that did not resolve in the SDS-PAGE gel and instead remained in the well, potentially due to high degree of branching such that the polymer prevented the sample from entering the gel (Figure 1A).

H-Y-E with short donor loop and long acceptor loop

PARP3 incorporated ADPr at its molecular weight in a pattern suggestive of MAR synthesis activity, consistent with previously published results (Figure 1A) (Loseva et al., 2010). Interestingly, PARP3 contains an H-Y-E catalytic triad and was therefore predicted to generate PAR (Kleine et al., 2008). These findings suggest that additional structural features of the PARP domain can impact catalytic activity.

H-Y-E with short donor and acceptor loop

PARP4 incorporation was consistent with MAR synthesis even though, similar to PARP3, it contains an H-Y-E catalytic motif (Figure 1). Previous reports on PARP4 also identified incorporation consistent with MAR synthesis for the bacterially purified PARP4 catalytic domain whereas incorporation activity of purified vault particles indicated PAR synthesis (Kickhoefer et al., 1999). Therefore, PARP4 activity may depend on

interactions with other components of vault particles. Another possibility is that there are minor levels of co-purifiying PARPs in vault particle preparations, contributing to the PAR synthesis activity identified. We confirmed previously reported results that PARP5a and 5b incorporated ADPr in a manner consistent with PAR synthesis (Figure 1) (Smith et al., 1998; Cook et al., 2002).

H-Y-I/L/Y

PARP6, 7, 8, 10, 11, 12, 14, 15 and 16 each incorporated ADPr in a manner consistent with MAR synthesis (Figure 1). Identification of MAR activity for PARP7, 10, 12, 14, 15 and 16 is consistent with previously published reports (Kleine et al., 2008; Leung et al., 2011; Di Paola et al., 2012; Jwa and Chang, 2012; MacPherson et al., 2013). Initial reports on PARP10 and 14 activity had originally identified poly(ADP-ribosyl)ation as their enzymatic activity (Aguiar et al., 2005; Yu et al., 2005). Interestingly, PARP15 appeared to have weak automodification activity and instead strongly modified a co-precipitating protein, suggesting that, unlike other PARPs, PARP15 is not a major target of PARP15 enzymatic activity.

Q/Y-Y-T/V

PARP9 failed to incorporate detectable amounts of ADPr, suggesting that it is catalytically inactive, in agreement with previous reports (Figure 1A) (Aguiar et al., 2005). Minimal NAD^+ incorporation was observed for both isoforms of PARP13, which are predicted to both be inactive due to the Q-Y-V catalytic motif for PARP13.1 and lack of catalytic domain for PARP13.2. Previous reports on the activity of the bacterially

purified PARP13 catalytic domain did not detect any NAD^+ incorporation (Kleine et al., 2008). Additionally, structural analysis of the PARP13 catalytic domain suggests that it cannot even bind NAD^+ due to a closed substrate binding pocket, and therefore the observed signal would not be due to bound ^{32}P-NAD. Instead the weak incorporation could be due to activity of a sub-stoichiometric co-purifiying PARP.

Enzymatic hydrolysis and chemical reversal of ADPr modifications confirms that majority of PARPs are mono (ADP-ribosyl)ases

While SDS-PAGE separation of NAD^+ incorporation reactions provides sufficient resolution to identify the generation of PAR modifications, the resolution is insufficient to distinguish between MAR or short oligomers of ADPr. Therefore we utilized two assays to improve resolution: 1) we treated *in vitro* automodified PARPs with ADPr hydrolytic enzymes specific for either PAR or MAR hydrolysis or 2) treated the identical reactions with chemicals known to release ADPr from proteins at the site of the protein linkage. We then examined the signal remaining attached to the PARP by resolving on SDS-PAGE followed by autoradiography (Figure 2), and examined the released reaction products by thin layer chromatography (TLC) (Figure 2) or high resolution TBE-polyacrylamide sequencing gels capable of resolving single units of ADPr (Figure 3). Each assay was performed a minimum of two times.

PAR is a substrate for hydrolysis by poly(ADP-ribose) glycohydrolase (PARG), which has been demonstrated to hydrolyze PAR chains, releasing ADPr as a product (Slade et al., 2011). Recently, enzymes with mono(ADP-ribose) hydrolase activity have been discovered which include MacroD1 and terminal (ADP-ribose) glycohydrolase (TARG) (Jankevicius et al., 2013; Rosenthal et al., 2013; Sharifi et al., 2013) . Both of

these enzymes have been shown to release the proximal ADPr unit. In addition, TARG was demonstrated to release PAR chains from the proximal ADPr unit, but does not hydrolyze the polymers to ADPr (Sharifi et al., 2013).

We first verified that the bead bound GFP-tagged protein did not affect the hydrolysis activity of these enzymes by comparing hydrolysis of automodified GFP-PARP10, SBP-PARP10 and soluble PARP10 (Figure S2A). We did not observe any effect of bead binding on hydrolysis activity. To determine an appropriate enzyme concentration for the reactions, we treated automodified GFP-PARP10 with a titration of TARG, MacroD1 and PARG ranging from 50nM to 500nM (Figure S2B). We confirmed that TARG and MacroD1 have identical activities using PARPs 1, 7, 10 and 14 and, in order to simplify subsequent assays, chose to use MacroD1 (Figure S2C). MacroD1 also released PAR chains from PARP1 but did not result hydrolyze the glycosidic ribose-ribose linkages as seen by TLC analysis of the release product, similar to what was previously shown for TARG (Figure S2C, S2D) (Sharifi et al., 2013).

There have been conflicting reports on the ability of PARG to hydrolyze the proximal ADPr-protein linkage (Kleine et al., 2008; Barkauskaite et al., 2013). In our assays, PARG failed to release signal from automodified PARP1^{E988Q} while some release was identified from automodified PARP10 (Figures 2 and S2E). While PARP1 has been shown to be automodifed on lysine residues, glutamate residues were identified as automodification targets for PARP10 (Kleine et al., 2008; Altmeyer et al., 2009). Therefore, this discrepancy could be due to differences in the specific amino acids on which the ADPr is attached on the two proteins, and the inability of PARG to hydrolyze the ADPr-lysine linkage.

Many chemicals have been identified that cleave various ADPr-protein linkages to release ADPr modifications (Jacobson et al., 1994). We tested three common chemical treatments: 2-(cyclohexylamino)ethanesulfonic acid (CHES), pH9, Hydroxylamine, pH 7.5 and sodium hydroxide, pH12 (Figure S3). While both CHES and NaOH treatment show similar levels of release of PAR from *in vitro* automodified PARP1, NaOH treatment results in the degradation of free ADPr to AMP, consistent with previous reports (Bredehorst et al., 1978). While treatment with neutral hydroxylamine has been shown to release carboxylate ADPr linkages robustly, we were unable to obtain samples that resulted in a clean PAR ladder from the PARP1 hydroxylamine released product. Therefore, we focused on CHES treatment for subsequent assays since it is reported to release ADPr from both acidic and lysine residues, allowing for the identification of ADPr modifications from both chemical linkages (Cervantes-Laurean et al., 1997)

As expected based on NAD^+ incorporation patterns and previously published results, CHES treatment of PARPs 1, 2, 5a and 5b resulted in the release of PAR chains of varying lengths, seen as ladders on sequencing gels (Figures 2A and 3). PARG treatment hydrolyzed PAR chains, releasing ADPr as the major product along with some short ADPr oligomers. This is consistent with previous work demonstrating that PARG has lower activity on short PAR chains (Hatakeyama et al., 1986). Finally, MacroD1 treatment also released PAR chains for PARPs 1, 2, 5a and 5b (Figure 2A).

The remaining PARPs showed release of ADPr as the major product of CHES and MacroD1 treatment (Figures 2B and 3). Interestingly, PARG treatment also resulted in a significant release of ADPr for some H-Y-E and H-Y-I PARPs, albeit to a

lesser extent than MacroD1 treatment, suggesting that ADPr linkages may be on acidic residues based on the differential hydrolysis activity for PARG on PARP1^{E988Q} and PARP10. While we observed a minor signal at 2 units of ADPr for CHES treatment, this signal may be due to artifact as it was also identified for PARP1^{E988Q} (Figure S4). These results suggest that the primary activity of PARPs is mono(ADP-ribosyl)ation.

Discussion

While the PARP protein family was originally identified as the source of intracellular PAR, recent work has demonstrated that many PARPs instead generate only MAR modifications. To systematically identify the enzymatic activity of each PARP protein, we performed NAD^+ incorporation assays for the whole family. The majority of the PARPs resolved as a discreet band, suggestive of MAR synthesis activity, and aside from a couple of exceptions, were in agreement with bioinformatics predictions. In order to further confirm the identity of ADPr modifications, we treated automodified PARPs with PARG, which hydrolyzes polymers, and MacroD1, which hydrolyzes MAR modifications. We also treated with CHES, a chemical that releases ADPr modifications at the site of protein linkage. These experiments indicated that the major activity for most of the PARP family is indeed mono(ADP-ribosyl)ation.

Interestingly, PARP3 and 4 had mono(ADP-ribosyl)ase activity despite containing a H-Y-E catalytic motif. While there is no structural information available for the catalytic domain of PARP4, based on the available structures of PARP1 and PARP3 catalytic domain, a key difference is the length of the D-loop, which partially shapes the NAD^+ binding pocket (Wahlberg et al., 2012). While the D-loop of PARP1 is long and contains 3 proline residues which contribute to rigidity of the loop, PARP3's D-loop is

shorter and more flexible, potentially affecting interactions with substrate NAD^+ and contributing to the lack of polymerase activity.

Why do cells need both types of ADPr modifications? MAR and PAR synthesis activities are both evolutionarily conserved, indicating that both have important functions in cellular physiology (Citarelli et al., 2010). PAR functions during many stress responses and physiological pathways that require the rapid assembly of multiprotein complexes, acting as a protein binding scaffold. The consequences of MAR modifications on target protein are less understood but recent work showing that ADPr binding macro domain containing proteins can specifically bind MARylated targets, suggests that one function could be to regulate specific protein-protein interactions, similar to SH3 domains binding to phosphoproteins (Karras et al., 2005; Forst et al., 2013). MAR modifications are also especially interesting because they may serve as primers for further elongation to PAR, with PARPs functioning cooperatively to synthesize polymer, allowing a cell to tightly regulate each step of PAR generation. This possibility is supported by the fact that PARPs with each activity are localized in both the cytoplasm and nucleus and that there are multiple physiological protein complexes containing MAR and PAR generating PARPs (Augustin et al., 2003; Kanai et al., 2003; Leung et al., 2011; Vyas et al., 2013)

Because of the possibility to either be capped by macro-domain containing proteins or elongated by polymerizing PARPs, MAR modifications could be poised for further elongation to PAR, allowing for a cell to rapidly respond to physiological or environmental signals. Further work examining the ability of PARPs to elongate MAR modifications will be important to determine if this type of regulation could occur in cells.

Materials and Methods

Cell culture and reagents

293F cells (from ATCC) were grown at 37°/5% CO_2 in F17 media supplemented with 2% glutamax (Life Technologies). ^{32}P-NAD$^+$ was from Perkin Elmer.

NAD Incorporation Reaction

GFP-PARPs or SBP-PARPs were expressed in 293F cells. Approximately 48hrs after transfection, cells were washed 3X in ice-cold PBS and lysed for 20min on ice in cell lysis buffer (CLB, 50mM HEPES, pH7.4, 150mM NaCl, 10mM $MgCl_2$, 1mM EGTA, 1mM DTT, 1% Triton-X 100, 1 µg/mL leupeptin, aprotinin, pepstatin, PMSF). Lysates were subject to ultracentrifugation at 100K*g for 30min. Cleared lysates were incubated for 1hr at 4 degrees either with anti-GFP antibody (3E6, Life Technologies) pre-bound protein A magnetic beads (Millipore) or streptavidin sepharose (GE Healthcare Life Sciences). Beads were than wash 1X 5min in CLB, followed by 3X 10min washed in CLB containing 1M NaCl, and 1X 5min wash in PARP reaction buffer (PRB; 50mM Tris, pH7.5, 50mM NaCl, 0.5mM DTT, 0.01% Triton-X 100, 1 µg/mL leupeptin, aprotinin, pepstatin).

NAD incorporation reactions were performed in PARP reaction buffer containing 10uM NAD (unless otherwise indicated) supplemented with ^{32}P-NAD at a 1:20 ratio for 30min at 25°C. Following NAD incorporation, beads were washed 6X 5min in PRB supplemented with 1M NaCl, 100uM NAD$^+$ and 10uM ATP and 2X 5min washed in PRB containing 100uM NAD$^+$ and 10uM ATP. Beads were then resuspended in Laemmli sample buffer, heated to 65°C for 10 minutes and run on 8% SDS-PAGE gels followed by autoradiography.

For enzymatic and chemical treatments, beads were treated with indicated enzyme or chemical following NAD incorporation and washes. Beads were then resuspended in Laemmli sample buffer while reaction supernatants were collected and either spotted on PEI-cellulose thin layer chromatography plates and resolved in 0.15M LiCl/0.15M Formic acid or diluted 1:1 in PAR loading buffer (50% urea, 25mM NaCl, 2mM EDTA, 2mM EGTA, 0.1% xylene cyanol, 0.1% bromophenol blue) and resolved on 20% polyacrylamide-TBE sequencing gels.

Figures and Tables

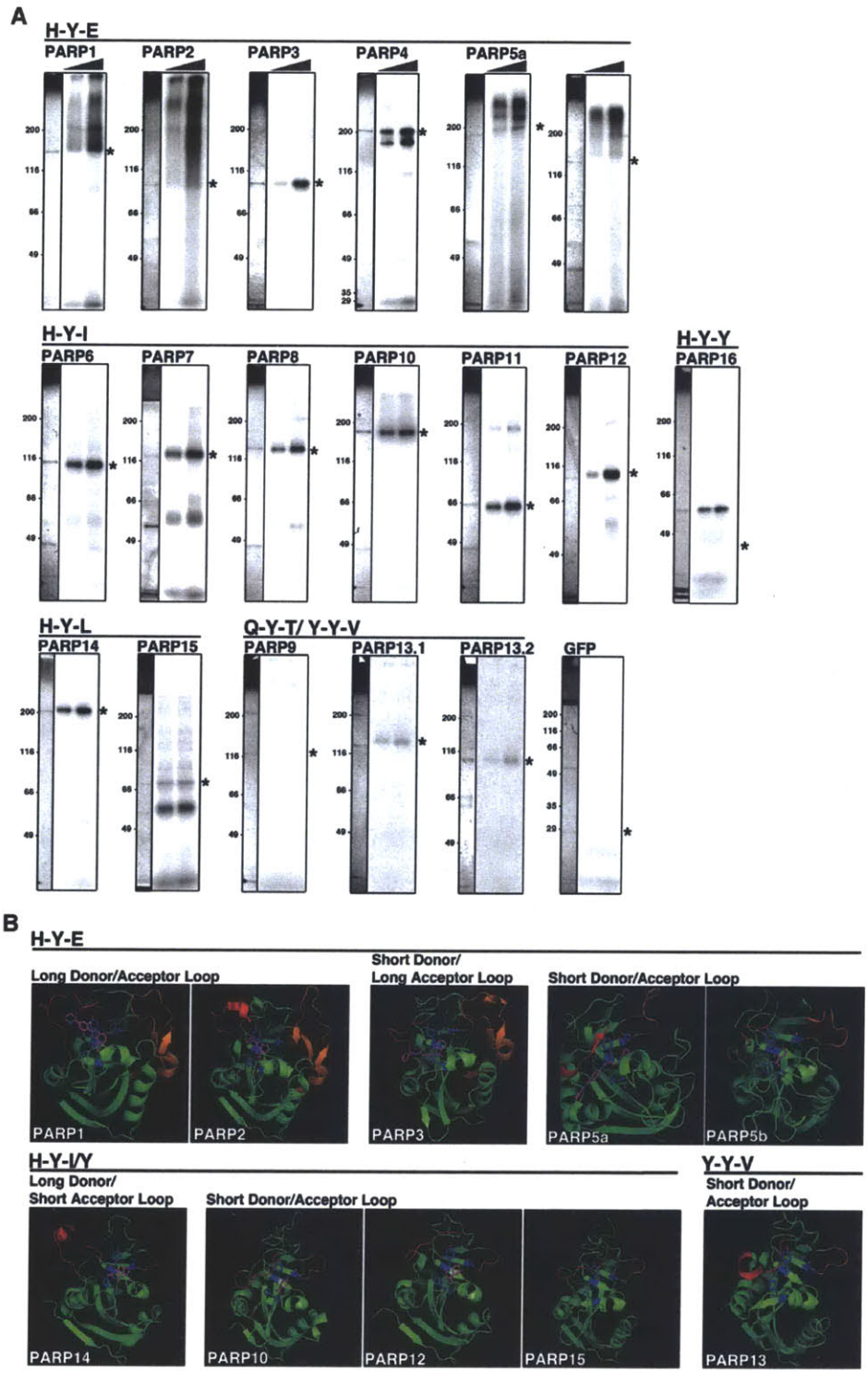

Figure 1. PARP enzymatic activity depends on catalytic triad motif and secondary structural elements of PARP catalytic domain
A) GFP-PARPs were immunoprecipitated from 293F cells and subjected to NAD^+ incorporation reactions *in vitro* with 5 or 10μM cold NAD^+ supplemented with a constant ratio of 32P-NAD^+. Automodifed PARPs were resolved on SDS-PAGE gels and subjected to autoradiography. Representative coomassies for each PARP purification are shown to the left the autoradiogram and the expected molecular weight of the PARP is indicated by an asterisk. Of the H-Y-E catalytic triad containing PARPs, PARP1, 2, 5a and 5b generated polymer, as evidenced by the smear of signal starting from the molecular weight of the PARP. The remaining PARPs resolve as a discreet, indicating that they do not generate poly(ADP-ribose). B) Crystal structures of PARP catalytic domains. The donor loop is shown in red, acceptor loop in orange, catalytic triad residues in blue and co-crystallized small molecule PARP inhibitors in magenta. Interestingly, PARP3, which contains an H-Y-E catalytic motif does not generate polymer, indicating that additional features such as the structure of the substrate binding pocket partially formed by the donor loop can contribute to catalytic activity. The following structures were used 3L3M (PARP1), 3KJD (PARP2), 4GV2 (PARP3), 4LI6 (PARP5a), 3U9H (PARP5b), 3HKV (PARP10), 2X5Y (PARP13), 3SMJ (PARP14) and 3GEY (PARP15).

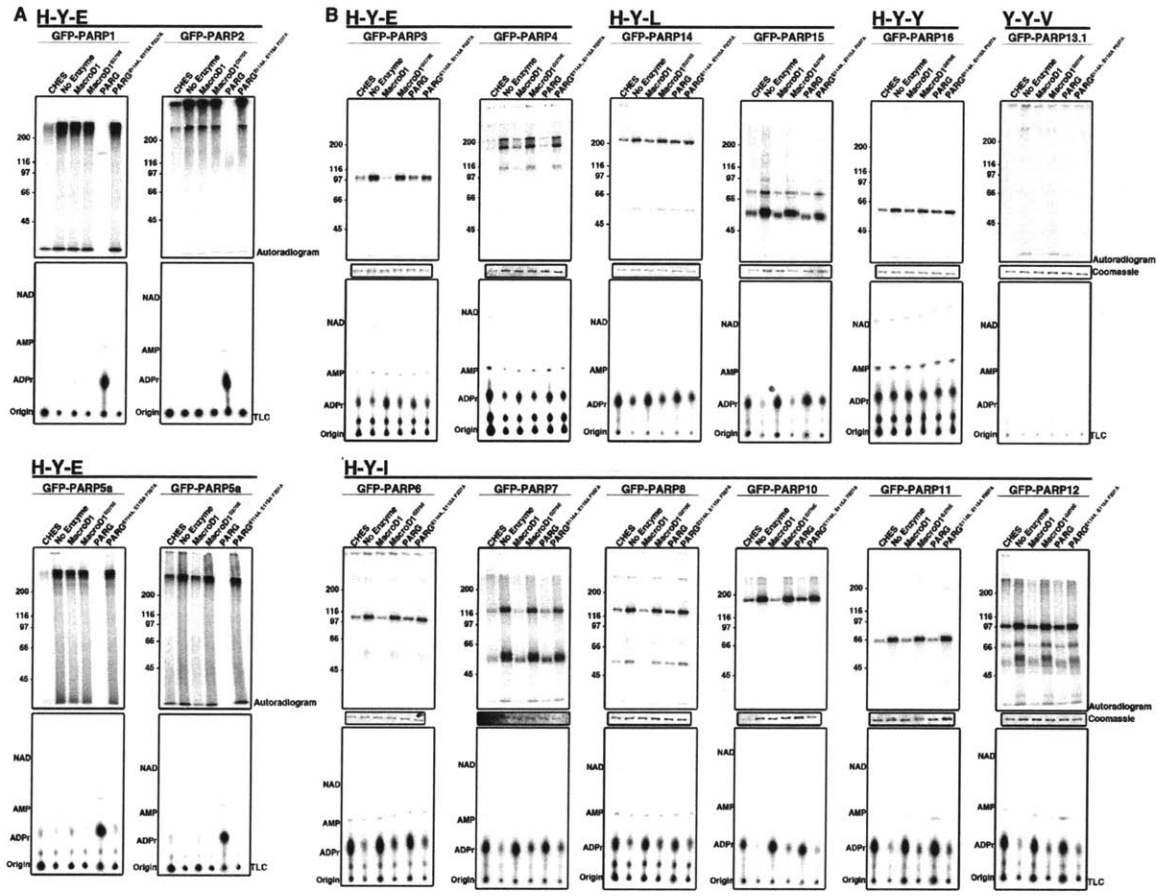

Figure 2. Enzymatic and chemical release of ADPr modifications confirms mono(ADP-ribosyl)ation as primary PARP activity

Automodified PARPs were treated with CHES or the indicated wild type and catalytically inactive ADPr hydrolytic enzyme. Signal remaining attached to protein was analyzed by SDS-PAGE and release product was analyzed by TLC. Clear differences are seen in the CHES and enzymatic hydrolysis patterns for poly(ADP-ribosyl)ating PARPs (A) and mono(ADP-ribosyl)ating/inactive PARPs (B).

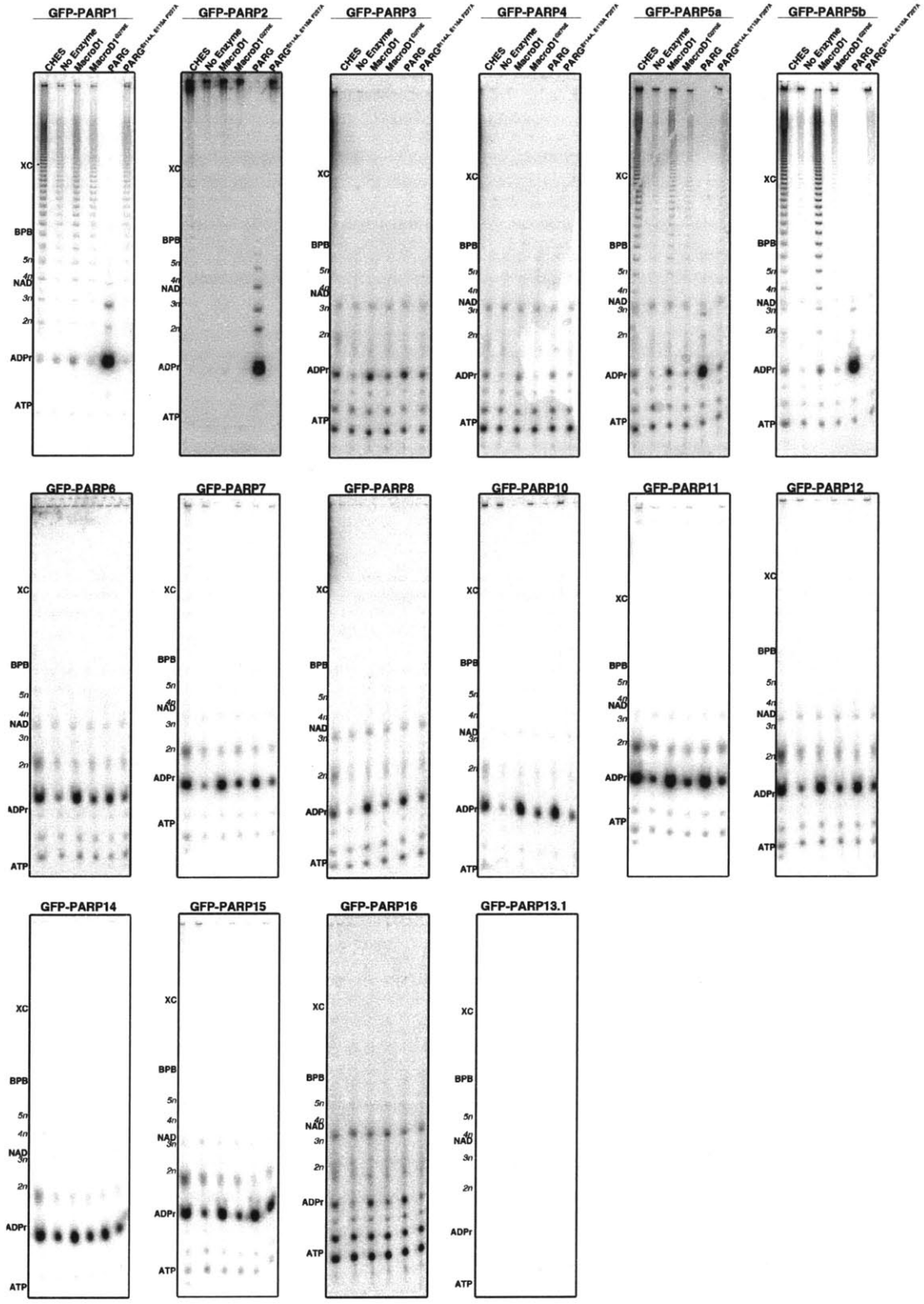
GFP-PARP1
GFP-PARP2
GFP-PARP3
GFP-PARP4
GFP-PARP5a
GFP-PARP5b
GFP-PARP6
GFP-PARP7
GFP-PARP8
GFP-PARP10
GFP-PARP11
GFP-PARP12
GFP-PARP14
GFP-PARP15
GFP-PARP16
GFP-PARP13.1
CHES
No Enzyme
MacroD1
MacroD1 E175Q
PARG
XC
BPB
NAD
ADPr
ATP

Figure 3. Analysis of PARP hydrolysis products by TBE-polyacrylamide sequencing gel.
CHES treatment of PARP1, 2, 5a and 5b results in the release of PAR ladders, while PARG treatment results in hydrolysis of PAR to ADPr. MacroD1 also results in release of PAR chains. The primary CHES release product for the remaining PARPs (except PARP13.1) is a single ADPr unit. MacroD1 and PARG treatment also results in release of ADPr for these PAPRs.

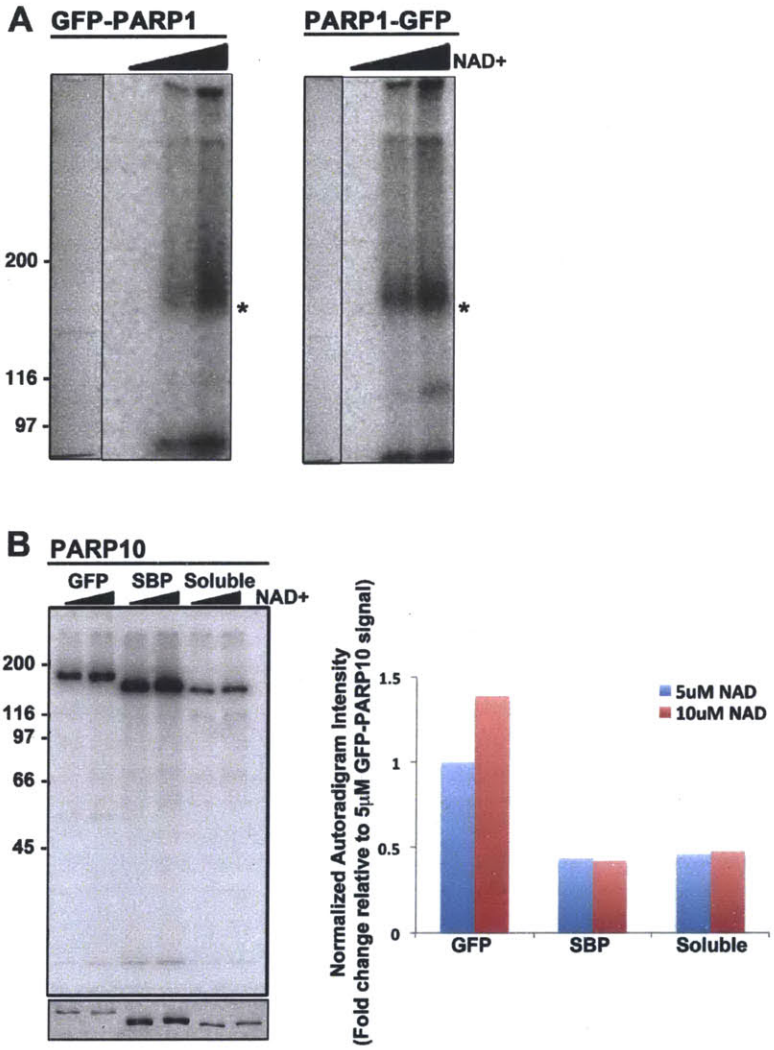

Figure S1. Effect of purification tags on *in vitro* NAD^+ incorporation activity.

A) PARP1 tagged with either a N- or C- terminal GFP fusion was subject to *in vitro* NAD^+ incorporation assays. Placement of tag did not affect enzymatic activity. Coomassie stained gel of each purification is shown the left and molecular of GFP-PARP protein is indicated by asterisk. B) Bead-bound PARP10 purifications tagged with either GFP or SBP and soluble PARP10 were subject to *in vitro* NAD^+ incorporation assays. Quantitation of NAD^+ incorporation signal, normalized for protein levels based on coomassie shown below, indicates that incorporation reactions are not affected by bead-bound GFP tagged protein.

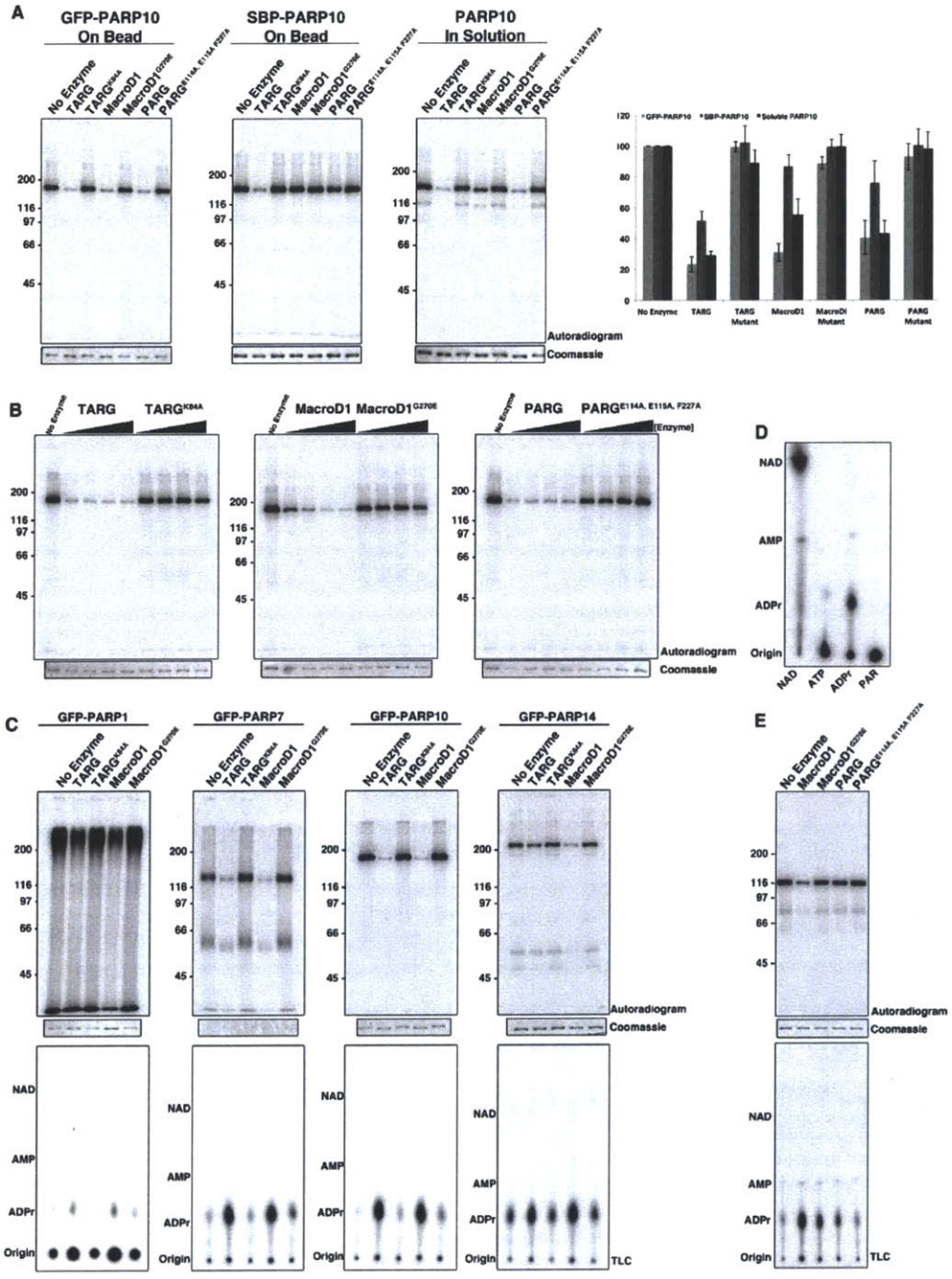
A
GFP-PARP10 On Bead
SBP-PARP10 On Bead
PARP10 In Solution
No Enzyme
TARG
TARG K84A
MacroD1
MacroD1 G270E
PARG
PARG E114A, E115A, F227A
200
116
97
66
45
Autoradiogram
Coomassie
GFP-PARP10
SBP-PARP10
Soluble PARP10
120
100
80
60
40
20
0
No Enzyme
TARG
TARG Mutant
MacroD1
MacroD1 Mutant
PARG
PARG Mutant
B
TARG
TARG K84A
MacroD1
MacroD1 G270E
PARG
PARG E114A, E115A, F227A
[Enzyme]
Autoradiogram
Coomassie
D
NAD
AMP
ADPr
Origin
NAD
ATP
ADPr
PAR
C
GFP-PARP1
GFP-PARP7
GFP-PARP10
GFP-PARP14
No Enzyme
TARG
TARG K84A
MacroD1
MacroD1 G270E
Autoradiogram
Coomassie
NAD
AMP
ADPr
Origin
TLC
E
No Enzyme
MacroD1
MacroD1 G270E
PARG
PARG E114A, E115A, F227A
Autoradiogram
Coomassie
NAD
AMP
ADPr
Origin
TLC

Figure S2. Enzyme treatments of automodified PARPs.
A) Automodified bead-bound GFP-PARP10, bead bound SBP-PARP10 and soluble PARP10 were treated with the 0.1μM TARG/TARG^{K84A}, 0.5μM MacroD1/MacroD1^{G270E}, or 0.1μM PARG/PARG$^{E114A, E115A, F227A}$. Quantitation of fold reduction in signal for each treatment compared to no enzyme control indicates that enzyme treatments are not affects by bead bound, GFP tagged protein. B) Titration of TARG, MacroD1, PARG and their respective catalytic point mutants from 50-500nM. Signal remaining on protein was analyzed by SDS-PAGE gel and coomassie below shows protein levels for each condition. C) Comparison of TARG and MacroD1 treatment for automodified PARP1, 7, 10 and 14. Signal remaining on protein was analyzed by SDS-PAGE gel and coomassie below shows protein levels for each condition. Released products were analyzed by TLC, showing TARG and MacroD1 mediated release PAR from PARP1 and ADPr from PARPs 7, 10 and 14. Migration of cold standards is indicated to the left D) Migration patterns of ^{32}P labeled NAD$^+$ standards on TLC, with migration of cold standards shown to the left. E) Treatment of automodified PARP1^{E988Q} with MacroD1 and PARG shows sensitivity to MacroD1 treatment and resistance to PARG mediated hydrolysis.

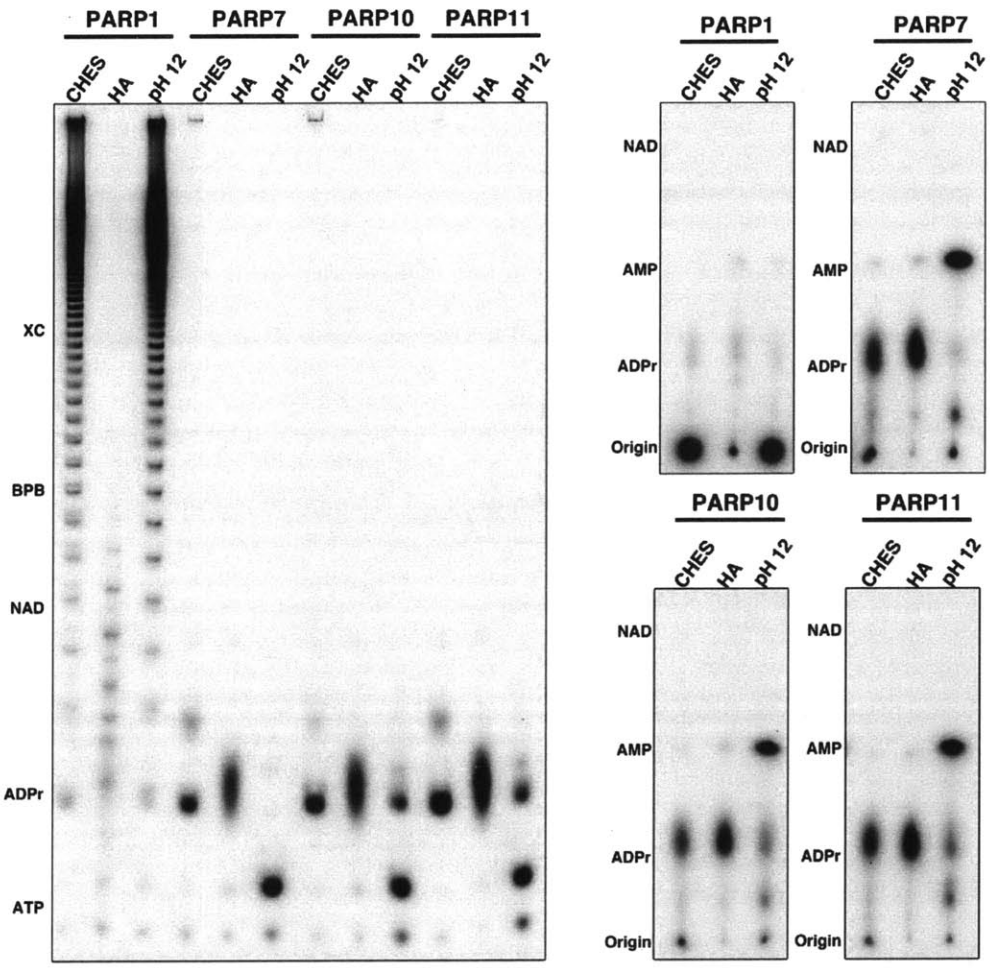

Figure S3. Comparison of chemical treatments to release ADPr linkages. Automodified PARP1, 7, 10 and 11 were treated with 100mM CHES, pH9, 2mM EDTA, 0.4M Hydroxylamine, pH 7.5, 2mM EDTA, or 100mM Tris, pH12, 1mM EDTA. Release products were analyzed both on 20% TBE-polyacrylamide sequencing gels (left) and TLC (right).

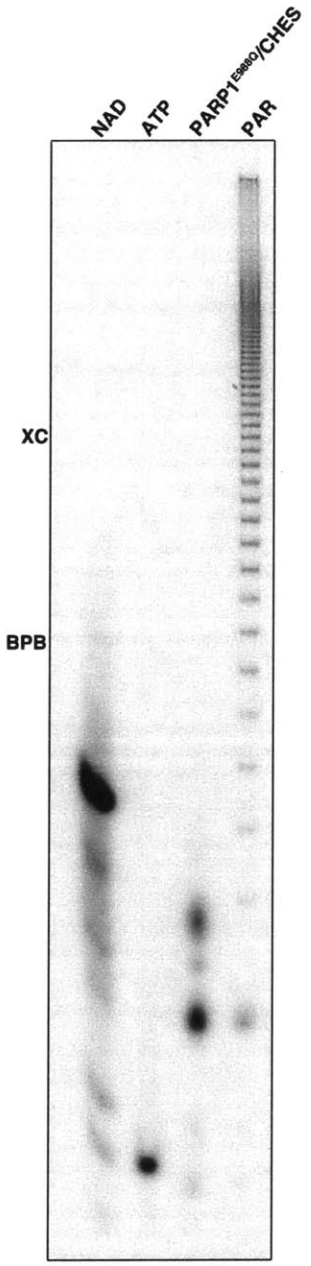

Figure S4. Further investigation of 2n ADPr signal.
Automodified PARP1^{E988Q} was treated with CHES and the released product analyzed by TBE-polyacrylamide sequencing gel. Although PARP1^{E988Q} has been shown to generate MAR, a signal is observed at 2n ADPr units, suggesting that this signal could be an artifact of the CHES treatment

Subfamily	PARP	Other Names	Catalytic Motif	D loop Length	Acceptor Loop Length	Postulated Activity	Experimental Evidence	Citation
DNA Dependent	1	PARP ARTD1	H-Y-E	12	37	P	SDS-PAGE Smear Sequencing Gel Phosphodiesterase Treatment	Alvarez-Gonzalez and Jacobson (1987). *Biochemistry* 26, 3218
	2	ARTD2	H-Y-E	12	40	P	SDS-PAGE Smear Sequencing Gel Phosphodiesterase Treatment	Amé et al. (1999). *J. Biol. Chem.* 274, 17860
	3	ARTD3	H-Y-E	8	42	P	(M) SDS-PAGE Band (P) Sequencing Gel	(M) Loseva et al. (2011). *J. Biol. Chem.* 285, 8054 (P) Rulten et al. (2011). *Mol. Cell* 41, 33.
Tankyrase	5a	TNKS1 ARTD5	H-Y-E	7	10	P	SDS-PAGE Smear Sequencing Gel Phosphodiesterase Treatment	Smith et al. (1998). *Science* 282, 1484. Rippmann et al. (2002). *J. Mol. Biol.* 323, 217.
	5b	TNKS2 ARTD6	H-Y-E	7	10	P	SDS-PAGE Smear	Cook et al. (2002). *Mol and Cell. Biol.* 22, 332. Sbodio et al. (2002). *Biochem. J.* 361, 451.
CCCH Zn Finger	7	tiPARP ARTD14	H-Y-I		6	M	SDS-PAGE Band	MacPherson et al. (2013). *Nuc. Acids. Rsrch.* 41, 1604
	12	ARTD12	H-Y-I	8	6	M	SDS-PAGE Band	Leung et al. (2011). *Mol. Cell* 42, 489
	13	ZC3HAV1 ARTD13	Y-Y-V	8	6	I	No Signal on SDS-PAGE	Kleine et al. (2008). *Mol. Cell* 32, 57
Macro	9	BAL1 ARTD9	Q-Y-T		6	I	No Signal on SDS-PAGE	Aguiar et al. (2005). *J. Biol. Chem.* 280, 33756.
	14	BAL2 ARTD8	H-Y-L	8	6	M	(M) SDS-PAGE Band (P) Poly(ADP-ribose) blot	(M) Kleine et al. (2008). *Mol. Cell* 32, 57 (P) Aguiar et al. (2005). J. Biol. Chem. 280, 33756.
	15	BAL3 ARTD7	H-Y-L	8	6	M	SDS-PAGE Band	Aguiar et al. (2005). *J. Biol. Chem.* 280, 33756.
Unclassified	4	vPARP ARTD4	H-Y-E		14	P	SDS PAGE Band/ Smear	Kickhoefer et al. (1999). *J. Cell Biol.* 146, 917.
	6	ARTD17	H-Y-I		2	M		
	8	ARTD16	H-Y-I		2	M		
	10	ARTD10	H-Y-I	8	6	M	(M) SDS-PAGE Band Sequencing Gel Phosphodiesterase Treatment Mass Spectrometry (P) SDS-PAGE MW shift	(M) Kleine et al. (2008). *Mol. Cell* 32, 57 (P) Yu et al. (2005). *Oncogene* 24, 1982
	11	ARTD11	H-Y-I		6	M		
	16	ARTD15	H-Y-Y	9	13	M	SDS-PAGE Band Sequencing gel	Jwa and Chang (2012). *Nat. Cell Biol.* 14, 1223 Di Paola et al. (2012). *PLoS One* 7, e37352

Table 1. Summary of PARP catalytic domain features and experimental evidence of enzymatic activity.

References

Aguiar, R., Takeyama, K., He, C., Kreinbrink, K., and Shipp, M. (2005). B-aggressive lymphoma family proteins have unique domains that modulate transcription and exhibit poly(ADP-ribose) polymerase activity. The Journal of biological chemistry 280, 33756-33765.

Ahel, I., Ahel, D., Matsusaka, T., Clark, A., Pines, J., Boulton, S., and West, S. (2008). Poly(ADP-ribose)-binding zinc finger motifs in DNA repair/checkpoint proteins. Nature 451, 81-85.

Altmeyer, M., Messner, S., Hassa, P., Fey, M., and Hottiger, M. (2009). Molecular mechanism of poly(ADP-ribosyl)ation by PARP1 and identification of lysine residues as ADP-ribose acceptor sites. Nucleic acids research 37, 3723-3738.

Alvarez-Gonzalez, R., and Jacobson, M. (1987). Characterization of polymers of adenosine diphosphate ribose generated in vitro and in vivo. Biochemistry 26, 3218-3224.

Amé, J., Rolli, V., Schreiber, V., Niedergang, C., Apiou, F., Decker, P., Muller, S., Höger, T., Ménissier-de Murcia, J., and de Murcia, G. (1999). PARP-2, A novel mammalian DNA damage-dependent poly(ADP-ribose) polymerase. The Journal of biological chemistry 274, 17860-17868.

Ame, J.C., Spenlehauer, C., and de Murcia, G. (2004). The PARP superfamily. Bioessays 26, 882-893.

Augustin, A., Spenlehauer, C., Dumond, H., Ménissier-De Murcia, J., Piel, M., Schmit, A.-C., Apiou, F., Vonesch, J.-L., Kock, M., Bornens, M., and De Murcia, G. (2003). PARP-3 localizes preferentially to the daughter centriole and interferes with the G1/S cell cycle progression. Journal of cell science 116, 1551-1562.

Barbarulo, A., Iansante, V., Chaidos, A., Naresh, K., Rahemtulla, A., Franzoso, G., Karadimitris, A., Haskard, D., Papa, S., and Bubici, C. (2013). Poly(ADP-ribose) polymerase family member 14 (PARP14) is a novel effector of the JNK2-dependent pro-survival signal in multiple myeloma. Oncogene 32, 4231-4242.

Barkauskaite, E., Brassington, A., Tan, E., Warwicker, J., Dunstan, M., Banos, B., Lafite, P., Ahel, M., Mitchison, T., Ahel, I., and Leys, D. (2013). Visualization of poly(ADP-ribose) bound to PARG reveals inherent balance between exo- and endo-glycohydrolase activities. Nature communications 4, 2164.

Bredehorst, R., Wielckens, K., Gartemann, A., Lengyel, H., Klapproth, K., and Hilz, H. (1978). Two different types of bonds linking single ADP-ribose residues covalently to proteins. Quantification in eukaryotic cells. Eur J Biochem 92, 129-135.

Brenda, A.W., Karl, A.R., Beth, R.W., and Collier, R.J. (1990). Active-site mutations of diphtheria toxin: effects of replacing glutamic acid-148 with aspartic acid, glutamine, or serine. Biochemistry 29.

Carroll, S.F., and Collier, R.J. (1984). NAD binding site of diphtheria toxin: identification of a residue within the nicotinamide subsite by photochemical modification with NAD. Proceedings of the National Academy of Sciences of the United States of America 81, 3307-3311.

Cervantes-Laurean, D., Jacobson, E., and Jacobson, M. (1997). Preparation of low molecular weight model conjugates for ADP-ribose linkages to protein. Methods in enzymology 280, 275-287.
Chang, P., Coughlin, M., and Mitchison, T.J. (2005). Tankyrase-1 polymerization of poly(ADP-ribose) is required for spindle structure and function. Nature cell biology 7, 1133-1139.
Chang, P., Coughlin, M., and Mitchison, T.J. (2009). Interaction between Poly(ADP-ribose) and NuMA contributes to mitotic spindle pole assembly. Molecular biology of the cell 20, 4575-4585.
Chang, P., Jacobson, M.K., and Mitchison, T.J. (2004). Poly(ADP-ribose) is required for spindle assembly and structure. Nature 432, 645-649.
Cho, S., Goenka, S., Henttinen, T., Gudapati, P., Reinikainen, A., Eischen, C., Lahesmaa, R., and Boothby, M. (2009). PARP-14, a member of the B aggressive lymphoma family, transduces survival signals in primary B cells. Blood 113, 2416-2425.
Citarelli, M., Teotia, S., and Lamb, R. (2010). Evolutionary history of the poly(ADP-ribose) polymerase gene family in eukaryotes. BMC evolutionary biology 10, 308.
Cook, B., Dynek, J., Chang, W., Shostak, G., and Smith, S. (2002). Role for the related poly(ADP-Ribose) polymerases tankyrase 1 and 2 at human telomeres. Molecular and cellular biology 22, 332-342.
Di Giammartino, D., Shi, Y., and Manley, J. (2013). PARP1 represses PAP and inhibits polyadenylation during heat shock. Molecular cell 49, 7-17.
Di Paola, S., Micaroni, M., Di Tullio, G., Buccione, R., and Di Girolamo, M. (2012). PARP16/ARTD15 is a novel endoplasmic-reticulum-associated mono-ADP-ribosyltransferase that interacts with, and modifies karyopherin-ß1. PloS one 7.
Domenighini, M., and Rappuoli, R. (1996). Three conserved consensus sequences identify the NAD-binding site of ADP-ribosylating enzymes, expressed by eukaryotes, bacteria and T-even bacteriophages. Molecular microbiology 21, 667-674.
Forst, A., Karlberg, T., Herzog, N., Thorsell, A.-G., Gross, A., Feijs, K., Verheugd, P., Kursula, P., Nijmeijer, B., Kremmer, E., Kleine, H., Ladurner, A., Schüler, H., and Lüscher, B. (2013). Recognition of mono-ADP-ribosylated ARTD10 substrates by ARTD8 macrodomains. Structure (London, England : 1993) 21, 462-475.
Goenka, S., and Boothby, M. (2006). Selective potentiation of Stat-dependent gene expression by collaborator of Stat6 (CoaSt6), a transcriptional cofactor. Proceedings of the National Academy of Sciences of the United States of America 103, 4210-4215.
Goenka, S., Cho, S., and Boothby, M. (2007). Collaborator of Stat6 (CoaSt6)-associated poly(ADP-ribose) polymerase activity modulates Stat6-dependent gene transcription. The Journal of biological chemistry 282, 18732-18739.
Han, S., and Tainer, J.A. (2002). The ARTT motif and a unified structural understanding of substrate recognition in ADP-ribosylating bacterial toxins and eukaryotic ADP-ribosyltransferases. International journal of medical microbiology : IJMM 291, 523-529.
Hatakeyama, K., Nemoto, Y., Ueda, K., and Hayaishi, O. (1986). Purification and characterization of poly(ADP-ribose) glycohydrolase. Different modes of action

on large and small poly(ADP-ribose). The Journal of biological chemistry 261, 14902-14911.
Huang, S.-M.A., Mishina, Y., Liu, S., Cheung, A., Stegmeier, F., Michaud, G., Charlat, O., Wiellette, E., Zhang, Y., Wiessner, S., Hild, M., Shi, X., Wilson, C., Mickanin, C., Myer, V., Fazal, A., Tomlinson, R., Serluca, F., Shao, W., Cheng, H., Shultz, M., Rau, C., Schirle, M., Schlegl, J., Ghidelli, S., Fawell, S., Lu, C., Curtis, D., Kirschner, M., Lengauer, C., Finan, P., Tallarico, J., Bouwmeester, T., Porter, J., Bauer, A., and Cong, F. (2009). Tankyrase inhibition stabilizes axin and antagonizes Wnt signalling. Nature 461, 614-620.
Jacobson, E.L., Cervantes-Laurean, D., and Jacobson, M.K. (1994). Glycation of proteins by ADP-ribose. Molecular and cellular biochemistry 138, 207-212.
Jankevicius, G., Hassler, M., Golia, B., Rybin, V., Zacharias, M., Timinszky, G., and Ladurner, A. (2013). A family of macrodomain proteins reverses cellular mono-ADP-ribosylation. Nature structural & molecular biology 20, 508-514.
Ji, Y., and Tulin, A.V. (2010). The roles of PARP1 in gene control and cell differentiation. Current opinion in genetics & development 20, 512-518.
Jwa, M., and Chang, P. (2012). PARP16 is a tail-anchored endoplasmic reticulum protein required for the PERK- and IRE1alpha-mediated unfolded protein response. Nature cell biology 14, 1223-1230.
Kanai, M., Tong, W.-M., Sugihara, E., Wang, Z.-Q., Fukasawa, K., and Miwa, M. (2003). Involvement of poly(ADP-Ribose) polymerase 1 and poly(ADP-Ribosyl)ation in regulation of centrosome function. Molecular and cellular biology 23, 2451-2462.
Karras, G., Kustatscher, G., Buhecha, H., Allen, M., Pugieux, C.I., Sait, F., Bycroft, M., and Ladurner, A. (2005). The macro domain is an ADP-ribose binding module. The EMBO journal 24, 1911-1920.
Kickhoefer, V.A., Siva, A.C., Kedersha, N.L., Inman, E.M., Ruland, C., Streuli, M., and Rome, L.H. (1999). The 193-kD vault protein, VPARP, is a novel poly(ADP-ribose) polymerase. The Journal of cell biology 146, 917-928.
Kleine, H., Poreba, E., Lesniewicz, K., Hassa, P.O., Hottiger, M.O., Litchfield, D.W., Shilton, B.H., and Luscher, B. (2008). Substrate-assisted catalysis by PARP10 limits its activity to mono-ADP-ribosylation. Molecular cell 32, 57-69.
Leung, A., Vyas, S., Rood, J., Bhutkar, A., Sharp, P., and Chang, P. (2011). Poly(ADP-ribose) regulates stress responses and microRNA activity in the cytoplasm. Molecular cell 42, 489-499.
Lindahl, T., Satoh, M., Poirier, G., and Klungland, A. (1995). Post-translational modification of poly(ADP-ribose) polymerase induced by DNA strand breaks. Trends in biochemical sciences 20, 405-411.
Loseva, O., Jemth, A.-S., Bryant, H., Schüler, H., Lehtiö, L., Karlberg, T., and Helleday, T. (2010). PARP-3 is a mono-ADP-ribosylase that activates PARP-1 in the absence of DNA. The Journal of biological chemistry 285, 8054-8060.
MacPherson, L., Tamblyn, L., Rajendra, S., Bralha, F., McPherson, J., and Matthews, J. (2013). 2,3,7,8-Tetrachlorodibenzo-p-dioxin poly(ADP-ribose) polymerase (TiPARP, ARTD14) is a mono-ADP-ribosyltransferase and repressor of aryl hydrocarbon receptor transactivation. Nucleic acids research 41, 1604-1621.

Malanga, M., and Althaus, F. (2005). The role of poly(ADP-ribose) in the DNA damage signaling network. Biochemistry and cell biology = Biochimie et biologie cellulaire 83, 354-364.

Marsischky, G.T., Wilson, B.A., and Collier, R.J. (1995). Role of glutamic acid 988 of human poly-ADP-ribose polymerase in polymer formation. Evidence for active site similarities to the ADP-ribosylating toxins. The Journal of biological chemistry 270, 3247-3254.

Otto, H., Reche, P., Bazan, F., Dittmar, K., Haag, F., and Koch-Nolte, F. (2005). In silico characterization of the family of PARP-like poly(ADP-ribosyl)transferases (pARTs). BMC genomics 6, 139.

Papini, E., Schiavo, G., Sandona, D., Rappuoli, R., and Montecucco, C. (1989). Histidine 21 is at the NAD+ binding site of diphtheria toxin. The Journal of biological chemistry 264, 12385-12388.

Petesch, S., and Lis, J. (2012). Activator-induced spread of poly(ADP-ribose) polymerase promotes nucleosome loss at Hsp70. Molecular cell 45, 64-74.

Pleschke, J., Kleczkowska, H., Strohm, M., and Althaus, F. (2000). Poly(ADP-ribose) binds to specific domains in DNA damage checkpoint proteins. The Journal of biological chemistry 275, 40974-40980.

Rippmann, J.F., Damm, K., and Schnapp, A. (2002). Functional characterization of the poly(ADP-ribose) polymerase activity of tankyrase 1, a potential regulator of telomere length. Journal of molecular biology 323, 217-224.

Rosenthal, F., Feijs, K., Frugier, E., Bonalli, M., Forst, A., Imhof, R., Winkler, H., Fischer, D., Caflisch, A., Hassa, P., Lüscher, B., and Hottiger, M. (2013). Macrodomain-containing proteins are new mono-ADP-ribosylhydrolases. Nature structural & molecular biology 20, 502-507.

Rouleau, M., Saxena, V., Rodrigue, A., Paquet, E., Gagnon, A., Hendzel, M., Masson, J.-Y., Ekker, M., and Poirier, G. (2011). A key role for poly(ADP-ribose) polymerase 3 in ectodermal specification and neural crest development. PloS one 6.

Ruf, A., Rolli, V., de Murcia, G., and Schulz, G. (1998). The mechanism of the elongation and branching reaction of poly(ADP-ribose) polymerase as derived from crystal structures and mutagenesis. Journal of molecular biology 278, 57-65.

Sharifi, R., Morra, R., Appel, C., Tallis, M., Chioza, B., Jankevicius, G., Simpson, M., Matic, I., Ozkan, E., Golia, B., Schellenberg, M., Weston, R., Williams, J., Rossi, M., Galehdari, H., Krahn, J., Wan, A., Trembath, R., Crosby, A., Ahel, D., Hay, R., Ladurner, A., Timinszky, G., Williams, R., and Ahel, I. (2013). Deficiency of terminal ADP-ribose protein glycohydrolase TARG1/C6orf130 in neurodegenerative disease. The EMBO journal 32, 1225-1237.

Slade, D., Dunstan, M., Barkauskaite, E., Weston, R., Lafite, P., Dixon, N., Ahel, M., Leys, D., and Ahel, I. (2011). The structure and catalytic mechanism of a poly(ADP-ribose) glycohydrolase. Nature 477, 616-620.

Smith, S., Giriat, I., Schmitt, A., and de Lange, T. (1998). Tankyrase, a poly(ADP-ribose) polymerase at human telomeres. Science (New York, NY) 282, 1484-1487.

Verheugd, P., Forst, A., Milke, L., Herzog, N., Feijs, K., Kremmer, E., Kleine, H., and Lüscher, B. (2013). Regulation of NF- κ B signalling by the mono-ADP-ribosyltransferase ARTD10. Nature communications 4, 1683.

Vyas, S., Chesarone-Cataldo, M., Todorova, T., Huang, Y.H., and Chang, P. (2013). A systematic analysis of the PARP protein family identifies new functions critical for cell physiology. Nature communications 4, 2240.

Wahlberg, E., Karlberg, T., Kouznetsova, E., Markova, N., Macchiarulo, A., Thorsell, A.-G., Pol, E., Frostell, Å., Ekblad, T., Öncü, D., Kull, B., Robertson, G., Pellicciari, R., Schüler, H., and Weigelt, J. (2012). Family-wide chemical profiling and structural analysis of PARP and tankyrase inhibitors. Nature biotechnology 30, 283-288.

Wang, Z., Michaud, G., Cheng, Z., Zhang, Y., Hinds, T., Fan, E., Cong, F., and Xu, W. (2012). Recognition of the iso-ADP-ribose moiety in poly(ADP-ribose) by WWE domains suggests a general mechanism for poly(ADP-ribosyl)ation-dependent ubiquitination. Genes & development 26, 235-240.

Yu, M., Schreek, S., Cerni, C., Schamberger, C., Lesniewicz, K., Poreba, E., Vervoorts, J., Walsemann, G., Grötzinger, J., Kremmer, E., Mehraein, Y., Mertsching, J., Kraft, R., Austen, M., Lüscher-Firzlaff, J., and Lüscher, B. (2005). PARP-10, a novel Myc-interacting protein with poly(ADP-ribose) polymerase activity, inhibits transformation. Oncogene 24, 1982-1993.

Zhang, Y., Liu, S., Mickanin, C., Feng, Y., Charlat, O., Michaud, G., Schirle, M., Shi, X., Hild, M., Bauer, A., Myer, V., Finan, P., Porter, J., Huang, S.-M.A., and Cong, F. (2011). RNF146 is a poly(ADP-ribose)-directed E3 ligase that regulates axin degradation and Wnt signalling. Nature cell biology 13, 623-629.

Chapter 4. Conclusions and Future Directions for the study of PARPs

The importance of cytoplasmic PARPs

For many years, PARP function was thought to be exclusive to the nucleus. Therefore, the majority of PARP research focused on nuclear functions including the maintenance of genome integrity (Meyer-Ficca et al., 2005), transcriptional regulation (Kraus and Lis, 2003), chromatin structure regulation (Dantzer and Santoro, 2013) and the DNA damage response (Malanga and Althaus, 2005). However, this work and recent data by other labs have highlighted the importance of cytoplasmic PARP functions including those in the unfolded protein response (Jwa and Chang, 2012), cytoplasmic signal transduction (Huang et al., 2009; Barbarulo et al., 2013; Verheugd et al., 2013), actin cytoskeleton regulation (Vyas et al., 2013), stress granules (Leung et al., 2011) and regulation of the miRNA silencing pathway (Seo et al., 2013). We have shown that the majority of PARPs are localized to the cytoplasm and that considerable amounts of cytoplasmic PAR exists throughout the cell cycle, demonstrating the importance of cytoplasmic PARP activity in cellular physiology (Vyas et al., 2013). These cytoplasmic PARPs have distinct sub-cytoplasmic localization patterns and function in diverse cellular processes. Identifying activating signals, binding partners and target proteins will be critical to understand how cytoplasmic PARPs are specifically and differentially regulated.

Regulation of PARP activity and identification of PARP specific protein targets

The ability of the PARP family to function in so many pathways must be due to the diversity of the protein domains outside the PARP catalytic domain. These domains are known to contribute to the regulation of catalytic activity by targeting PARPs to

specific subcellular localizations, specifying interactions with target proteins and activating PARP enzymatic activity (Altmeyer et al., 2009; Loeffler et al., 2011; Jwa and Chang, 2012; Langelier et al., 2012). However, exogenous regulatory signals such as posttranslational modifications that can stimulate PARP activity in response to various stresses or physiological conditions also exist and are not well understood. PARP1 can be activated by multiple protein kinases including ERK (extracellular signal-regulated kinases), JNK1 (c-Jun-N-terminal kinase 1) and CDK2 (cyclin dependent kinase 2) independent of DNA damage via phosphorylation and is required for full transcriptional activation of downstream target genes within these signaling pathways (Kauppinen et al., 2006; Cohen-Armon et al., 2007; Zhang et al., 2007; Wright et al., 2012). Interestingly, many of the phosphorylation sites in PARP1 have been mapped to known PARP1 regulatory domains including the zinc-finger, BRCT, WGR and catalytic domains. Mutation of some of the identified sites affects PARP1 recruitment and persistence at sites of microirradiation-induced DNA damage, suggesting that a further layer of PARP regulation is posttranslational modification of the protein domains outside of the PARP catalytic domain (Gagné et al., 2009). PARP5a also can be regulated by phosphorylation and is a target of PLK1 (polo-like kinase 1), with phosphorylation upregulating its ADP-ribosylation activity (Ha et al., 2012). Additional posttranslational modifications are known to regulate PARP activity and localization. For example, PARP1 function as a transcriptional co-regulator is regulated by acetylation and sumoylation and PARP13 is targeted to membranes by farnesylation (Hassa et al., 2005; Messner et al., 2009; Charron et al., 2013). The role of posttranslational modifications in the regulation of the remaining PARP family members is largely

unknown and their identification will be critical for a mechanistic understanding of how PARPs are activated.

The identification of PARP specific target proteins will be critical to understand mechanisms of PARP function in distinct cellular processes. Multiple studies using immunoprecipitation of proteins from cell lysates with anti-PAR antibodies have been used to identify poly(ADP-ribose) associated proteins (Gagné et al., 2003; Lai et al., 2008). However, this approach cannot differentiate between proteins that are covalently modified or non-covalently bound to PAR and, importantly, will not detect mono(ADP-ribosyl)ated proteins. The use of alkyne containing NAD^+ analogs that can be labeled with affinity tags by click chemistry and the development of proteome-wide mass spectrometry based methods to detect ADPr modified peptides have been useful in identifying the ADP-ribosylome (Dani et al., 2009; Jiang et al., 2010; Rosenthal et al., 2011). However, the issue of identification of PARP specific targets still remains unaddressed in these approaches. Recent work has used protein microarrays to identify specific targets by incubating with different recombinant PARPs (Feijs et al., 2013). Modified proteins identified by this approach must be further validated *in vivo* to determine if they are physiologically relevant targets. Another approach to identify PARP specific targets is candidate-based, where modification status of a target is determined in control versus PARP knockdown cells (Di Paola et al., 2012; Jwa and Chang, 2012). This type of approach coupled with the use of gene-editing strategies and proteome-wide mass spectrometry will no doubt be effective in identifying key targets of PARP specific ADP-ribosylation.

In addition to ADP-ribosylation target identification, determination of the sites of

modification within a protein will also be essential to understand the effect of ADPr modification on protein function. For example, if ADPr modification sites are located at sites of proteins required for binding to proteins or nucleic acids, it would suggest that ADPr modifications can function to modulate target protein interactions. Additionally, identification of ADP-ribosylation sites can allow for generation of point mutants that cannot be modified, a critical tool for further understanding of the role of ADPr modifications on protein function. Again, modern mass spectrometry methods such as electron transfer dissociation have allowed for such analyses for proteins such as PARP1 and histones (Messner et al., 2010).

Mono(ADP-ribose) as the prevailing product of PARP activity

Interestingly, the majority of the PARP family does not synthesize PAR and instead has mono(ADP-ribosyl)ase activity. This finding has direct consequences for the mechanism of function of ADPr modifications. While PAR can function as a protein binding scaffold to nucleate multiprotein complexes, MAR modifications lack this ability and the effects of MAR modifications on target protein activity are less well understood. Recently, it has been demonstrated that MAR-modified proteins can be specifically bound by macro domain-containing proteins (Forst et al., 2013). Additional mono(ADP-ribosyl)ating bacterial mART toxins can ADP-ribosylate many different host proteins, resulting in the disruption of protein-protein interactions (Deng and Barbieri, 2008). For example, ADP-ribosylation of the small GTPase Ras interferes with its ability to bind to the Cdc25 guanine exchange factor and modification of G-actin results in the depolymerization of actin filaments (Aktories et al., 1986; Ganesan et al., 1999). Therefore, one mechanism of MAR function can be to modulate protein-protein binding,

either by inducing interactions via macro domain recognition of a MARylated protein or by disrupting protein-protein interactions.

The finding that active PARPs synthesize either PAR or MAR leads to the hypothesis that PARPs can function together in the generation of ADPr modifications. In this case, MAR generating PARPs may prime polymer synthesis by transferring the initial ADPr unit onto a target, which is subsequently elongated by PAR generating PARPs. PARPs with each type of ADPr synthesis activity co-localize at multiple cellular structures including cytoplasmic stress granules, the mitotic spindle pole and the centrosome, each of which is also enriched in PAR (Leung et al., 2011; Vyas et al., 2013). Whether the MAR generating PARPs are required for the PAR accumulation or affect the kinetics of PAR synthesis at these structures is unknown. If PARPs function cooperatively in PAR synthesis, polymer generation could be finely tuned via differential regulation of each PARP's enzymatic activity.

The ability to stain and blot for PAR has been critical for identifying targets of PAR modification and cellular structures enriched in PAR. Therefore, the generation of similar reagents for MAR detection will be crucial for identifying MAR modified proteins and sites of MAR modifications within the cell. Since MAR is structurally identical to the terminal unit of PAR, generating antibodies that exclusively recognize MAR may prove difficult. While polyclonal antibodies against MAR have been generated and display specificity for MAR binding over PAR *in vitro*, no controls such as immunoblotting of a PARylated protein were performed to explicitly demonstrate that these antibodies cannot recognize PAR (Meyer and Hilz, 1986). Using immunofluorescence of untreated and DNA damaged cells, anti-MAR antibodies did show an increase in nuclear staining

upon DNA damage, but it not clear if the antibodies exclusively recognize MAR over PAR *in vivo* (Meyer and Hilz, 1986). Direct labeling of ADPr binding macro domains is an attractive candidate for MAR detection since specificity of certain macro domains for MAR binding has been demonstrated (Karras et al., 2005; Forst et al., 2013). Macro domains could be developed for use in immunofluorescence analogous to antibody based detection, as reporters for MARylation in real time by exogenous expression in live cells, or immobilized and used to isolate MARylated proteins from cell lysates. Indeed, the ability to pull down MARylated proteins using a macro domain has already been utilized to identify *in vivo* targets of ADP-ribosylation (Dani et al., 2009).

Impact of structural features of the catalytic domain on activity

The identification of mono(ADP-ribosyl)ase activity for PARPs 3 and 4, both of which contain an H-Y-E catalytic motif predictive of polymerase activity, highlights the potential impact of secondary structural features on PARP enzymatic activity (Loseva et al., 2010). The differences in donor loop structures across the PARP family likely affects the affinity for substrate NAD^+ and could account for differences in catalytic activity among the H-Y-E PARPs. The K_M for NAD^+ binding has been experimentally determined for a few PARPs including PARP1 (50μM) and PARP2 (130μM) but this analysis has not been done for the majority of the PARP family (Amé et al., 1999). Therefore, to determine if differences in substrate binding pocket structures, partly shaped by the D-loop, affect NAD^+ binding affinities, K_M analysis for NAD^+ binding should be performed across the whole PARP family. Similar studies have been done to determine inhibitor binding affinities to purified catalytic domains, demonstrating that this type of analysis can be easily performed family-wide (Wahlberg et al., 2012).

The structure of the acceptor pocket, lined by the loop between β4 and 5 within the catalytic domain, can also impact enzymatic activity by dictating what targets can be modified by each PARP. The acceptor loop varies greatly within the PARP family and is longest in the DNA dependent PARPs, presumably enabling them to processively bind PAR chains. PARPs 5a and 5b have a mid length acceptor loop potentially explaining why they generate only linear PAR as opposed to branched chains (Alvarez-Gonzalez and Jacobson, 1987; Rippmann et al., 2002). The majority of remaining active PARPs have short acceptor loops and are therefore predicted to be unable to remain bound to PAR chains, partly explaining their mono(ADP-ribosyl)ase activity.

Generating chimeric PARP catalytic domains can experimentally test these structural predications. For example, since the catalytic domains of PARP1 and 3 have high structural similarity other than within the D-loop, the requirement of the D-loop for polymerase activity can be determined by creating a PARP3 catalytic domain which contains the D-loop of PARP1. Similarly the importance of the acceptor loop in polymer binding and elongation can be tested by making a chimeric PARP domain where the acceptor loop of a mono(ADP-ribosyl)ating PARP is replaced with that of a poly(ADP-ribosyl)ating PARP. Finally, making PARP1/2 and 5a/5b catalytic domain chimeras in which the acceptor loops are switched can test the importance of acceptor loop structure in the generation of linear versus branched PAR.

Concluding remarks

PARPs have many functions in cellular physiology and the PARP family is evolutionarily conserved from amoeba to mammals, demonstrating the importance of this enzyme family (Citarelli et al., 2010). PARPs and PARG activity have even been

found in ancient bacteria, although it is possible that this is due to lateral transfer (Hassa and Hottiger, 2008; Slade et al., 2011). Determining mechanisms of PARP and ADPr function, including identification of targets and the effects of ADPr modifications on target activity, will be important to determine how PARPs execute their various cellular roles. This is especially critical due to the emergence of the PARP family as therapeutic targets for multiple human diseases. Currently, PARP1 is a major target for cancer treatment due to its function in the DNA damage response and recent work has implicated additional PARPs in the pathology of cancers including multiple myeloma and B cell lymphomas (Rouleau et al., 2010; Cho et al., 2011; Barbarulo et al., 2013). In addition, PARP inhibitors have had therapeutic benefits in multiple cardiovascular disease models (Pacher and Szabó, 2007). Since many of the small molecules used in these studies are non-specific PARP inhibitors, the inhibition of which PARP results in therapeutic benefit is unclear (Wahlberg et al., 2012). Therefore, gaining mechanistic insight into PARP functions and targets of PARP modification will be important to identify the therapeutically relevant PARPs.

References

Aktories, K., Bärmann, M., Ohishi, I., Tsuyama, S., Jakobs, K., and Habermann, E. (1986). Botulinum C2 toxin ADP-ribosylates actin. Nature 322, 390-392.

Altmeyer, M., Messner, S., Hassa, P., Fey, M., and Hottiger, M. (2009). Molecular mechanism of poly(ADP-ribosyl)ation by PARP1 and identification of lysine residues as ADP-ribose acceptor sites. Nucleic acids research 37, 3723-3738.

Alvarez-Gonzalez, R., and Jacobson, M. (1987). Characterization of polymers of adenosine diphosphate ribose generated in vitro and in vivo. Biochemistry 26, 3218-3224.

Amé, J., Rolli, V., Schreiber, V., Niedergang, C., Apiou, F., Decker, P., Muller, S., Höger, T., Ménissier-de Murcia, J., and de Murcia, G. (1999). PARP-2, A novel mammalian DNA damage-dependent poly(ADP-ribose) polymerase. The Journal of biological chemistry 274, 17860-17868.

Barbarulo, A., Iansante, V., Chaidos, A., Naresh, K., Rahemtulla, A., Franzoso, G., Karadimitris, A., Haskard, D., Papa, S., and Bubici, C. (2013). Poly(ADP-ribose) polymerase family member 14 (PARP14) is a novel effector of the JNK2-dependent pro-survival signal in multiple myeloma. Oncogene 32, 4231-4242.

Charron, G., Li, M., MacDonald, M., and Hang, H. (2013). Prenylome profiling reveals S-farnesylation is crucial for membrane targeting and antiviral activity of ZAP long-isoform. Proceedings of the National Academy of Sciences of the United States of America 110, 11085-11090.

Cho, S., Ahn, A., Bhargava, P., Lee, C.-H., Eischen, C., McGuinness, O., and Boothby, M. (2011). Glycolytic rate and lymphomagenesis depend on PARP14, an ADP ribosyltransferase of the B aggressive lymphoma (BAL) family. Proceedings of the National Academy of Sciences of the United States of America 108, 15972-15977.

Citarelli, M., Teotia, S., and Lamb, R. (2010). Evolutionary history of the poly(ADP-ribose) polymerase gene family in eukaryotes. BMC evolutionary biology 10, 308.

Cohen-Armon, M., Visochek, L., Rozensal, D., Kalal, A., Geistrikh, I., Klein, R., Bendetz-Nezer, S., Yao, Z., and Seger, R. (2007). DNA-independent PARP-1 activation by phosphorylated ERK2 increases Elk1 activity: a link to histone acetylation. Molecular cell 25, 297-308.

Dani, N., Stilla, A., Marchegiani, A., Tamburro, A., Till, S., Ladurner, A., Corda, D., and Di Girolamo, M. (2009). Combining affinity purification by ADP-ribose-binding macro domains with mass spectrometry to define the mammalian ADP-ribosyl proteome. Proceedings of the National Academy of Sciences of the United States of America 106, 4243-4248.

Dantzer, F., and Santoro, R. (2013). The expanding role of PARPs in the establishment and maintenance of heterochromatin. The FEBS journal 280, 3508-3518.

Deng, Q., and Barbieri, J. (2008). Molecular mechanisms of the cytotoxicity of ADP-ribosylating toxins. Annual review of microbiology 62, 271-288.

Di Paola, S., Micaroni, M., Di Tullio, G., Buccione, R., and Di Girolamo, M. (2012). PARP16/ARTD15 is a novel endoplasmic-reticulum-associated mono-ADP-ribosyltransferase that interacts with, and modifies karyopherin-ß1. PloS one 7.

Feijs, K., Kleine, H., Braczynski, A., Forst, A., Herzog, N., Verheugd, P., Linzen, U., Kremmer, E., and Lüscher, B. (2013). ARTD10 substrate identification on protein microarrays: regulation of GSK3 β by mono-ADP-ribosylation. Cell communication and signaling : CCS 11, 5.

Forst, A., Karlberg, T., Herzog, N., Thorsell, A.-G., Gross, A., Feijs, K., Verheugd, P., Kursula, P., Nijmeijer, B., Kremmer, E., Kleine, H., Ladurner, A., Schüler, H., and Lüscher, B. (2013). Recognition of mono-ADP-ribosylated ARTD10 substrates by ARTD8 macrodomains. Structure (London, England : 1993) 21, 462-475.

Gagné, J.-P., Hunter, J., Labrecque, B., Chabot, B., and Poirier, G. (2003). A proteomic approach to the identification of heterogeneous nuclear ribonucleoproteins as a new family of poly(ADP-ribose)-binding proteins. The Biochemical journal 371, 331-340.

Gagné, J.-P., Moreel, X., Gagné, P., Labelle, Y., Droit, A., Chevalier-Paré, M., Bourassa, S., McDonald, D., Hendzel, M., Prigent, C., and Poirier, G. (2009). Proteomic investigation of phosphorylation sites in poly(ADP-ribose) polymerase-1 and poly(ADP-ribose) glycohydrolase. Journal of proteome research 8, 1014-1029.

Ganesan, A., Vincent, T., Olson, J., and Barbieri, J. (1999). Pseudomonas aeruginosa exoenzyme S disrupts Ras-mediated signal transduction by inhibiting guanine nucleotide exchange factor-catalyzed nucleotide exchange. The Journal of biological chemistry 274, 21823-21829.

Ha, G.H., Kim, H.S., Go, H., Lee, H., Seimiya, H., Chung, D., and Lee, C.W. (2012). Tankyrase-1 function at telomeres and during mitosis is regulated by Polo-like kinase-1-mediated phosphorylation. Cell death and differentiation 19, 321-332.

Hassa, P., Haenni, S., Buerki, C., Meier, N., Lane, W., Owen, H., Gersbach, M., Imhof, R., and Hottiger, M. (2005). Acetylation of poly(ADP-ribose) polymerase-1 by p300/CREB-binding protein regulates coactivation of NF-kappaB-dependent transcription. The Journal of biological chemistry 280, 40450-40464.

Hassa, P.O., and Hottiger, M.O. (2008). The diverse biological roles of mammalian PARPS, a small but powerful family of poly-ADP-ribose polymerases. Front Biosci 13, 3046-3082.

Huang, S.-M.A., Mishina, Y., Liu, S., Cheung, A., Stegmeier, F., Michaud, G., Charlat, O., Wiellette, E., Zhang, Y., Wiessner, S., Hild, M., Shi, X., Wilson, C., Mickanin, C., Myer, V., Fazal, A., Tomlinson, R., Serluca, F., Shao, W., Cheng, H., Shultz, M., Rau, C., Schirle, M., Schlegl, J., Ghidelli, S., Fawell, S., Lu, C., Curtis, D., Kirschner, M., Lengauer, C., Finan, P., Tallarico, J., Bouwmeester, T., Porter, J., Bauer, A., and Cong, F. (2009). Tankyrase inhibition stabilizes axin and antagonizes Wnt signalling. Nature 461, 614-620.

Jiang, H., Kim, J., Frizzell, K., Kraus, W., and Lin, H. (2010). Clickable NAD analogues for labeling substrate proteins of poly(ADP-ribose) polymerases. Journal of the American Chemical Society 132, 9363-9372.

Jwa, M., and Chang, P. (2012). PARP16 is a tail-anchored endoplasmic reticulum protein required for the PERK- and IRE1alpha-mediated unfolded protein response. Nature cell biology 14, 1223-1230.

Karras, G., Kustatscher, G., Buhecha, H., Allen, M., Pugieux, C.I., Sait, F., Bycroft, M., and Ladurner, A. (2005). The macro domain is an ADP-ribose binding module. The EMBO journal 24, 1911-1920.
Kauppinen, T., Chan, W., Suh, S., Wiggins, A., Huang, E., and Swanson, R. (2006). Direct phosphorylation and regulation of poly(ADP-ribose) polymerase-1 by extracellular signal-regulated kinases 1/2. Proceedings of the National Academy of Sciences of the United States of America 103, 7136-7141.
Kraus, W., and Lis, J. (2003). PARP goes transcription. Cell 113, 677-683.
Lai, Y., Chen, Y., Watkins, S., Nathaniel, P., Guo, F., Kochanek, P., Jenkins, L., Szabó, C., and Clark, R. (2008). Identification of poly-ADP-ribosylated mitochondrial proteins after traumatic brain injury. Journal of neurochemistry 104, 1700-1711.
Langelier, M.-F., Planck, J., Roy, S., and Pascal, J. (2012). Structural basis for DNA damage-dependent poly(ADP-ribosyl)ation by human PARP-1. Science (New York, NY) 336, 728-732.
Leung, A., Vyas, S., Rood, J., Bhutkar, A., Sharp, P., and Chang, P. (2011). Poly(ADP-ribose) regulates stress responses and microRNA activity in the cytoplasm. Molecular cell 42, 489-499.
Loeffler, P., Cuneo, M., Mueller, G., DeRose, E., Gabel, S., and London, R. (2011). Structural studies of the PARP-1 BRCT domain. BMC structural biology 11, 37.
Loseva, O., Jemth, A.-S., Bryant, H., Schüler, H., Lehtiö, L., Karlberg, T., and Helleday, T. (2010). PARP-3 is a mono-ADP-ribosylase that activates PARP-1 in the absence of DNA. The Journal of biological chemistry 285, 8054-8060.
Malanga, M., and Althaus, F. (2005). The role of poly(ADP-ribose) in the DNA damage signaling network. Biochemistry and cell biology = Biochimie et biologie cellulaire 83, 354-364.
Messner, S., Altmeyer, M., Zhao, H., Pozivil, A., Roschitzki, B., Gehrig, P., Rutishauser, D., Huang, D., Caflisch, A., and Hottiger, M. (2010). PARP1 ADP-ribosylates lysine residues of the core histone tails. Nucleic acids research 38, 6350-6362.
Messner, S., Schuermann, D., Altmeyer, M., Kassner, I., Schmidt, D., Schär, P., Müller, S., and Hottiger, M. (2009). Sumoylation of poly(ADP-ribose) polymerase 1 inhibits its acetylation and restrains transcriptional coactivator function. FASEB journal : official publication of the Federation of American Societies for Experimental Biology 23, 3978-3989.
Meyer, T., and Hilz, H. (1986). Production of anti-(ADP-ribose) antibodies with the aid of a dinucleotide-pyrophosphatase-resistant hapten and their application for the detection of mono(ADP-ribosyl)ated polypeptides. Eur J Biochem 155, 157-165.
Meyer-Ficca, M., Meyer, R., Jacobson, E., and Jacobson, M. (2005). Poly(ADP-ribose) polymerases: managing genome stability. The international journal of biochemistry & cell biology 37, 920-926.
Pacher, P., and Szabó, C. (2007). Role of poly(ADP-ribose) polymerase 1 (PARP-1) in cardiovascular diseases: the therapeutic potential of PARP inhibitors. Cardiovascular drug reviews 25, 235-260.
Rippmann, J., Damm, K., and Schnapp, A. (2002). Functional characterization of the poly(ADP-ribose) polymerase activity of tankyrase 1, a potential regulator of telomere length. Journal of molecular biology 323, 217-224.

Rosenthal, F., Messner, S., Roschitzki, B., Gehrig, P., Nanni, P., and Hottiger, M. (2011). Identification of distinct amino acids as ADP-ribose acceptor sites by mass spectrometry. Methods in molecular biology (Clifton, NJ) 780, 57-66.

Rouleau, M., Patel, A., Hendzel, M., Kaufmann, S., and Poirier, G. (2010). PARP inhibition: PARP1 and beyond. Nature reviews Cancer 10, 293-301.

Seo, G., Kincaid, R., Phanaksri, T., Burke, J., Pare, J., Cox, J., Hsiang, T.-Y., Krug, R., and Sullivan, C. (2013). Reciprocal Inhibition between Intracellular Antiviral Signaling and the RNAi Machinery in Mammalian Cells. Cell host & microbe.

Slade, D., Dunstan, M., Barkauskaite, E., Weston, R., Lafite, P., Dixon, N., Ahel, M., Leys, D., and Ahel, I. (2011). The structure and catalytic mechanism of a poly(ADP-ribose) glycohydrolase. Nature 477, 616-620.

Verheugd, P., Forst, A., Milke, L., Herzog, N., Feijs, K., Kremmer, E., Kleine, H., and Lüscher, B. (2013). Regulation of NF- κ B signalling by the mono-ADP-ribosyltransferase ARTD10. Nature communications 4, 1683.

Vyas, S., Chesarone-Cataldo, M., Todorova, T., Huang, Y.H., and Chang, P. (2013). A systematic analysis of the PARP protein family identifies new functions critical for cell physiology. Nature communications 4, 2240.

Wahlberg, E., Karlberg, T., Kouznetsova, E., Markova, N., Macchiarulo, A., Thorsell, A.-G., Pol, E., Frostell, Å., Ekblad, T., Öncü, D., Kull, B., Robertson, G., Pellicciari, R., Schüler, H., and Weigelt, J. (2012). Family-wide chemical profiling and structural analysis of PARP and tankyrase inhibitors. Nature biotechnology 30, 283-288.

Wright, R.H.G., Castellano, G., Bonet, J., Dily, F.L., Font-Mateu, J., Ballare, C., Nacht, A.S., Soronellas, D., Oliva, B., and Beato, M. (2012). CDK2-dependent activation of PARP-1 is required for hormonal gene regulation in breast cancer cells. Genes & Development 26.

Zhang, S., Lin, Y., Kim, Y.S., Hande, M., Liu, Z.G., and Shen, H.M. (2007). c-Jun N-terminal kinase mediates hydrogen peroxide-induced cell death via sustained poly(ADP-ribose) polymerase-1 activation. Cell death and differentiation 14, 1001-1010.

Acknowledgements

First and foremost, I thank my parents for their continuous support and encouragement from the very start of my primary schooling throughout graduate school. Their emphasis on the importance of hard work and not taking the easy way out has forever stuck with me and prepared me for the many challenges I've had to face along the way. I also thank my brother for his support and encouragement to aim high.

I of course would like to thank my advisor, Paul Chang, for all his support and advice in both the ups and downs of grad school and in my future career. As the first student in his lab, I was able to learn a lot from him first hand as I started in the lab, which gave me a great foundation for independent work.

I thank my thesis committee, Phil Sharp and Peter Reddien, who have followed my progress from the start of my time in the lab and always been supportive and provided thoughtful advice.

I thank everyone I worked with while in the Chang lab (Jenny, Anthony, Tanya, Lilen, Robert, Tenzin, Miri, Melissa, Hannah, Stephanie, Alan, Tiffany, Florian, Thomas) for their support and helpful discussion, for sitting through practice talks and lab meetings and for making our lab a fun environment in which to work. I especially want to thank Tanya for being a great baymate and for her critical function in the proofreading of this thesis. I also thank all the members of biograd2007, who were always there for discussions about work as well as fun nights out to unwind.

I thank my undergraduate advisor, Wendy Hanna-Rose, and my intern advisor at Merck, Russell Lingham, who both took me into their labs and taught me not only the technical aspects of designing and performing experiments but also how to think critically about scientific questions.

Finally, I thank all my biology teachers from high school to undergrad who made me believe that there was nothing more interesting than figuring out how cells work.

Curriculum Vitae

Sejal Vyas

Education

Ph.D. in Biology, Massachusetts Institute of Technology, Cambridge, MA, 2007-2013

B.S. in Biochemistry and Molecular Biology, Penn State University, Schreyer Honors College, University Park, PA, 2003-2007
Summa cum laude graduate with honors in Biochemistry & Molecular Biology
Minor in Chemistry
GPA 3.98/4.0

Research Experience

2007-2013: Graduate Thesis
Laboratory of Dr. Paul Chang, Koch Institute for Integrative Cancer Research, MIT
A systematic analysis of the poly(ADP-ribose) polymerase protein family

Summer 2006, Summer 2007: Research Intern
Immunology Dept., Merck and Co.
Investigated the timing of HIF1α nuclear translocation, gene expression, and protein translation following hypoxic induction or treatment with hypoxia mimetics

2005-2007: Undergraduate Research
Laboratory of Dr. Wendy Hanna-Rose, Penn State University
Investigated the regulation of gene expression in the *Caenorhabditis elegans* uterine seam cell

Publications

Vyas, S., Chesarone-Cataldo, M., Todorova, T., Huang, Y-H., and Chang, P. (2013) A systematic analysis of the PARP protein family identifies new functions critical for cell physiology. Nature Communications *4*, doi:10.1038/ncomms3240.

Vyas, S. and Chang, P. (2013) Dual roles for PARP1 during heat shock: transcriptional activator and posttranscriptional inhibitor of gene expression. Molecular Cell *49*, 1.

Leung, A.K.L., Vyas, S., Rood, J.E., Bhutkar, A., Sharp, P.A., and Chang, P. (2011) Poly(ADP-Ribose) Regulates Stress Responses and microRNA Activity in the Cytoplasm. Molecular Cell *42*, 489.

Patents

U.S. Patent No: 8,268,550
Compositions and method for identification of PARP function, inhibitors, and activators

U.S. Provisional Application Serial No. 61/269,614
Compositions and methods for treating cancer and modulating stress granule formation

U.S. Provisional Application Serial No. 61/552,210
Methods of diagnosis and treatment of endoplasmic reticulum (ER) stress-related conditions

Teaching Experience

Fall 2010. Teaching Assistant, Cell Biology (7.06), MIT.
Spring 2009. Teaching Assistant, Introductory Biology (7.013), MIT.

Presentations and Conferences

March 2012: Keystone Symposium: RNA protein interactions in physiology and human disease
Poster: PARP-7 localizes to nuclear speckles via a CCCH ZnF domain and is upregulated during heat shock.

December 2009: American Society for Cell Biology Annual Meeting
Poster: A systematic analysis of PARP function

June 2009: Gordon Research Conference: Stress Proteins in Growth, Development & Disease
Poster: Poly(ADP-ribose) is required for cytoplasmic stress granule function.

February 2009: Koch Institute for Integrative Cancer Research Seminar Talk
Title: Poly(ADP-ribose) function in stress granules

October 2008: Koch Institute for Integrative Cancer Research Annual Retreat Talk
Title: A systematic analysis of PARP function

Awards

Ludwig School of Science Graduate Fellowship Award (2011)
Evan Pugh Scholar Award (2007)
Schraer Scholarship for Women in Science (2006)
Life Sciences Scholarship (2005)
Academic Excellence Scholarship (2003-2007)

Appendix I. Poly(ADP-Ribose) Regulates Stress Responses and microRNA Activity in the Cytoplasm

Anthony K.L. Leung[1,3], Sejal Vyas[1,2], Jennifer E. Rood[1,2], Arjun Bhutkar[1], Phillip A. Sharp[1,2*] and Paul Chang[1,2*]

[1]Koch Institute for Integrative Cancer Research, [2]Department of Biology Massachusetts Institute of Technology, Cambridge, MA 02139, USA. [3]Present Address: Department of Biochemistry and Molecular Biology, Bloomberg School of Public Health, Johns Hopkins University, Baltimore, MD 21205, USA

Published as

Leung, A.K.L., Vyas, S., Rood, J.E., Bhutkar, A., Sharp, P.A., and Chang, P. (2011) Poly(ADP-Ribose) Regulates Stress Responses and microRNA Activity in the Cytoplasm. Molecular Cell *42*, 489.

Molecular Cell
Article

Poly(ADP-Ribose) Regulates Stress Responses and MicroRNA Activity in the Cytoplasm

Anthony K.L. Leung,[1,3] Sejal Vyas,[1,2] Jennifer E. Rood,[1,2] Arjun Bhutkar,[1] Phillip A. Sharp,[1,2,*] and Paul Chang[1,2,*]
[1]Koch Institute for Integrative Cancer Research
[2]Department of Biology
Massachusetts Institute of Technology, Cambridge, MA 02139, USA
[3]Present Address: Department of Biochemistry and Molecular Biology, Bloomberg School of Public Health, Johns Hopkins University, Baltimore, MD 21205, USA
*Correspondence: sharppa@mit.edu (P.A.S.), pchang2@mit.edu (P.C.)
DOI 10.1016/j.molcel.2011.04.015

SUMMARY

Poly(ADP-ribose) is a major regulatory macromolecule in the nucleus, where it regulates transcription, chromosome structure, and DNA damage repair. Functions in the interphase cytoplasm are less understood. Here, we identify a requirement for poly(ADP-ribose) in the assembly of cytoplasmic stress granules, which accumulate RNA-binding proteins that regulate the translation and stability of mRNAs upon stress. We show that poly(ADP-ribose), six specific poly(ADP-ribose) polymerases, and two poly(ADP-ribose) glycohydrolase isoforms are stress granule components. A subset of stress granule proteins, including microRNA-binding Argonaute family members Ago1–4, are modified by poly(ADP-ribose), and such modification increases upon stress, a condition when both microRNA-mediated translational repression and microRNA-directed mRNA cleavage are relieved. Similar relief of repression is also observed upon overexpression of specific poly(ADP-ribose) polymerases or, conversely, upon knockdown of glycohydrolase. We conclude that poly(ADP-ribose) is a key regulator of posttranscriptional gene expression in the cytoplasm.

INTRODUCTION

Poly(ADP-ribose), or pADPr, is a macromolecular polymer and posttranslational modification best known for its functions in the nucleus (Schreiber et al., 2006). These include DNA damage repair, chromatin remodeling, and transcriptional regulation (Krishnakumar and Kraus, 2010). However, increasing evidence suggests that pADPr also functions in the cytoplasm. For example, pADPr is required for the structure and function of the spindle in the mitotic cytoplasm (Chang et al., 2004). Furthermore, the majority of enzymes regulating pADPr synthesis and degradation are localized to the cytoplasm. These include two of the three isoforms of pADPr glycohydrolase (PARG) (Meyer-Ficca et al., 2004) and five pADPr polymerase (PARP) family members whose cellular localizations are characterized (Juszczynski et al., 2006; Kickhoefer et al., 1999; Liu et al., 2004; Smith and de Lange, 1999; Yu et al., 2005). Seventeen PARPs exist in humans, all defined by a conserved PARP domain, and are classified as pADPr synthesizing, mono-ADP-ribose (mADPr) synthesizing, or enzymatically inactive based primarily on the presence of a triad of histidine, tyrosine, and glutamate (HYE) thought to be required for synthesizing the initial mADPr and/or subsequent pADPr subunits (Hottiger et al., 2010; Kleine et al., 2008).

The ability to synthesize mADPr or pADPr is not a prerequisite for PARP function. For example, PARP-13/ZAP (zinc finger *a*ntiviral *p*rotein) lacks catalytic activity yet inhibits certain viruses by degrading viral RNAs in the cytoplasm (Gao et al., 2002). PARP-13 proteins either lack a PARP domain (PARP-13.2 isoform) or contain a domain lacking key residues of the HYE motif (PARP-13.1 contains YYV). Such a lack of catalytic activity does not rule out the possibility that PARP-13 function requires ADPr modification by another PARP. Such *trans*-modification is common among PARPs from the same subfamily, including modifications between PARP-1 and PARP-2 (Schreiber et al., 2002) and between PARP-5a and PARP-5b (Sbodio et al., 2002). Consistent with PARP-13's role in regulating RNA in the cytoplasm, pADPr's synthesizing and degrading activities were previously identified in cytoplasmic mRNA-protein complexes (mRNPs) (Elkaim et al., 1983; Thomassin et al., 1985). In this study, we discover two functions of pADPr in the cytoplasm—modulating the expression of microRNA (miRNA) targets and assembling mRNP-rich structures called stress granules (SGs).

miRNAs are ~22 nt short noncoding RNAs that regulate targets via translational inhibition and mRNA degradation (Fabian et al., 2010). Despite the diverse fates of mRNA targets, all processes are mediated through the miRNA-binding protein Argonaute (Ago1–4 in humans). Recent data suggest that the activities of miRNAs can be modulated by multiple mechanisms, including posttranslational modifications of Argonaute (Qi et al., 2008; Rüdel et al., 2011; Zeng et al., 2008), association with other RNA-binding proteins, and relocalization of Argonaute to subcellular locations, such as SGs (reviewed in Leung and Sharp, 2010).

SGs assemble upon stalled translation initiation (Anderson and Kedersha, 2008), which can be triggered via two pathways: (1) phosphorylation of initiation factor eIF2α, which commonly

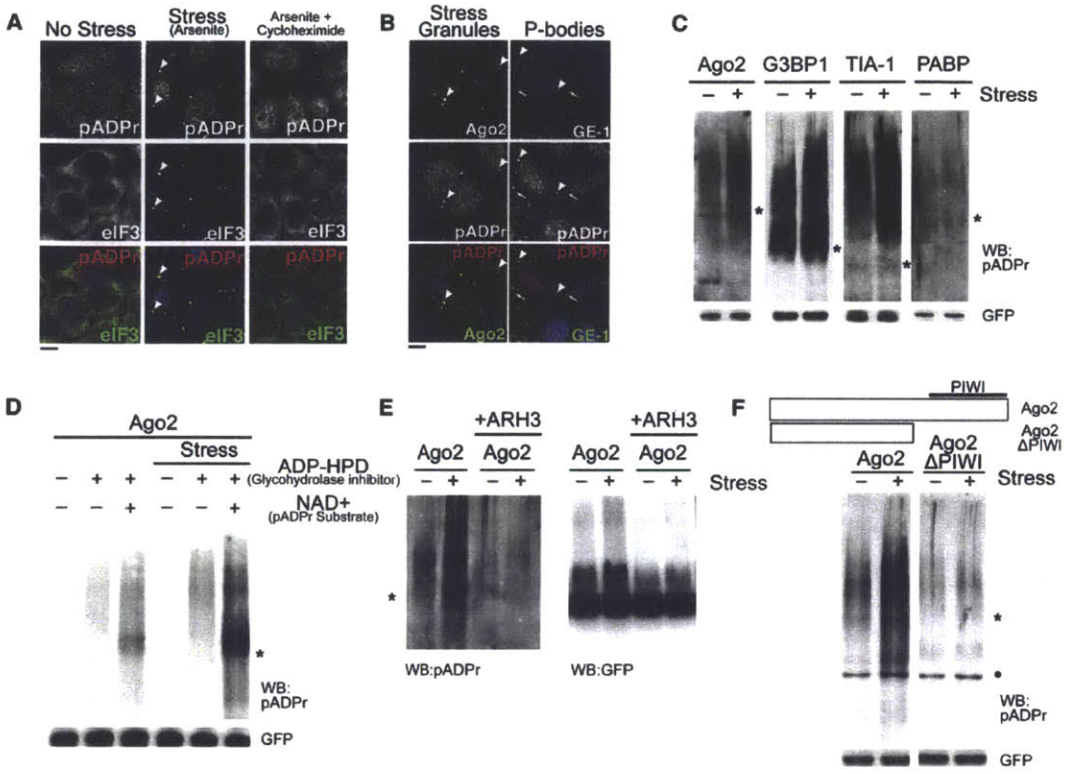

Figure 1. pADPr Is Enriched in SGs upon Multiple Types of Stresses and Modifies Specific Cytoplasmic RNA-Binding Proteins Dependent on RNA-Binding Domain

(A) pADPr staining using LP96-10 antibodies in HeLa cells untreated or treated with 100 μM arsenite for 60 min or for 30 min followed by 100 μM arsenite + 100 μg/ml cycloheximide for 30 min. Arrowheads, SGs; scale bar, 10 μm.

(B) HeLa cells treated with 100 μM arsenite were stained for pADPr, SG component Ago2 (arrowheads), or PB component GE-1 (arrows). DNA was stained with Hoechst 33342 (blue); scale bar, 10 μm.

(C) Immunoprecipitates of four GFP-tagged SG-localized RNA-binding proteins from cells treated with or without 20 nM pateamine A were probed for pADPr.

(D) Immunoprecipitates of GFP-Ago2 from cells treated with or without 20 nM pateamine A were probed for pADPr. The cell extracts either included or excluded 1 μM ADP-HPD and with or without 1 mM NAD^+ before immunoprecipitation by anti-GFP.

(E) pADPr modification of Ago2 from cells treated with or without 20 nM pateamine A was verified by treating the immunoprecipitates with ARH3. The immunoprecipitates were probed for pADPr (left) and GFP (right).

(F) Immunoprecipitates of wild-type and PIWI mutant of GFP-Ago2 from cells treated with or without 20 nM pateamine A were probed for pADPr. For (C)–(F), cell extracts included 1 μM ADP-HPD unless stated otherwise; shown are western blots for pADPr (LP96-10) and GFP levels in each immunoprecipitate. Asterisks indicate the position of the corresponding GFP-tagged RNA-binding protein constructs. Black dots indicate nonspecific binding to BSA by LP96-10. See also Figure S1.

occurs during cell stresses, such as heat shock or arsenite-mediated oxidative stress, or (2) by addition of translation initiation inhibitors that do not involve the phosphorylation of eIF2α. Here, we show that pADPr is important for SG assembly and identify six PARPs including PARP-13 that function in these processes. Interestingly, the majority of these PARPs also bind to Ago2, suggesting that they have overlapping activities in miRNA and SG function.

RESULTS

Poly(ADP-Ribose) Localizes to Stress Granules in the Cytoplasm

Previous work by us and others identified binding interactions between pADPr and cytoplasmic RNA-binding proteins (Chang et al., 2009; Gagne et al., 2008); included among these are SG components. To determine whether pADPr is present in SGs, cells were stressed with arsenite then stained with antibodies generated against pADPr (LP96-10) and SG marker eIF3. Four human cell lines were analyzed: retinal primary epithelial cells (RPE-1) and three cancer lines, 293T, U2OS, and HeLa (Figures 1A and S1A). In each case, pADPr was enriched in SGs. To confirm, five additional anti-pADPr antibodies were tested (Figure S1B and data not shown). This panel of antibodies includes monoclonal antibody 10H specific for polymers containing ≥20 ADP-ribose subunits (Kawamitsu et al., 1984). Each antibody stained the interphase cytoplasm and nucleus in untreated cells and demonstrated a clear colocalization with eIF3-positive puncta in the cytoplasm upon stress, regardless of fixation method (methanol or paraformaldehyde; data not shown).

Moreover, such colocalization was also observed in all examined stress conditions that result in SG assembly, including heat shock, glucose deprivation, treatment with the proteasome inhibitor MG132, or with translation initiation inhibitors (pateamine A and hippuristanol) (Figure S1C and data not shown). Together, these data indicate that pADPr is enriched in SGs upon multiple stresses and contain polymers of at least 20 ADP-ribose subunits.

SGs can be disassembled by cycloheximide, which shifts the equilibrium of mRNA pools from stalled initiation complexes at SGs to polyribosomes (Anderson and Kedersha, 2008). Upon addition of cycloheximide to arsenite-treated cells, pADPr no longer localized as punctate structures (Figure 1A, rightmost panel), suggesting that the pADPr originally at SGs relocated with mRNA and/or their binding proteins. Thus, pADPr colocalization with other mRNA-binding proteins was further analyzed (Anderson and Kedersha, 2008). pADPr colocalized with miRNA-binding protein Ago2, RNA decay factor G3BP1, translational suppressor TIA-1, and poly(A)-binding protein PABP (Figures 1B and S1D). In contrast, no significant pADPr colocalization was observed with GE-1, a marker for P-bodies, another cytoplasmic structure enriched in RNA-binding proteins (Figures 1B and S1E and legends for statistics). Thus, pADPr localization to SGs is not the result of nonspecific binding of pADPr with mRNA-binding proteins.

pADPr Modification of Cytoplasmic RNA-Binding Proteins Requires the Presence of an RNA-Binding Domain

Although pADPr modifications occur primarily on PARP proteins, pADPr also modifies other targets (Schreiber et al., 2006). Because Ago2, G3BP1, TIA-1, and PABP colocalized with pADPr at SGs, we examined their pADPr modification status. Proteins were expressed as GFP-fusions, immunoprecipitated from extracts of either unstressed or stressed cells in the presence of PARG-specific inhibitor ADP-HPD, then immunoblotted for pADPr. If the protein is modified, a slower migrating material stained positively with anti-pADPr is expected and would appear as a "smear" as a result of heterogeneity in the length of polymer attached (Figure 1C). Such pADPr-positive material was observed for Ago2, G3BP1, and TIA-1, but not PABP. Upon stress, Ago2, G3BP1, and TIA-1, but not PABP, exhibited significantly increased pADPr modification (Figure 1C). Similarly, other Argonaute family members—Ago1, Ago3, and Ago4—are modified by pADPr during nonstress conditions, suggesting that all Argonaute proteins are actively regulated by pADPr in unstressed cells and such modification increases upon stress (Figure S1F).

The presence of pADPr modification was further verified for Ago2 in four different ways. First, endogenous Ago2 was immunoprecipitated from unstressed and stressed cells and probed for pADPr (Figure S1G). Similar to GFP-Ago2, endogenous Ago2 exhibited moderate amounts of pADPr modification during nonstress conditions and the modification increased upon stress. Second, the pADPr staining associated with GFP-Ago2 under nonstress and stress conditions decreased when PARG-specific inhibitor ADP-HPD was omitted, and increased upon addition of NAD^+, a substrate for ADPr synthesis, suggesting that pADPr modification of Ago2 is actively regulated even in in vitro conditions (Figure 1D). Third, treatment of a pADPr glycohydrolase, ARH3, but not RNase A, eliminated the anti-pADPr signal from the immunoprecipitates (Figure 1E and data not shown). These slow-migrating, pADPr-positive materials were also GFP-positive, confirming that the observed signal was derived from GFP-Ago2 (Figure 1E). Finally, the ADP-ribosylating activities in the GFP-Ago2 immunoprecipitates were further examined by incubating with increasing concentrations of NAD^+ containing trace amounts of radioactive NAD^+. The reactions were then resolved via SDS-PAGE and were visualized by autoradiography (Figure S1H). A heterogeneous mobility of radioactive signal was observed immediately above where GFP-Ago2 migrated (denoted by asterisk). The intensity of this signal was directly dependent on the concentration of NAD^+ added. These data suggest that PARPs associated with Ago2 in the immunoprecipitates can synthesize pADPr. Importantly, addition of the general PARP inhibitor 3-aminobenzamide (3-AB) to the reactions completely eliminated any incorporation of radioactivity in the Ago2 precipitates, suggesting that the signal observed is due to ADP-ribosylating activities (Figure S1H).

Because pADPr modification was observed on mRNA-binding proteins Ago2, G3BP1, and TIA-1, we next tested whether their modification requires mRNA binding. To test this, fragments of each protein were expressed at levels comparable to wild-type, immunoprecipitated from unstressed and stressed cells, and immunoblotted for pADPr. In all cases, pADPr modification required the presence of an mRNA-binding domain, such as Ago2's PIWI domain (Figure 1F) or RRM in G3BP1 and TIA-1 (Figures S1I and S1J) in both nonstress and stress conditions. These data suggest that either the pADPr modification site is within or proximal to the RNA-binding domains of these proteins, or that the modification begins with the activation of PARP(s) that is/are associated via mRNAs.

Specific PARPs and PARG Isoforms Associate with Cytoplasmic mRNP Complexes

We reasoned that PARPs responsible for such modification are likely associated with these cytoplasmic RNA-binding proteins during nonstress conditions and that these associations may be retained in SGs upon stress. Thus, SGs were used as a surrogate to identify such PARPs. We screened a library of GFP fusions (S.V., unpublished data) to 17 of the 18 human PARPs (PARP-13.2 isoform included, but not PARP-14 because the full-length cDNA was unavailable) for colocalization with known SG markers (Figures 2A and S2A and data not shown). Five of 17 PARPs localized to SGs: PARP-5a, -12, -13.1, -13.2, and -15 (Figure S2B). Specific SG localization of these PARPs was confirmed using live-cell imaging. In each case, GFP-tagged PARPs strongly colocalized with RFP-G3BP1 at the assembling SGs (Movie S1). To further rule out overexpression artifacts, we repeated the colocalization screen in HeLa (Figure 2B) and RPE-1 cells (Figure S2C) using a library of affinity purified and characterized antibodies against each PARP (S.V., unpublished data). Antibody staining confirmed the GFP-PARP screen results and also identified PARP-14 as a SG protein (confirmed via two distinct antibodies) (Figures 2B and S2C and data not shown). Consistent with the GFP localization screen, the remaining

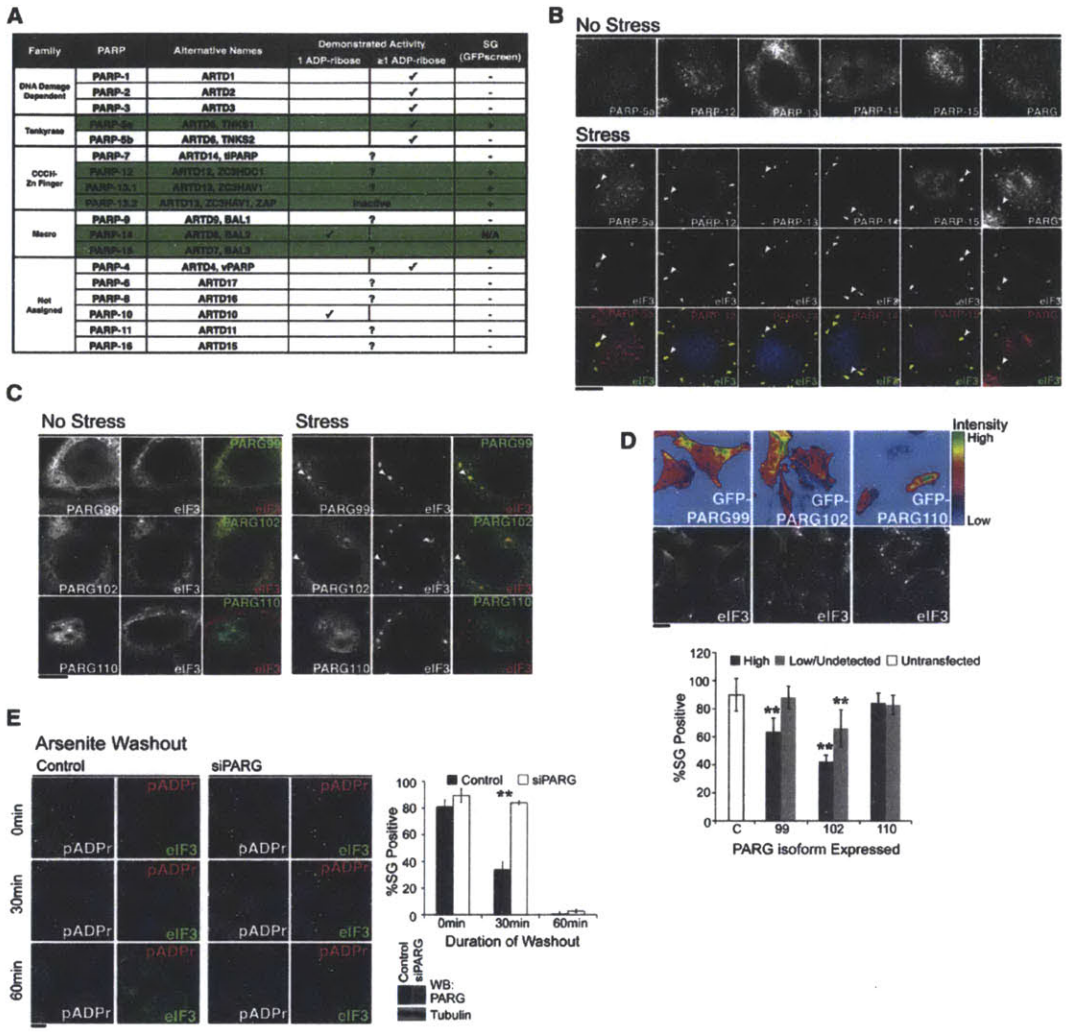

Family	PARP	Alternative Names	Demonstrated Activity: 1 ADP-ribose	Demonstrated Activity: ≥1 ADP-ribose	SG (GFPscreen)
DNA Damage Dependent	PARP-1	ARTD1		✓	-
	PARP-2	ARTD2		✓	-
	PARP-3	ARTD3		✓	-
Tankyrase	PARP-5a	ARTD5, TNKS1		✓	+
	PARP-5b	ARTD6, TNKS2		✓	-
CCCH-Zn Finger	PARP-7	ARTD14, tiPARP		?	-
	PARP-12	ARTD12, ZC3HDC1		?	+
	PARP-13.1	ARTD13, ZC3HAV1		?	+
	PARP-13.2	ARTD13, ZC3HAV1, ZAP		Inactive	+
Macro	PARP-9	ARTD9, BAL1		?	-
	PARP-14	ARTD8, BAL2	✓		N/A
	PARP-15	ARTD7, BAL3		?	+
Not Assigned	PARP-4	ARTD4, vPARP		✓	-
	PARP-6	ARTD17		?	-
	PARP-8	ARTD16		?	-
	PARP-10	ARTD10	✓		-
	PARP-11	ARTD11		?	-
	PARP-16	ARTD15		?	-

Figure 2. Specific PARPs and PARG Isoforms Localize in the Cytoplasmic SGs and the Level of PARG Modulates the Kinetics of SG Assembly and Disassembly

(A) Summary of SG localization screen of PARP family. Green shading indicates SG-PARPs as determined by GFP-PARP fusions or PARP-specific antibodies.

(B) HeLa cells were treated with or without 100 μM arsenite for 60 min and stained using antibodies against SG-PARPs and PARG.

(C) HeLa cells expressing GFP-tagged PARG isoforms were treated with or without 250 μM arsenite for 30 min.

(D) Overexpression of cytoplasmic PARG isoforms inhibits SG assembly. Experiment performed as in (C), but heat map shows level of GFP-PARG isoforms (99, 102, 110) compared with untransfected control (C). Accompanying graph shows quantitation of image data (≥200 cells for each condition from at least six independent fields). Cells with GFP intensity above background are classified as "High" whereas cells with intensity indistinguishable from background levels as "Low/Undetected." Paired t test $p < 0.01$ (**), derived from comparison to untransfected control; error bars indicates SD.

(E) pADPr hydrolysis is required for SG disassembly. Shown are representative images taken 0, 30, and 60 min after washout of 30 min 100 μM arsenite treatment in control and PARG knockdown HeLa cells. Quantitation: ≥100 cells for each condition, n = 3. Paired t test $p < 0.01$ (**) and error bars indicate SD. Accompanying blot shows level of PARG knockdown with tubulin as loading control. For (B)–(E), pADPr were stained by LP96-10 antibodies, SGs (arrowheads) by anti-eIF3, and DNA by Hoechst 33342 (blue); scale bars = 10 μm. See also Figure S2 and Movie S1.

12 PARPs did not localize to SGs endogenously, confirming these six PARPs as SG proteins (hereafter referred as SG-PARPs) (Figure S2B).

We next examined the localization of pADPr-hydrolyzing enzyme PARG. Immunostaining suggests that a fraction of endogenous PARG localizes to the cytoplasm (Figure 2B). Similar to the SG-PARPs, PARG was enriched in SGs upon stress (Figure 2B). Three major PARG isoforms exist: PARG99, PARG102, and PARG110 (Figure S2D). To determine which localize to SGs, GFP fusions of each were screened. Both PARG99 and PARG102 strongly colocalized with SGs upon stress and were dispersed in the cytoplasm during nonstress

conditions. PARG110 was nuclear and unaffected by stress (Figure 2C). Although nuclear PARG110 is known to function in DNA damage repair (Schreiber et al., 2006), PARG99 and PARG102 isoforms are functionally uncharacterized; thus, their identification at SGs uncovers potential function for these cytoplasmic isoforms.

The presence of six PARPs and two PARG isoforms in SGs suggests that the pADPr concentration may be dynamically regulated there. Overexpression of each SG-PARP resulted in de novo assembly of SGs without altering eIF2α phosphorylation levels (Figure S2E). This finding suggests that these enzymes and/or their product, pADPr, play a structural role in SG function rather than causing a general impairment of translation via eIF2α regulation. Overexpression of cytoplasmic PARG99 or PARG102 inhibited SG assembly, whereas overexpression of nuclear PARG110 had no effect (Figure 2D). Moreover, three distinct siRNAs targeting the first exon of PARG102 coding region individually delayed SG disassembly (Figures 2E and S2F). No such effect was observed upon knockdown of a nuclear PARG ARH3 (Figure S2G). Interestingly, all tested proteins that can nucleate SGs upon overexpression, including Ago2, TIA-1, and G3BP1, but not nonnucleator PABP (Anderson and Kedersha, 2008), serve as acceptors of pADPr modification (Figure 1C), suggesting a strong correlation between polymer synthesis and SG assembly. Consistent with this, no pADPr modification was identified on mutants of TIA-1 and G3BP1 that are dominant negative in SG formation (Kedersha et al., 1999; Tourriere et al., 2003) (Figures S1I and S1J). Taken together, these data suggest that both assembly and maintenance of SG structure depends on regulating pADPr concentration locally in the cytoplasm.

Stress or Specific PARP Overexpression Alleviates miRNA-Mediated Repression

To identify a possible function for pADPr modification of RNA-binding proteins on their activities, we focused on Argonautes because of their critical function in regulating >60% of all mRNAs (Bartel, 2009). Given that Argonaute localization to SGs is dependent on miRNAs (Leung et al., 2006) and pADPr modification of Ago2 increases upon stress, we examined miRNA activity during stress. miRNA activity was monitored using a luciferase reporter that contains six bulged sites for an siRNA, siCXCR4, in its 3′ UTR (Doench et al., 2003). The luciferase protein contains a destabilization signal that reduces its half-life to 20 min so that any change in expression is rapidly monitored. Under nonstress conditions, the luciferase construct was repressed 15-fold by targeting siCXCR4 relative to a control siRNA. Consistent with Bhattacharyya et al. (2006), we observed a relief of miRNA-mediated silencing under stress conditions. Under stress conditions, the relative fold repression is reduced to ~5-fold (Figure 3A). Notably, following these stresses, the translation rate was globally reduced; however, the expression of the luciferase mRNA targeted by siCXCR4 decreased to a lesser extent than the nontargeted reporter.

Because SGs can be assembled via SG-PARP overexpression in the absence of exogenous stress, we next examined whether miRNA activity is correlated with SG induction or specific SG-PARP overexpression (Figure 3B). Interestingly, overexpression of PARP-13.1 or PARP-13.2 each resulted in a ~3-fold

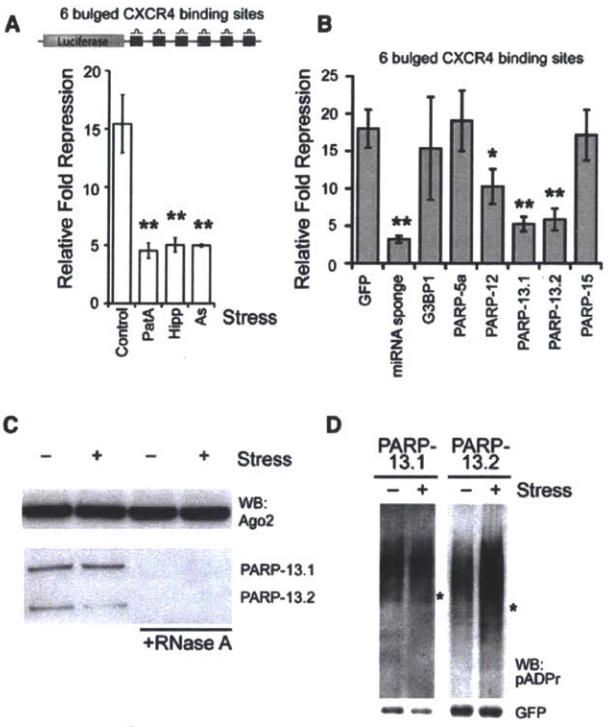

Figure 3. Stress or PARP-13 Overexpression Alleviates miRNA-Mediated Repression

(A) miRNA activity assay in untreated 293T cells or cells treated with 30 nM pateamine A (PatA), 1 μM hippuristanol (Hipp), or 250 μM arsenite (As) for 2 hr, where relative fold repression was measured as the activity of luciferase (upper panel) in the presence of the targeting siRNA normalized to a control siRNA; n = 3.

(B) miRNA activity assay upon overexpression of SG-PARPs. Relative fold repression was measured as in (A); n = 4. For (A) and (B), error bars indicate SD; paired t test $p < 0.05$ (*) and < 0.01 (**).

(C) Antibodies against endogenous Ago2 were used for immunoprecipitation from cytoplasmic extract of HeLa cells treated with or without 250 μM arsenite for 30 min. On the right, the extract was pretreated with 200 μg/ml RNase A for 20 min at 25°C.

(D) Immunoprecipitates of GFP-tagged PARP-13.1 or -13.2 from cells treated with or without 20 nM pateamine A for 30 min were probed for pADPr, where cell extracts included 1 μM ADP-HPD. Asterisks indicate the position of the corresponding GFP-tagged PARPs. See also Figure S3.

decrease in repression of miRNA activity, and overexpression of PARP-12 resulted in a modest ~1.8-fold decrease, whereas overexpression of other SG-PARPs or another SG nucleator G3BP1 had no effect. As controls, overexpression of GFP had no effect, whereas the repression can be relieved by a competitive inhibitor miRNA sponge (Ebert et al., 2007). Thus, the observed decrease in miRNA-mediated repression is not likely due to an overall increase in SG assembly or SG-PARP overexpression, but instead is due to the specific function of PARP-13.1/13.2.

To further explore the role of PARP-13 in miRNA silencing, the association between PARP-13 and Ago2 was investigated (Figure 3C). Immunoprecipitation of endogenous Ago2 identified

PARP-13.1 and PARP-13.2 as binding partners mediated by mRNA. Given that the amount of PARP-13 bound to Ago2 remains unchanged in nonstress and stress conditions, it seems that other properties, such as posttranslational modifications, of PARP-13 are likely altered during stress, resulting in enhanced Ago2 modification.

We therefore examined whether PARP-13 proteins are modified by pADPr. GFP-PARP-13.1 and -PARP-13.2 were immunoprecipitated from unstressed or stressed cells and probed for pADPr. Both isoforms were modified under nonstress conditions. Remarkably, PARP-13.2 exhibited a dramatic increase in modification upon stress, whereas PARP-13.1 modification remained roughly the same (Figure 3D). Similarly, immunoprecipitation of endogenous PARP-13 via a pan-PARP-13 antibody demonstrated an increase in pADPr modification upon stress (Figure S3A). PARP-13 modification was further confirmed by antibody 10H, which recognizes pADPr with $\geq$ 20 subunits (Figures S3A and S3B), and the pADPr staining can be eliminated by glycohydrolase ARH3 or PARG (Figure S3C) but not RNase A (data not shown). Interestingly, the amount of pADPr modification shifted among the SG-PARPs during stress conditions; similar to PARP-13.1, there was no change in PARP-12 modification, whereas PARP-5a and PARP-15 modifications were reduced (Figure S3D). These results suggest a possible shift in PARP activity from auto-modification to modification of stress targets, including Ago1-4, TIA-1, G3BP1, and PARP-13 family members.

PARP-13 Family Members Are pADPr-Modified by Other SG-PARPs

The pADPr modifications attached to PARP-13 proteins are not due to auto-ADP-ribosylating activities because PARP-13.1's PARP domain is inactive in vitro and PARP-13.2 lacks a PARP domain (Kleine et al., 2008). To determine which PARPs modify PARP-13, we examined the catalytic activity of each SG-PARP. GFP-tagged SG-PARPs were purified by immunoprecipitation from either unstressed or stressed cells (PARP-1 serves as a positive control), and the immunoprecipitates were washed twice with buffer containing high salt (450 mM NaCl) and then divided into equal aliquots for ADP-ribosylating activity (Figures 4A and S4A). As expected, PARP-1 and PARP-5a demonstrated auto-poly(ADP-ribosylating) activities, as shown by the mobility shifts above their respective molecular weights (asterisks in Figure 4A). On the other hand, PARP-12 and PARP-15 exhibited mono(ADP-ribosylating) activities, as demonstrated by single radioactive bands at their respective molecular weights. Consistent with their lack of active PARP domains, significant amounts of radioactivity were not associated with PARP-13.1 or PARP-13.2. Interestingly, PARP-12 and PARP-15 samples also contained single bands of radioactivity near the expected mobility of endogenous PARP-13.1 (circle) and PARP-13.2 (triangle). Similar results were observed from stress conditions (data not shown). These results suggest that PARP-12 and PARP-15 could be part of complexes that modify PARP-13 family members even in high salt conditions.

To determine whether SG-PARPs bind to and modify one another, the binding interactions between different PARPs

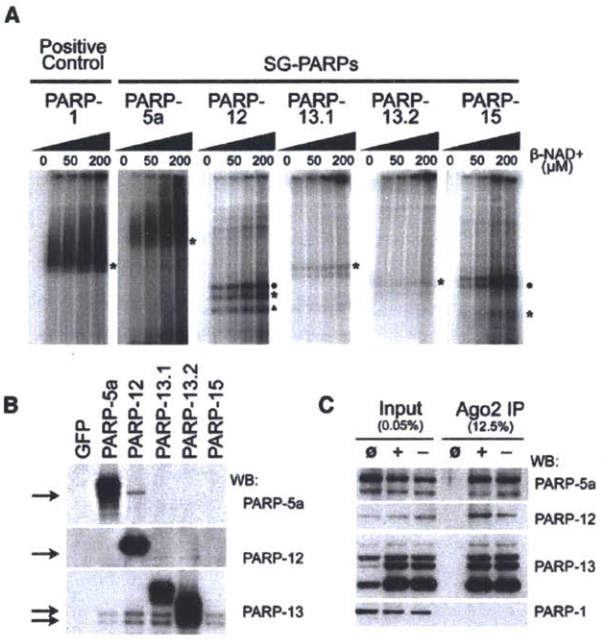

Figure 4. PARP-13 Family Members Are Poly(ADP-Ribosylated) by Other SG-PARPs

(A) In vitro ADP-ribosylating assay for PARP-1, -5a, -12, -13.1, -13.2, and -15. HeLa S3 cells were transfected with individual GFP-tagged SG-PARPs, and GFP-PARP immunoprecipitates were washed twice with 450 mM NaCl, then once with 150 mM NaCl. The immunoprecipitates were incubated with 0, 25, 50, 100, or 200 μM NAD^+ (with 1/175-fold of P32-labeled NAD^+) at 16°C for 30 min, separated on a 6% SDS-PAGE gel, and visualized by autoradiography. Asterisks indicate the position of the corresponding GFP-tagged SG-PARPs; circles and triangle indicate the endogenous position of PARP-13.1 and PARP-13.2, respectively.

(B) Western blots of the immunoprecipitates from (A) were probed with PARP-5a, -12, and -13 (antibodies for PARP-15 are not good for detecting endogenous protein). Immunoprecipitates from cells transfected with GFP were used as a negative control.

(C) HeLa S3 cells were transfected with GFP-tagged Ago2 and cells either treated with (+) or without (−) 20 nM pateamine A for 30 min. Untransfected cells treated with 20 nM pateamine A were used as a negative control (ø). The cytoplasmic lysates were immunoprecipitated with anti-GFP and washed thrice with cytoplasmic lysis buffer. The input and immunoprecipitates were probed with antibodies against PARP-1, -5a, -12, and -13. See also Figure S4.

were analyzed in the immunoprecipitates. Samples were analyzed either by immunoblot (Figure 4B) or mass spectrometry (LC-MS/MS) (Figure S4B). Both endogenous PARP-13 isoforms were detected in immunoprecipitates from PARP-12, -13.1, -13.2, and -15 by both methods. The interaction between PARP-13.1 and PARP-13.2 confirms that both isoforms function as a complex (Law et al., 2010). In comparison, the associations of PARP-5a and both PARP-13 isoforms are relatively weak, because they were only detected by immunoblot but not by mass spectrometry. However, the association with PARP-13 is specific with these PARPs because it was not observed with the negative control, GFP (Figure 4B). Interestingly, we also observed an association between PARP-12 and PARP-5a.

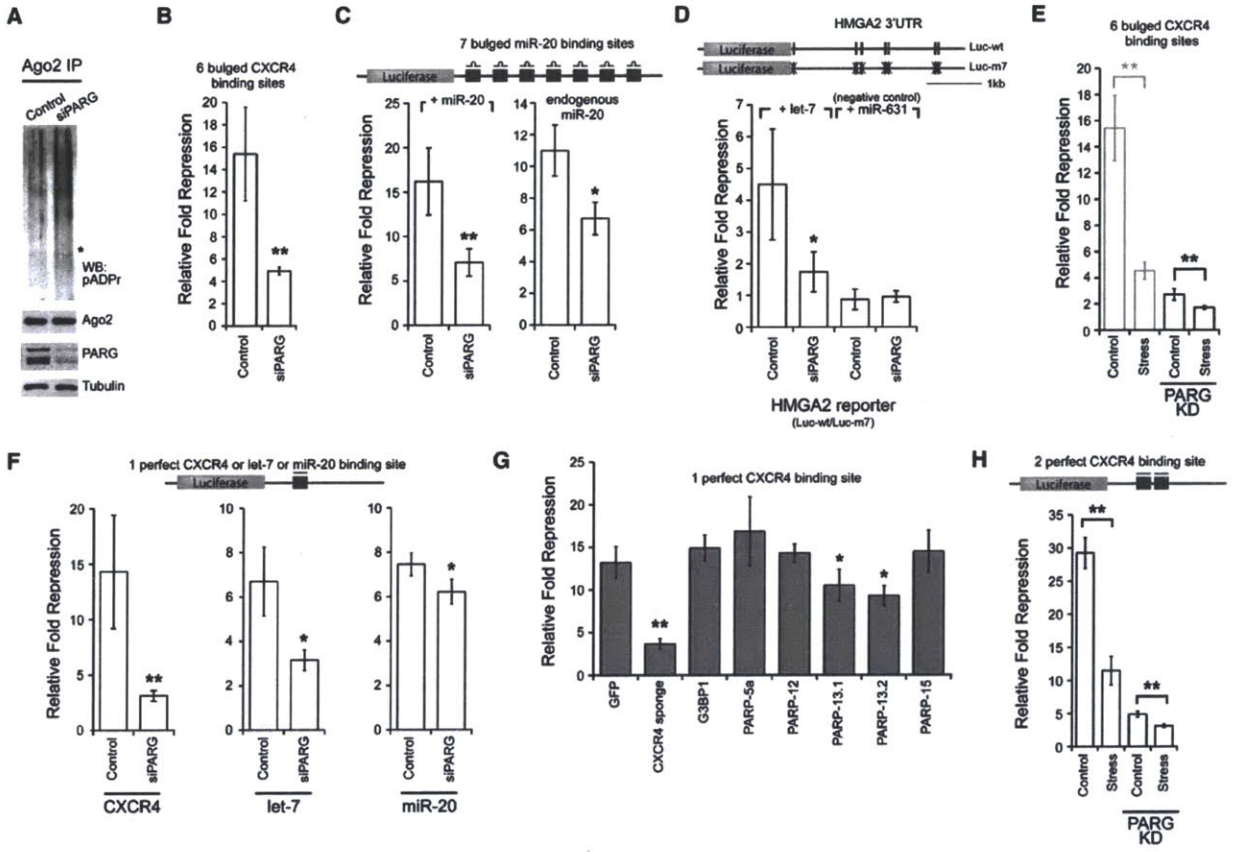

Figure 5. PARG Knockdown Alleviates miRNA-Mediated Repression and miRNA-Directed Cleavage

(A) pADPr modification levels of endogenous Ago2 in HeLa S3 cells transfected with 25 nM control siRNA or siPARG for 48 hr. Asterisk indicates where Ago2 migrated. Shown are western blots for Ago2, PARG, and tubulin.

(B) 293T cells were transfected with 25 nM control siRNA or siPARG for 72 hr. Relative fold repression was measured as in Figure 3A; n = 3.

(C) PARG knockdown effect observed in luciferase reporter with seven artificial miR-20 binding sites. The relative fold repression was calculated by the amount of expression of the construct normalized to a construct with all binding sites mutated at their seed positions. The assay was tested with exogenous addition of miR-20 (left) or with endogenous miR-20 (right); n = 4.

(D) PARG knockdown effect observed in luciferase reporter with endogenous HMGA2 3′ UTR. The relative fold repression is calculated by the amount of expression by the wild-type construct (Luc-wt) normalized to the mutant construct Luc-m7; n = 4.

(E) siPARG-transfected cells were either treated with or without 30 nM pateamine A for 2 hr (right). As a comparison, part of Figure 3A is reproduced here on the left to show cells transfected with a control siRNA.

(F) The effect of PARG knockdown on miRNA-directed cleavage was examined for luciferase construct with one perfect siCXCR4-, let-7-, or miR-20-binding site; n = 4 in each case.

(G) The effect of SG-PARP overexpression on miRNA-directed cleavage assay as in (F); n = 5.

(H) The effect of stress on miRNA-directed cleavage was tested with a luciferase reporter with two perfect binding sites for siCXCR4 using the same transfection conditions and drug treatment as in (E); n = 3. For (B)–(H), error bars indicate SD; paired t test $p < 0.05$ (*) and < 0.01 (**). See also Figure S5.

Therefore, it seems likely that individual PARPs associate with other PARPs and account for their respective ADP-ribosylating activities in vitro and in cells.

In light of these findings, we re-examined whether Ago2 binds to other SG-PARPs. GFP-Ago2 was immunoprecipitated from either unstressed or stressed cells and probed for individual PARPs (Figure 4C). Immunoblots identified associations between GFP-Ago2 and PARP-5a and PARP-12, in addition to PARP-13, in both unstressed and stressed cells. No such association was observed for the nuclear PARP-1. Such association of Ago2 with catalytically active PARPs is consistent with the in vitro ADP-ribosylating activities observed in GFP-Ago2 immunoprecipitates (Figure S1H).

Knockdown of Glycohydrolase PARG Alleviates miRNA-Mediated Repression

Because pADPr modification is dynamically regulated by PARP and PARG activities, we next examined the effect of miRNA activity upon knocking down PARG. PARG knockdown results in an increase in pADPr modification on endogenous Ago2 (Figure 5A) and a ~5-fold decrease in miRNA-mediated repression (Figures 5B and S5A). Thus, similar to stress conditions, an

inverse correlation between the pADPr modification of Ago2 and miRNA-mediated repression was observed upon PARG knockdown in nonstress conditions.

The effect of PARG knockdown on miRNA activity in nonstress conditions was further examined with other constructs. Using a luciferase construct with seven miR-20 binding sites, the expression was reduced ~15-fold upon addition of exogenous miR-20, but such repression was reduced by half upon PARG knockdown (Figure 5C). Given that miR-20 is expressed in 293T cells (Landgraf et al., 2007), the repression mediated by endogenous miR-20 was examined. Under this condition, ~11-fold repression was observed, and such repression was reduced 1.8-fold in siPARG-transfected cells (Figure 5C). Similarly, miRNA-mediated repression was examined with a luciferase construct (Luc-wt) fused with the endogenous HMGA2 3′ UTR, which contains seven let-7-binding sites (Mayr et al., 2007) (Figure 5D). As a control, a luciferase (Luc-m7) construct with each miRNA-binding site mutated was used to normalize expression. Upon addition of exogenous let-7, the wild-type construct was repressed by 4.5-fold compared to the mutant. On the other hand, there is no such repression upon addition of miR-631, which does not bind anywhere in the HMGA2 3′ UTR. Similar to other constructs, the let-7-mediated repression is reduced by half upon PARG knockdown.

Because both PARG knockdown and stress can alleviate miRNA-mediated silencing individually, we asked whether the combination of both results in further relief in miRNA-mediated silencing (Figures 5E and S5B). Indeed, a significant further reduction of miRNA-mediated repression was observed upon stress in siPARG-treated cells, though the magnitude is less than multiplicative. Although stress resulted in a ~3.4-fold repression in control cells, only ~1.6-fold repression was observed upon stress in siPARG-treated cells. Given that stress and PARG knockdown did not synergistically attenuate miRNA silencing, it is likely that the stress pathway involved in modulating the miRNA-mediated silencing is not independent of the pathway that regulates pADPr level via PARG.

PARG Knockdown, PARP-13 Overexpression, or Stress Alleviates miRNA-Directed Cleavage

Apart from inhibiting translation or accelerating mRNA decay, miRNAs can also induce mRNA cleavage when the miRNA binds to its mRNA target in a perfectly complementary manner (e.g., Yekta et al., 2004). The effect of PARG knockdown on the miRNA-directed cleavage was next examined. First, a luciferase construct with a perfectly complementary binding site for siCXCR4 or let-7 was tested (Figures 5F and S5C). Upon addition of siCXCR4 or let-7, expression is reduced 15- or 7-fold, respectively. As in the case of the constructs with bulged configuration for siRNA/miRNA, this repression is relieved upon PARG knockdown (4.5-fold for siCXCR4 and 2-fold for let-7). Such relief in repression upon PARG knockdown was also examined for endogenous miR-20 and the repression was reduced ~1.2-fold upon PARG knockdown (Figure 5F). Because Ago2 is the only member of the Argonaute family that is capable of mediating miRNA-directed cleavage, these statistically significant decreases in repression must reflect inhibition of a complex containing this factor.

Given that the relief of miRNA-mediated translational inhibition/mRNA decay can result from overexpression of specific PARPs or stress, their effects on miRNA-directed cleavage were also examined. In the reporter construct containing one (or two) perfect siCXCR4-binding site(s), overexpression of PARP-13.1 and -13.2 reduced the level of miRNA-mediated directed cleavage by 1.3- (1.6-) and 1.4- (1.7-) fold, respectively (Figures 5G and S5D). Thus, both major miRNA-mediated processes involve PARP-13 family members. Similarly, stress reduced the repression ~2.5-fold using the reporter containing two perfect siCXCR4-binding sites (Figures 5H and S5E). When stress and siPARG treatment were combined, the repression was reduced to ~1.6-fold (Figures 5H and S5F). Thus, similar to miRNA-mediated silencing (Figure 5E), the reduced magnitude observed upon stress in siPARG-treated cells, as compared to untreated cells, is likely because the stress pathway involved in modulating the miRNA-directed cleavage overlaps with the pathway that regulates pADPr level via PARG.

DISCUSSION

pADPr Regulates Posttranscriptional Gene Expression in the Cytoplasm

We report a previously uncharacterized function for pADPr—cytoplasmic posttranscriptional regulation of mRNA. pADPr regulates miRNA silencing and catalyzes the assembly of microscopically visible SG structures. This posttranscriptional regulation occurs in the interphase cytoplasm, further extending the function of pADPr outside the nucleus. Our findings help explain several intriguing observations regarding pADPr function in the cytosol. First, pADPr synthesis and hydrolysis activities are enriched in postnuclear, postmitochondrial fractions and in the free mRNP fractions (Elkaim et al., 1983; Thomassin et al., 1985). Free mRNP fractions are enriched in factors that regulate translation and decay of mRNAs, many of which are SG components. Second, our data indicate potential functions for the two cytoplasmic isoforms of PARG, which together are more active than the single nuclear isoform (Meyer-Ficca et al., 2004). Third, large amounts of RNA-binding proteins were associated with pADPr in our previous analyses and by global proteomic analyses; some of them are SG components, including G3BP1 and PABP (Chang et al., 2009; Gagne et al., 2008).

Here, we report that specific cytoplasmic RNA-binding proteins—Ago2, G3BP1, and TIA-1—are pADPr-modified depending on the presence of their RNA-binding domains. Each protein is increasingly modified by pADPr upon stress and enriched in SGs (though not all components, such as PABP, are modified). Perhaps one general function of pADPr is to recruit RNA-binding proteins to specific locations, such as SGs, thus functioning as a scaffold for protein recruitment. This scaffold function in the cytoplasm is conceptually similar to the role pADPr plays in other complexes or structures, such as the mitotic spindle, where pADPr recruits spindle pole proteins (Chang et al., 2005, 2009); Cajal bodies, a nuclear organelle enriched in nucleic acid-binding proteins that can bind pADPr (Kotova et al., 2009); or at DNA damage sites, pADPr recruits nucleic acid-binding proteins for chromatin remodeling and DNA repair (Ahel et al., 2009). However, in contrast to these examples

involving the activation of a single PARP, we identified multiple PARPs in SGs from distinct subfamilies: Tankyrase PARP-5a; RNA-binding PARP-12 and PARP-13 isoforms; and PARP-14 and PARP-15 that contain pADPr-binding macro-domains. These pADPr-synthesizing activities along with PARG99 and PARG102 isoforms likely regulate the local pADPr concentration that determines the assembly and maintenance of SGs.

pADPr Regulates miRNA Function in the Interphase Cytoplasm

miRNA targets are preferentially expressed relative to total protein synthesis under three conditions: stress, PARP-13 overexpression, and PARG knockdown. Two of these conditions, PARP-13 overexpression and stress, trigger SG assembly. Yet this apparent correlation is paradoxical because SGs are not sites of active translation as they do not contain 60S ribosomes (Anderson and Kedersha, 2008). Therefore, any preferential translation of miRNA targets probably occurs outside SGs in the cytoplasm. Several results suggest that the two phenomena are likely to be coincidental events that are not necessarily mechanistically linked. For example, overexpression of G3BP1, a known inducer of SG assembly, does not result in the relief of miRNA silencing, whereas PARG knockdown results in the relief of miRNA silencing in the presence or absence of SG formation. This is not surprising because the majority of Ago/miRNA complexes are located in the diffuse cytoplasm; only 5% are localized in SGs upon stress and such pool is rapidly exchanging with the cytoplasm (Leung et al., 2006). Thus, the relief of miRNA silencing as a result of poly(ADP-ribosylation) likely occurs in the diffuse cytoplasm.

At what step does pADPr modulate miRNA silencing? Given that the miRNA silencing is alleviated upon increase in pADPr modification level for both endogenous miRNAs and exogenously added siRNA, pADPr likely regulates a step downstream of miRNA processing in the cytoplasm. Consistent with this, the expression levels of nearly all (>99%) miRNAs examined using miRNA microarray remained unchanged upon PARG knockdown (data not shown). In addition, the relief of miRNA silencing was observed in constructs that can be cleaved through perfectly complementary sites and silenced through partially complementary sites. Thus, pADPr likely regulates miRNA function at a step upstream of the direct activity of the Argonaute complex.

Here, we propose that the accessibility of Argonaute/miRNA complex to its target mRNA is affected by an increase in local pADPr modification on multiple proteins that bind to the target, resulting in the relief of miRNA silencing (Figure 6). Those proteins that are modified by pADPr include all Argonaute members and PARP-5a, -12, -13.1, and -13.2, among which Ago1-4 and PARP-13.2 are increasingly modified upon stress when miRNA silencing is relieved. Consistent with the importance of poly(ADP-ribosylation), relief of miRNA silencing was observed upon PARG knockdown when pADPr modification on proteins is generally increased. Such high concentration of negatively charged pADPr modification near the sites of miRNA:mRNA-binding likely disrupts the electrostatic interaction between similarly charged miRNA and mRNA. Alternatively, the sizeable pADPr modification might cause steric hindrance to

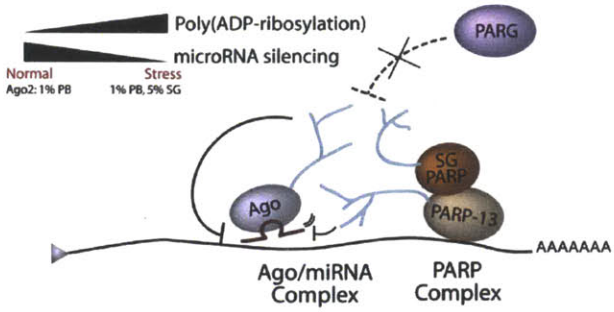

Figure 6. A Working Model: A High Local Concentration of pADPr at miRNA Complex Results in Relief of miRNA Silencing

Upon stress, multiple proteins including all Argonaute family members and PARP-13.1/2 complex are increasingly modified by pADPr. Such increase in poly(ADP-ribosylation) during stress could be due to increase in PARP activity and/or decrease in PARG activity (dotted line). High concentration of pADPr near the Argonaute/miRNA complex might disrupt electrostatic interaction or cause steric hindrance for effective miRNA silencing. Similar relief of miRNA silencing is also observed upon overexpression of PARP-13 or, conversely, upon knockdown of PARG.

prohibit effective miRNA silencing. Recently, it has been shown that in vitro addition of pADPr inhibits the RNA-binding ability of a *Drosophila* heterogeneous nuclear ribonucleoprotein (Ji and Tulin, 2009). Given that pADPr also exhibited binding affinity to RNA-binding proteins (Chang et al., 2009; Gagne et al., 2008), one function of pADPr could be to regulate the binding of RNAs to RNA-binding proteins.

One interesting observation from this study is that overexpression of PARP-13 family members affects both miRNA-mediated repression and miRNA-directed cleavage, yet these PARPs are not catalytically active. Instead, our data suggest that PARP-5a, PARP-12, and PARP-15 are likely the source of pADPr modification, given that (1) PARP-5a has demonstrated poly(ADP-ribosylating) activities and PARP-12 and PARP-15 mono(ADP-ribosylating) activities, (2) PARP-5a and PARP-12, but not PARP-1, associate with Ago2, and (3) all of these PARPs associate with endogenous PARP-13 family members. We note that the association of an inactive PARP with active PARPs resembles the case of the receptor tyrosine kinase erbB-3, which, though itself has no active kinase domain, can mediate signaling through heterodimerization with active EGF family kinases like Her2 (Holbro et al., 2003). Perhaps, because of their ability to bind mRNA, the function of the inactive PARP-13 isoforms is to anchor the activity of the catalytically active PARPs to the mRNP complex. This might partly explain why the mRNA-binding domain is required for pADPr modification of Ago2.

In conclusion, our data point to two functions for pADPr in the cytoplasm. At SGs, pADPr modulates the assembly and maintenance of an mRNP-enriched structure. At submicroscopic miRNP complexes, pADPr relieves miRNA-mediated repression and miRNA-directed cleavage under stress conditions. These cytoplasmic functions are likely mediated through the concerted activities of catalytically inactive and mADPr- and pADPr-synthesizing PARPs. Such cross-subfamily mechanism of pADPr synthesis suggests that pADPr polymerization could be

more complex than previously thought. Given that other post-transcriptional factors such as G3BP1 and TIA-1 are increasingly modified by pADPr upon stress and that these modifications depend on the presence of an RNA-binding domain, it is likely that pADPr is a key regulator of mRNA functions in the interphase cytoplasm.

EXPERIMENTAL PROCEDURES

Immunofluorescence

Following SG induction, coverslips were rinsed twice in PBS and either extracted for 30 s with buffer A, fixed for 15 min in 4% paraformaldehyde in buffer B, or fixed in ice-cold methanol for 5 min, followed by slow rehydration with PBS. Coverslips were incubated with 1° antibodies for 45 min and 2° antibodies for 35 min. See Supplemental Experimental Procedures for buffer recipes.

Immunoprecipitation

HeLa S3 cells (8×10^7) were transfected with GFP-PARPs or RNA-binding proteins for 48 hr using 293fectin, such that the expression did not induce visible SGs. Cells were either treated with or without 20 nM pateamine A or 250 μM Arsenite for 30 min. At 10 min before stress, latruculin B was added to 0.5 μg/ml. Cells were lysed with cytoplasmic lysis buffer C. Lysate was spun at 18,407 g for 10 min and a final concentration of 10 μg/ml cytochalasin B and 25 μM nocodazole was added to the supernatant. The supernatants were incubated with anti-GFP and Protein A beads for 90 min. The immunoprecipitates were washed for 10 min with buffer C, then twice in buffer C containing 300 mM NaCl and again with buffer C. Beads were then eluted with sample buffer and heated for 10 min at 70°C. For endogenous Ago2 modification, anti-Ago2 antibody was preincubated with Protein A beads. The supernatant was made by spinning the lysate at 2,300 g or 18,407 g for 10 min, and the beads were washed 3 × 5 min with buffer C before eluting with sample buffer. See Supplemental Experimental Procedures for buffer receipes.

miRNA Reporter Assay

Twenty-four hours after transfection, cells were either untreated or stressed with 30 nM pateamine A, 1 μM hippuristanol, or 250 μM arsenite for 2 hr before lysis for luciferase assay. Firefly and Renilla luciferase signals were measured using the Dual Luciferase reporter assay system (Promega). Shown are representative luciferase assay results from 3–5 replicates, as indicated in the figure legend, in each experimental condition, and each condition has been independently examined 2–4 times.

SUPPLEMENTAL INFORMATION

Supplemental Information includes Supplemental Experimental Procedures, five figures, and one movie and can be found with this article online at doi:10.1016/j.molcel.2011.04.015.

ACKNOWLEDGMENTS

We thank M. Miwa, J. Tazi, P. Anderson, N. Kedersha, and J. Pelletier for kind gifts of reagents; A. West, T. Lai, and E. Vasile for technical support; A. Young, M. Ebert, J. Wilusz, and P. Boutz for comments; and M. Lindstrom for illustrations. A.K.L.L was a special fellow of Leukemia and Lymphoma Society. P.C. is a Rita Allen Foundation Scholar, a Kimmel Foundation for Cancer Research Scholar, and a Howard S. and Linda B. Stern Career Development Professor. This work was supported by the National Institutes of Health (grant RO1-CA133404 to P.A.S.), the National Cancer Institute (grant PO1-CA42063 to P.A.S.), and partially by Cancer Center Support (core; grant P30-CA14051).

Received: December 8, 2010
Revised: March 11, 2011
Accepted: April 25, 2011
Published: May 19, 2011

REFERENCES

Ahel, D., Horejsi, Z., Wiechens, N., Polo, S.E., Garcia-Wilson, E., Ahel, I., Flynn, H., Skehel, M., West, S.C., Jackson, S.P., et al. (2009). Poly(ADP-ribose)-dependent regulation of DNA repair by the chromatin remodeling enzyme ALC1. Science *325*, 1240–1243.

Anderson, P., and Kedersha, N.L. (2008). Stress granules: the Tao of RNA triage. Trends Biochem. Sci. *33*, 141–150.

Bartel, D.P. (2009). MicroRNAs: target recognition and regulatory functions. Cell *136*, 215–233.

Bhattacharyya, S.N., Habermacher, R., Martine, U., Closs, E.I., and Filipowicz, W. (2006). Relief of microRNA-mediated translational repression in human cells subjected to stress. Cell *125*, 1111–1124.

Chang, P., Jacobson, M.K., and Mitchison, T.J. (2004). Poly(ADP-ribose) is required for spindle assembly and structure. Nature *432*, 645–649.

Chang, W., Dynek, J.N., and Smith, S. (2005). NuMA is a major acceptor of poly(ADP-ribosyl)ation by tankyrase 1 in mitosis. Biochem. J. *391*, 177–184.

Chang, P., Coughlin, M., and Mitchison, T.J. (2009). Interaction between Poly(ADP-ribose) and NuMA contributes to mitotic spindle pole assembly. Mol. Biol. Cell *20*, 4575–4585.

Doench, J.G., Petersen, C.P., and Sharp, P.A. (2003). siRNAs can function as miRNAs. Genes Dev. *17*, 438–442.

Ebert, M.S., Neilson, J.R., and Sharp, P.A. (2007). MicroRNA sponges: competitive inhibitors of small RNAs in mammalian cells. Nat. Methods *4*, 721–726.

Elkaim, R., Thomassin, H., Niedergang, C., Egly, J.M., Kempf, J., and Mandel, P. (1983). Adenosine diphosphate ribosyltransferase and protein acceptors associated with cytoplasmic free messenger ribonucleoprotein particles. Biochimie *65*, 653–659.

Fabian, M.R., Sonenberg, N., and Filipowicz, W. (2010). Regulation of mRNA translation and stability by microRNAs. Annu. Rev. Biochem. *79*, 351–379.

Gagne, J.P., Isabelle, M., Lo, K.S., Bourassa, S., Hendzel, M.J., Dawson, V.L., Dawson, T.M., and Poirier, G.G. (2008). Proteome-wide identification of poly(ADP-ribose) binding proteins and poly(ADP-ribose)-associated protein complexes. Nucleic Acids Res. *36*, 6959–6976.

Gao, G., Guo, X., and Goff, S.P. (2002). Inhibition of retroviral RNA production by ZAP, a CCCH-type zinc finger protein. Science *297*, 1703–1706.

Hottiger, M.O., Hassa, P.O., Luscher, B., Schuler, H., and Koch-Nolte, F. (2010). Toward a unified nomenclature for mammalian ADP-ribosyltransferases. Trends Biochem. Sci. *35*, 208–219.

Ji, Y., and Tulin, A.V. (2009). Poly(ADP-ribosyl)ation of heterogeneous nuclear ribonucleoproteins modulates splicing. Nucleic Acids Res. *37*, 3501–3513.

Juszczynski, P., Kutok, J.L., Li, C., Mitra, J., Aguiar, R.C., and Shipp, M.A. (2006). BAL1 and BBAP are regulated by a gamma interferon-responsive bidirectional promoter and are overexpressed in diffuse large B-cell lymphomas with a prominent inflammatory infiltrate. Mol. Cell. Biol. *26*, 5348–5359.

Holbro, T., Beerli, R.R., Maurer, F., Koziczak, M., Barbas, C.F., 3rd, and Hynes, N.E. (2003). The ErbB2/ErbB3 heterodimer functions as an oncogenic unit: ErbB2 requires ErbB3 to drive breast tumor cell proliferation. Proc. Natl. Acad. Sci. USA *100*, 8933–8938.

Kawamitsu, H., Hoshino, H., Okada, H., Miwa, M., Momoi, H., and Sugimura, T. (1984). Monoclonal antibodies to poly(adenosine diphosphate ribose) recognize different structures. Biochemistry *23*, 3771–3777.

Kedersha, N.L., Gupta, M., Li, W., Miller, I., and Anderson, P. (1999). RNA-binding proteins TIA-1 and TIAR link the phosphorylation of eIF-2 alpha to the assembly of mammalian stress granules. J. Cell Biol. *147*, 1431–1442.

Kickhoefer, V.A., Siva, A.C., Kedersha, N.L., Inman, E.M., Ruland, C., Streuli, M., and Rome, L.H. (1999). The 193-kD vault protein, VPARP, is a novel poly(ADP-ribose) polymerase. J. Cell Biol. *146*, 917–928.

Kleine, H., Poreba, E., Lesniewicz, K., Hassa, P.O., Hottiger, M.O., Litchfield, D.W., Shilton, B.H., and Luscher, B. (2008). Substrate-assisted catalysis by PARP10 limits its activity to mono-ADP-ribosylation. Mol. Cell *32*, 57–69.

Kotova, E., Jarnik, M., and Tulin, A.V. (2009). Poly (ADP-ribose) polymerase 1 is required for protein localization to Cajal body. PLoS Genet. *5*, e1000387.

Krishnakumar, R., and Kraus, W.L. (2010). The PARP side of the nucleus: molecular actions, physiological outcomes, and clinical targets. Mol. Cell *39*, 8–24.

Landgraf, P., Rusu, M., Sheridan, R., Sewer, A., Iovino, N., Aravin, A., Pfeffer, S., Rice, A., Kamphorst, A.O., Landthaler, M., et al. (2007). A mammalian microRNA expression atlas based on small RNA library sequencing. Cell *129*, 1401–1414.

Law, L.M., Albin, O.R., Carroll, J.W., Jones, C.T., Rice, C.M., and Macdonald, M.R. (2010). Identification of a dominant negative inhibitor of human zinc finger antiviral protein reveals a functional endogenous pool and critical homotypic interactions. J. Virol. *84*, 4504–4512.

Leung, A.K., Calabrese, J.M., and Sharp, P.A. (2006). Quantitative analysis of Argonaute protein reveals microRNA-dependent localization to stress granules. Proc. Natl. Acad. Sci. USA *103*, 18125–18130.

Leung, A.K., and Sharp, P.A. (2010). MicroRNA functions in stress responses. Mol. Cell *40*, 205–215.

Liu, L., Chen, G., Ji, X., and Gao, G. (2004). ZAP is a CRM1-dependent nucleocytoplasmic shuttling protein. Biochem. Biophys. Res. Commun. *321*, 517–523.

Mayr, C., Hemann, M.T., and Bartel, D.P. (2007). Disrupting the pairing between let-7 and Hmga2 enhances oncogenic transformation. Science *315*, 1576–1579.

Meyer-Ficca, M.L., Meyer, R.G., Coyle, D.L., Jacobson, E.L., and Jacobson, M.K. (2004). Human poly(ADP-ribose) glycohydrolase is expressed in alternative splice variants yielding isoforms that localize to different cell compartments. Exp. Cell Res. *297*, 521–532.

Qi, H.H., Ongusaha, P.P., Myllyharju, J., Cheng, D., Pakkanen, O., Shi, Y., Lee, S.W., and Peng, J. (2008). Prolyl 4-hydroxylation regulates Argonaute 2 stability. Nature *455*, 421–424.

Rüdel, S., Wang, Y., Lenobel, R., Korner, R., Hsiao, H.H., Urlaub, H., Patel, D., and Meister, G. (2011). Phosphorylation of human Argonaute proteins affects small RNA binding. Nucleic Acids Res. *39*, 2330–2343.

Sbodio, J.I., Lodish, H.F., and Chi, N.W. (2002). Tankyrase-2 oligomerizes with tankyrase-1 and binds to both TRF1 (telomere-repeat-binding factor 1) and IRAP (insulin-responsive aminopeptidase). Biochem. J. *361*, 451–459.

Schreiber, V., Ame, J.C., Dolle, P., Schultz, I., Rinaldi, B., Fraulob, V., Menissier-de Murcia, J., and de Murcia, G. (2002). Poly(ADP-ribose) polymerase-2 (PARP-2) is required for efficient base excision DNA repair in association with PARP-1 and XRCC1. J. Biol. Chem. *277*, 23028–23036.

Schreiber, V., Dantzer, F., Ame, J.C., and de Murcia, G. (2006). Poly(ADP-ribose): novel functions for an old molecule. Nat. Rev. Mol. Cell Biol. *7*, 517–528.

Smith, S., and de Lange, T. (1999). Cell cycle dependent localization of the telomeric PARP, tankyrase, to nuclear pore complexes and centrosomes. J. Cell Sci. *112*, 3649–3656.

Thomassin, H., Niedergang, C., and Mandel, P. (1985). Characterization of the poly(ADP-ribose) polymerase associated with free cytoplasmic mRNA-protein particles. Biochem. Biophys. Res. Commun. *133*, 654–661.

Tourriere, H., Chebli, K., Zekri, L., Courselaud, B., Blanchard, J.M., Bertrand, E., and Tazi, J. (2003). The RasGAP-associated endoribonuclease G3BP assembles stress granules. J. Cell Biol. *160*, 823–831.

Yekta, S., Shih, I.H., and Bartel, D.P. (2004). MicroRNA-directed cleavage of HOXB8 mRNA. Science *304*, 594–596.

Yu, M., Schreek, S., Cerni, C., Schamberger, C., Lesniewicz, K., Poreba, E., Vervoorts, J., Walsemann, G., Grotzinger, J., Kremmer, E., et al. (2005). PARP-10, a novel Myc-interacting protein with poly(ADP-ribose) polymerase activity, inhibits transformation. Oncogene *24*, 1982–1993.

Zeng, Y., Sankala, H., Zhang, X., and Graves, P.R. (2008). Phosphorylation of Argonaute 2 at serine-387 facilitates its localization to processing bodies. Biochem. J. *413*, 429–436.

Supplemental Information
Molecular Cell, *Volume 42*

Poly(ADP-Ribose) Regulates Stress Responses and MicroRNA Activity in the Cytoplasm

Anthony K.L. Leung, Sejal Vyas, Jennifer E. Rood, Arjun Bhutkar, Phillip A. Sharp, and Paul Chang

Supplemental Experimental Procedures

Cell Culture and Reagents

U2OS (from ATCC), HeLa (from Puck Ohi, Vanderbilt University, TN, USA) and HeLa S3 (from ATCC) cells were grown in DMEM containing 10% FBS and penicillin/streptomycin at 37°C and 5% CO_2. 293T (from ATCC) were grown in DMEM containing 10% FBS at 37°C and 5% CO_2. RPE1 cells (from ATCC) were grown in 1:1 Ham's F12 and DMEM mixture (15mM HEPES, 0.5mM sodium pyruvate, 1.2 g/L sodium bicarbonate) containing 10% FBS, penicillin/streptomycin, and 0.01mg/mL hygromycin B at 37°C and 5% CO_2. DMEM, Trypsin-EDTA, and penicillin/streptomycin solution were from Mediatech. FBS was from Tissue Culture Biologicals. 1:1 Ham's F12:DMEM, Optimem and Lipofectamine 2000 were from Invitrogen. Sodium arsenite and cycloheximide were from Sigma Aldrich. RNase A was from Qiagen. Pateamine A and hippuristanol were gifts from Jerry Pelletier (McGill University, Montreal, QC, Canada). pADPr antibodies were from BD-Pharmingen (LP96-10 and #551813), Tulip Biolabs (10H and chIgY) and Trevigen. PARP-5a antibody (H350), TIA-1 antibody (C-20), GE-1 antibody (sc-8418) and eIF3 antibody (N20) were from Santa Cruz Biotechnology. Ago2 (4G8) antibody was from WAKO chemicals USA. G3BP1 antibody (611127) was from BD-Pharmingen. GFP antibodies were from Abcam (ab1218, ab290) and Invitrogen (3E6 for immunoprecipitation). Protein A beads from Bio-rad #156-0005 or Protein A Dynabead from Invitrogen. One PARP-14 antibody

(HPA012063) was from Sigma Aldrich. PARG antibodies were either generated in house or a gift from Dr. Tanuma (RIKEN, Japan) and Dr. Urana (RIKEN, Japan). PARP-12, PARP-13, PARP-14 and PARP-15 antibodies were generated in house. Alexa Fluor® secondary antibodies were from Invitrogen. Control siRNA was from Qiagen (cat. # 1027280). siPARG1 (5'-CCAGUUGGAUGGACACUAAUU-3'), siPARG2 (5'-AGGAAUCAAG ACAGCGGAAUU-3'), siPARG3 (5'- UGGAUGGACACUAAAGGAAUU-3') and siARH3 (5'-GGACAG AAGCCUUGUACUAUU-3') siRNAs were from Dharmacon.

Buffer Recipes

Cell lysis buffer A:

0.1% Triton X-100, 50 mM HEPES, pH 7.4, 150 mM NaCl, 1 mM $MgCl_2$, 1 mM EGTA

Cell lysis buffer B:

50 mM HEPES, pH 7.4, 150 mM NaCl, 1 mM $MgCl_2$, 1 mM EGTA

Cell lysis buffer C/Cytoplasmic Lyiss Buffer (in the text):

50 mM HEPES, pH 7.4, 150 mM NaCl, 1 mM $MgCl_2$, 1 mM EGTA, 1% Triton X-100, 1 mM DTT, 1 mM ADP-HPD and Complete protease inhibitor cocktail (Roche)

Immunofluorescence Staining and Imaging Conditions

Cells were split onto coverslips 6 hr after transfection using lipofectamine 2000 and grown overnight. Following SG induction, coverslips were either rinsed twice in PBS and then extracted for 30 sec with buffer A or fixed in ice cold methanol for 5 min, followed by slow rehydration with PBS. For pre-extracted coverslips, cells were fixed for 15 min in 4% paraformaldehyde in buffer B. Coverslips were incubated with primary antibodies for 45 min and secondary antibodies for 35 min. For pADPr staining, coverslips were further treated with 100 mM $NaIO_4$ for 5 min followed by 25 mM succinic dihydrazide for 30 min

(Chang et al., 2009). Images were collected on a Nikon TE2000 confocal microscope using a 60X objective with NA = 1.40, equipped with a Yokogawa CSU-X1 spinning disc head and Hamamatsu ORCA ER digital camera.

Live Cell Imaging

HeLa cells were cotransfected with RFP-G3BP1 and GFP-SG-PARPs and split into 24 well glass bottom plates (Greiner Bio-One) ~5 hours post transfection and grown overnight. At time 0, 250 μM arsenite was added to cells and 4 fields/transfection were imaged every minute for 45 min using a 40X objective (NA = 0.95) on a Nikon TE2000 inverted microscope equipped with an environmental chamber, Yokagawa CSU-X1 spinning disc head, Hamamatsu ORCA-ER digital camera and NIS Elements Imaging Software.

miRNA Reporter Constructs

pRCP-6X is a modified version of pRL-6X (Doench et al., 2003) where Renilla luciferase CDS is replaced with pGL4.81. Using pRCP-6X as the backbone, the 6 bulged CXCR4 binding sites is replaced by a heptamer of miR-20 binding site "CCGGTACCTGCACTCGCGCACTTTA" to make pRCP-miR-20x7 and "CCGGTACCTGCACTCGCGGAGTATA" to make pRCP-miR20m7. pRCP-wtHMGA2 and pRCP-mutHMGA2 were made by replaced the 6 bulged CXCR4 binding site in pRCP-6X with the wild-type and Luc-m7 mutants from Mayr et al., 2007, respectively. Similar to pRCP-6X, RCP-CXCR4-1P and RCP-CXCR4-2P were modified versions of pRL-1P and pRL-2P (Doench et al., 2003), respectively, where the coding sequence of Renilla

luciferase is replaced with pGL4.81 (Promega). pRCP-let7-1P, pRCP-let7mut-1P, pRCP-miR-20-1P and pRCP-miR-20mut-1P were made by replacing one perfect CXCR4 binding site with one perfect let-7 binding site "TCTAGAAACTATACAACCTA CTACCTCATCTAGA" and its mutant "TCTAGAAACTATACAACCTACTTCGTGATCT AGA", or one perfect miR-20 binding site "TCTAGACTACCTGCACTATAAGCACTTTA TCTAGA" and its mutant "TCTAGACTACCTGCACTATAAGCTCATAATCTAGA" respectively, using restriction enzyme XbaI.

Transfection Conditions

For overexpression analysis, $4x10^4$ 293T cells were seeded per well of 96 well-plate 24 hr prior to transfection of 11.1 ng pGL3 plasmid, 33.3 ng pRCP-6X, 155.6 ng GFP-tagged construct and 5 nM targeting siRNA, siCXCR4 (Doench et al., 2003), or control siRNA using 0.5 μl Lipofectamine 2000. 24 hr after transfection, cells were washed once with 1X PBS and lysed with 1X Passive Lysis Buffer (Promega). For knockdown analysis, $5x10^5$ 293T cells were seeded per well of 12 well-plate 24 hr prior to transfection of specific siRNAs using 4 μl Lipofectamine 2000. 24 hr after transfection, $4x10^4$ siRNA-transfected cells were seeded per well of a 96 well-plate 24 hour prior to transfection of 25 ng pGL3 plasmid, 175 ng pRCP-6X and specific siRNAs using 0.5 μl Lipofectamine 2000.

SG Assembly and Disassembly Assays

For assembly assay, HeLa cells were transfected with GFP-PARG isoforms for 24 hours and stressed with 250 μM Arsenite for 30 min. Heat maps were generated using Adobe Photoshop based on the GFP-intensity of the construct and the amount of stress granules were counted based on co-staining with eIF3. For disassembly assay, HeLa cells were

seeded at $9x10^5$ cells/well and grown overnight in 6-well plates. Cells were transfected with either 30 nM control or PARG siRNA using lipofectamine 2000 (Invitrogen). After 24 hours, cells were split into 96-well glass bottom plates at $2.5x10^4$ cells/well and grown overnight. Following SG induction by 100 μM arsenite treatment for 30 min, disassembly was induced by arsenite washout for 0, 15, 30, 45 or 60 min. eIF3 signal was used to count the number of cells containing SGs for at least 100 cells for each condition in triplicate.

Figure S1

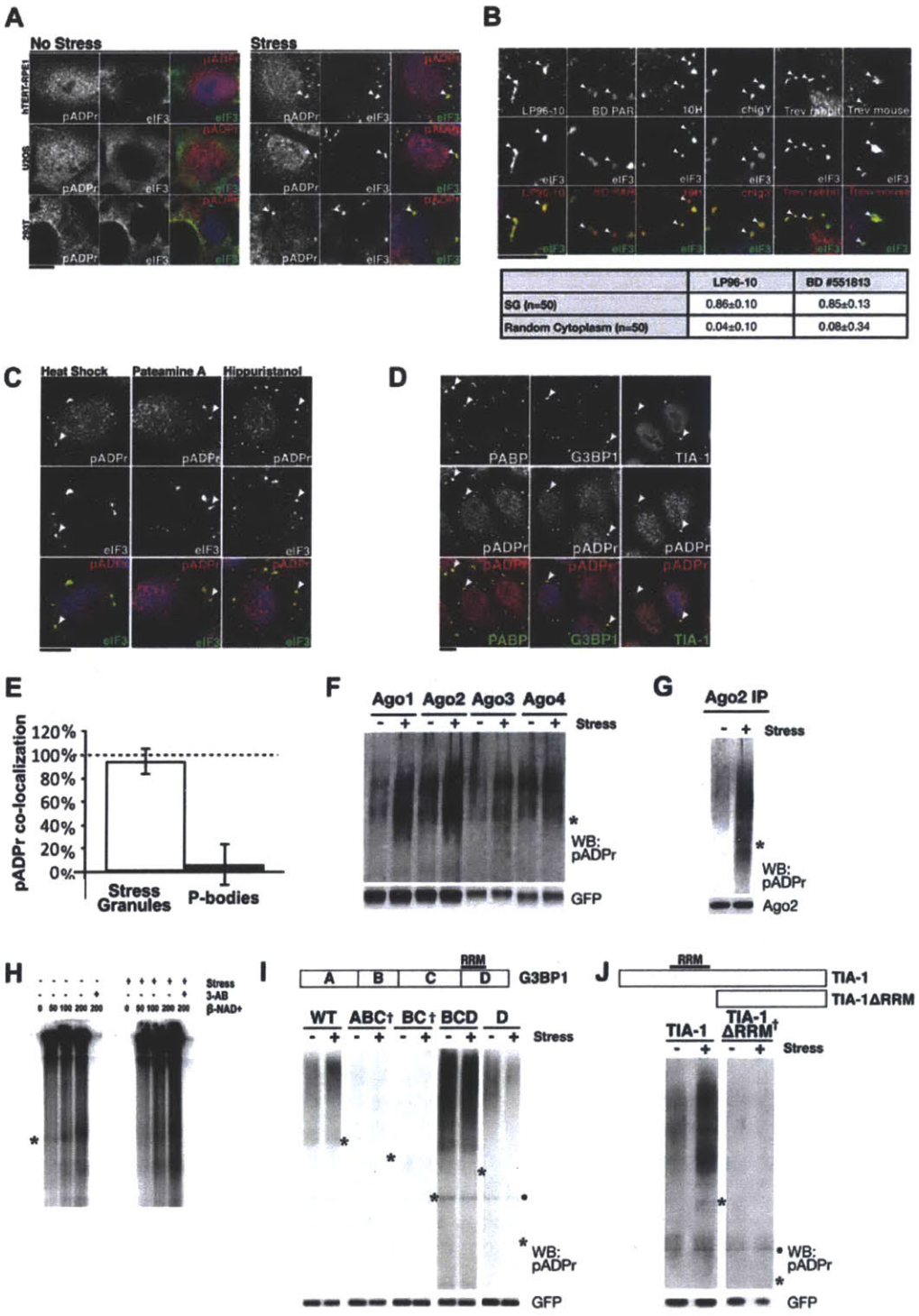

	LP96-10	BD #551813
SG (n=50)	0.86±0.10	0.85±0.13
Random Cytoplasm (n=50)	0.04±0.10	0.08±0.34

Figure S1, related to Figure 1 (A) hTERT immortalized primary RPE-1 cells, human osteosarcoma U2OS cells and embryonic kidney 293T cells were either treated with or without 250 μM arsenite for 1 hour. pADPr, detected using LP96-10, co-localizes with SG marker eIF3 upon stress, indicated by arrowheads; scale bar, 10 μm. (B) pADPr staining of HeLa cells treated with 100 μM arsenite for 1 hour using six antibodies: LP96-10, BD rabbit antibodies #551813, 10H, Tulip chIgY, Trevigen rabbit and mouse antibodies. SGs are indicated by arrowheads; scale bar, 10 μm. Pearson coefficients of linescan intensity between pADPr staining and SG localization were measured at 50 SGs in each case for two different antibodies LP96-10 and BD #551813. (C) pADPr staining using LP96-10 in HeLa cells treated for 1 hour with 42°C heat shock, 20 nM pateamine A or 1 μM hippuristanol. SGs are indicated by arrowheads; scale bar, 10 μm. (D) HeLa cells treated with 100 μM arsenite for 1 hour were stained for pADPr with LP96-10 and for SGs (arrowheads) with antibodies against PABP, G3BP1 or TIA-1. DNA was stained with Hoeschst 33342 (blue); scale bar, 10 μm. (E) Quantitation of the percent co-localization of pADPr with SGs and PBs; >200 SGs (46 cells) and >400 P-bodies (60 cells) were counted. 1st quartile, median and 3rd quartile and mean = 100%, 100%, 100%, 95% for SGs and 0%, 0%, 1.6%, 6.5% for PBs, respectively. (F) Immunoprecipitates of GFP-tagged Ago1-Ago4 from cells treated with or without 20 nM pateamine A were probed for pADPr, where cell extracts included 1 μM ADP-HPD. Shown are western blots for pADPr (LP96-10) and GFP levels in each immunoprecipitate. Asterisk indicates the position of the GFP-tagged Argonaute constructs. Note: compared with the increase in modification of Ago1-3 upon stress, the change for Ago4 pADPr modification was relatively modest. (G) pADPr modification levels of endogenous Ago2 in HeLa S3 cells treated with or without 20 nM pateamine A for 30 min, where cell extracts included 1 μM ADP-HPD. Asterisk indicates where Ago2 migrated. (H) pADPr modification of Ago2 is sensitive to a general PARP inhibitor 3-aminobenzamide (3-AB). HeLa S3 cells were transfected with GFP-tagged Ago2 and cytoplasmic lysates from untreated cells and cells treated with 20nM pateamine A were immunoprecipitated using an anti-GFP antibody, where cell extracts included 1 μM ADP-HPD, and washed twice with 450 mM NaCl then once with 150 mM NaCl. GFP-Ago2 immunocomplexes were incubated with 0, 50, 100, 200 μM NAD^+ for 30 min at 16°C, and, in addition, one sample with 200 μM NAD^+ was co-incubated with 1 mM 3-AB in the reaction. Shown is the autoradiograph of each reaction separated by 6% PAGE. (I, J) Immunoprecipitates of the wild-type and mutant of (I) G3BP1 and (J) TIA-1 from cells treated with or without 250 μM arsenite were probed for pADPr, where cell extracts included 1 μM ADP-HPD. Daggers indicate mutants that have been shown to be dominant negative in SG formation (Kedersha et al., 1999; Tourriere et al., 2003). Shown are western blots for pADPr (LP96-10) and GFP levels in each immunoprecipitate. Asterisk indicates the position of the GFP-tagged RNA-binding proteins.

Figure S2

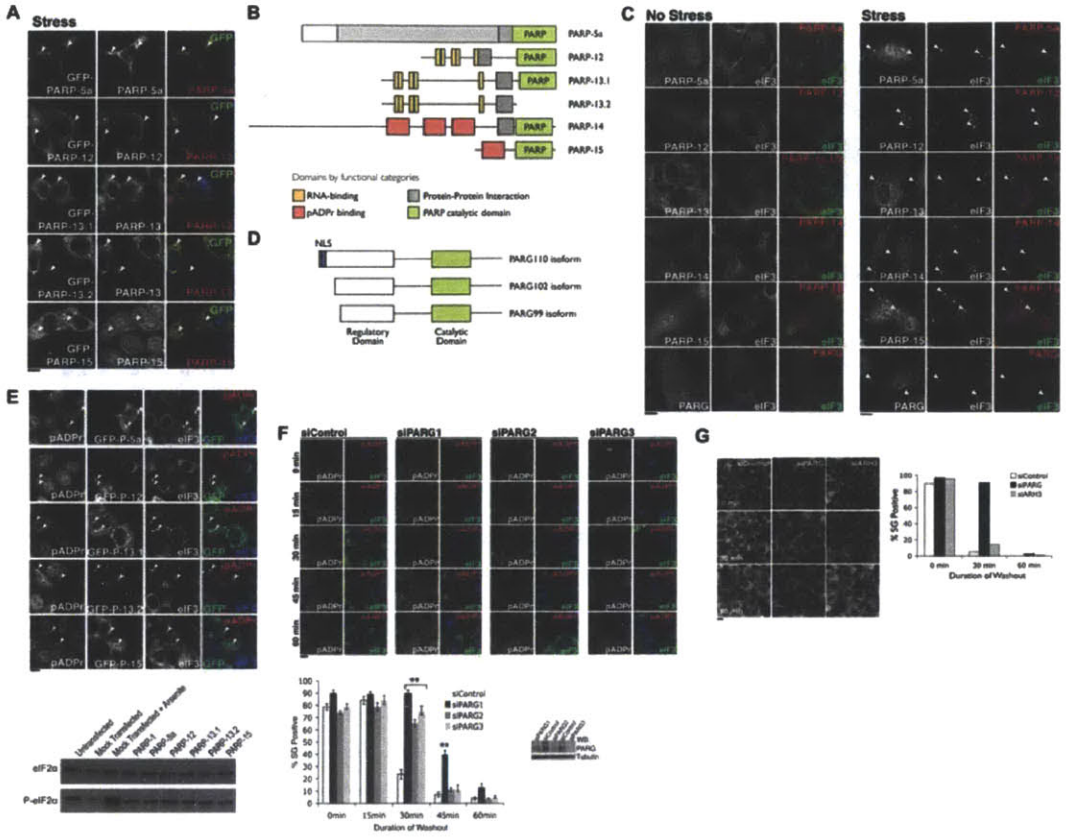

Figure S2, related to Figure 2. (A) HeLa cells expressing GFP tagged PARP-5a, PARP-12, PARP-13.1, PARP-13.2 or PARP-15 were treated with 100 μM arsenite for 30 min and co-stained with respective PARP specific antibodies. DNA was stained with Hoechst 33342 (blue). Arrowheads indicate SGs; scale bar, 10 μm. (B) Schematics for domain structures of SG-PARPs. (C) SG-PARP and PARG localization in control RPE1 cells and in cells following 250 μM arsenite treatment for 1 hour. Cells were stained with respective antibodies and DNA was stained with Hoechst 33342 (blue). Arrowheads indicate SGs; scale bar, 10 μm. (D) Schematics for domain structures of PARG isoforms. (E) High expression of SG-PARPs nucleates stress granule assembly in HeLa cells in the absence of drug treatment. The presence of SGs correlates with the presence of pADPr, detected using LP96-10, even in the absence of stress. A range of DNA and transfection reagent concentrations were used and PARPs -13.1, -13.2, and -15 were able to nucleate SGs in all conditions tested in a dose-dependent manner. However, SG nucleation by PARP-5a and PARP-12 was more sensitive to the level of protein overexpression and was not seen when a lower concentration of transfection reagent was used. DNA is stained with Hoechst 33342 (blue). Arrowheads indicate SGs; scale bar, 10 μm. Bottom panel indicated the corresponding level of

eIF2α and eIF2α phosphorylation upon SG-PARP overexpression. (F) pADPr hydrolysis is required for SG disassembly. Shown are representative images taken 0, 15, 30, 45 and 60 min after washout of 30 min 100 μM arsenite treatment in control and PARG knockdown HeLa cells; scale bar, 10 μm. pADPr was detected using LP96-10. Graph shows quantitation of image data; >100 cells were counted for each condition, n = 3. Error bars indicate SD and p-values were derived from paired t-tests comparing with a control siRNA (** indicates p-values < 0.01). Accompanying blot shows level of knockdown for 3 siRNAs directed against PARG with tubulin as a loading control. siPARG1 is the same siRNA shown in Figure 2E. (G) Knockdown of PARG but not ARH3, another pADPr glycohydrolase, slowed down the kinetics of SG disassembly. Representative images taken 0, 30 and 60 min after washout of 30 min 100 μM arsenite treatment in control, PARG and ARH3 knockdown HeLa cells; scale bar, 10 μm. Graph shows quantitation of image data (200 cells were counted for each condition).

Figure S3

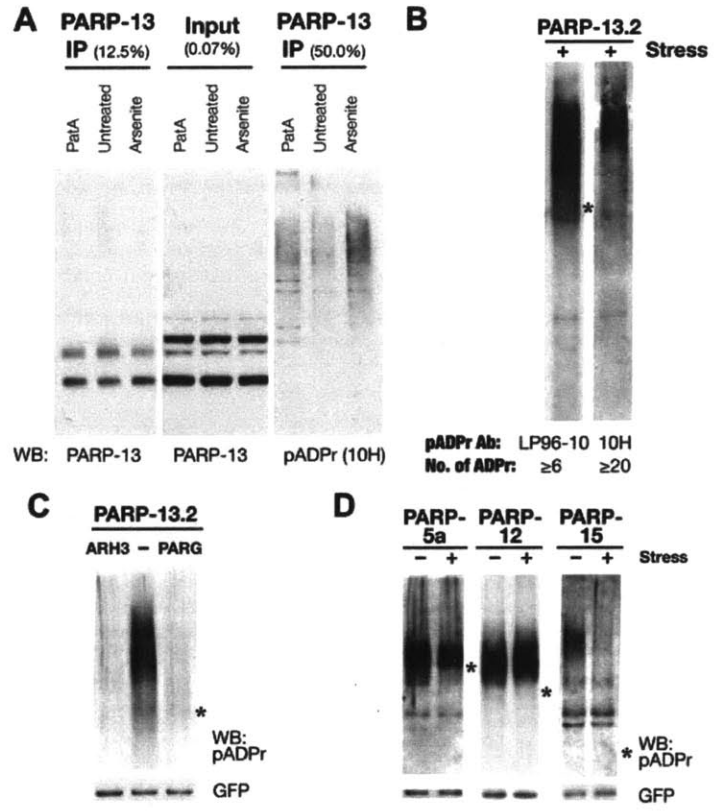

Figure S3, related to Figure 3. (A) pADPr modification of endogenous PARP-13 in untreated cells or cells treated with 250 μM Arsenite or 20 nM pateamine A for 30 min. Shown are western blots for PARP-13 and pADPr (10H antibodies). (B) pADPr modification of GFP-PARP-13.2 as shown in Figure 3D were stained positively by two anti-pADPr antibodies, LP96-10 and 10H, which recognize different chain lengths of the polymer. (C) Immunoprecipitates of GFP-tagged PARP-13.2 are sensitive to *in vitro* treatment with glycohydrolase ARH3 and PARG. In this experiment, GFP-PARP-13.2 was immunoprecipitated from lysate of transfected cells treated with 30 min of 250 μM arsenite, where cell extracts included 1 μM ADP-HPD. Asterisks indicate the position of the corresponding GFP-tagged PARP-13.2. (D) Immunoprecipitates of GFP-tagged PARP-5a, PARP-12 and PARP-15 from untreated cells or cells treated with 20 nM pateamine A for 30 min were probed for pADPr, where cell extracts included 1 μM ADP-HPD. Asterisks indicate the position of the corresponding GFP-tagged PARPs.

Figure S4

A

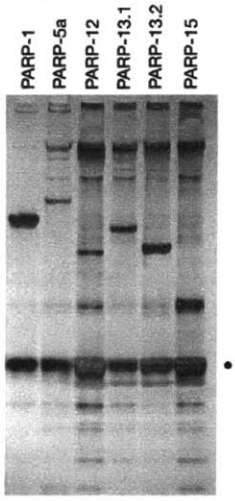

B

Peptides identified	Immunoprecipitation				
	PARP-5a	PARP-12	PARP-13.1	PARP-13.2	PARP-15
PARP-5a	25	0	0	0	0
PARP-12	1	17	0	0	0
PARP-13	0	1	6	20	3
PARP-15	0	0	0	0	7

Figure S4, related to Figure 4. (A) Corresponding silver stain of SG-PARP immunoprecipitates used for in vitro ADP-ribosylating assay in Figure 4A. Black dot indicates IgG used for immunoprecipitation. (B) LC-MS/MS data for individual SG-PARP immunoprecipitates from stressed conditions (20 nM pateamine A, 30 min). The top row indicates which PARPs were immunoprecipitated and the columns indicate how many peptides for a particular PARP were detected.

Figure S5

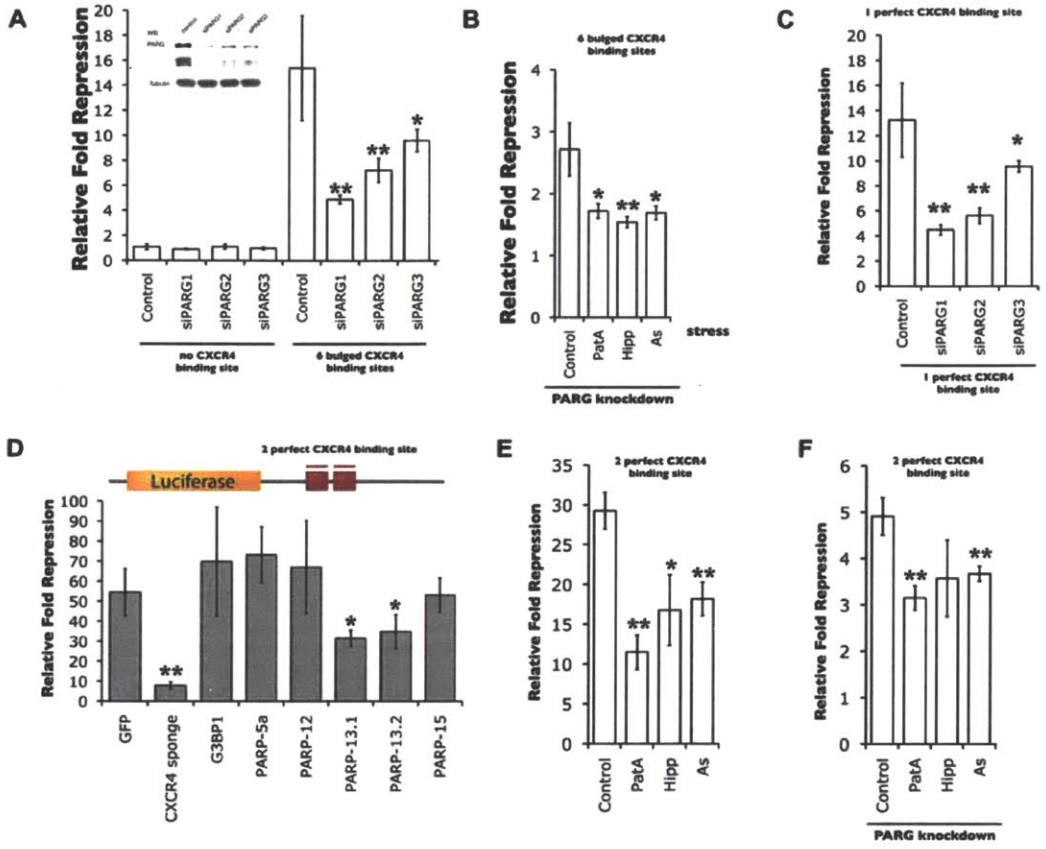

Figure S5, related to Figure 5. (A) Effect of PARG knockdown on luciferase construct with either 0 or 6 bulged binding sites for siCXCR4. Upper panel indicates their activities upon knockdown of PARG using 3 different siRNAs in 293T cells. Luciferase assays and transfection conditions were performed as in Figure 5B and siRNAs targeting PARG are the same as in Figure 2E and S2F; n = 4. Upper panel shows western blots for PARG along with tubulin as control in each lysate. (B) miRNA activity assay in siPARG-transfected 293T cells treated with or without 30 nM pateamine A (PatA), 1 μM hippuristanol (Hipp) or 250 μM arsenite (As) for 2 hours; luciferase assays were performed as in Figure 3A. (C) Effect of PARG knockdown on luciferase construct with 1 perfect binding site for siCXCR4. Left panel indicates their activities upon knockdown of PARG using 3 different siRNAs in 293T cells. Luciferase assays and transfection conditions were performed as in Figure 5F and siRNAs targeting PARG are the same as in Figure 2E and S2E; n = 4. (D) The effect of SG-PARP overexpression on miRNA-directed cleavage assay as in Figure 5G except that a luciferase with 2 perfect siCXCR4 binding site was used; n = 4. (E-F) miRNA activity assay in 293T cells transfected with 25 nM of a control siRNA (E) or siPARG (F) treated with or without 30 nM pateamine A (PatA), 1

μM hippuristanol (Hipp) or 250 μM arsenite (As) for 2 hours; n=3; luciferase assays and transfection conditions were performed as in Figure 5H. For all panels, error bars indicate SD; paired t-test $p < 0.05$ (*) and < 0.01 (**).